2016

Determining the Angle of Impact from the Analysis of Bullets Following Perforation with Glass

Roger L. Jeffreys II

Determining the Angle of Impact from the Analysis of Bullets Following Perforation with Glass

Roger L. Jefferys II

Thesis submitted
to the Eberly College of Arts and Sciences
at West Virginia University

in partial fulfillment of the requirements for the degree of

Master of Science in
Forensic & Investigative Science

Keith Morris, Ph.D., Chair

Casper Venter, M.S.

Patrick Buzzini, Ph.D.

Department of Forensic & Investigative Science

Morgantown, West Virginia
2016

Keywords: bullets, glass, angle of impact, shooting reconstruction

ABSTRACT

Determining the Angle of Impact from the Analysis of Bullets Following Perforation with Glass

Roger L. Jefferys II

When two objects come into contact with one another, there is a potential for the transfer of material between those objects. The goal of this research was to develop statistical models to aid investigators in the reconstruction of a shooting incident. Specifically, the determination of the direction of fire from the angle of impact of the bullet was addressed by assessing the deformation of the bullet and the transfer of glass onto the bullet. Transfer of material to bullets is an underexploited area of trace evidence. Current research has mainly been observational and no attempt has been made to provide a quantitative measure to the results. Four aspects of bullet deformation after perforation of a glass target were studied during the research: (1) the shape of the bullet holes, (2) the side view of bullet deformation, (3) the frontal view of bullet deformation, and (4) the distribution of glass onto the bullets. A Ruger® SR9® 9mm pistol was used to fire 100 cartridges at individual glass samples at angles of 45°, 50°, 60°, 75°, and 90° using full metal jacket and lead round nose ammunition. The following methodologies were employed for image capture and analysis: (1) focus stacking was used to generate high-quality images of the frontal view of the bullet, (2) analysis of the bullet holes in the glass targets using HemoSpat, (3) analysis of bullet deformation and distribution of glass onto bullets using ImageJ. Regression modeling and principal component analysis were performed on the data. The research found that examining bullet holes in glass is not a viable method for determining angle of impact. It also found that the side view deformation of full metal jacket bullets can be used to distinguish between some impact angles, for example, 90° and 65°, but cannot be used for lead round nose bullets. Furthermore, the front view deformation and distribution of glass on full metal jacket bullets can be used to distinguish between some impact angles, for example, 75° and 50°, but cannot be used for lead round nose bullets.

Acknowledgements

I would like to thank the West Virginia University Department of Forensic and Investigative Science for providing funding for the supplies needed to build my firing system.

I would also like to thank Jennifer Ho for assisting with image capturing and processing.

I would like to dedicate this thesis to my parents, brothers, and grandparents who have always supported me in my endeavors.

Contents

List of Figures

List of Tables

1. Introduction

Glass evidence is commonly found at many types of crime scenes including burglaries, murders, assaults, and other types of crimes. The evidence can come from a variety of sources such as windows, automobiles, bottles, and other glass objects [18]. The size of the evidence will depend on the event which created the evidence. Smaller fragments may result from a criminal breaking a window with a weapon, while larger fragments may result from a glass object falling and breaking onto a surface. While large fragments are able to provide more shape, detail, and striations, smaller fragments are more commonly found and collected at crime scenes [18].

Glass evidence can be analyzed in many ways, including the identification of source, analysis of glass fractures, and the analysis of small glass fragments using the density and refractive index [18].

To identify a proof of origin for an unknown piece of glass, the piece will fit back together with the glass of known source. The pieces should fit tightly together and resist lateral movement when pressed together [18].

To analyze glass fractures, one starts by looking at the longest dimension of the triangular shape of the individual pieces of glass. This typically indicates the initial breakage position of a particular glass fragment. Next, each fragment is examined for striations, which diagrams the lines of stress. The path of the break is across and toward the convex side of the striations. This will allow one to determine the direction of break, the direction of the force which produced the break, and which side ruptured first [18].

A refractive index analysis can also be performed to determine whether or not a glass fragment could have come from a particular source of glass.

Bullet evidence is often left at the scene of a shooting. This evidence can, in turn, help the examiner determine if a suspected gun fired a specific bullet, the type of gun that fired the bullet, the type of ammunition used, and from what position the bullet was fired [18].

To determine if an unknown bullet was fired from a suspected firearm, an examiner will first compare class characteristics between an unknown bullet found at the crime scene and a test fired bullet from a suspected firearm. Class characteristics include the direction of twist, number of lands (raised areas created by the rifling in the barrel of a firearm) and

grooves (depressed areas created by the rifling in the barrel of a firearm), width of the lands and grooves, and depth of the lands and grooves. If these are the same between bullets, the examiner will then compare the striation marks on the bullets under a comparison microscope to determine whether or not the unknown bullet was fired from the suspected firearm.

To determine the type of gun that fired the bullet or the type of ammunition used, an examiner will often use the class characteristics listed above. It is important to note that class characteristics differ between manufacturers and between firearms. An examiner will also measure the bullet dimensions and weight to determine the caliber of the firearm used. In some cases, the material the bullet is made from may help the examiner determine the type of ammunition.

In order to determine the position from which the bullet was fired, the examiner may look at trace evidence, such as glass, that has been deposited onto the bullet. If more than one type of trace evidence is present, the examiner may also try to determine the sequence in which the evidence was deposited. They may also look at how the bullet deformed to help make an inference about the possible angle at which the bullet impacted a surface.

As a forensic scientist, one needs to know the physical and chemical properties of evidence before any analysis can be conducted.

1.1 Physical and chemical properties of glass

Glass is defined as an inorganic product of fusion that has cooled to a rigid condition without crystallization [19]. Glass is a mixture of inorganic components including, among others, sand or silicon dioxide (SiO_2), soda ash or sodium carbonate (Na_2CO_3), and limestone or calcium oxide (CaO) [20]. It is a hard, brittle, amorphous substance. Glass is a very important piece of evidence for forensic scientists and it plays a significant role in the reconstruction of a case for several reasons [21]:

1. It has a wide range of uses and is common in the environment.
2. It is easily broken producing fragments of various sizes.
3. Glass fragments or particles are left at the scene if glass is broken during the commission of a crime.
4. Small fragments can be transferred to objects.
5. It is not affected by normal environment conditions and is extremely stable.
6. It is produced in different ranges of compositions and by different processes.

7. There is a range of composition within a given type of glass.

Plate glass (windows), laminated glass (windshields), and tempered glass (side and rear vehicle windows) are the types of glass commonly found in shooting incidents [22]. Plate glass or single-strength glass is produced using the float method, which involves one side of the glass floating on a bath of molten tin during the manufacturing process for flattening purposes [21]. Sodium, calcium, magnesium, and aluminum are common metal oxides found in plate glass [23]. The resulting glass tends to be smooth, have a uniform thickness, and fluoresce on the float side when examined under ultraviolet light.

Laminated glass consists of two sheets of plate glass with a polyvinyl plastic layer placed between them and can be manufactured with a curvature [22].

Tempered glass is made by heating single-strength glass until it begins to soften and then rapidly cooling it with streams of compressed air [21]. As a result, stresses and a surface-tension effect are created due to the outside of the glass cooling down faster than the inside [24]. This process creates a layer of compression stresses on the surface, offsetting any surface tension caused by applied forces. Tensile stress is also created in the glass mid-plane, and as a result, upper stress limits are established [24]. These properties make tempered glass more resistant to breakage.

1.2 Physical and chemical properties of bullets

Handgun bullets commonly encountered in casework are full metal jackets (FMJ), hollow points (HP), and lead round nose (LRN) bullets while jacketed soft points (JSP) are less common [25].

FMJ bullets have a lead core with a copper jacket which encapsulates the entire core except the base. HP bullets have an opening at the nose of the bullet. The opening causes the bullet to expand upon impact, but also introduces drag limiting the range of the bullet.

LRN bullets are entirely lead and are similar to the FMJ as both have a round nose. It has a high ballistic coefficient due to its weight and round nose [26]. JSP bullets have a lead core surrounded by a copper jacket with some of the lead core protruding from the front [27].

When a bullet contains a jacket, the jacket is normally harder than the core itself. The jacket can be composed of a variety of materials, including gilding metal, cupronickel, cupronickelcoated steel, nickel, zinc–, chromium–, or copper-coated steel, lacquered steel, brass, nickelor chromium-plated brass, copper, bronze, aluminum/aluminum alloy, Nylon (Nyclad), Teflon- and cadmium-coated steel [28]. Tin is also sometimes used in jacket material due to its lubricating properties. Depending on the desired effects of the bullet, for example, how

much the bullet will penetrate, the base and nose of the jacket will have different thickness and hardness [28]. The way in which the jacket is attached to the core can also be different as well between manufacturers.

The core can vary between manufacturers, but is normally made from lead. One reason for this is due to its high density [28]. Other materials can include copper, brass, bronze, aluminum, steel, depleted uranium, zinc, tungsten, rubber, and various plastics [28]. However, bullets which contain a lead core and copper alloy jacket are the most common. When it comes to the hardness between the base and the nose, a combination of core materials are sometimes used. The lead used to form the core can either be a soft lead or a lead that has been hardened by antimony, tin, or both [28]. If the lead core is hardened, antimony is typically used.

The components of a FMJ bullet can be seen in Figure 1.1 on the following page. The shape of the nose of a bullet is one important factor that plays a crucial role in the aerodynamics of the bullet, thus determining the distance a specific bullet can travel. The ogive is represented by the curved shape forming on the bullet and, along with the nose, is one of the parts that is involved in the impact when a bullet strikes a surface [29]. The bearing surface, or cylindrical portion of the bullet, is typically what firearms examiners use to conduct comparisons and encompasses the center portion of the bullet, which contacts the rifling in the barrel of a firearm [29]. A comparison involves the examiner placing both a known and unknown bullet onto a comparison microscope and viewing the bearing surfaces of each bullet at a high magnification to observe the lands (raised portions) and grooves (depressed portions). The lands and grooves are created on the bearing surface of the bullets by the rifling inside the barrel of the firearm from which each particular bullet was fired. Within the lands and grooves, the examiner will compare striations, or linear markings, to conclude whether both bullets were fired from the same firearm or from different firearms. The base, or side opposite the nose, helps the bullet maintain its seal as it travels down the barrel.

By understanding the physical and chemical properties of these two types of evidence, an examiner can better understand the interaction that takes place between glass and bullets.

Figure 1.1: Parts of a full metal jacket bullet (FMJ) [1]

1.3 Interaction between two evidence types (glass and bullets)

When a bullet contacts a surface, it will either perforate the material (completely pass through the material), penetrate the material (impacting the material causing the surface to depress), or ricochet (deflect off the surface of the material) [30].

When two objects come into contact with one another, there is a potential for the transfer of materials from one to the other [31]. A drive-by shooting is a good example of how glass and bullets may interact with each other. If a shot is fired at a home from a moving vehicle, the bullet could travel into the home by way of perforation through a window. This impact between the bullet and the glass creates an interaction between these two types of evidence and allows for the possible transfer of glass onto the bullet. Figure 1.2 demonstrates how the transfer of material to the ogive area of a FMJ bullet can provide crucial information in a reconstruction. The observation of the x-ray map shows that steel (through the monitoring of iron) was transferred around the ogive area of the bullet, creating a ring like shape. One can hypothesize, from this information, that the angle of impact was approximately 90° based on the how the steel was distributed on the bullet during impact.

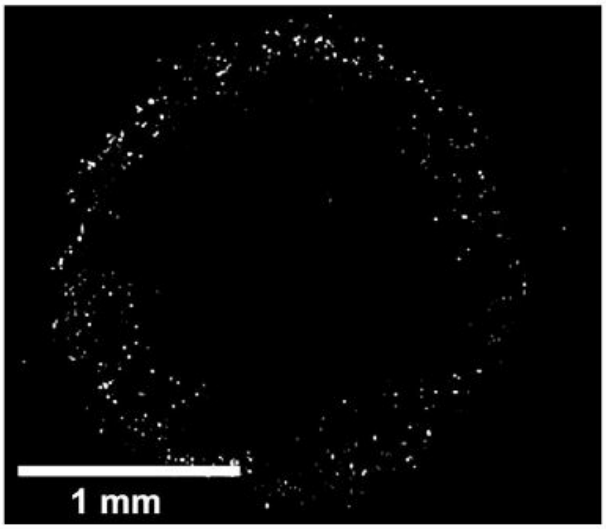

Figure 1.2: Iron X-ray map of the nose of a FMJ bullet following perforation with a steel plate [2]

Not much attention has been given to target specific markings on and trace evidence from bullets. From observing trace evidence on bullets following impact, an association between people, places, and things involved in crimes can be developed [32]. The examination of the distribution of glass on fired bullets will allow for the determination of angle of impact and distance fired which will aid in the reconstruction of a crime scene. This is an underexploited area of trace evidence, as limited research has been performed on this topic. Previous research has only been observational and no attempt has been made to provide a quantitative measure of the results.

The characterization of glass samples is needed to ensure similar properties of glass types before experimentation. Proper control for the continuation of the methods and eventual evaluation of the results are thus maintained. When referring to glass, refractive index and elemental composition are the two main methods used in forensic analysis for characterizing glass samples.

There are a few types of instrumentation that allow examiners to perform analysis on glass, bullets, and their resulting states following interaction with each other.

1.4 Instrumentation for the analysis of glass and bullets

1.4.1 Refractive index (RI) and the glass refractive index measurement (GRIM) system

The physical property of refractive index is used for characterizing glass particles [33][34][35]. In forensic casework, the small size of glass fragments allows for an accurate refractive index measurement.

Refraction refers to the bending of a light wave due to a change in velocity. When light waves travel through air of the same temperature, they do so at a constant velocity until they move into another medium. This is demonstrated in Figure 1.3.

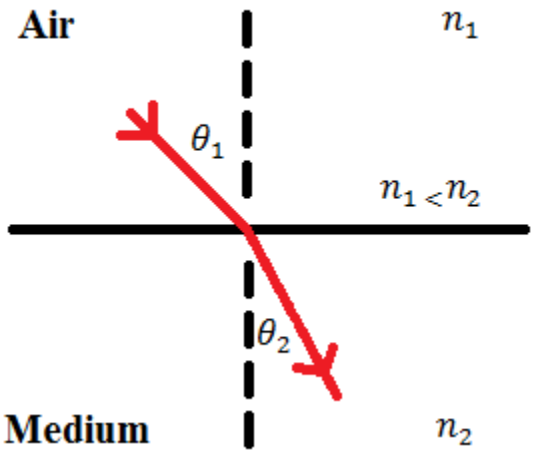

Figure 1.3: Diagram of refraction [3]

At this point, the waves will slow and the rays of light will bend. This can be described by Snells law of refraction by the following equation :

$$n_1 \times \sin\theta_1 = n_2 \times \sin\theta_2 \tag{1.1}$$

where θ_1 and θ_2 are the angles of incidence and refraction, respectively, and n_1 and n_2 are the refractive indices of air and the second medium, respectively. The refractive index of that medium can be defined as the ratio of the velocity of light in a vacuum to the velocity of light in that medium, or mathematically as [36]:

$$RI = \frac{\text{velocity of light in vacuum}}{\text{velocity of light in medium}} \tag{1.2}$$

It should be noted that refractive index varies with temperature and wavelength, thus requiring them to be monitored and controlled. Glass is isotropic and therefore is always extinct under double polarization at all angles [37]. To determine the refractive index of a glass sample, two methods can be used. The immersion method involves observing a glass fragment mounted in a series of immersion oils of different refractive indices. By observing the direction of the Becke line, which is a bright halo near the edge of glass sample while immersed in a medium, one can determine the refractive index of the glass sample [38]. If the distance between the sample and objective lens is increased, the Becke line will move into the medium of higher refractive index. If this distance in decreased, the Becke line will move into the medium of lower refractive index.

The hot stage method varies the refractive index of the immersion oil by adjusting the temperature. The glass fragment is placed in the immersion oil on a hot stage, and the temperature is adjusted based on properties of the immersion oil. Figure 1.4 demonstrates what is known as a match point; this is the point at which the temperature reaches 80°C the refractive index of the glass is the same as the refractive index of the immersion oil (RI = 1.518). A match point is any combination of temperature and wavelength, at which two media have indistinguishable refractive indices.

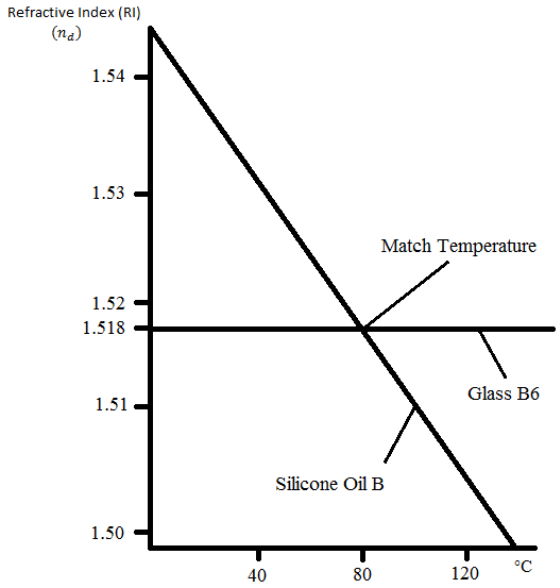

Figure 1.4: Curve showing relationship between the temperature of an immersion oil and its refractive index. Adapted from Locke Scientific Reference Glasses and Silicon Oils for Refractive Index Determination [4].

The refractive index can be calculated using linear equations or graphically determined using a Hartmann net and plotting the corresponding wavelength at the match temperature [38]. Figure 1.5 shows a Hartman net which is a graph representing the refractive index versus wavelength at fixed temperatures for an immersion oil. [39].

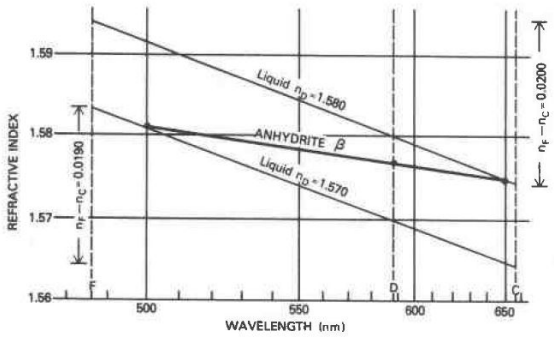

Figure 1.5: Hartmann net [5]

The glass refractive index measurement (GRIM) system can be used to automatically measure the refractive index of a glass sample. The instrument uses the hot stage method to automate the measurements of the match temperature and refractive index. Contrast on a video image is measured until the match point is detected as viewed in Figure 1.6. This contrast is measured while the immersion oil is heated or cooled. Once the match point is detected, the refractive index is determined using stored calibration data in the system [23].

Figure 1.6: GRIM3® and its graphical user interface [6]

The hot stage method as well as the GRIM3® both make use of a phase contrast microscope which enhances contrast between the glass fragment and immersion oil. The principle

of phase contrast microscopy enables phase differences in a glass fragment to be converted to amplitude differences resulting in an image of good contrast [7]. Figure 1.7 depicts the schematic of a phase microscope and displays the resulting path rays of direct (background light) and diffracted light. The enhanced contrast is a result of diffracted and direct beams interfering on recombination in the final image [7].

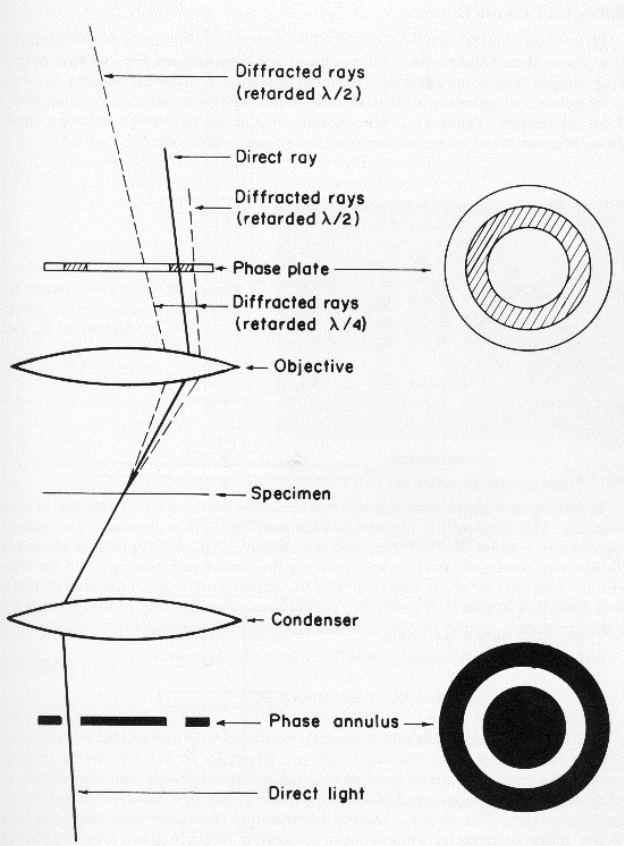

Figure 1.7: Phase contrast microscope schematic [7].

Central undeviated rays and diffracted deviated rays form spectra in the back focal plane of the objective as light passes through a glass fragment [7]. Retardation occurs as light is diffracted and passes through the glass fragment.

An image is produced of the annular ring of light in the back focal plane as a result of the annular stop being focused by the objective, thus separating the direct rays from the diffracted rays [7]. The intensity of direct light from the condenser is reduced by a ring of absorbent material in the phase plate.

A transparent phase retarding film is applied causing retardation in either the direct or diffracted beam, resulting in the direct and diffracted beams interfering destructively in the

intermediate image plane [7]. This causes the phase differences to be detected into visible light and dark.

Another common method for the observation and analysis of glass on a bullet involves the use of a scanning electron microscope with energy dispersive x-ray spectroscopy (SEM-EDX).

1.4.2 Scanning electron microscopy with energy dispersive x-ray spectroscopy (SEM-EDX)

Image formation

The SEM-EDX produces high resolution images with high magnification [9]. It allows for the analysis of small sized samples such as gunshot residue particles and glass fragments.

The SEM column contains a tungsten filament, which is used as the electron beam source. The beam itself is produced by the operation of electromagnetic lenses in the SEM column. High energy electrons are focused into a fine beam, and the beam is scanned or rastered over the surface of the sample in a series of lines and frames [9]. The beam electrons and the sample interact both elastically and inelastically, resulting in radiation products including backscattered electrons, secondary electrons, and x-rays [9]. These are generated as a result of the complex interactions of the beam electrons with the atoms of the sample.

Figure 1.8 displays secondary electrons that are used to represent morphological features of the sample, backscattered electrons that are used to create an image based on the average atomic mass of the elements in the sample, and x-rays that provide the elemental composition which is used to generate a spectrum.

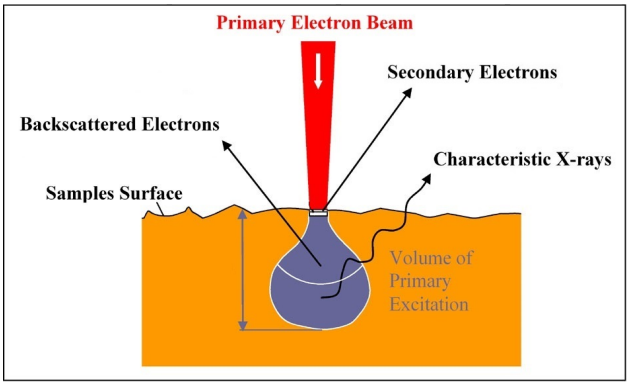

Figure 1.8: Interaction of electron beam with the sample [8].

The radiation products are commonly collected by an Everhart-Thornley scintillator-photomultiplier detector [9]. The radiation signals are amplified and displayed on screen

which scans in sync with the scan of the sample [9]. An image is constructed using a scanning system which scans over the image point by point. Figure 1.9 shows a schematic of the scanning system of the SEM.

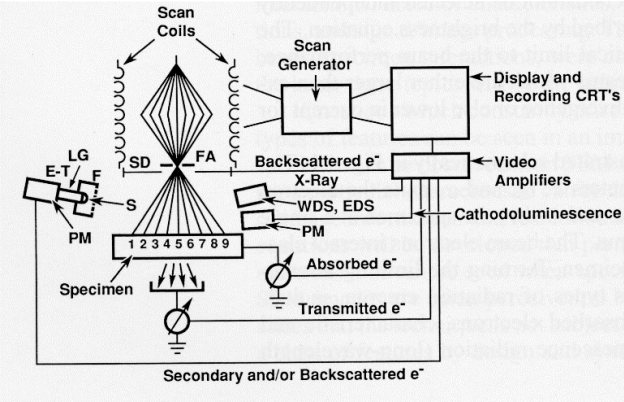

Figure 1.9: Schematic of the SEM [9].

Deflection occurs in both the X and Y directions as a result of electromagnetic scan coils being energized [9]. The strength of the current in the scan coils are altered as a function of time. This way, the beam moves according to a sequence of points on the sample.

The resulting image displayed by the SEM represents a two-dimensional map with a single pixel corresponding to each individual point on the sample that was scanned [9]. The brightness at each pixel is proportional to the intensity of the signal.

Energy dispersive X-ray spectrometry (EDX)

EDX is combined with the SEM allowing for the elemental analysis at a point on the sample. The x-ray photon is converted into an electrical pulse with specific characteristics (amplitude and width) by the EDX system [40]. Depending on the energy received by the detector, individual peaks are generated corresponding to the electrical pulses. Each particular element making up a sample will have a peak proportional to the amount of energy received by the detector [40].

The location, height, and presence of a peak from the EDX spectrum allows for the identification of specific elements present in the sample. An example of an EDX spectrum is shown in Figure 1.10 on the following page. Multiple elements can be found in the spectrum including oxygen (O), aluminum (Al), and sulfur (S). Common elements found in glass can also be seen in the spectrum including silicon (Si) and calcium (Ca). It would be expected that these common elements would be present in a glass sample EDX spectrum

along with another common element, sodium (Na). A quantitative analysis can be performed to calculate the weight percentages of each element found to be in the sample [40].

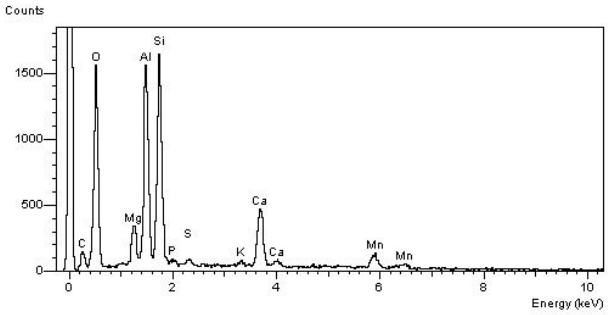

Figure 1.10: Example of an EDX spectrum [10].

X-ray mapping

An X-ray map is an image of the sample formed from a selected part of the X-ray spectrum [40]. They show the spatial distribution of elements in a sample.

An electron beam is rastered over one or more areas of interest point by point as shown in Figure 1.11. The regions selected represent the intensities (energies) of the X-rays of the elements of interest [11]. The electron beam will dwell over each pixel in the image for a specified time. The number of X-rays detected in each pixel region are stored, and the electron beam moves to the next pixel until the entire region of interest is scanned [11]. The resolution of the X-ray image is determined by the beam size, and the relative response of each element is determined both by how long the beam scans each point and the concentration of each specific element in the sample. An image is created, which is made up of a matrix of integers representing the number of X-ray counts at each pixel. A single band image with 0-255 greyscale levels is then created from these integers [11]. A pseudo-color image can also be created.

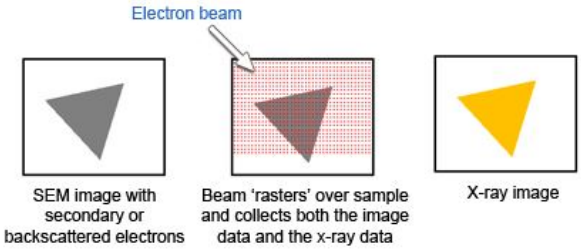

Figure 1.11: Diagram of x-ray mapping creation [11].

Figure 1.12 demonstrates that a combination map of common elements in glass can be created using X-ray mapping to show the distribution of these elements of interest in a single image. As the electron beam rasters over the sample point by point, X-rays are generated by each individual element (silicon, calcium, and sodium) and measured by the EDX detector. The intensity (number of counts) of the X-rays from each element at each point is then converted into a greyscale value. This process continues until the beam has rastered over the entire area of interest, thus resulting in the combination X-ray map.

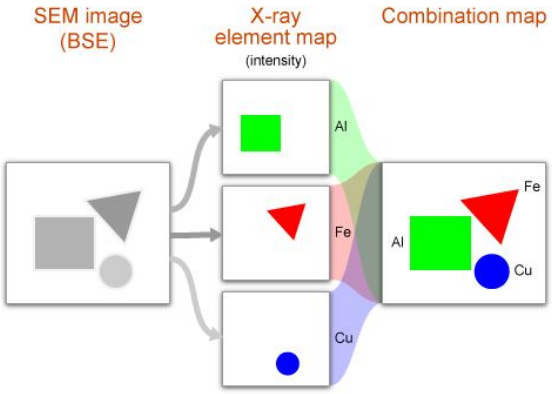

Figure 1.12: Diagram of an elemental combination x-ray map [11].

In order to properly photograph the interaction between glass and bullets, certain devices and software can be used to generate high-quality photographs, allowing an examiner to observe the glass distribution onto a bullet following perforation.

Although the SEM was used in this research, there are other methods, such as inductively coupled plasma mass spectrometry (ICP-MS), which are better at characterizing glass.

1.5 Data processing and analysis

1.5.1 ImageJ

ImageJ is an image processing and analysis program created to perform multiple functions on images. An examiner can use ImageJ to calculate area and pixel value statistics, measure distances and angles, and create density histograms and line profile plots based on the selection within an image that examiner chooses [41]. For example, an examiner can recover a bullet at a crime scene and use ImageJ to measure the angle deformation of the bullet as well as that bullets length, width, and height. This can provide insight into the type of

material that the bullet may have impacted and at what angle the bullet impact a certain material.

ImageJ serves as an image processing program that consists of several plugins with the purpose of statistical analysis of multidimensional images [42]. One of the basic functions is the ability to measure area statistics, line lengths and angles, or point coordinates. From those measured particles, the program is able to create 8-bit images with outlines of those said particles. Another feature is the calculation of area within a selected boundary of the image using square pixels or calculating the perimeter of that boundary [42]. The center point, or centroid, of a selection can also be determined by averaging the x and y coordinates of the pixels. Similar to that, the center of mass can be determined by taking the brightness-weighted average of the x and y coordinates of the pixels. ImageJ also allows the implication of fit ellipses, which identifies the primary (major) and secondary (minor) axes of the best fitting ellipse as well as the angle between the primary axis and a line parallel to the X-axis of the image [42]. This feature can be used in conjunction with centroid to calculate the center coordinates of a given ellipse. Similarly, the shape descriptors function calculates and identifies the shape in reference to circularity, aspect ratio, fit ellipse, roundness, and solidity. The shape descriptors are represented by specific equations [42]:

Circularity is defined as

$$\text{circularity} = 4\pi \times \frac{\text{area}}{\text{perimeter}^2} \tag{1.3}$$

where the area is the combined space of a selected particle, and perimeter is the outside distance around the selected particle.

Aspect Ratio is defined as

$$\text{aspect ratio} = \frac{\text{major axis}}{\text{minor axis}} \tag{1.4}$$

where the minor axis is the short axis of the best fitting ellipse from the selected particle area, and the major axis is the long axis of the best fitting ellipse from the selected particle area.

Roundness is defined as

$$\text{roundness} = 4 \times \frac{\text{area}}{\pi \times \text{major axis}^2} \tag{1.5}$$

where the area is the combined space of a selected particle, and the major axis is the long axis of the best fitting ellipse from the selected particle area.

Solidity is defined as

$$\text{solidity} = \frac{\text{area}}{\text{convex area}} \tag{1.6}$$

where the area is the combined space of a selected particle, and the convex area is the combined space inside the convex hull (or a compressed particle).

1.5.2 R and RStudio®

R is a programming language specifically designed for statistical computing and graphics and incorporates data manipulation, calculation, and graphical display [43]. Linear and nonlinear modeling, classical statistical tests, time-series analysis, classification, clustering, and graphical techniques are just some of the techniques available in R [43]. RStudio® is designed for R and serves as an integrated development environment which includes a console for viewing run command scripts, an editor for direct code execution, and numerous tools [44].

Using the data generated from these programs, an examiner can then perform statistical analysis in order to help study the data so that new methods can be developed for use in forensic science.

1.6 Regression modeling

1.6.1 Simple linear regression

When one wishes to describe the behavior of one continuous variable in relation to another continuous variable, a simple linear regression can be used to try and model this relationship [12]. For example, simple linear regression could be used if one wished to describe measured angles resulting from a particular method in relation to the known or true angles. The response variable, or dependent variable, is represented by y while the explanatory variable, or independent variable, is represented by x. The simple linear regression model is described as

$$y_i = \beta_0 + \beta_1 \times x_i + \epsilon_i, \epsilon_i \sim N(0, \sigma^2), i = 1, \ldots, n \tag{1.7}$$

where y_i is described by a straight line relationship ($y = mx + b$) with x_i [12]. The intercept and slope, also known as regression coefficients, are represented by β_0 and β_1. ϵ_i is the error that describes the difference between an observation and a mean, and $\epsilon_i \sim N(0, \sigma^2)$ states that ϵ_i has a normal error distribution [12].

Given a particular data set, the data model is described as [12]:

$$y_i = \hat{y_i} + r_i \tag{1.8}$$

where r_i is the estimated errors (residuals), and $\hat{y_i}$ represents fitted values. These values are obtained from the fitted model described as [12]:

$$y_i = \beta_0 + \beta_1 \times x_i \tag{1.9}$$

1.6.2 Multiple linear regression

In order to relate more than one explanatory variable to the response variable, multiple linear regression is used. A model for p linearly independent explanatory variables, $x_1, x_2, \ldots, x_p$, can be described as [12]:

$$y_i = \beta_0 + \beta_1 \times x_{1i} + \beta_2 \times x_{2i} + \cdots + \beta_p \times x_{pi} + \epsilon_i, \epsilon_i \sim N(0, \sigma^2), i = 1, \ \ldots, \ n \tag{1.10}$$

A general principle of regression modeling is to find the simplest model that best explains the data.

1.6.3 Linear models in R

Linear regression is used to describe a relationship between variables based on statistical data. In R, a command (shown below) is able to compute that relationship using a linear regression model.

As seen in Figure 1.13 on the next page, the output consists of a series of information, or data. Lines 1-2 are the call, which serves as a label to ensure the command was operated on the correct data set with the designated model [12]. Lines 4-6 are a five number summary, describing the minimum, maximum, lower and upper quartiles, and the median of the residuals [12]. Lines 8-11 are the coefficient values, most often referred to as the regression table. This section includes the variable name; estimated coefficients, which are sometimes referred to as the beta-hats; the standard error, which is used to test the significance of the regression coefficient or importance of the variables; and the p-values, which either support

or nullify the hypotheses [12]. In this case, it is a test of the hypotheses: $H_0 : \beta_j = 0$ and $H_0 : \beta_j \neq 0$. The closer the p-value is to zero, the more likely the evidence is not in favor of the null hypothesis. Line 13 lists how R identifies significance. If $P < 0.001$ there are three asterisks, if $0.001 \leq P \leq 0.01$ two asterisks, if $0.01 \leq P \leq 0.05$ one asterisk, and if $0.05 \leq P \leq 0.10$ either a period or full stop [12]. If there is any other value, nothing is displayed.

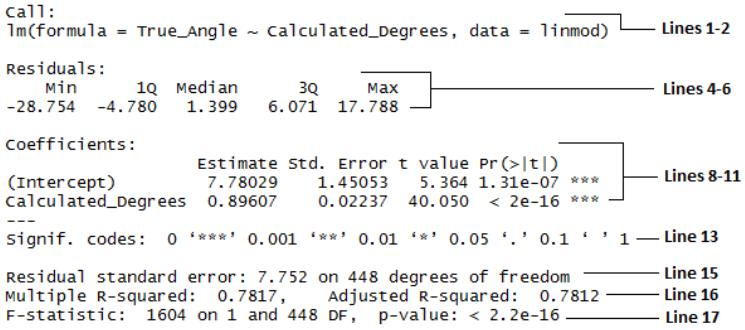

Figure 1.13: Example of a linear model output from R for simple linear regression.

Line 15 is the residual standard error, which describes the standard deviation of the residuals [12]. Line 16 gives the multiple R^2 and adjusted R^2 values which provide measures of model performance. R^2, or multiple R^2, is called the squared multiple correlation coefficient and measures the (squared) correlation between the fitted values and the observed values [12]. To obtain the fitted values, also referred to as the predicted values, estimated regression coefficients are tested in the model and the output is recorded. The adjusted R^2 can be described by the following equation [12]:

$$\text{Adjusted}R^2 = 1 - (1 - R^2)\frac{n-1}{n-p-1} \tag{1.11}$$

The adjusted R^2, shown in Equation 1.11 above, accounts for the addition of variables to a regression model. Because of that, adjusted R^2 is considered important in multiple linear regressions because it ensures that the models are not over-parameterized (as an increase in variables causes an increase in the adjusted R^2) [12]. The adjusted R^2 value is always lower than that of R^2 and has the potential to be a negative value, which would indicate that the model had been extremely over-parameterized. Line 17 of the output provides an F-statistic and the respective P-value [12]. With these values, the following hypotheses are being looked at: $H_0 : \beta_1 = \beta_2 = \cdots = \beta_p = 0$ $H_1 : \text{some}\beta_j \neq 0, j = 1, \ldots, p$

The hypothesis being tested predicts that all of the regression coefficients, save for the intercept, will come out to zero. If this hypothesis is proven false, then the explanatory

variable is considered important in predicting responses. Under linear regression models, three general assumptions exist to ensure that statistical inferences can be made: (1) all observations and errors are orthogonal (independent) from one another, (2) all errors have consistence variance about the line, and (3) all errors have a mean of zero [12].

The idea that the observations and errors are independent is the hardest assumption to check as there is no statistical test that can prove or disprove independence. However, the use of fit models can aid in dealing with dependency although they typically consist of series models, mixed effect models, and/or multivariate analyses [12]. Therefore, the assumption is made that if the data was collected correctly, the observations would be independent unless the measurements made were done on "the same subject and time or space effects."

The second assumption is considered the next most important. In the case that the errors have dynamic variances, the regression coefficient estimates result in extremely large standard errors in some areas and extremely small standard errors in others [12].

A pred-res plot plots the model residuals against their corresponding fitted values [12]. In order to validate the assumption of constant scatter, a pred-res plot is created. According to the third assumption, if the resulting graph shows the points to center around zero, both assumptions are met [12].

In Figure 1.14 on the next page, the left side shows the fitted line plots while the right side shows the pred-res plots. As seen with the above, pred-res plots are able to identify non-constant scatter and non-linearity. These plots also allow for the assessment of data normality. The normal Q-Q plot, or normal quantile-quantile plot, is a scatter plot that depicts the empirical quantiles obtained from the data against the theoretical quantiles [12]. Two methods of plotting that do so are the use of a normal Q-Q plot and a density estimate of the residuals.

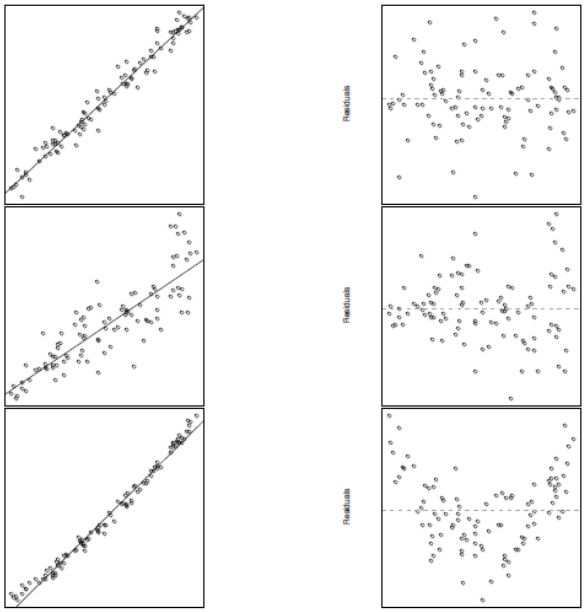

Figure 1.14: Residuals versus predicted value (pred-res) plots [12].

If the data is considered normal, the points of the plot will follow a general linear line as seen in Figure 1.15 - graph A [12]. From the line, an estimate of the mean can be determined based on the intercept while the slope of the line gives the estimated standard deviation.

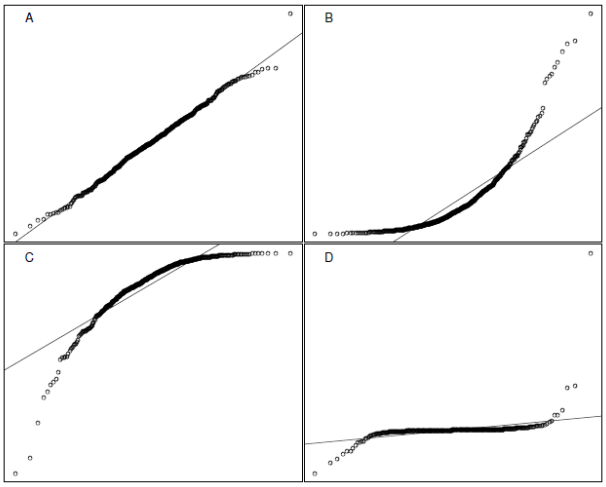

Figure 1.15: Possible shapes for a normal Q-Q plot. The theoretical quantiles are plotted on the x-axis, and the empirical quantiles are plotted on the y-axis [12].

In multiple linear regressions, when there are several variables, some may be considered borderline significant. One of the strategies to combat this is called backward elimination,

where the least significant variables are removed one by one until the refitted model reads that all variables are significant [12]. If multiple variables are removed at once, the chances are that two or more of those variables are "highly linearly correlated." If that is the case, multi-collinearity (the presence of those correlated variables) may cause the significance of the remaining variables to change drastically [12].

1.6.4 Confidence and prediction intervals

Determining the 95% confidence interval can be achieved using the following equation [45]:

$$\hat{y} \pm T_{crit} \times s.e. \tag{1.12}$$

where $\hat{y}$ denotes the forecasted values $\hat{y}$ of x, t_{crit} is the critical value of t (or a point on the continuous probability distribution), and $s.e.$, is the standard error, represented by the equation:

$$s.e. = S_{yx}\sqrt{\frac{1}{n} + \frac{(x - \bar{x})^2}{SS_x}} \tag{1.13}$$

where S_{yx} is the standard error of the predicted y-value for their respective x, n is the sample size number, $\bar{x}$ is the sample mean, and SS_x is the sum of all squared deviations from the sample mean.

An example of a confidence interval can be seen in Figure 1.16 on the next page. A confidence interval represents the 95% probability that the true regression line of the population will fall within the interval calculated using Equation 1.12 [45].

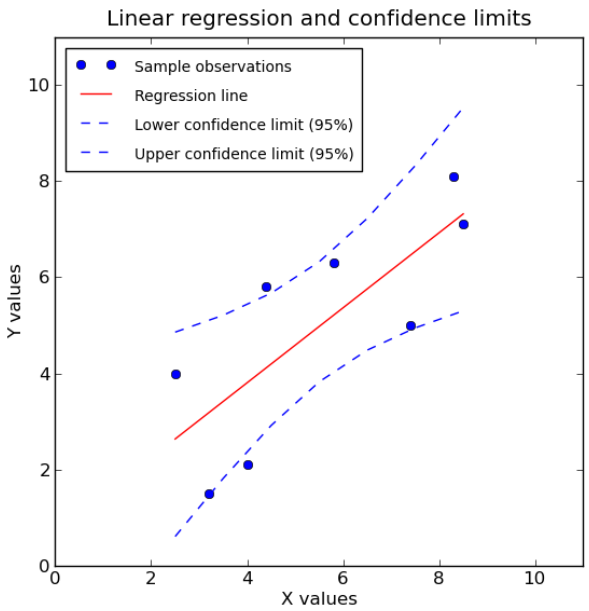

Figure 1.16: A linear regression line calculated to fit data points and the lower and upper confidence limits [13].

Determining the 95% prediction interval can be achieved using the following equation [45]:

$$\hat{y_0} \pm t_{crit} \times s.e. \tag{1.14}$$

where $\hat{y_0}$ represents the forecasted value for $\hat{y_0}$ for x, t_{crit} is the critical value of t (or a point on the continuous probability distribution), and $s.e.$ is the standard error, which is represented by the equation:

$$s.e. = S_{yx}\sqrt{1 + \frac{1}{n} + \frac{(x_0 - \bar{x})^2}{SS_x}} \tag{1.15}$$

where S_{yx} is the standard error of the predicted y-value for their respective x, n is the sample size number, x_0 represents any specified value, $\bar{x}$ is the sample mean, and SS_x is the sum of all squared deviations from the sample mean.

The prediction interval indicates that there is a 95% probability that the true value of $\hat{y_0}$ corresponding to x_0 is within the interval calculated from Equation 1.14 [45].

The prediction interval tells you about where you can expect to see the next data point sampled and describes the distribution of values [46]. It accounts for the scatter of the data as well as the uncertainty of the data mean and therefore tends to be much larger than the

confidence interval [46]. It, on the other hand, describes the possible best-fit line location and, in turn, depicts how well the mean of the data was determined [46].

1.7 Principal component analysis (PCA)

Principal component analysis (PCA) is a form of multidimensional scaling that constructs new characteristics, or variables, from the original ones and allows that high-dimensional data to be optimized and then summarized into a linear multivariate model of orthogonal variables [14]. This method allows the analysis of variance in a set of data that otherwise reads non-statistically significant.

For example, an original data set, composed of chemical data, could consist of a high number of variables where there is a high correlation between those variables. As seen in Figure 1.17, a total of sixty gasoline samples, each consisting of 401 reflectance values could not be differentiated from one another. The similiarity between the samples causes overlapping information creating smooth curves that are hard to tell apart [14].

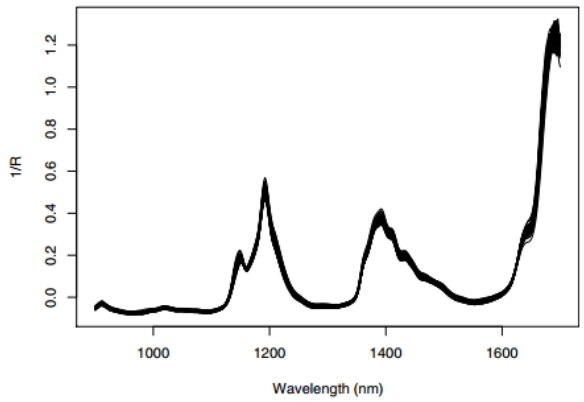

Figure 1.17: Near-infrared spectra of sixty gasoline samples, consisting of 401 reflectance values measured at equally spaced wavelengths between 900 and 1700 nm [14].

As a means to create easier interpretable data, and statistically significant data, PCA isolates and defines latent variables in such a way that all samples are represented and now distinguishable. To do so, PCA creates linear representations using orthogonal basis vectors, or eigenvectors [47]. These are also known as principal components, or PCs. PCs model the statistically significant variation in the data set as well as the random measurement error [47]. The first PC will account for the highest percentage of the variance, while the next PC

will account for the next highest percentage, and so on, while remaining uncorrelated with each other.

The data being used and analyzed is a result of a multiplication matrix, or approximation of the original data, (represented by $\bar{X}$), as shown in Equation 1.16:

$$\bar{X} = T_a P_a^T \tag{1.16}$$

where T represents the scores, P represents the loadings, $superscript^T$ refers to the transposition of the matrix, and $subscript_a$ refers to the number of components used.

Equation 1.16 forms a multiplication matrix, which has the purpose of forming the lower-dimensional, and easier interpretable, data. This is done by multiplying the scores and loadings [14]. With any given a, it indicates the maximum number of PCs and likewise describes the minimum number of rows and columns in the created matrix, which is summarized in equation 1.17:

$$\bar{a}_{min} = min(n, p) \tag{1.17}$$

where n and p refer to the rows and columns of the matrix, respectively.

The resulting matrix consists of PCs where the scores vary as much as possible, the linear distance between each score is as large as possible, and the resulting matrix is as similar to the original as possible. From there, an algorithm referred to as Singular Value Decomposition (SVD) is used to empirically define the PCs and lower the rank of the matrix, which can be seen in equation 1.18:

$$X = UDV^T \tag{1.18}$$

where X indicates an $n \times p$ mean-centered data matrix, U refers to an $n \times a$ orthonormal matrix containing the left singular vectors, D refers to a diagonal matrix $(a \times a)$ composed of the singular values, and V refers to a $p \times a$ orthonormal matrix containing the right singular values.

Equation 1.18 shows that by multiplying the orthonormal matrix composed of U, D, and V, you are able to obtain that mean-centered data matrix, X [14]. However, as shown in Equation 1.19, by multiplying the left singular vectors and the right singular vectors, you obtain the scores, represented by T, while V^T is, in reference with PCA, synonymous with loadings, represented with P. In the case that $a_{max} = a$ in Equation 1.16, the approximation is equivalent to the original matrix, causing Equation 1.16 to appear the same as the modified Equation 1.18. This can be observed in Equation 1.19:

$$X = (UD)V^T = TP^T \tag{1.19}$$

where the scores (the columns in T) describe the object weights per PC, or the location in the latent variables obtained from PCA, while the loadings (the columns in P) provide the weights of the original variables per PC.

While the columns in U have the same coordinates, or location, as that of T, the coordinates in U are normalized and not orthogonal, while the coordinates in T are orthonormal. Because of this, while the columns in U consist of unit variances, the columns in T consist of variances parallel to the variances of each PC [14]. That variance relationship described in the scores matrix (T) can be described by the following equation:

$$\lambda_i = \frac{d_i^2}{n-1} \tag{1.20}$$

where λ_i are the variances, and d_i^2 refers to the squaring of the diagonal elements in matrix D.

The fraction of variance resulting from PC_i can be calculated using Equation 1.21:

$$FV(i) = \frac{\lambda_i}{\sum_{j=1}^{a} \lambda_j} \tag{1.21}$$

A different viewpoint puts this process into another perspective in reference to spectroscopic-chromatographic data. Under this is an equation similar to Equation 1.16 on the previous page. The equation is shown below:

$$A = CP^T + \epsilon \tag{1.22}$$

where A refers to a data matrix composed of mixture spectra, C is a matrix of pure chromatograms, P is a matrix of pure-component spectra, and $\grave{\epsilon}$ refers to the measurement error [47].

The same concept is present in Equation 1.16 on the preceding page with the goal being creating a lower-dimensional data set. Equation 1.22 describes the C and P matrices spectra as "row basis vectors" and "column basis vectors," respectively.

Under the Principal Component Model, the following equation is presented:

$$A = T^k V_k^T + \epsilon \tag{1.23}$$

where A represents a set of basis vectors condensed into a data matrix, V_k represents the eigenvectors, which are also referred to as loadings or eigenspectra, and T_k represents the scores, where the columns of T_k are considered orthogonal but not orthonormal [47].

Again, this equation is equivocal to Equation 1.16 on page 24 and Equation 1.22 on the previous page while also accounting for measurement error. In summation, these equations allow for creating an empirical model of the original data.

In terms of PCA, possible pre-processing options include centering, and if necessary, baseline correction. The idea behind mean-centering data analysis is to calculate the average data vector throughout all rows of that data set, which subsequently moves the origin of the model to the "center" of the data. This normalizes each column of variables to give proportional weighting to all aspects of the measured data vectors, forming what is called "scaled to unit variance." This sets the data up for SVD and is particularly useful with large signal-to-noise ratios [47]. In the case that there is a baseline offset, typically identified by upward or downward slopes, the average signal over a frequency region is calculated and then subtracted from each frequency in order to form a baseline-corrected spectrum.

1.8 Box-Cox transformation

The Box-Cox Normality Plot is a plot of correlation coefficients obtained from a Box-Cox transformation [15]. This is a procedure with the purpose of converting a data set into normalized data in order to be optimal for statistical tests. The transformation required to normalize data can be determined using Equation 1.24:

$$T(Y) = \frac{Y^{\lambda} - 1}{\lambda} \tag{1.24}$$

where λ refers to the transformation parameter and Y is the response variable. In the case that $\lambda = 0$, the natural log is taken of the data in place of the formula [15]. To determine the measure of the normality of the resulting transformation, a number of normal probability plots are formed based on the transformations using a series of λ values.

A correlation coefficient is calculated from each normal probability plot, which is then plotted into a Box-Cox normality plot against the corresponding value of λ used as seen in the top right of Figure 1.18 on the next page.

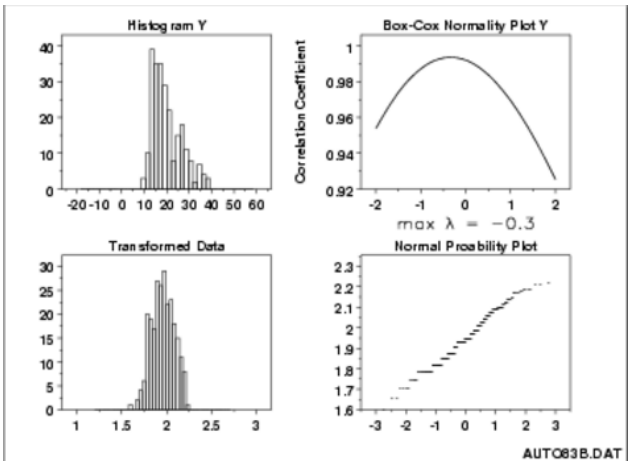

Figure 1.18: Example of transforming the data using a Box-Cox Transformation. The top left graph represents the data before the transformation while the bottom left graph represents the data after the transformation. The graphs on the right represent the normal probability and Box-Cox normality plots. [15].

2. Literature Review

2.1 Characterization of glass evidence

In a study by Munger *et al.*, refractive indices of seven double-paned vehicle windshields were measured to assess the variation across each pane of glass [17]. Thickness measurements were taken of the glass fragments from each pane using a digital caliper. A Foster + Freeman® GRIM3® was used to measure the refractive indices. At least 240 measurements were made for each pane of glass depending on its size. The largest pane resulted in 540 measurements.

The mean standard deviation of the refractive indices values for all the panes of glass were found to be 4×10^{-5}. The individual pane standard deviations were found to be from 3×10^{-5} to 5×10^{-5}. This data can be found in Table 2.1. The range of the mean for the refractive index values across all panes was found to be from 1.51864 to 1.52264.

Table 2.1: Refractive index values for a single windshield pane [17].

Section	Measured RI Min–Max	RI Average	RI Standard Deviation
A	1.52254–1.52271	1.52264	0.000042
B	1.52256–1.52275	1.52266	0.000042
C	1.52255–1.52278	1.52266	0.000049
D	1.52259–1.52274	1.52266	0.000036
E	1.52255–1.52273	1.52264	0.000043
F	1.52251–1.52277	1.52262	0.000050
G	1.52256–1.52276	1.52265	0.000048
H	1.52256–1.52275	1.52265	0.000055
I	1.52258–1.52271	1.52266	0.000037
J	1.52256–1.52277	1.52262	0.000042
K	1.52257–1.52269	1.52263	0.000031
L	1.52258–1.52279	1.52264	0.000039
M	1.52258–1.52269	1.52262	0.000024
N	1.52260–1.52269	1.52264	0.000026
O	1.52255–1.52269	1.52261	0.000028

Zadora and Brozek-Mucha discussed the usefulness of the SEM-EDX in forensic examinations [48]. The ability to analyze samples based on elemental composition makes the SEM-EDX a powerful tool. Since glass samples are usually small in forensic casework, there is a strong need for an appropriate analytical method of analysis. The elemental composition could be very different between samples depending on the product from which the glass frag-

ment originates. Using the SEM-EDX to analyze various glass samples, one should be able to develop a classification scheme which will allow a glass sample to be placed into a specific class based on the elemental composition retrieved from the SEM-EDX. It was confirmed in the Forensic Testing Program that the SEM-EDX is useful for solving problems that involve the analysis of microtraces, including that of glass [40].

Falcone et al. studied the ability of the SEM-EDX to analyze small glass fragments [49]. The glass fragments used in the study were retrieved from a green silica-soda-lime container glass of known composition. The analyses provided accurate results of the components of embedded and polished glass particles down to 0.30mm in size. It was found that trace element concentrations of oxides in the range of 500–100ppm could be detected and that non-embedded irregular shaped glass particles could be classified using the SEM-EDX.

Andrasko and Maehly attempted to differentiate four different groups of window glass [16]. Group A consisted of two panes, one fifteen years old and one new. Group B contained twenty-nine samples collected from a town over a period of several weeks. Group C had ten samples of show window glass with similar thickness, densities, and refractive index values. Group D consisted of three glass samples from casework, which were indistinguishable based on refractive index values. The elements found in the glass samples included: silicon, calcium, sodium, magnesium, aluminum, potassium, sulfur, chlorine, iron, and barium.

It was concluded that the elemental ratios obtained by the SEM-EDX analysis allowed for nearly all of the glass samples to be distinguished from one another although the refractive index values were the same for some samples. This can be seen in Figure 2.1.

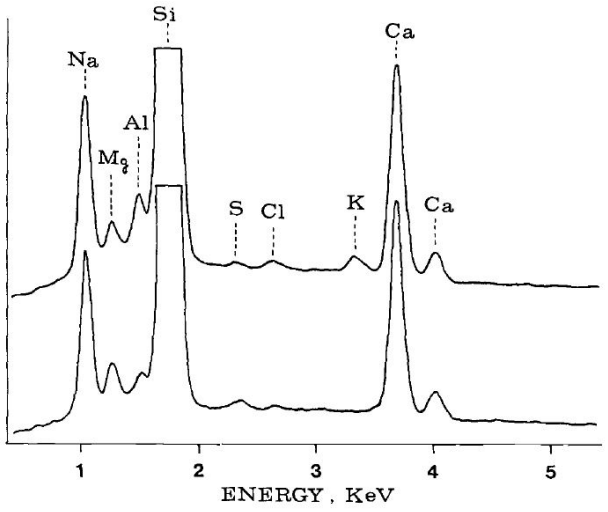

Figure 2.1: X-ray spectrum resulting from a 400-s analysis of glass samples 23 and 24 of Group B. The refractive index of both of these samples was 1.5198 [16].

2.2 Interaction between glass and bullets

In a study by Vermeij *et al.*, the transfer of glass onto bullets following perforation of 8mm layered glass and 4mm single sheet glass was examined [2]. The study found that the best method to catch the bullets was to use a cotton wool trap which limited the amount of damage to the bullet and transferred a limited amount, if any, of cotton to the bullet itself. Sellier & Bellot® 9mm Luger FMJ 115 grain and PMC .38 Special 158 grain lead round nose (LRN) ammunition were used in the study. The 9mm Luger ammunition was fired using a Sig Sauer P226 9mm pistol. The .38 Special ammunition was fired using a Smith & Wesson Model 586-3 .357 revolver. Ten FMJ bullets were fired through layered glass and nine were fired through single plate glass. Eight LRN bullets were fired through layered glass and ten were fired through single plate glass. The study used SEM-EDX to observe the glass on the bullets.

For single-sheet glass, the noses of the bullets were strongly flattened. Finely powdered glass fragments covered the noses. The very tip of the bullet, however, was relatively free of glass. Three zones were noticed on the bullet as shown in Figure 2.2. The first zone consisted of the center of the nose which remained mainly unharmed with very few traces of glass. The second zone consisted of the area surrounding the center of the nose which was rough and contained only a few glass particles. The third zone is outside of the second zone and contains larger particles of glass.

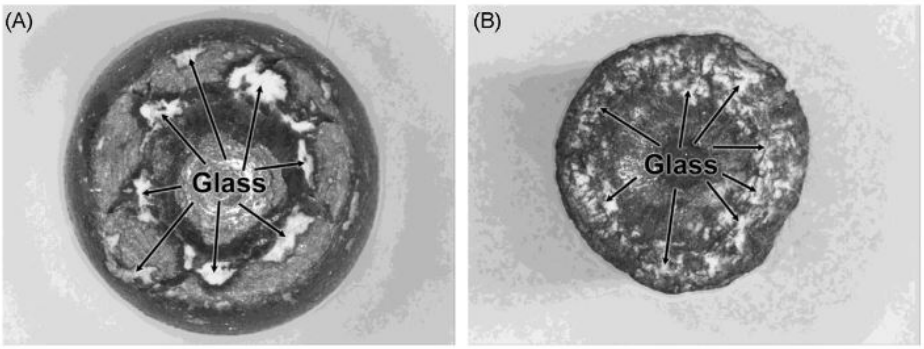

Figure 2.2: Nose of FMJ bullet (A) and LRN (B) after perforation of single sheet glass [2].

For layered glass, both the FMJ and LRN bullets were more damaged [2]. The jackets separated from the core, and, at times, there was fragmentation of the core itself. If part of the jacket remained intact, glass dust was observed in a ring around the nose. Glass powder was also found on the edges of the opened jackets. There were glass fragments found embedded in the flattened faces of the bullets.

The glass fragments embedded into the bullets were easily recognized using SEM-EDX due to the angularity of the particles and the EDX spectra of the particles [2]. These glass fragments can be observed in Figure 2.3.

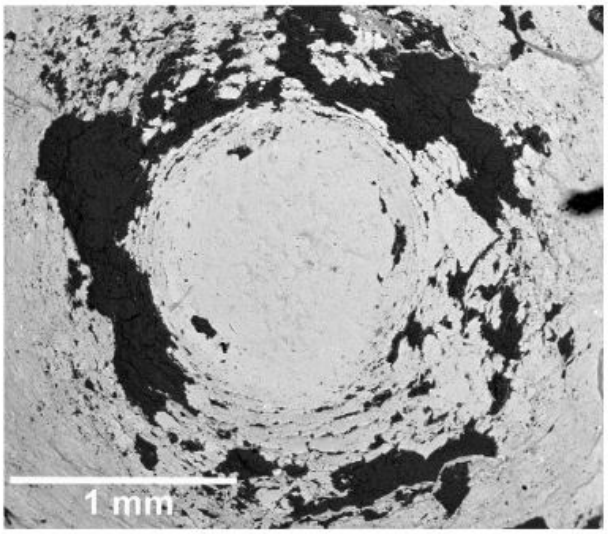

Figure 2.3: SEM image of glass (black) surrounding the tip of an FMJ bullet [2].

Karger *et al.* examined the transfer of glass to bullets using a SEM-EDX [50]. A Sig Sauer P225 9mm pistol was used to fire Geco 9mm FMJ round nose bullets through 3mm thick flat glass (lime-sodium-silicate). Five bullets were fired through the glass. After firing, the glass on the bullets was located using SEM-EDX. The major elements observed were silicon and calcium. Upon observation of the bullets, there was a hollow in the tip of the bullet along with a finely tapered rim. A few small glass fragments were observed at the tip of the bullet. Glass dust was also located on the sides and rear of the bullets.

Scientists Wong and Jacobson conducted a study on bullet hole shapes to determine angles of impact in 2012 [51]. They created bullet impacts using a Walther P4 with PMC copper-jacketed ammo into three different flat media surfaces — 5/8 wood, sheetrock, and sheet metal from a van. The 54 holes were then examined using an ellipse template method and caliper and half-length method. With the wood pressboard media, 39 of the calculated angles were within the 10° true angle using the ellipse template while 46 were within the range using the caliper. With the sheetrock, 38 of the template-method angles were within range while 44 of the caliper-method angles were. With the sheet metal, the bullets were unable to penetrate at the 10 degree angle due to the nature of the media. However, the ellipse template was used on the ricochet imprints, resulting in 20 of the 48 calculated angles within the 10° range and 23 of the 48 to be within range using the caliper.

2.3 Image capture

Baviskar discussed a method to measure area from a set of features in a photomicrograph using ImageJ [52]. In this process, a scale is calibrated using `Set Scale` and the image must be 8-bit greyscale. Variables to be measured, such as area, standard deviation, minimum and maximum grey scale value, and mean grey scale value, are selected using the `Set Measurements` function. Automatic thresholding is used to set pixels for objects of interest at a certain greyscale value so that they appear brighter than the background. The `Analyze Particles` function is used to analyze the image and generate characteristic data for the objects of interest. A Microsoft® Excel® spreadsheet stores the data which can then be used to conduct further analyses.

2.3.1 Zerene Stacker

In a study conducted by Brecko *et al.* in 2014, an inexpensive approach to focus stacking systems used Zerene Stacker results for comparison against two high-end stacking systems – a Leica® MZ16A with DFC500 and a Leica® Z6APO with DFC290 [53]. Using an ant and beetle as subjects, photos were taken within an Ikea® kitchen closet with flashlights for lighting and Stackshot™ as the focus-adjuster. Afterwards, the results were tested with a number of stacking software including CombineZP, Auto-Montage, Helicon Focus, and Zerene Stacker using the PMax and DMap stacking methods. When comparing the results between the two stacking methods, DMap resulted in halos in areas of fine detail, such as hairs, and blurry images while PMax created detailed and clear images. The study results showed that out of all the high-end focus stacking solutions used, Zerene Stacker (using PMax) in combination with their stacking system gave the best resolution and highest detailed photos.

2.4 Analysis of data

2.4.1 HemoSpat

A study considering the calculations of one-sided bloodstains and the methods to do so was carried out by Maloney *et al.* in 2010 [54]. After creating 64 one-sided, incomplete bloodstains using hockey pucks, 20 were selected to be analyzed using a laser distance finder and right angles. The same 20 stains were then analyzed by a version of HemoSpat specifically for one-sided stains and compared to the previous results. HemoSpat gave both angles and a two-dimensional view at the estimated locations of the pucks, and it was found that the

areas of origin using the laser distance finder were within an acceptable range for that of HemoSpat.

An attempt to calculate areas of origin on non-orthogonal surfaces by Maloney *et al.* in 2009 used HemoSpat to reduce limitations and create precise results [55]. A small tabled surface was set up at an angle in a room where, after impact, 78 stains were chosen to be analyzed and were categorized by location on that table. After being processed through HemoSpat, the two-dimensional images showed estimated origins of impact that were within 1cm of the actual source. As a result, the analyst found it nondestructive to remove objects from scenes to be analyzed in controlled environments using software similar to HemoSpat.

2.5 Regression modeling

A study by Rowe & Hanson in 1985 used regression analysis to model range of fire estimates of various spreads of shotgun pellet patterns [56]. The study used test fires from two different 12-gauge shotguns. Each firearm used a different buckshot cartridge. A number of questioned pellet patterns were fired at ranges between 10 and 50 feet, and test fires were conducted using the same firearms and ammunition. Using the data obtained from the spread of the pellet patterns, regression analysis was applied and regression coefficients were determined. The estimates of the ranges of fire were derived from the regression coefficients. Confidence intervals were then calculated for the estimates, and the ranges of fire were found to be within the 99% confidence interval. An approach using regression functions in R to model the data from this study was performed by Curran, 2011 [12].

In an experiment conducted by Heaney and Rowe in 1982, a series of shotgun pellet patterns were shot at varying ranges using a Remington 12-gauge and chilled No. 2 shot cartridges [57]. Using the linear regression model $y = a+bx$, a and b (the intercept and slope, respectively) were calculated and used to determine the correlation coefficient and standard error for three different sets of ranges. The correlation coefficients calculated ranged from 0.993–0.999, meaning that for the ranges tested at, there existed a strong linear relationship between the range at which the bullets were shot and the $\sqrt{area}$ of the smallest rectangle that would enclose the shotgun pellet pattern. These results were consistent with the already-existing belief that shotgun pellets traveled together for x distance before they actually spread out.

In 1983, a study done by Wray, McNeil, and Rowe looked at the spread of pellet patterns by three methods: the "effective shot dispersion" method, calculating the area of the smallest rectangle that would enclose the pellet pattern, and an overlay method that calculated the radius of the smallest circle that would enclose the pellet pattern [58]. Using a Remington

12-gauge with 00 buckshot cartridges, 72 shot patterns were created at 24 different ranges. To find a relationship between the dispersion of the pattern (S), the radius of the smallest circle (R), and the area of the smallest rectangle (A), regression analysis was applied. The relationship was found to be expressed by $y = a + bx$ where $y = S$, R, or $\sqrt{A}$ and a and b represented the regression coefficients. The result of the study showed that the dispersion method resulted in the best fit to a linear function according to range while giving the smallest confidence interval in terms of range-of-fire estimates.

2.6 Principal component analysis

An experiment conducted by Virkler and Lednev in 2009 used a combination of Raman spectroscopy, significant factor analysis, mean-centering, and principal component analysis to isolate the principal components that could be used to separate three different species [59]. They measured Raman spectra for 24 samples from 16 points at random, and then normalized the spectra into a single matrix. PCA was performed, assuming six principal components, and then cross-validated to verify that number of components. A graph was made by plotting the root-mean-square error of cross validation against the number of principal components. Only the first three PCs proved to be differentiable, and a three-dimensional plot of the species was created based on the information provided by the PCs. A 99% confidence interval was used for each species–it was found that none of the ellipsoids created overlapped one another. Assuming that since there is no overlap in two- and three-dimensional space, there must be no overlap in a six-dimensional space, meaning there is a low likelihood of a false positive identification using this nondestructive method.

An attempt to identify the limitations of chemometric methods on spectroscopic data by Muehlethaler *et al.* in 2011 consisted of using principal component analysis to reinforce data obtained from other variable selection methods [60]. Using paint samples for spectroscopic data, PCA was performed on the FTIR data matrix, which provided four principal components. These PCs corresponded to binder types and the presence/absence of calcium carbonate. 83% of the total variance was explained by the four first PCs.

However, from using the Raman data matrix, six PCs were identified. These corresponded to the different pigment compositions when plotting the first two PCs, which accounted for 37% and 20%, respectively, of the total variance. They determined that when separating at a more specific, higher level, PCA works efficiently while at a general, lower level of separation, Raman spectra are more likely to experience reproducibility problems. If both methods of variable selection (hierarchical cluster analysis (HCA) principal component analysis) are used combined, it was found that all samples could be individually separated as long as the

samples could be separated into different groups. They concluded that chemometrics is a valuable tool for objective decision-making, a reduction of the possible classification errors, and a better efficiency, having robust results with time saving data [60].

2.7 Box-Cox transformation

A study by Osborne in 2010 assessed Box-Cox transformations as a primary means to enhance data analysis [61]. The idea was that the use of power transformations improves the effectiveness of normalizing for all variables. Osborne applied Box-Cox transformations on data of Prussian cavalrymen deaths via horses, U.S. universities and faculty salary, and student test grades, all of which were non-normal data. Following the implementation of the transformation, the effect sizes of a correlation in all three cases increased over 80%.

3. Methods

3.1 Glass targets and bullets

All samples of glass were obtained from a closed glass factory and are part of the same sheet of glass produced. The samples were cleaned and labeled with a unique identifier. The width and length of the samples were measured with the same tape measure. The thickness on all four sides of each glass sample was measured using the same caliper.

Table 3.1 and Table 3.2 lists a subset of the samples used for the full metal jacket bullet and lead round nose bullet analysis. The unique identifier, which represents each glass sample, also represents the bullet that was fired through that specific piece of glass. Each bullet was fired from a distance of approximately 80 inches from the glass using a Ruger® SR9® 9mm pistol. The bullets perforated the glass samples at angles of 45°, 50°, 60°, 75°, and 90°.

Table 3.1: Subset of samples used for all full metal jacket bullets

Sample Name	Angle (°)	Average Thickness of all 4 sides (inches)	Standard Deviation of Thickness (inches)	Length (inches)	Width (inches)
5A	90	0.1873	0.00050	8.625	4.500
1D	75	0.1888	0.00050	9.125	4.375
1A	60	0.1885	0.00058	9.000	4.375
1L	50	0.1853	0.00050	9.500	5.000
1Q	45	0.1870	0.00082	10.500	4.875

Table 3.2: Subset of samples used for all lead round nose bullets

Sample Name	Angle (°)	Average Thickness of all 4 sides (inches)	Standard Deviation of Thickness (inches)	Length (inches)	Width (inches)
5I	90	0.1920	0.00000	7.875	4.000
3W	75	0.1888	0.00050	10.500	4.125
3R	60	0.1880	0.00000	10.625	4.000
3U	50	0.1893	0.00050	10.500	4.375
1U	45	0.1883	0.00050	10.500	5.000

Ten full metal jacket bullets and ten lead round nose bullets were used for this study at each angle. The sample set consisted of a total of 100 samples (50 full metal jacket and 50 lead round nose).

Winchester® 115 grain full metal jacket 9mm Luger ammunition was used for the full metal jacket bullet analysis. Reloaded 9mm lead round nose ammunition was used for the lead round nose bullet analysis. The reloaded ammunition consisted of 115 grain Missouri Bullet Company lead, 4.1 grains of Hodgdon® Titegroup powder, and Sellier & Bellot® 4,4 small pistol boxer primers.

3.2 Firing system

Three devices were designed to form a system for the testing and collection of bullets. The firearm mount device, as seen in Figure 3.1, was used to stabilize the firearm while each shot was fired. There was a Ransom Masters Series Vise mounted into the center of the device to place the firearm into before being fired. Three cinder blocks were used to weigh down the device to restrict movement during firing. The device was designed to allow for vertical adjustment of the firearm.

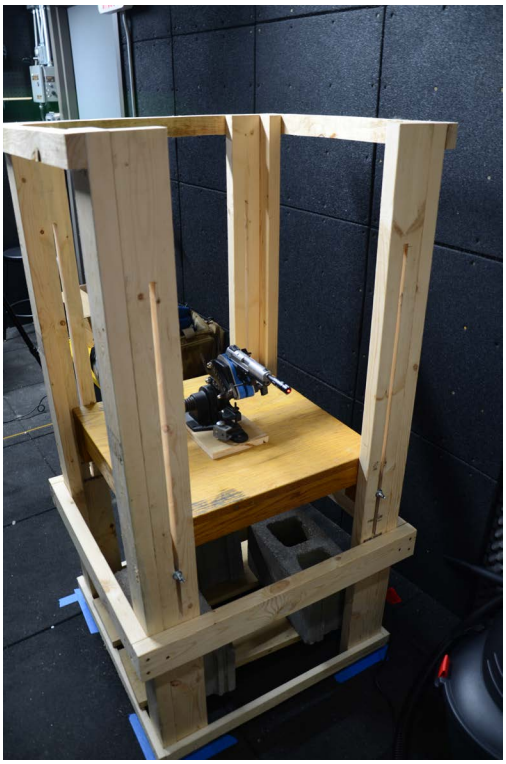

Figure 3.1: Firearm mount device

The glass frame and angle adjustment device, as seen in Figure 3.2, was used to frame the glass samples prior to firing. A swivel from a chair was mounted in the center of the main table in order to adjust the angle at which the bullet would perforate the glass. The frame itself was placed onto the top of the swivel. The bottom and sides of the frame consisted of two pieces of wood with a V-shape groove to ensure that the glass samples would fit tightly into the frame. For the top part of the frame, two pieces of wood with tightening screws for the glass sample were placed on each side of the frame and locked down using clamps. Angles from 45° to 90° in increments of 5° were measured out and labeled on the main table. This allowed for the centering of the frame and alignment of the desired angle.

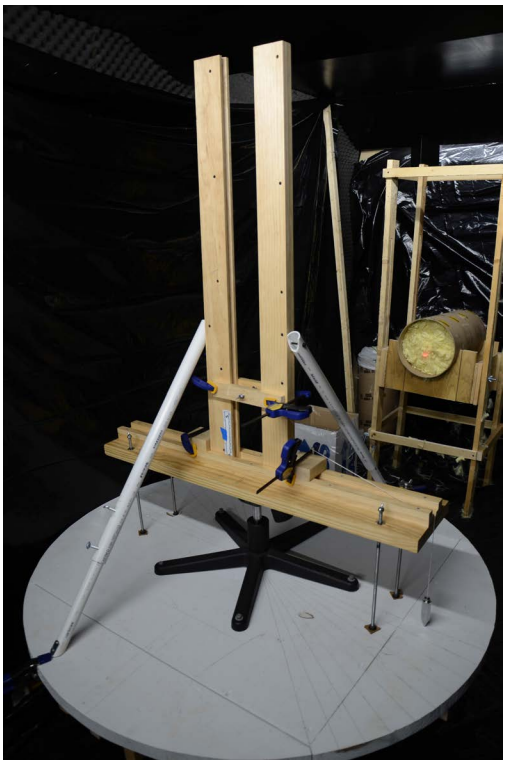

Figure 3.2: Glass frame and angle adjustment device

The Kevlar® bullet trap holder device, as seen in Figure 3.3 on the following page, served as the bullet trap holder. It consisted of a wood piece that was cut and designed to fit the cylindrical bullet trap that was used to catch the bullets. This piece could be moved vertically to align the trap with the bullet's path. The bullet trap itself contained Kevlar® fibers.

Figure 3.3: Kevlar® bullet trap holder device

3.3 Firing process and collection

The following steps were repeated for each sample at an indoor firing facility:

1. The firearm was placed into a vice and tightened down. The firearm was checked to ensure it was level in the vice (Figure 3.4 on the next page). The wood surface, which the vice was mounted on, was checked to ensure it was level on all four sides with a larger level.

Figure 3.4: Process to ensure firearm is level in the vice

2. A plumb bob was attached to the frame and allowed to hang down over the side of the frame until it contacted the main table at the desired angle (Figure 3.5). The swivel was then secured down to the main table using four tightening screws. The frame was checked to ensure it was leveled. A glass sample was then inserted into the frame and secured on all four sides.

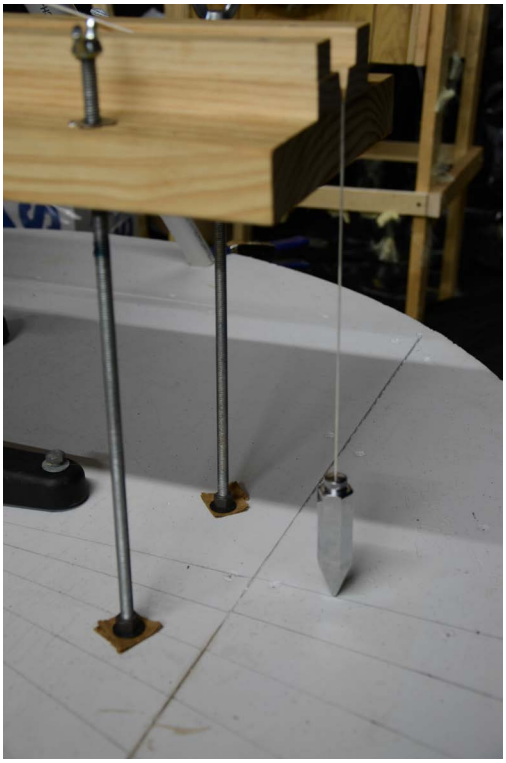

Figure 3.5: Plumb bob measuring the proper angle

3. A laser was inserted into the barrel of the firearm, and the path of travel of the bullet was aligned with the center of the glass sample and also with the center of the bullet trap (Figure 3.6).

Figure 3.6: Laser inserted into barrel to view the path of the bullet

4. The firearm was pulled up in the vice so the magazine could be ejected. A single cartridge was inserted into the magazine. The magazine was then inserted into the

firearm, and the firearm was pressed back down into place. The firearm was cocked, and the muzzle was pressed down to ensure it was leveled. The handle was pulled backward, pulling the trigger and thus discharging the round into the glass sample. The magazine was then immediately removed from the firearm.

5. As shown in Figure 3.7, a scale was placed in front of the glass sample. Two photographs were taken of the bullet hole in the glass. The first photograph was taken by looking at the glass from the angle at which the bullet perforated it. The second was taken perpendicular to the hole. One photograph was taken for samples at 90°.

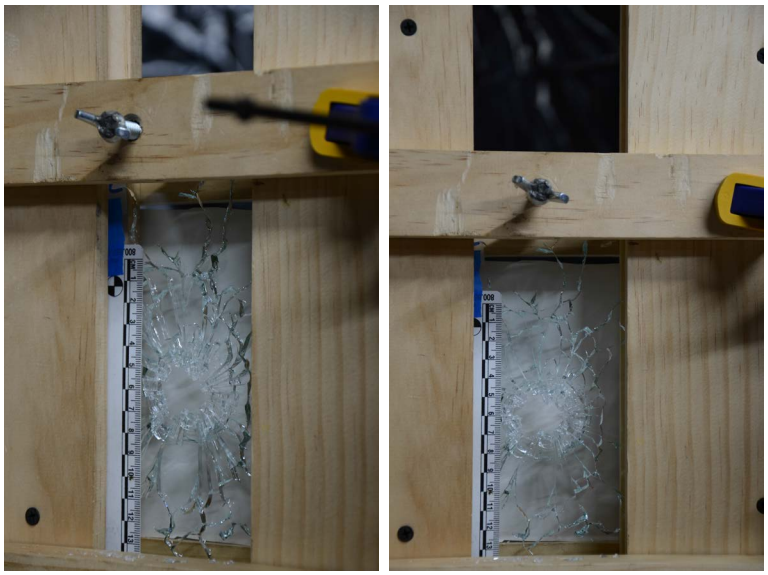

Figure 3.7: A 60° angle photograph (left) and perpendicular photograph (right)

6. A small glass sample was retrieved and placed into an envelope and labeled. The rest of the glass was discarded.

7. The bullet was retrieved from the bullet trap and placed into a small envelope and labeled.

8. The area was cleaned of glass, and the bullet trap was reset for the next sample.

9. Steps 1-8 were repeated for each sample for both the full metal jacket and lead round nose bullet analysis.

3.4 Using HemoSpat to determine the angle of impact

HemoSpat is a software designed specifically for bloodstain pattern analysis and recognition in order to easily determine areas of impact [62]. By applying the same concept of traditional methods like stringing, HemoSpat is able to effectively perform directional analysis of bloodstains in much less time than traditional methods. This software utilizes a combination of physical stringing, mathematical formulae, and bloodstain pattern analysis software to accurately calculate the area of origins of bloodstain patterns [62]. It offers the ability to invert colors to allow a greater contrast from the background for hard-to-see bloodstains, analyze non-orthogonal surfaces by allowing the addition of any flat surface to a scene for analysis relative to that surface, and automatic bloodstain ellipse detection to make quicker and easier analysis [63]. As stain data is edited and changed, the area of origin calculations are also automatically updated in real time [63]. HemoSpat takes away the time-consumption traditional methods applied at crime scenes and condenses it into a simpler program.

The interface for HemoSpat during the processing of a glass sample can be seen in Figure 3.8. The following steps were repeated for each sample of the full metal jacket and lead round nose bullet analysis within the HemoSpat program:

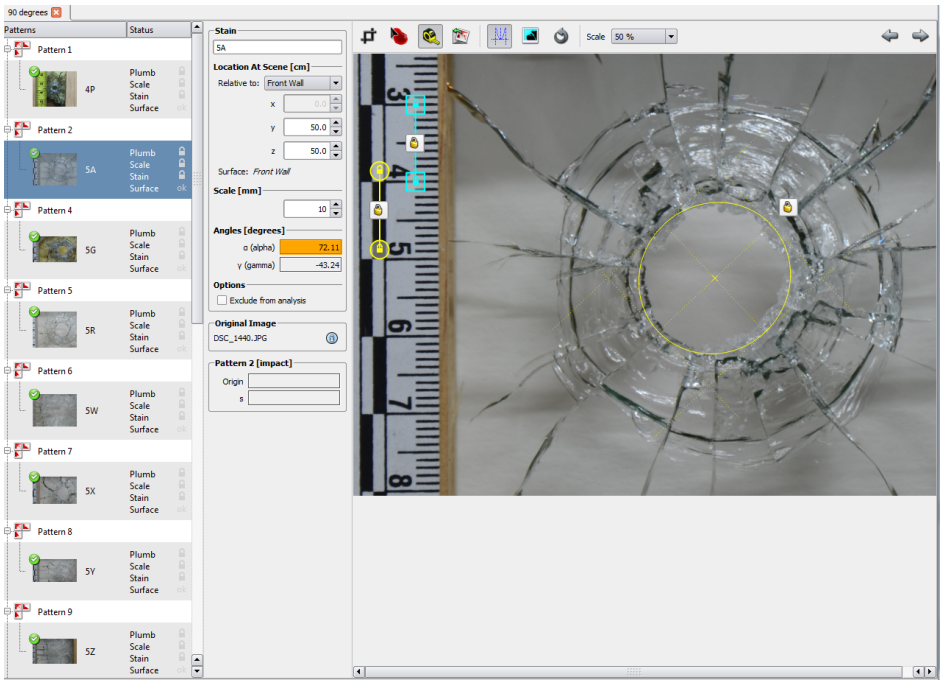

Figure 3.8: Interface of HemoSpat while measuring angle of impact

1. The perpendicular photograph taken at the indoor facility of the bullet hole in the glass was loaded into the HemoSpat program.

2. The photograph was cropped to include the bullet hole and scale only.

3. The bullet hole was selected using the `Select Stain` tool.

4. The scale was set to 10mm using the `Set Scale` tool.

5. The vertical direction was selected using the `Select Plumb Line` tool.

6. The location of the hole was chosen to be the front wall. The x and z coordinates were both set to 50 cm.

7. The four sides of the yellow selection area were adjusted in three different ways to select the bullet hole. The tail of the yellow selection area was moved in the direction where the bullet hole was elongated the most.

   First, they were adjusted to include the largest possible ellipse that could be made while selecting areas that contained no glass (Figure 3.9).

   Secondly, they were adjusted to include the smallest possible ellipse that could be made while selecting areas that contained no glass. The yellow selection area touched the innermost glass piece on all four sides (Figure 3.10 on the next page).

   Finally, the sides were adjusted to include the best fitting ellipse (Figure 3.11 on the following page). This took into account areas with and without glass present.

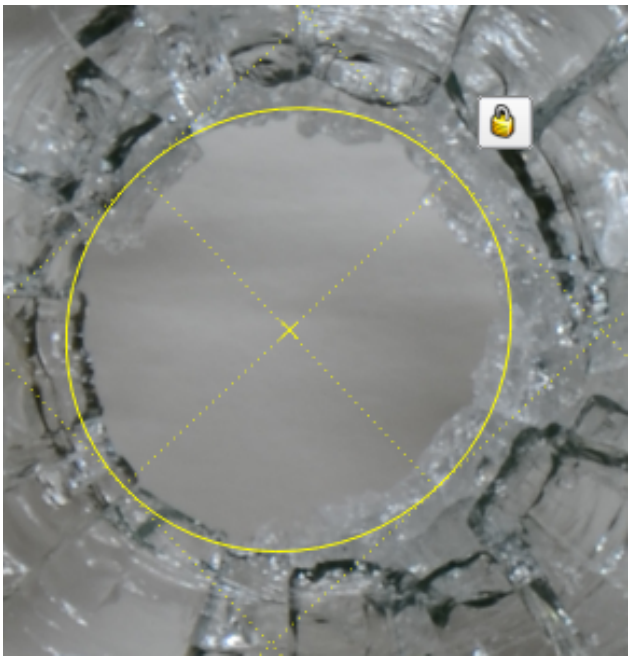

Figure 3.9: Measuring angle of impact by selecting the largest possible ellipse while including all areas that do not contain glass

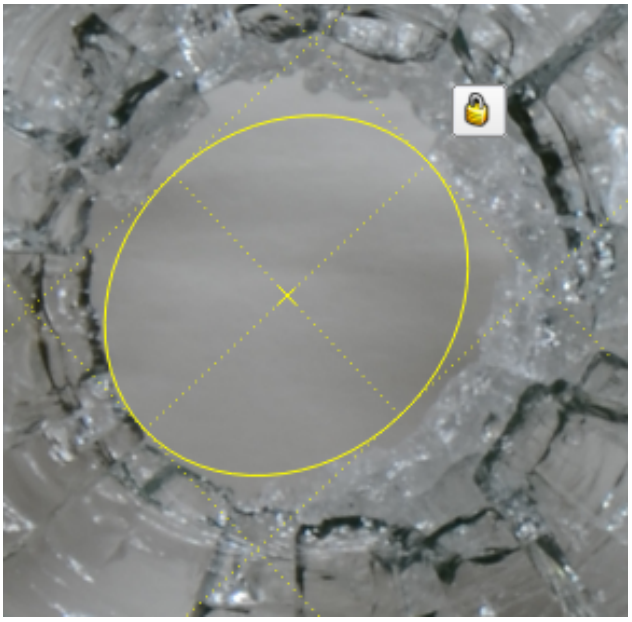

Figure 3.10: Measuring angle of impact by selecting the smallest possible ellipse while including all areas that do not contain glass

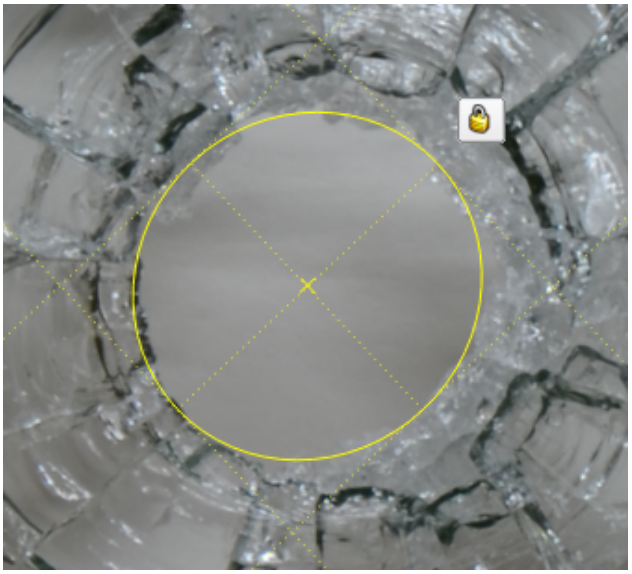

Figure 3.11: Measuring angle of impact by selecting the best fitting ellipse

8. The measured alpha angle, or angle of impact, was recorded for each of the three methods.

The data retrieved from HemoSpat was used to develop linear models using R. Four linear models were created for the full metal jacket data and four for the lead round nose data.The four models include an overall model, inner model, middle model, and outside model. Plots showing the linear models and their 95% confidence and prediction intervals were created.

In addition, a pred-res plot (residuals versus fitted values), normal Q-Q plot, histogram, and 95% confidence and prediction intervals only plot were created for each model.

A regression table for each model was created, which included the estimated coefficients, standard errors of the estimates, t-values, p-values, and the multiple R^2 and adjusted R^2 values.

3.5 Refractive index analysis of glass deposited on bullets

Glass from three bullets were tested on the GRIM3® to determine if the refractive index could be measured following the perforation of the bullets.

A new case was created on the GRIM3® system. To calibrate the GRIM3®, a small piece of a B6 standard glass fragment was placed onto a glass slide. Two drops of silicon B6 immersion oil was placed onto the fragment. Forceps were used to push down on the fragments to break it into smaller pieces for better observation under the microscope. Another drop of oil was placed onto the slide, and a circular glass cover slip was placed over the oil and fragments. The slide was placed into the GRIM3®. The lighting and focus were both adjusted. Four glass fragments were selected for analysis. The resulting refractive index measurements for the standard fragments selected fell into the acceptable range.

For analysis, glass, which was deposited on a bullet during impact, was scraped onto a clean microscope slide. Two drops of silicon B6 immersion oil were placed on the slide at the location of the glass fragments. A circular glass cover slip was placed over the oil and fragments, and the slide was then placed into the GRIM3®. The lighting and focus were adjusted.

After careful observation under the microscope, the fragments retrieved from the bullets were determined to be too fine for selection using the GRIM3®.

3.6 Scanning electron microscopy with energy dispersive X-ray analysis on FMJ and LRN bullets

A section of a full metal jacket (sample 8G) and lead round nose (sample 8X) bullet was observed in BEC (backscattered electron composition image) mode on a Joel JSM-6490 LV scanning electron microscope under x50 magnification with an accelerating voltage of 20kV and pressure of 27Pa.

Energy dispersive X-ray analysis was performed on the samples using an Oxford Instruments INCAx-sight Model 7623. X-ray maps were created of calcium (glass), silicon (glass), copper (jacket), and lead (bullet) for sample 8G and of calcium, silicon, and lead for sample 8X.

Table 3.3 displays the conditions for the full metal jacket sample.

Table 3.3: Conditions for the x-ray map of sample 8G

Type	Label	Auto width	Low (keV)	High (keV)	Width (keV)
Line	Si Ka1	Yes	1.651	1.829	0.177
Line	Ca Ka1	Yes	3.594	3.79	0.196
Line	Pb Ma1	Yes	2.254	2.437	0.183
Line	Cu Ka1	Yes	7.932	8.164	0.231

Table 3.4 displays the conditions for the lead round nose sample.

Table 3.4: Conditions for the x-ray map of sample 8X

Type	Label	Auto width	Low (keV)	High (keV)	Width (keV)
Line	Si Ka1	Yes	1.651	1.829	0.178
Line	Ca Ka1	Yes	3.594	3.79	0.196
Line	Pb Ma1	Yes	2.254	2.437	0.184

3.7 Using ImageJ to measure side view bullet deformation

The following steps were repeated for each sample of the full metal jacket and lead round nose bullet analysis:

1. As seen in Figure 3.13, each bullet was placed onto a rotating mount and rotated until the steepest slope of the non-glass side of the deformed bullet was aligned to the right. As seen in Figure 3.13, for some 90° bullets, no noticeable slope was observed no matter the rotation. The setup can be seen in Figure 3.12. For bullets that perforated the glass at angles of 45°, 50°, 60°, and 75°, a majority of the glass was located on the left side of the bullet once aligned. For 90°, the glass was located throughout the surface of the bullet once aligned.

Figure 3.12: Bullet deformation setup

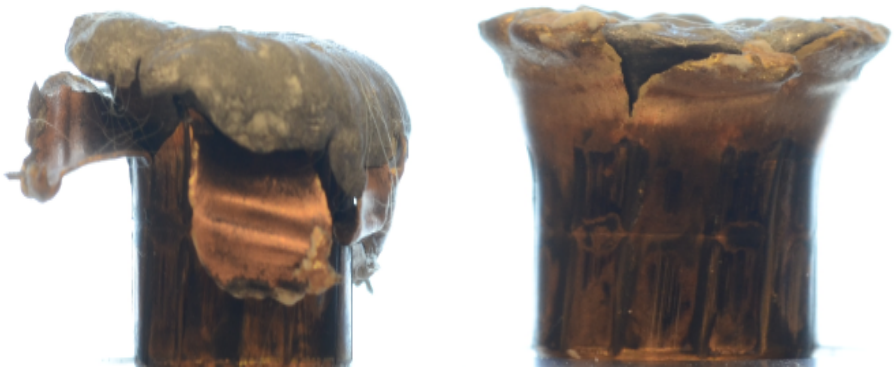

Figure 3.13: Noticeable slope present on a 90° bullet (left), no noticeable slope present on a 90° bullet (right)

2. A photograph was taken using a Nikon® D7000 with a 60mm macro lens. An example photograph can be seen in Figure 3.14. The settings used were an ISO of 100, shutter speed of one fifth of a second, and f/stop of 16.

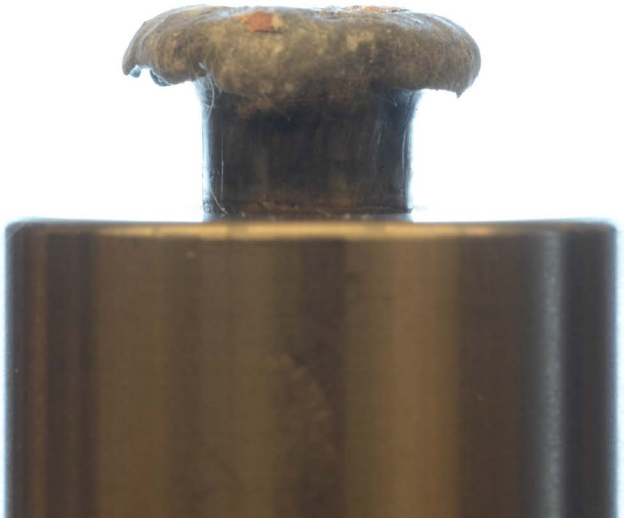

Figure 3.14: Example of a photographed bullet

3. The photograph was loaded into ImageJ. Using the `multi-point selection` tool, three different methods were used to measure the deformed bullet. If a bullet did not have a noticeable angle (distinct rise and fall before the left vertical tangent of the bearing surface) on the nose of the bullet, the following methods were used:

   The first method, called AA, is shown in Figure 3.15 and incorporated placing points from the steepest right vertical tangent to the steepest left vertical tangent. Five, ten, and fifteen points were marked between these locations.The points were spaced approximately an equal distance apart.

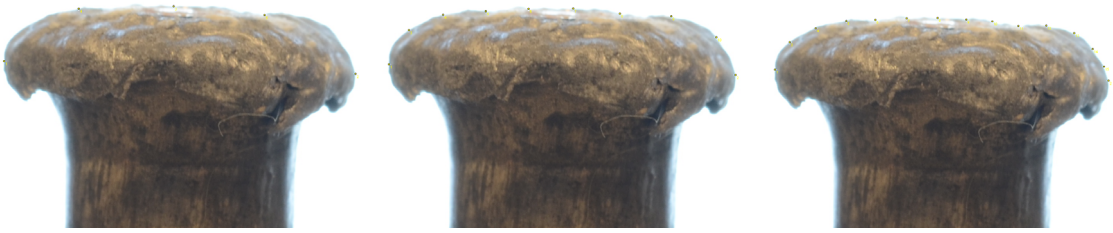

Figure 3.15: Measuring 5 (left), 10 (middle), and 15 (right) points on a 90° bullet using method AA.

The second method, called VV, incorporated placing points from above the right vertical of the bearing surface to above the left vertical of the bearing surface. Five, ten, and fifteen points were marked between these locations. The points were spaced approximately an equal distance apart. Method VV is demonstrated in Figure 3.16.

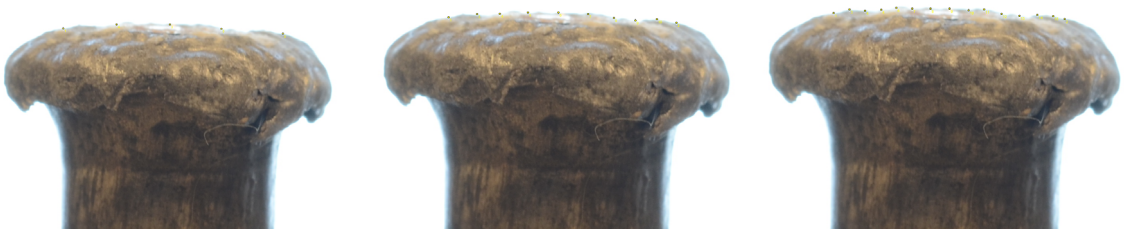

Figure 3.16: Measuring 5 (left), 10 (middle), and 15 (right) points on a 90° bullet using method VV.

The third method, called HH, is shown in Figure 3.17. This method incorporated placing points from half way between the right vertical tangent and above the right vertical of the bearing surface to half way between the left vertical tangent and above the left vertical of the bearing surface. Five, ten, and fifteen points were marked between these locations. The points were spaced approximately an equal distance apart.

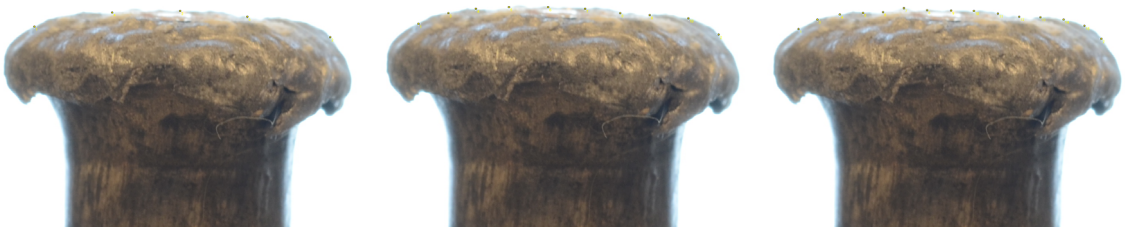

Figure 3.17: Measuring 5 (left), 10 (middle), and 15 (right) points on a 90° bullet using method HH.

4. If there was a noticeable angle (distinct rise and fall before the left vertical tangent of the bearing surface), the following methods were used:

   Method AA, shown in Figure 3.15 on the preceding page, incorporated placing points from the highest peak on the nose of the bullet to the steepest left vertical tangent. Five, ten, and fifteen points were marked between these locations.The points were spaced approximately an equal distance apart.

Figure 3.18: Measuring 5 (left), 10 (middle), and 15 (right) points on a 60° bullet using method AA.

Method VV, shown in Figure 3.19, incorporated placing points from the highest peak of the bullet's nose to above the left vertical of the bearing surface. Five, ten, and fifteen points were marked between these locations. The points were spaced approximately an equal distance apart.

Figure 3.19: Measuring 5 (left), 10 (middle), and 15 (right) points on a 60° bullet using method VV.

Method HH, shown in Figure 3.20 on the following page, incorporated placing points from the highest peak of the bullet's nose to half way between the steepest left vertical tangent and above the left vertical of the bearing surface. Five, ten, and fifteen points were marked between these locations. The points were spaced approximately an equal distance apart.

Figure 3.20: Measuring 5 (left), 10 (middle), and 15 (right) points on a 60° bullet using method HH.

5. The X and Y coordinates for the points selected for each method were retrieved from ImageJ by first selecting `Analyze`, then `Set Measurements`, and then choosing the `Center of Mass` in the `Set Measurements` window. Secondly, `Analyze` then `Measure` was selected, which displayed the coordinates in a table that could be saved.

The following steps were completed in R for each method used:

1. A new variable `yprime` was created which included the subtracted y-coordinate of each point from 2,500. This allowed for a consistent y-axis to be created.

2. A linear model was created for the new yprime values as a function of the corresponding X coordinates.

3. The theoretical degree value was calculated by taking the arc tangent of the gradient (or slope) of the regression line from the linear model created in Step 2 and converting it from radians to degrees.

4. The theoretical degree value was subtracted (or added as appropriate) from 90° to obtain the measured degrees.

The data retrieved from ImageJ was used to develop linear models using R. Seven linear models were created for the full metal jacket data and seven for the lead round nose data. The seven models include an overall model and models for methods AA, VV, HH, 5 points, 10 points, and 15 points. Plots showing the linear models and their 95% confidence and prediction intervals were created.

In addition, a pred-res plot (residuals versus fitted values), normal Q-Q plot, histogram, and 95% confidence and prediction intervals only plot were created for each model.

A regression table for each model was created, which included the estimated coefficients, standard errors of the estimates, t-values, p-values, and the multiple R^2 and adjusted R^2 values.

3.8 Using focus stacking and ImageJ to measure frontal view bullet deformation and distribution of glass onto bullets

3.8.1 Image capture

Stackshot™

With the purpose of making image collection easier, Stackshot™ consists of a macro rail system that allows the electronic control of positioning and triggering of an attached camera [64]. It was designed to make the general focus stacking procedure more effective and less time consuming by providing an automated approach to maco rails, which would traditionally be adjusted manually between photo runs. With Stackshot™, exposure settings can be easily replicated between photo series runs while also giving access to shot timing, the amount of photos taken, the speed at which they are taken, ramp time, and more. It consists of a length of up to 100 mm, which can be controlled by two buttons, and an auto-return option that returns the camera to the position it originally started in for easier, consistent setup [64].

Nikon® Camera Control Pro 2™

Nikon® Camera Control Pro 2™ is software that allows remote control access to most functions offered by Nikon® DSLRs via cable connection or wireless LAN [65]. Settings including exposure mode, shutter speed, aperture, and preview and selection become modifiable from a computer while also allowing images to be directly transferred from camera to computer. Camera Control Pro 2™ also includes adjustment of focal points and gives previews of images in real time as they are taken [65]. In addition, a number of other Nikon® software are integrable such as ViewNX browser or Capture NX photo-finishing.

Zerene Stacker

Intended for macro photography subjects, Zerene Stacker utilizes focus stacking, or z-stacking, software to create the sharpest photos possible [66]. This is accomplished by taking a series

of photos of the subject in varying focused depth planes and then stacking all of the photos into one. With a no-limit on load depth, Zerene Stacker uses stacking algorithms to isolate the sharpest portions of each photo and automatically aligns and interpolates those portions into an image as sharp as possible [66].

The two main stacking methods are PMax, a pyramid method, and DMap, a depth map method [67]. Although it is best to process the image frames from one side of the object to the other, PMax works well to align no matter the order or how many photos are stacked while DMap results in degraded images with a large number of photos. PMax also focuses on locating and preserving detail, even in blurred or low contrast areas, and processes overlapping objects as small as hairs or fibers true to form [67]. However, as a tradeoff, this method tends to create higher contrast in images as well as an increase in noise and color alteration. DMap oppositely keeps the original smoothness and colors of the image while not being able to enhance details quite as well [67].

Zerene Stacker enables high-quality images of bullets to be created following perforation with glass. The software takes multiple photographs, which are taken at different focal distances and combines these photographs together to create one high-quality image. The resulting image allows the examiner to observe the distribution of glass on the bullet and other characteristics, including striation marks.

To analyze these high-quality photographs for data, an examiner can take advantage of different image processing and analysis programs that allow the examiner to conduct analyses on different aspects of a glass and bullet interaction.

3.8.2 Analysis process

A Nikon® D7200 with an AF Micro Nikkor 200mm lens was used to take all photographs. The settings used were ISO 100, shutter speed of seven tenths of a second, and an f/stop of 16. The Cognisys Stackshot 3X™ system was used to move the camera toward and away from the bullet on a rail system and to simultaneously stack photographs while they were being taken. ZereneStacker was used to focus stack the photographs. Nikon® Camera Control Pro 2™ software was used in conjunction with the ZereneStacker to store the photographs in a specified folder for stacking.

The focus stacking setup can be seen in Figure 3.21 on the next page.

Figure 3.21: Focus stacking setup with Stackshot 3X^{TM}

The following steps were repeated for the image capture of each sample of the full metal jacket and lead round nose bullet analysis:

1. A small piece of putty was placed around the base of the bullet. The bullet was then secured in the center of a square white platform by placing the bullet in a designated hole. If distinctive striations were present, such as with a 50° as shown in Figure 3.22 on the following page, the bullets were oriented with the striations pointing to the right (striations flow to the right center edge). If there were no distinctive striations present, such as with a 90° bullet as shown in Figure 3.22, the bullet was not oriented in any specific way.

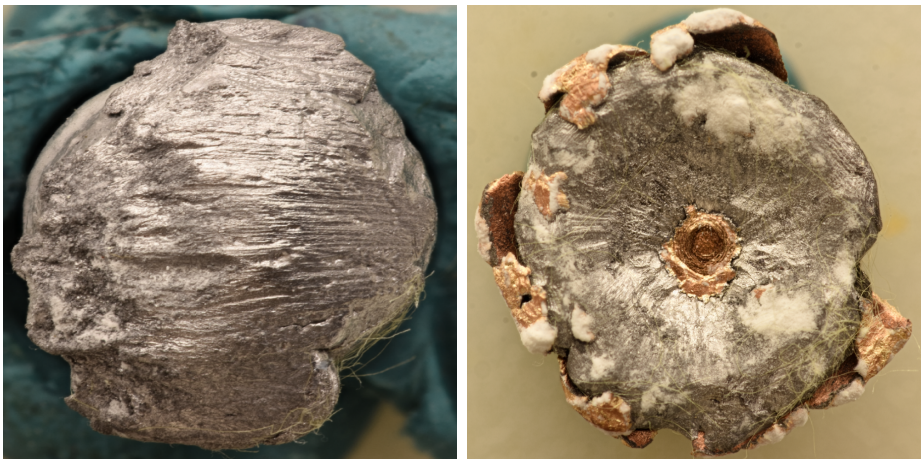

Figure 3.22: Distinctive striations present on a 50° bullet (left), no distincitve striations present on a 90° bullet (right)

2. On the Stackshot™ system, the step size was set to 10 micrometers. This refers to the distance the camera moves toward the bullet after every photograph.

3. Looking through the viewfinder of the camera, start and stop points were chosen. The start point refers to the location of the camera where the very center of the bullet is in focus. The stop point refers to the location of the camera where the very outside edge of the bullet is in focus.

4. Zerene Stacker and Camera Control Pro 2™ software was loaded and setup for stacking.

5. The focus stacking process was completed which included taking all photographs, stacking those photographs together, and saving them. The PMax algorithm was used for all stacking. On average, the system captured between 300 and 650 photographs.

The following steps were repeated for the image analysis of each sample of the full metal jacket and lead round nose bullet analysis:

1. The photograph was opened in ImageJ. Each photograph was 6000x4000 pixels.

2. Using the `freehand selection` tool, the bullet outline was selected. This is shown in Figure 3.23 on the next page. If the jacket was not separated on an FMJ bullet, this included the areas containing copper that were still pressed against the lead core.

Figure 3.23: Selection of the bullet outline using the ***freehand selection*** *tool*

3. Specific data was chosen by selecting `Analyze` then `Set Measurements`. The following were chosen: `Area`, `Center of Mass`, `Shape descriptors`, `Perimeter`, and `Fit ellipse`. The data were retrieved and saved by selecting `Analyze` and then `Measure`.

4. Continuing with the same image, the area selected was made white by selecting the `Fill` option in the `Edit` menu.

5. The image was made an 8-bit greyscale by going to `Image`, `Type`, then `8-bit`.

6. The threshold was adjusted so that only the area selected remained after the threshold was applied. This was done by going to `Image`, `Adjust`, then `Threshold`.

7. The best fitting ellipse was generated by going to `Analyze` then `Analyze Particles`, and in the `Analyze Particles` window under `Show`, `Ellipses` was selected.

8. The threshold and fitted ellipse images were combined into one image by going to `Process` then `Image Calculator`. An example can be seen in Figure 3.24 on the following page. In the `Image Calculator` window, the threshold image was chosen in the `Image1` drop down menu, and the fitted ellipse was chosen in the `Image2` drop down menu. Under the `Operation` drop down menu, `Average` was selected.

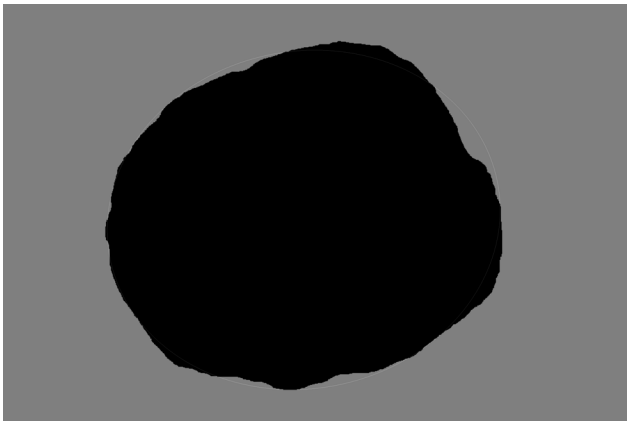

Figure 3.24: Threshold and fitted ellipse images combined

9. Using the same original image and the `straight line` tool, a vertical line was drawn at the location on the bullet where the last distinctive white patch of glass was observed (moving from left to right). The line was drawn on the rightmost edge of the patch.

10. The X coordinate for this line was retrieved by going to `Analyze` then `Measure`. A variable called X_Patch was created by subtracting the X coordinate of the line with the X coordinate for the center of mass of the bullet obtained in Step 7.

11. Using the `freehand selections` tool, the area where glass was distributed on the bullet was selected. Areas that were obvious and distinct were chosen. This is shown in Figure 3.25.

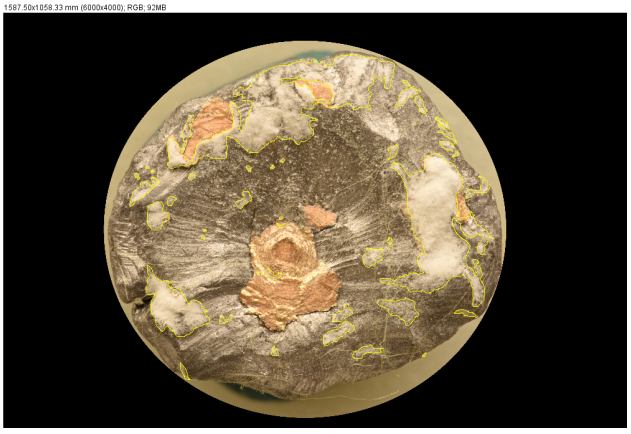

Figure 3.25: Selecting glass that was transferred to the bullet using the ***`Freehand Selection`*** *tool*

12. The areas selected were then made white by selecting the `Fill` option in the `Edit` menu.

13. The image was made an 8-bit greyscale by going to `Image`, `Type`, then `8-bit`. This can be seen in Figure 3.26.

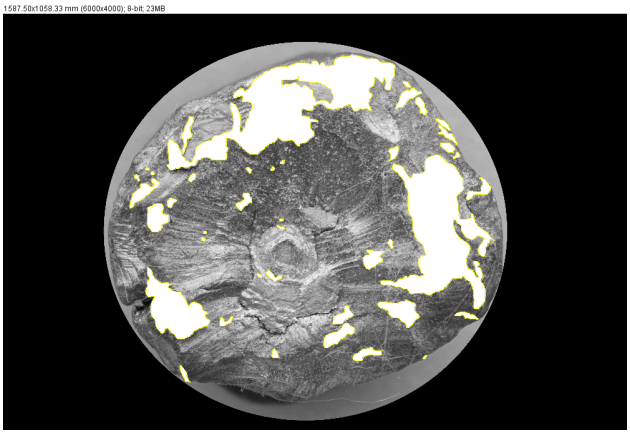

Figure 3.26: Image as an 8-bit greyscale with areas selected filled in white

14. The threshold was adjusted so that only the areas selected remained after the threshold was applied. This was done by going to `Image`, `Adjust`, then `Threshold`. This can be seen in Figure 3.27.

Figure 3.27: Areas that were selected after using the ***`threshold`*** *option*

15. `Area` was selected in ImageJ by going to `Analyze` then `Set Measurements`. The area data was retrieved and recorded by selecting `Analyze` then `Analyze Particles`. The analyze particles window can be seen in Figure 3.28 on the following page.

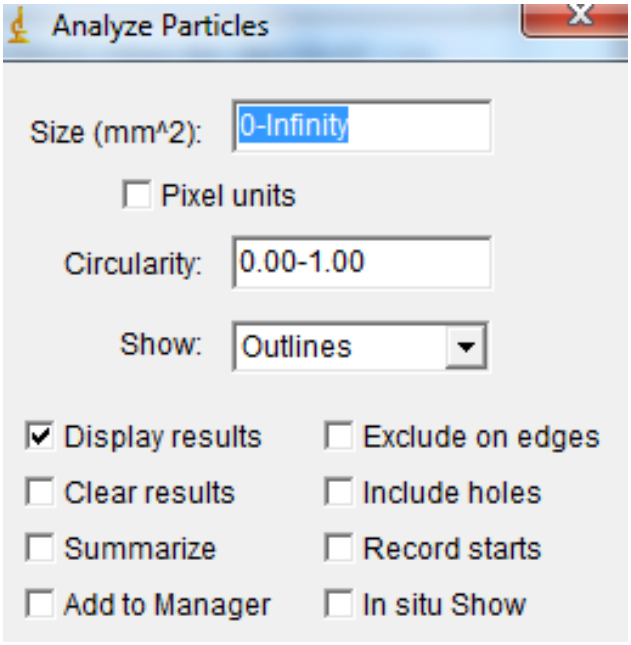

Figure 3.28: ***Analyze Particles*** *window*

16. Using all of the data recorded, the following was calculated: total particle area, area of the largest particle, total area of the five largest particles, total area of the ten largest particles, and total number of particles selected. All of the data was combined into one spreadsheet.

17. Using R, principal component analysis was performed on the full metal jacket and lead round nose bullet data. Combinations of the above variables were used to test which group of variables would perform the best. `Area`, `X_Patch`, `Circ.`, `Area Largest Particle`, `Minor`, and `AR` were determined to provide the best results and were therefore used in the final analysis for both the FMJ and LRN data.

    Summary tables showing the standard deviations of the PCs and rotations (or loadings) were created along with tables displaying the proportion of variance and cumulative proportion. Scree plots were created to show the proportion of variance of each PC. Biplots were created to show resulting PCs and the corresponding vectors of each variable. The normal contour line for each group has a probability of 95% confidence.

    A testing set was created for both the FMJ and LRN principal component analysis to gain an understanding of the variability in the data for each angle. The new values were based on the distributions of the original data means and the covariances between these parameters. New random data consisting of 20,000 test samples for each true angle

was created. The `MASS` package was used to calculate correlated/unvarying random numbers using this information. Principal component analysis was performed on the new data, and a table of new projected PC values for each angle were created using the `predict` function. Plots of the original data (10 samples) and 95% confidence bounds for the projected PCs of each angle were created.

The `devtools`, `ggbiplot`, `caret`, and `scatterplot3d` packages were also used.

18. Using R, an attempt was made to create a multiple linear regression model, which showed a significant linear relationship between the above variables and the true angle. If the resulting regression table for the model showed that a variable had little or no significance, that variable was removed from the model. A multiple linear regression model for the full metal jacket data was created for $X\_Patch \times Minor$ as a function of the $TrueAngle$. The lead round nose bullet data showed little or no significance for all variables, and, therefore, no regression analysis was performed.

    For the full metal jacket data, plots of the linear models for X_Patch and Minor were created. A pred-res plot (residuals versus fitted values), normal Q-Q plot, and histogram were created for the model. A regression table for the model was created, which included the estimated coefficients, standard errors of the estimates, t-values, p-values, and the multiple R^2 and adjusted R^2 values. An XY scatter plot of X_Patch and Minor was created along with a 3D scatterplot of X_Patch, Minor, and True Angle. Contour plots were created for the lower, fitted, and upper prediction values for the model.

    Testing and training were performed using the full metal jacket model prediction values. 1000 iterations of the testing and training were performed. During each iteration, 20% of the data was used for testing while the other 80% was used for training. An XY jitter plot was created to show the results.

    The `lattice`, `fields`, `graphics`, and `scatterplot3d` packages were used.

4. Results and Discussion

4.1 Bullet information obtained from laboratories

Information concerning the submission of bullet evidence to forensic laboratories was obtained. The submitted questions are based on the type of bullets being used in this study and were asked to assess the usefulness of bullets submitted to laboratories and the prevalence of specific bullets in crime scenes. Two firearms examiners, one from the Kentucky State Police Eastern Branch Crime Laboratory (KSP) [25] and one from the West Virginia State Police Crime Laboratory (WVSP) [68], were contacted.

Table 4.1 displays the four questions asked to each agency and their responses.

Table 4.1: Bullet information from laboratories

Question Asked	KSP	WVSP
1. What percentage of 9mm Luger FMJ bullets submitted to the laboratory are in good condition for further analysis?	>75%	>75%
2. What percentage of handgun bullets submitted are FMJ and LRN?	25% FMJ	35% FMJ and 25% LRN
3. What percentage of bullets submitted are 9mm Luger?	25%	20%
4. What percentage of 9mm Luger bullets submitted are 115 grain?	50%	50%

4.2 Bullet observations

4.2.1 FMJ bullets

Bullets fired at 90°

As shown in Figure 4.1 on the following page, all bullets fired at 90° contained part of the jacket in the center of the deformed nose.

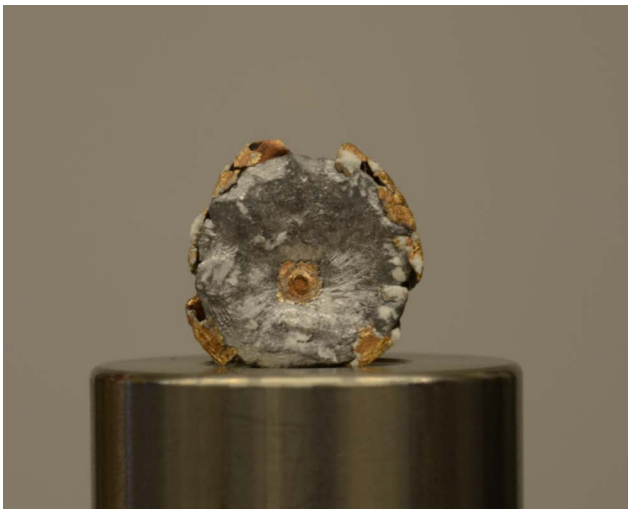

Figure 4.1: Part of jacket in center of bullet nose. The bullet perforated the glass at 90°.

With the retrieval of the 90° samples, the jackets of samples 6C, 6G, 8A, 8D, and 8K did not separate from their bullets. Samples 5A, 8G, 8J, and 8L had jackets that separated but were located immediately behind their bullets, while only sample 8I had a jacket that separated towards the front of the fiber trap.

Two of the jackets completely folded inside out as shown in Figure 4.2. This only happened at 90°.

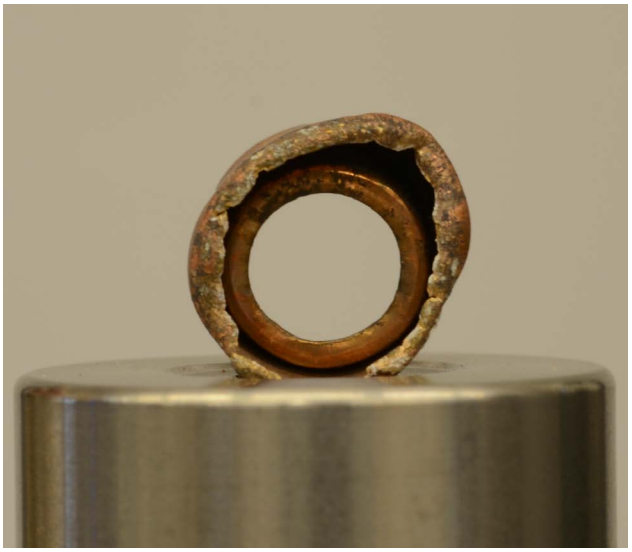

Figure 4.2: Jacket of a 90° bullet folded inside-out

Bullets fired at 75°

For the 75° samples, the jacket was found separated and towards the front of the fiber trap for samples 1D, 1F, 1G, 1J, 1K, 4L, and 4M. The jacket also separated for sample 1E, but it was located on the floor, underneath the trap. Samples 8F and 1H had jackets that were still intact with the bullet.

Bullets fired at 60°

The jackets of samples 4I, 4J, 5C, 5E, 1M, and 1A were found separated from their bullets towards the front of the fiber trap while that of sample 1B was found immediately behind the bullet within the fiber trap. Sample 8H's jacket also separated but penetrated and was lodged into the wood of the fiber trap. The jacket of sample 5D dispersed into three separate pieces, one of which fell in front of the glass sample and two of which were found inside of the trap. Similarly, sample 1C's jacket resulted in two separate pieces, but only part of it was found in the fiber trap, while the other part was lodged into the wood of the trap.

Bullets fired at 50°

For the 50° samples, the bullets of samples 3G, 3I, 3D, 3L, 1L, 5B, and 6A were all found to have separated jackets that were located toward the front of the fiber trap. For sample 3J, the jacket was located directly behind the bullet within the trap. Samples 3H and 3E had jackets that were retrieved on the floor, located beneath the fiber trap.

Bullets fired at 45°

The jackets of samples 1R, 1W, 3A, 3B, and 3C were found towards the front of the fiber trap, separated from their bullets. There were also portions of sample 3C that were found below the trap, lodged into the wood. The jacket for sample 3K was also found lodged into the wood. Samples 1S and 1X had separated jackets as well, but all or some of their jacket was found perpendicular to the line of fire. The jacket of sample 1Q was located in front of the glass sample, as well as lodged into the wood of the fiber trap, while the jacket of sample 1T was the only one to have a separated jacket that was not located.

4.2.2 LRN bullets

As shown in Figure 4.3 on the following page, all bullets fired at 90° contained a circular mark in the center of the nose of the bullet. This was not observed on bullets fired from 75°, 60°, 50°, or 45°.

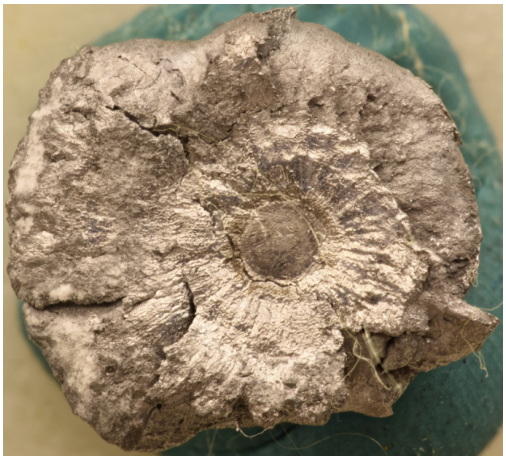

Figure 4.3: Circular mark in the center of the nose of the bullet. The bullet perforated glass at 90°

Lead round nose bullets deformed and broke apart much more than full metal jacket bullets. This was more apparent at 90° as can be seen in Figure 4.3. As the angle decreased to 45°, fewer bullets deformed and broke apart. However, some samples at low angles did present these characteristics as can be seen in Figure 4.4.

Figure 4.4: Bullet fired at 45°

4.2.3 General bullet observations

As full metal jacket bullets are fired at lower angles, the jackets are smaller and separate into more pieces.

From 75° down to 45°, glass is distributed toward one side of the bullet, whereas with 90°, the glass is distributed on all parts of the bullet. This was more apparent in full metal jacket bullets since they did not break apart and deform as much as lead round nose bullets.

The glass samples fractured into more pieces at lower angles. An example is shown in Figure 4.5.

Figure 4.5: Glass sample perforated by a bullet at 45° (left), glass sample perforated by a bullet at 90° (right)

At 60°, bullets begin to form an apparent V-shaped nose. This is clear at 45° as shown in Figure 4.6 on the following page.

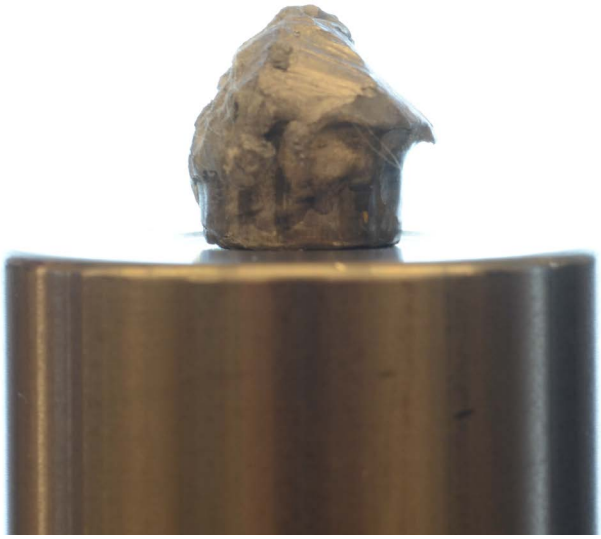

Figure 4.6: Bullet fired at 45° viewed from the side

4.3 Energy dispersive X-ray analysis

Figure 4.7 on the next page displays a backscattered electron image of a section of sample 8G and corresponding x-ray maps of calcium, silicon, copper, and lead. These specific elements are clearly visible in the x-ray maps.

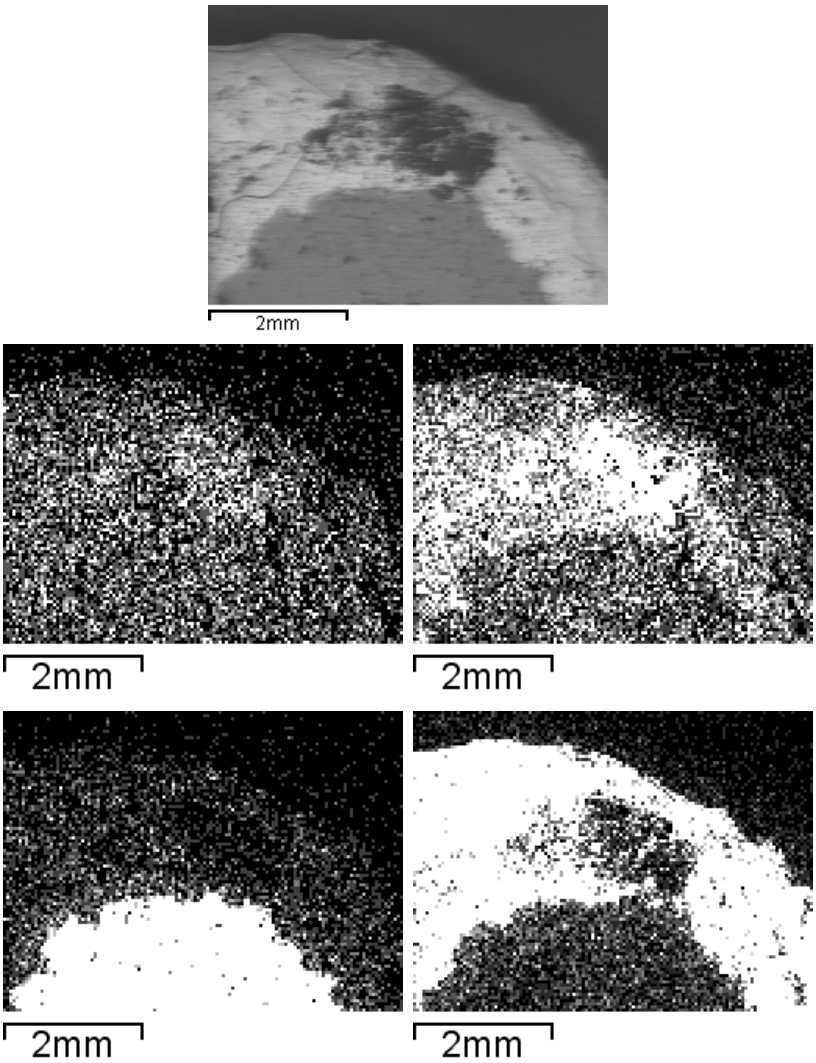

Figure 4.7: Backscattered electron image of a section of sample 8G (top), and corresponding x-ray maps of calcium (second row, left), silicon (second row, right), copper (bottom row, left), and lead (bottom row, right).

Figure 4.7 displays a backscattered electron image of a section of sample 8X and corresponding x-ray maps of calcium, silicon, and lead. These specific elements are clearly visible in the x-ray maps.

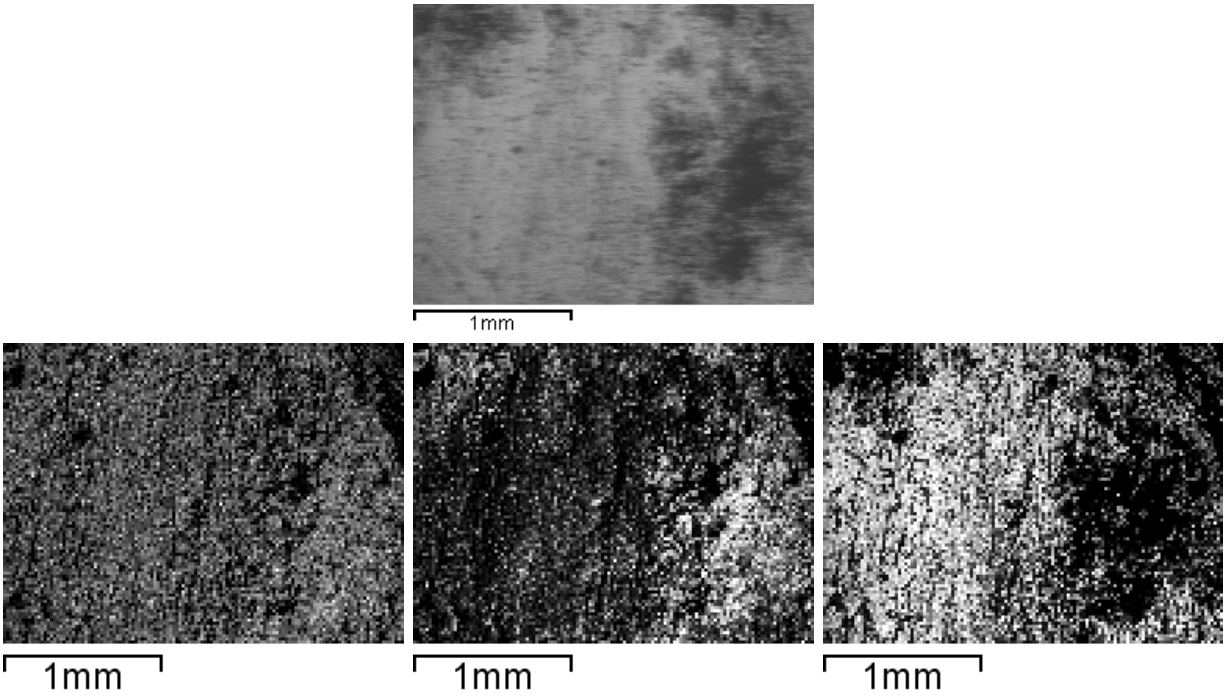

Figure 4.8: Backscattered electron image of a section of sample 8X (top), and corresponding x-ray maps of calcium (second row, left), silicon (second row, middle), and lead (bottom row, right)

4.4 HemoSpat

For all linear model plots in the results section, the solid horizontal lines represents a measured angle. In other words, if a bullet is recovered from a crime scene and the bullet deformation method is performed, the resulting angle would be the measured angle. The position that a line intersects the x-axis (Measured Angle) represents the calculated angle from the model. The position that a line intersects the y-axis (True Angle) represents the predicted angle from the model. The vertical dashed lines of each color represent the lower and upper prediction values for each measured angle. The vertical dotted lines of each color represent the lower and upper confidence values for each measured angle. The solid vertical line of each color represents the fitted value for each measured angle.

4.4.1 FMJ bullets

From Table 4.2, the gradient (or measured degrees) has an extremely low p-value, meaning that there appears to be a significant linear relationship between true angle and measured degrees (calculated values).

Table 4.2: Regression table for combined full metal jacket bullet HemoSpat data

Variable	Estimated Coefficient	Standard Error	T-Value	P-Value
Intercept	25.87390617	4.527000457	5.715463564	5.83E-08
Measured Degrees	0.689555005	0.079388748	8.68580271	6.42E-15
Multiple R-Squared	0.337639182		**Adjusted R-Squared**	0.333163771

Based on the R^2 value, the model performs poorly at explaining the variation in true angle. The estimated regression equation for this model is

$$\hat{y} = 0.6896 \times MeasuredDegrees + 25.8739 \tag{4.1}$$

The standard error (or standard deviation) of the intercept is 4.5270 while the standard error of the slope is 0.0794.

Figure 4.9 on the following page displays the linear model for the combined HemoSpat methods and the corresponding confidence and prediction intervals. Bullets fired at 90°, 75°, 60°, 50°, and 45° cannot be distinguished from each other.

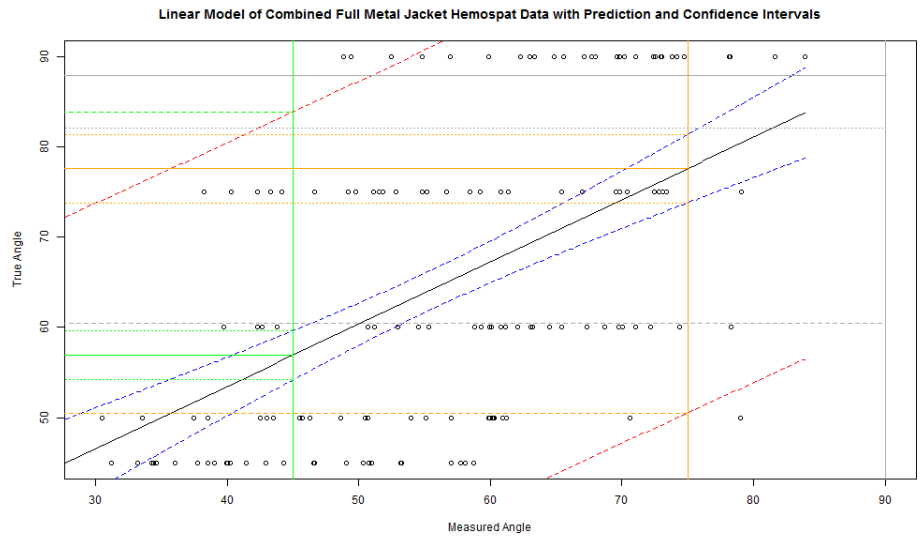

Figure 4.9: Linear model for combined full metal jacket bullet HemoSpat data

From Table 4.3, the gradient (or measured degrees) has an extremely low p-value, meaning that there appears to be a significant linear relationship between true angle and measured degrees (calculated values).

Table 4.3: Regression table for inside full metal jacket bullet HemoSpat data

Variable	Estimated Coefficient	Standard Error	T-Value	P-Value
Intercept	31.83980241	6.191560853	5.142451663	4.95E-06
Measured Degrees	0.633606087	0.116238552	5.450911741	1.71E-06
Multiple R-Squared	0.382338262		**Adjusted R-Squared**	0.369470309

Based on the R^2 value, the model performs poorly at explaining the variation in true angle. The estimated regression equation for this model is

$$\hat{y} = 0.6336 \times MeasuredDegrees + 31.8398 \tag{4.2}$$

The standard error (or standard deviation) of the intercept is 6.1916 while the standard error of the slope is 0.1162.

Figure 4.10 on the following page displays the linear model for the inside method and the corresponding confidence and prediction intervals. Bullets fired at 90°, 75°, 60°, 50°, and 45° cannot be distinguished from each other.

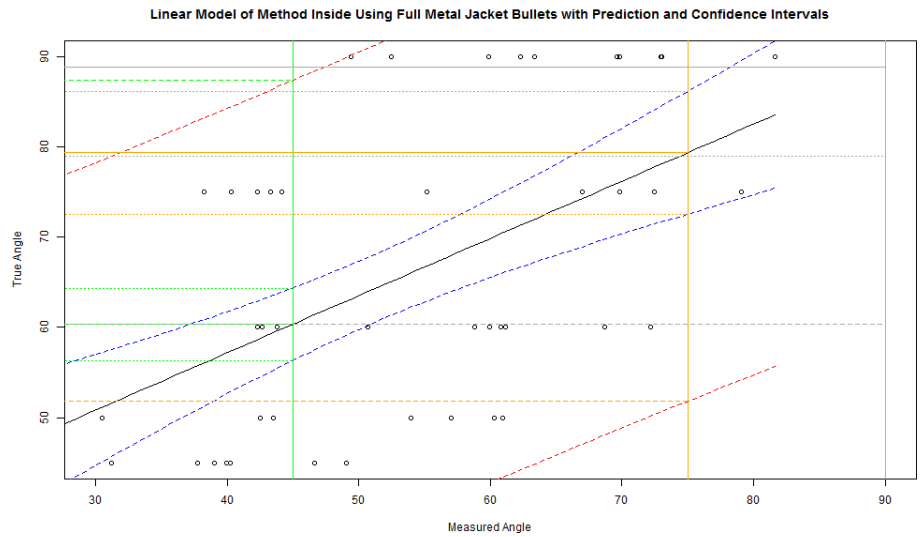

Figure 4.10: Linear model for inside full metal jacket bullet HemoSpat data

From Table 4.4, the gradient (or measured degrees) has an extremely low p-value, meaning that there appears to be a significant linear relationship between true angle and measured degrees (calculated values).

Table 4.4: Regression table for middle full metal jacket bullet HemoSpat data

Variable	Estimated Coefficient	Standard Error	T-Value	P-Value
Intercept	5.551772454	7.516374836	0.738623682	0.463731991
Measured Degrees	1.056479107	0.132866885	7.951410225	2.61E-10
Multiple R-Squared	0.568442054		**Adjusted R-Squared**	0.559451263

Based on the R^2 value, the model does not perform well at explaining the variation in true angle. The estimated regression equation for this model is

$$\hat{y} = 1.0565 \times MeasuredDegrees + 5.5518 \tag{4.3}$$

The standard error (or standard deviation) of the intercept is 7.5164 while the standard error of the slope is 0.1329.

Figure 4.11 on the following page displays the linear model for the middle method and the corresponding confidence and prediction intervals. Bullets fired from 45° can be distinguished from bullets fired from 90°, but bullets fired from 46° cannot be distinguished from 90°. Bullets fired from 90°, 75°, 60°, and 50° cannot be distinguished from each other.

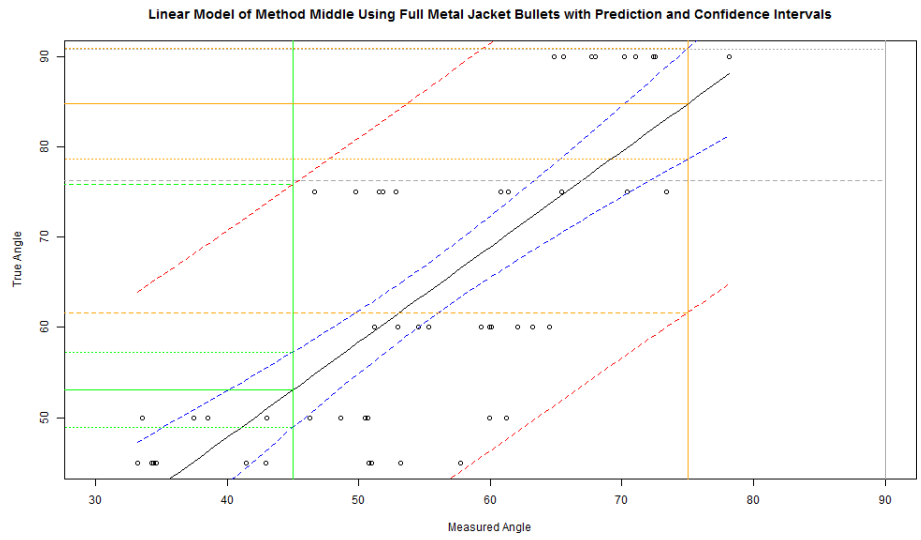

Figure 4.11: Linear model for middle full metal jacket bullet HemoSpat data

From Table 4.5, the gradient (or measured degrees) has an extremely low p-value, meaning that there appears to be a significant linear relationship between true angle and measured degrees (calculated values).

Table 4.5: Regression table for outside full metal jacket bullet HemoSpat data

Variable	Estimated Coefficient	Standard Error	T-Value	P-Value
Intercept	26.32365314	10.87561449	2.420429041	0.019335688
Measured Degrees	0.630127758	0.178374471	3.532611778	0.000920942
Multiple R-Squared	0.206340624		**Adjusted R-Squared**	0.189806053

Based on the R^2 value, the model does not perform well at explaining the variation in true angle. The estimated regression equation for this model is

$$\hat{y} = 0.6301 \times MeasuredDegrees + 26.3237 \tag{4.4}$$

The standard error (or standard deviation) of the intercept is 10.8756 while the standard error of the slope is 0.1784.

Figure 4.12 on the following page displays the linear model for the inside method and the corresponding confidence and prediction intervals. Bullets fired at 90°, 75°, 60°, 50°, and 45° cannot be distinguished from each other.

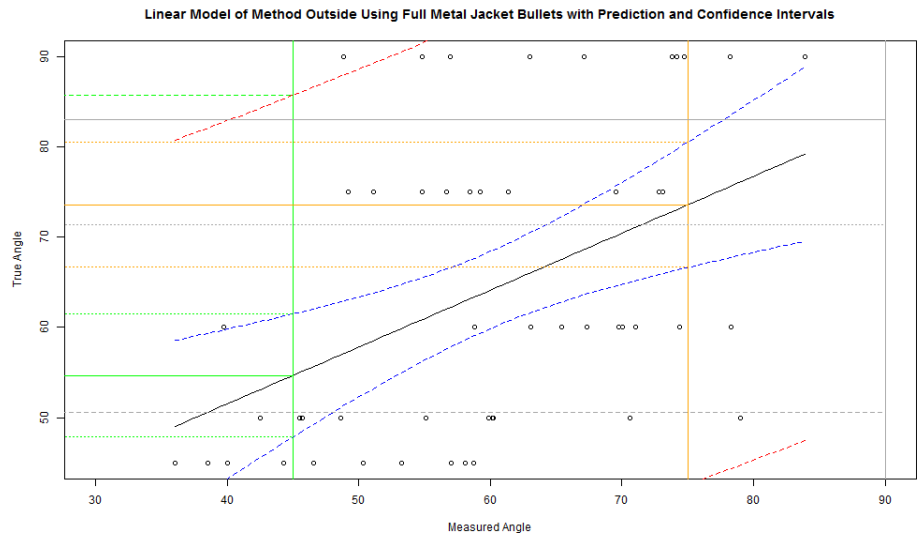

Figure 4.12: Linear model for outside full metal jacket bullet HemoSpat data

All other pred-res plots, normal Q-Q plots, histograms, and confidence and prediction interval plots for the full metal jacket combined methods, as well as for methods inside, outside, and middle can be found in Appendix A.

4.4.2 LRN bullets

From Table 4.6, the gradient (or measured degrees) has an extremely low p-value, meaning that there appears to be a significant linear relationship between true angle and measured degrees (calculated values).

Table 4.6: Regression table for combined lead round nose bullet HemoSpat data

Variable	Estimated Coefficient	Standard Error	T-Value	P-Value
Intercept	38.60618194	4.38133815	8.811504754	3.08E-15
Measured Degrees	0.499859941	0.082838727	6.034133518	1.23E-08
Multiple R-Squared	0.197443825		**Adjusted R-Squared**	0.192021148

Based on the R^2 value, the model performs poorly at explaining the variation in true angle. The estimated regression equation for this model is

$$\hat{y} = 0.4999 \times MeasuredDegrees + 38.6018 \tag{4.5}$$

The standard error (or standard deviation) of the intercept is 4.3813 while the standard error of the slope is 0.0828.

Figure 4.13 displays the linear model for the combined methods and the corresponding confidence and prediction intervals. Bullets fired at 90°, 75°, 60°, 50°, and 45° cannot be distinguished from each other.

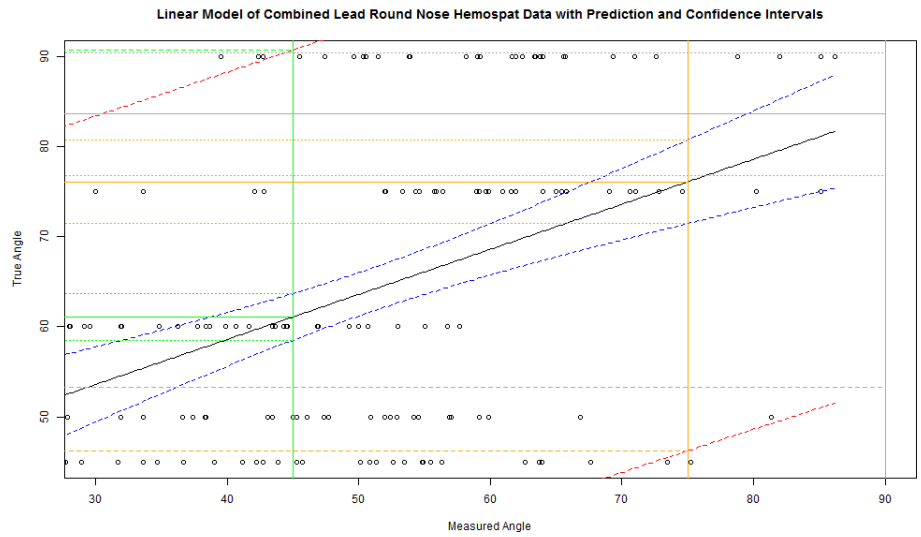

Figure 4.13: Linear model for combined lead round nose bullet HemoSpat data

From Table 4.7, the gradient (or measured degrees) has an extremely low p-value, meaning that there appears to be a significant linear relationship between true angle and measured degrees (calculated values).

Table 4.7: Regression table for inside lead round nose bullet HemoSpat data

Variable	Estimated Coefficient	Standard Error	T-Value	P-Value
Intercept	37.22985777	5.076887571	7.33320509	2.27E-09
Measured Degrees	0.593465096	0.104810926	5.662244545	8.19E-07
Multiple R-Squared	0.400457251		**Adjusted R-Squared**	0.387966777

Based on the R^2 value, the model performs poorly at explaining the variation in true angle. The estimated regression equation for this model is

$$\hat{y} = 0.5935 \times MeasuredDegrees + 37.2299 \tag{4.6}$$

The standard error (or standard deviation) of the intercept is 5.0769 while the standard error of the slope is 0.1048.

Figure 4.14 displays the linear model for the inside method and the corresponding confidence and prediction intervals. Bullets fired at 90°, 75°, 60°, 50°, and 45° cannot be distinguished from each other.

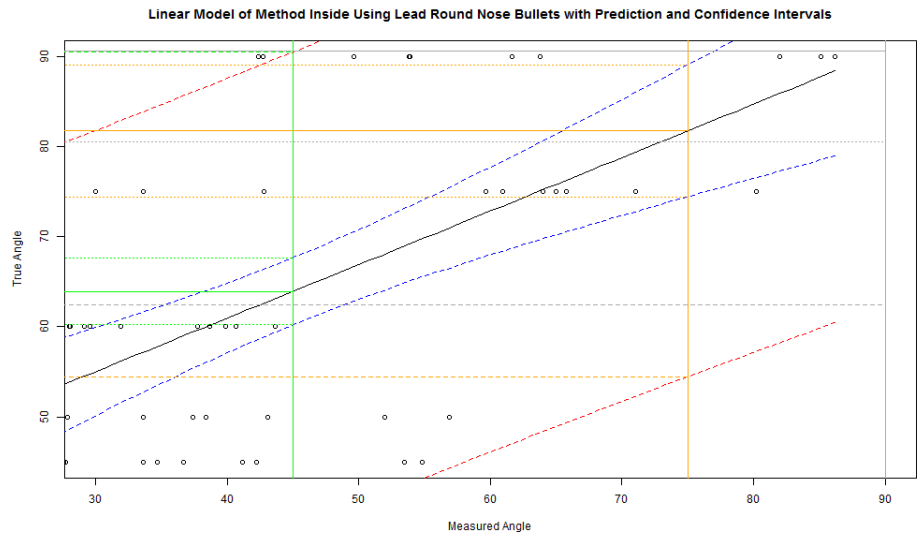

Figure 4.14: Linear model for inside lead round nose bullet HemoSpat data

From Table 4.8, the gradient (or measured degrees) has a low p-value, meaning that there appears to be a significant linear relationship between true angle and measured degrees (calculated values).

Table 4.8: Regression table for middle lead round nose bullet HemoSpat data

Variable	Estimated Coefficient	Standard Error	T-Value	P-Value
Intercept	32.26717674	9.028588008	3.573889595	0.00081355
Measured Degrees	0.61370459	0.16973743	3.615611415	0.000717235
Multiple R-Squared	0.214050754		**Adjusted R-Squared**	0.197676811

Based on the R^2 value, the model performs poorly at explaining the variation in true angle. The estimated regression equation for this model is

$$\hat{y} = 0.6137 \times MeasuredDegrees + 37.2672 \tag{4.7}$$

The standard error (or standard deviation) of the intercept is 9.0286 while the standard error of the slope is 0.1697.

Figure 4.15 displays the linear model for the middle method and the corresponding confidence and prediction intervals. Bullets fired at 90°, 75°, 60°, 50°, and 45° cannot be distinguished from each other.

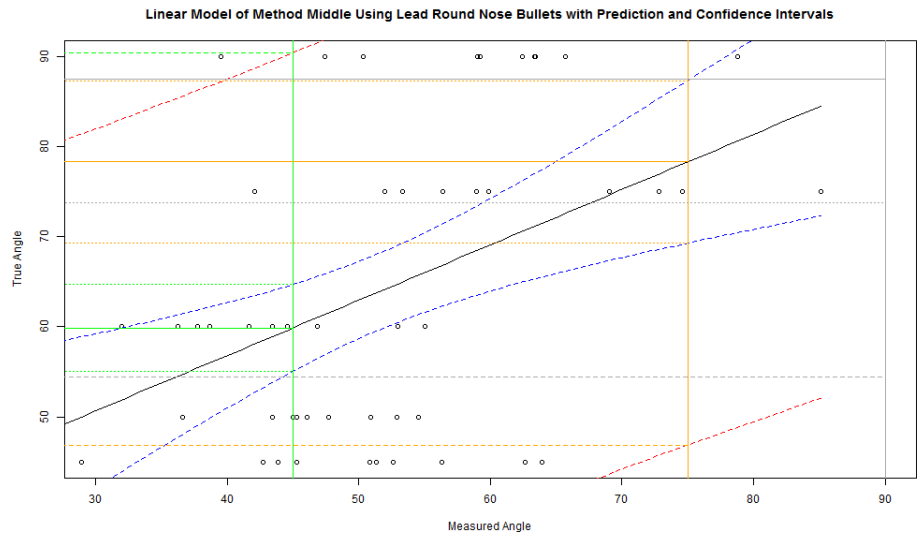

Figure 4.15: Linear model for middle lead round nose bullet HemoSpat data

From Table 4.9, the gradient (or measured degrees) has a low p-value, meaning that there appears to be a significant linear relationship between true angle and measured degrees (calculated values).

Table 4.9: Regression table for outside lead round nose bullet HemoSpat data

Variable	Estimated Coefficient	Standard Error	T-Value	P-Value
Intercept	44.50485388	11.71869223	3.797766252	0.000410586
Measured Degrees	0.350692676	0.206629673	1.697203847	0.096134076
Multiple R-Squared	0.056613061		**Adjusted R-Squared**	0.036959166

Based on the R^2 value, the model does a very poor job at explaining the variation in true angle. The estimated regression equation for this model is

$$\hat{y} = 0.3507 \times MeasuredDegrees + 44.5049 \tag{4.8}$$

The standard error (or standard deviation) of the intercept is 11.7187 while the standard error of the slope is 0.3366.

Figure 4.16 displays the linear model for the middle method and the corresponding confidence and prediction intervals. Bullets fired at 90°, 75°, 60°, 50°, and 45° cannot be distinguished from each other.

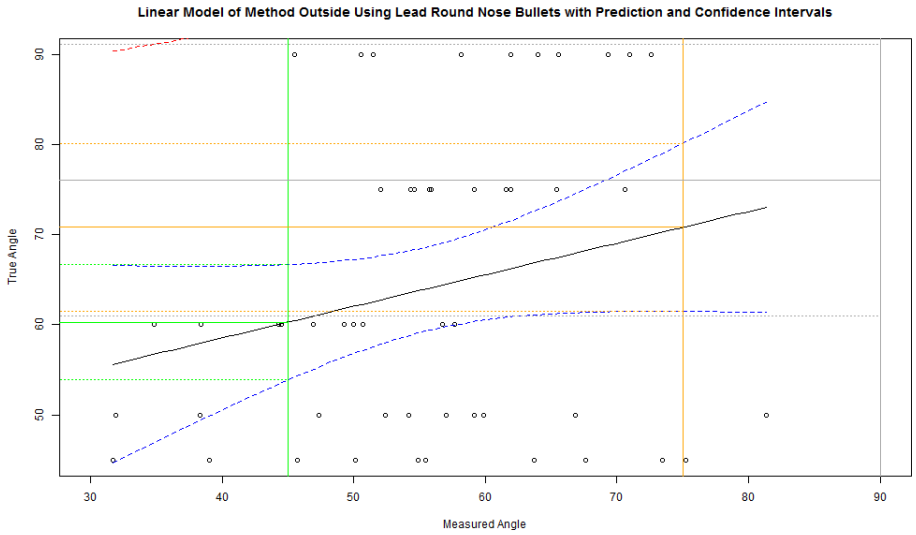

Figure 4.16: Linear model for outside lead round nose bullet HemoSpat data

4.4.3 Discussion of the HemoSpat results

For the full metal jacket bullets, the middle method performed the best, followed by the inside method, and then the outside method. For the lead round nose bullets, the inside performed the best, followed by the middle, and then the outside. The inside method being the best for the lead round nose bullets could be a result of those particular bullets being softer than the full metal jacket bullets causing there to be a smoother inside edge around the bullet hole from not as much glass breaking off.

Photographs of bullet holes (FMJ bullets)

There was only one method where a bullet fired from one angle (45°) could be distinguished from a bullet fired from another (90°). This was the case for the full metal jacket middle method where the best fitting ellipse was selected for the bullet hole. No other angles could be distinguished from each other using any method for both types of bullets. Figures 4.17, 4.18, 4.19, 4.20, and 4.21 for full metal jacket bullets and Figures 4.22, 4.23, 4.24, 4.25, and

4.26 for lead round nose bullets show that there is a significant amount of variation in the size, shape, and total structure of the bullet holes within the same angle group, which in turn causes a large range of measured angles to result when measuring the bullet holes in HemoSpat. For example, a 90° bullet hole for the FMJ inside method resulted in measured values ranging from 48.8° to 83.89°.

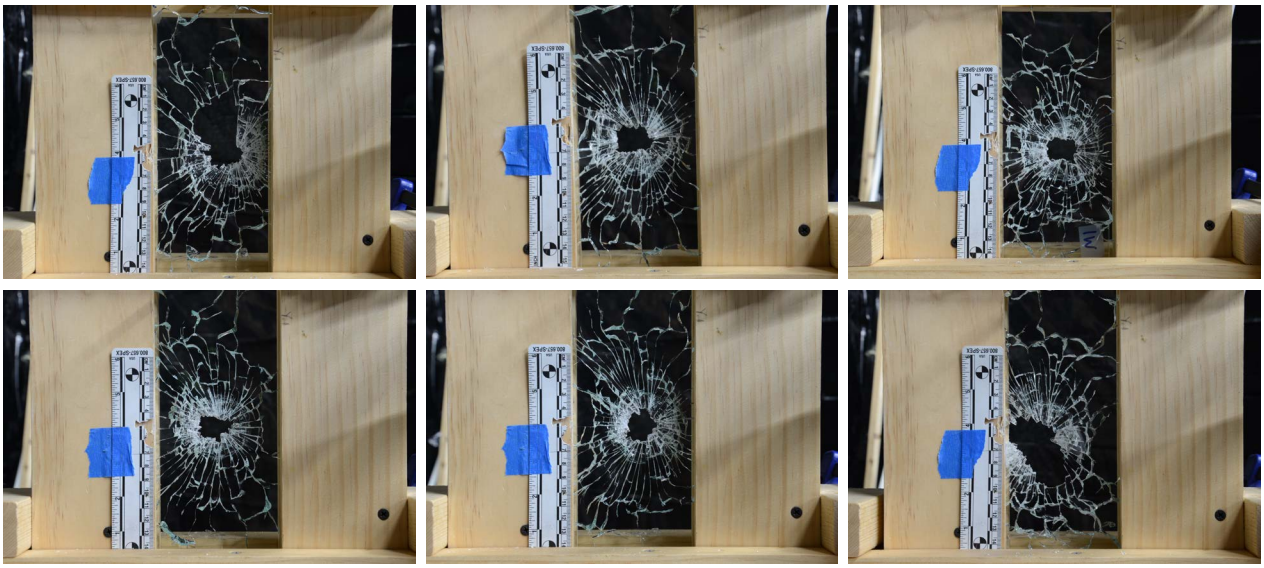

Figure 4.17: 45° full metal jacket bullet holes in glass. (Top row): 1Q, 1S, 1W, (Bottom row): 3B, 3C, 3K

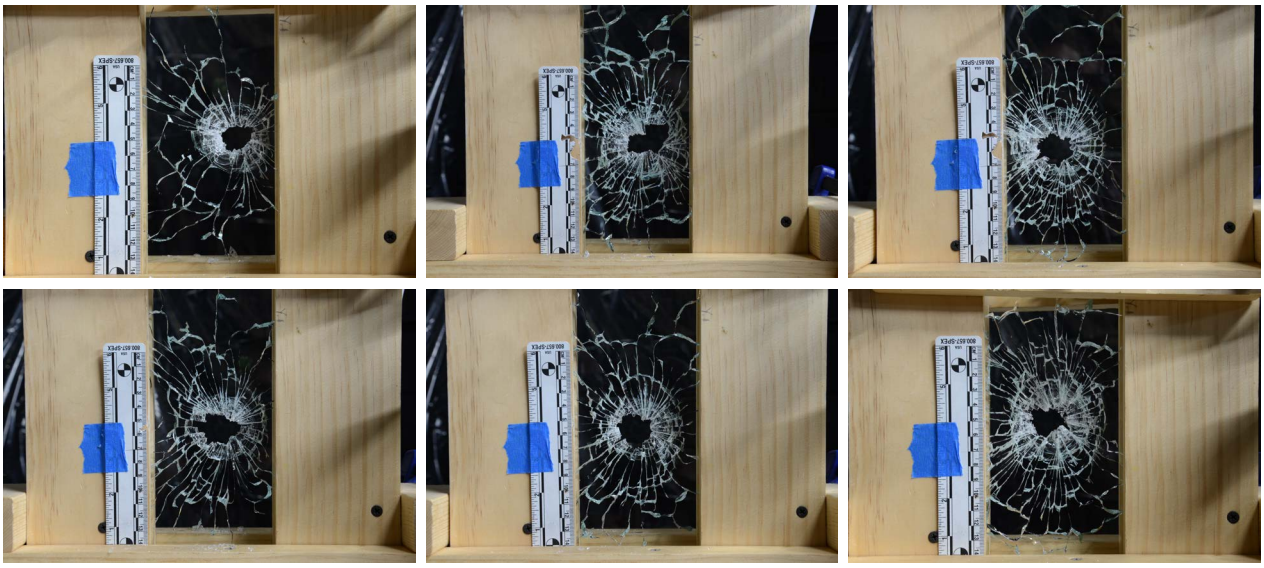

Figure 4.18: 50° full metal jacket bullet holes in glass. (Top row): 1L, 3D, 3G, (Bottom row): 3I, 3J, 3L

Figure 4.19: 60° full metal jacket bullet holes in glass. (Top row): 1A, 1B, 4I, (Bottom row): 4J, 5D, 8H

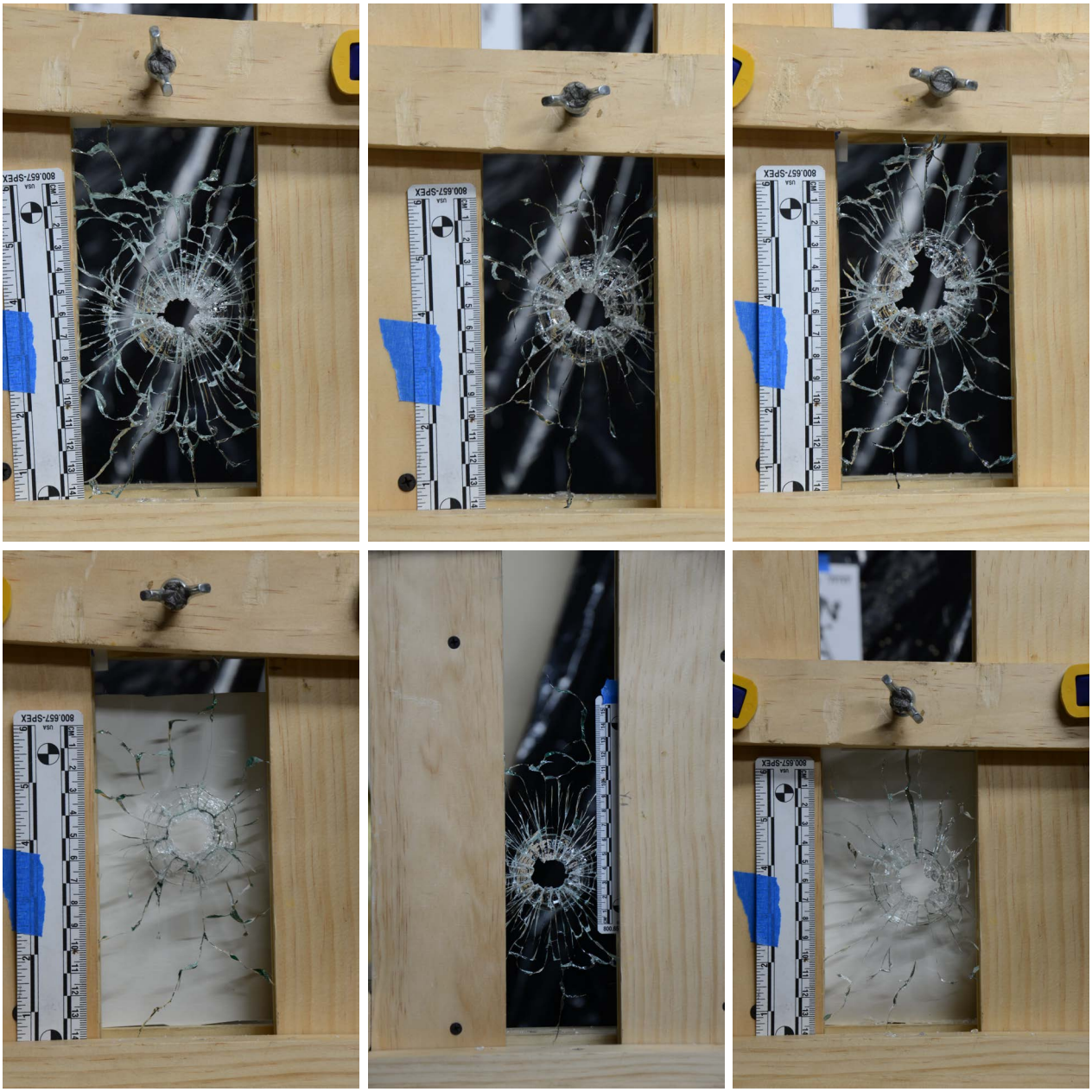

Figure 4.20: 75° full metal jacket bullet holes in glass. (Top row): 1D, 1F, 1G, (Bottom row): 1H, 4L, 8F

Photographs of bullet holes (LRN bullets)

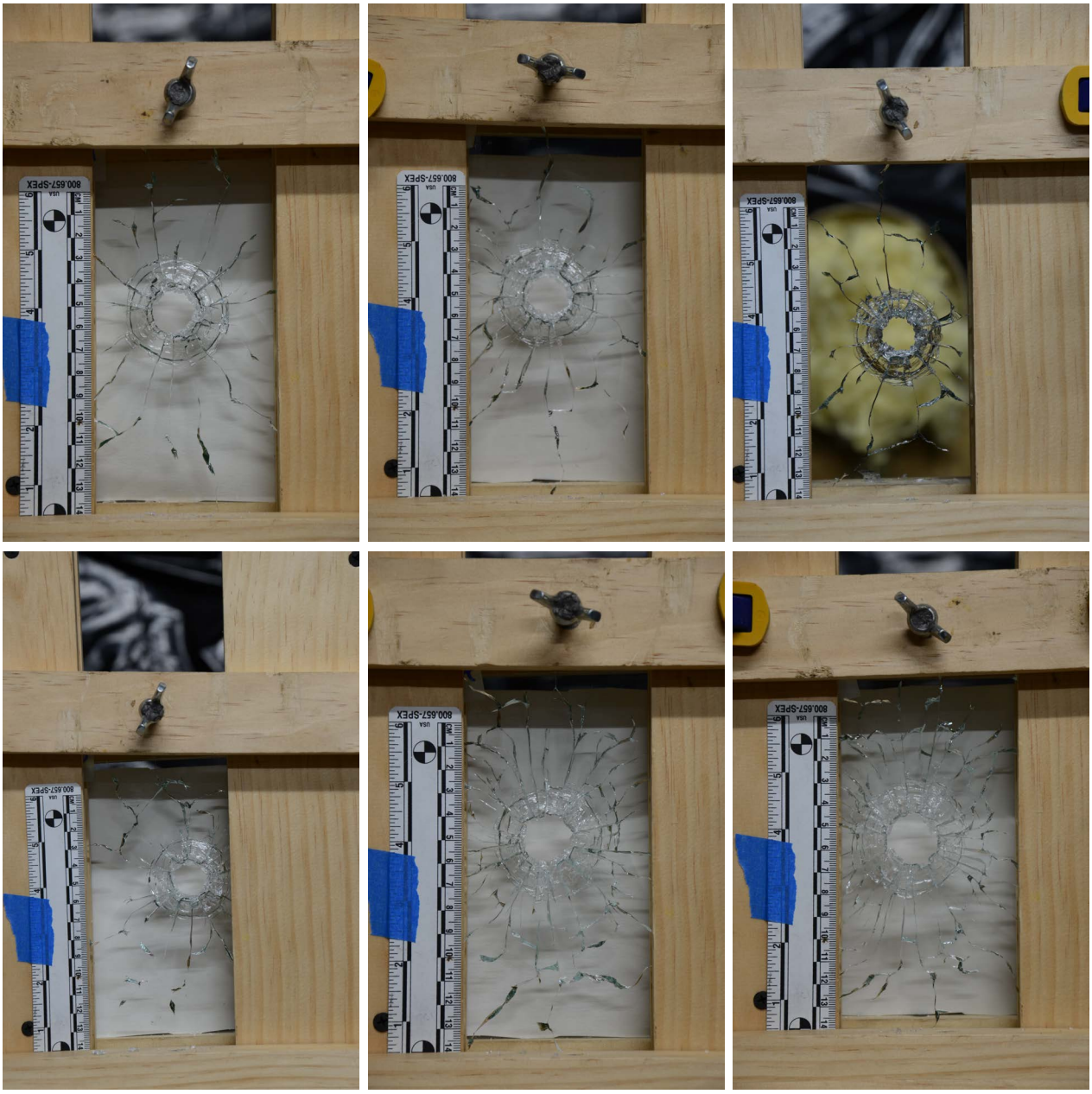

Figure 4.21: 90° full metal jacket bullet holes in glass. (Top row): 5A, 6C, 6G, (Bottom row): 8G, 8K, 8L

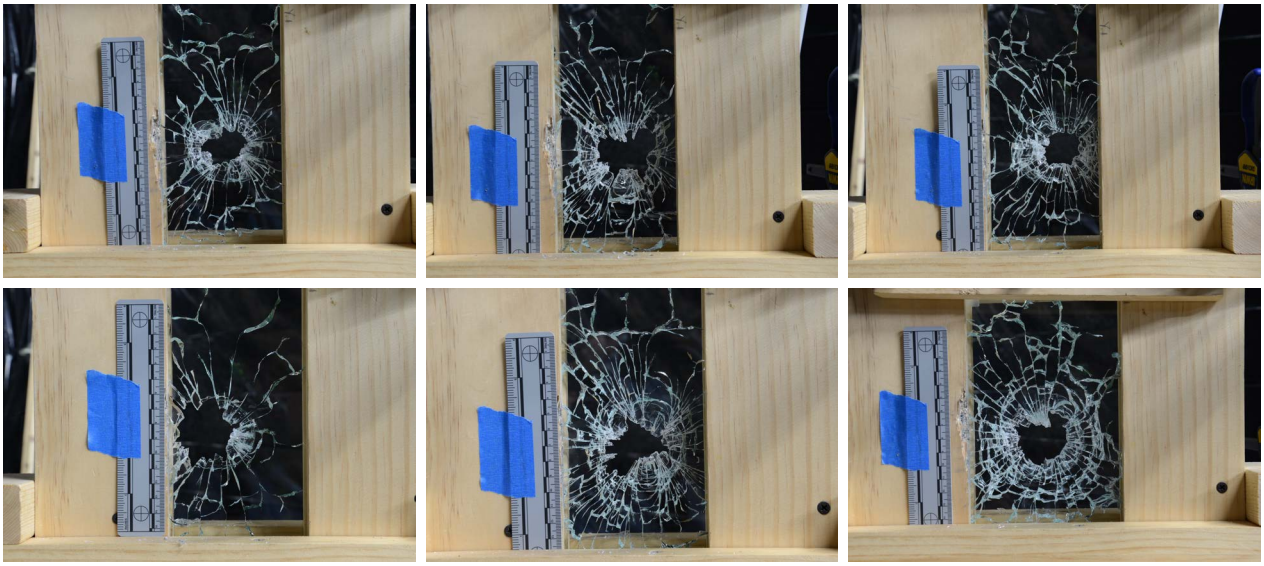

Figure 4.22: 45° lead round nose bullet holes in glass. (Top row): 1U, 1V, 1Y, (Bottom row): 2A, 2C, 3M

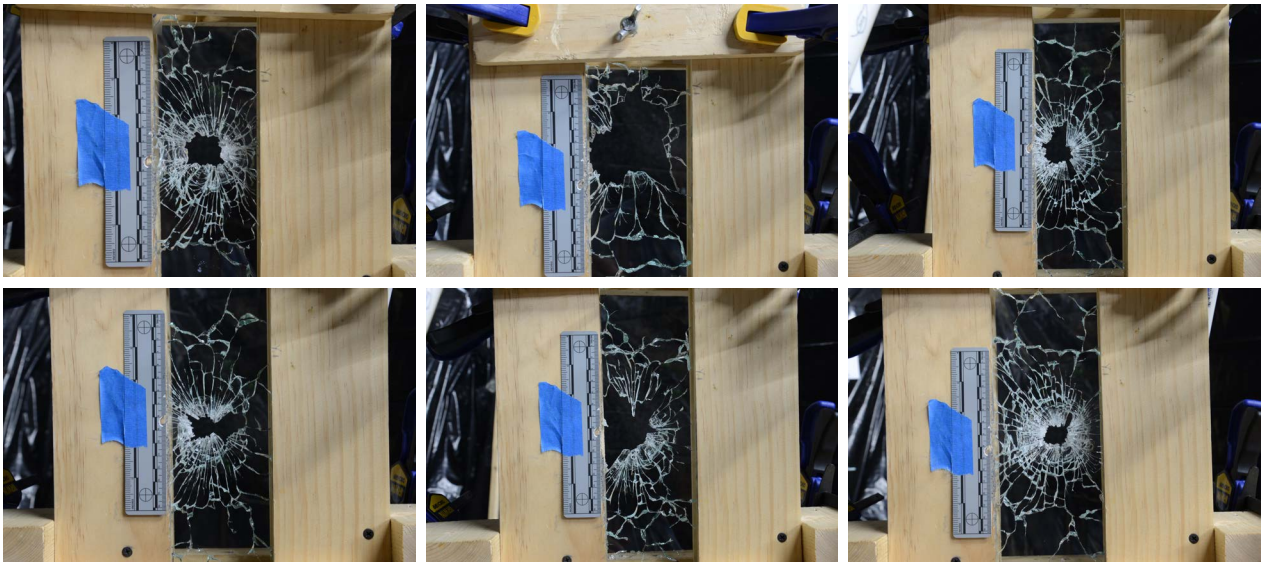

Figure 4.23: 50° lead round nose bullet holes in glass. (Top row): 6P, 61, 6T, (Bottom row): 6U, 8Y, 8Z

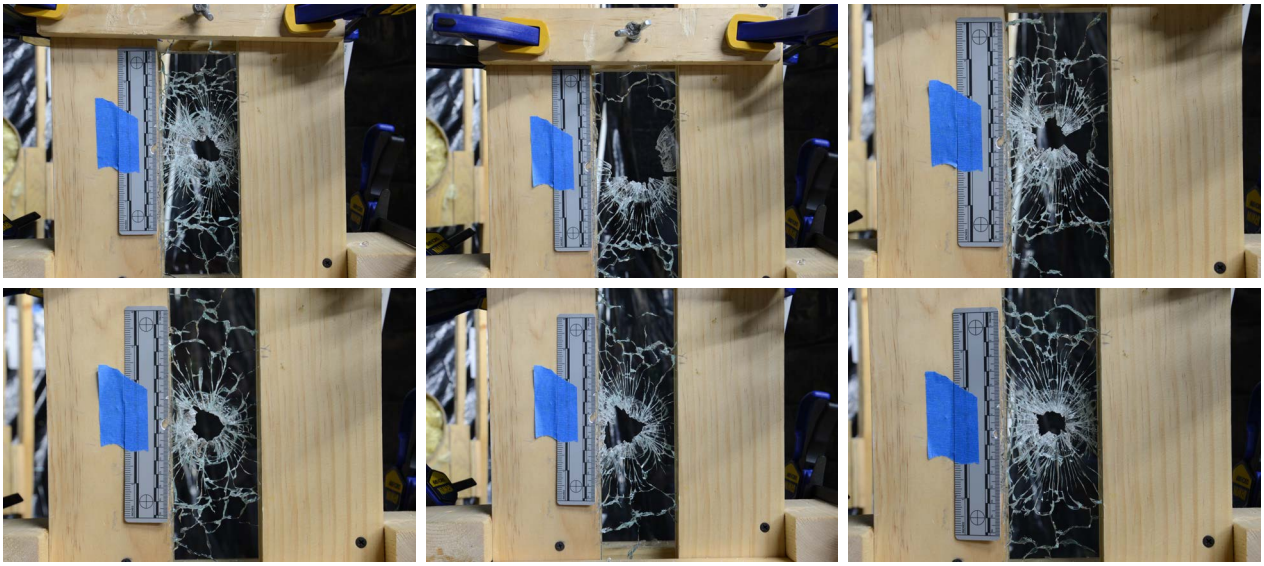

Figure 4.24: 60° lead round nose bullet holes in glass. (Top row): 3R, 3S, 3T, (Bottom row): 8R, 8S, 8V

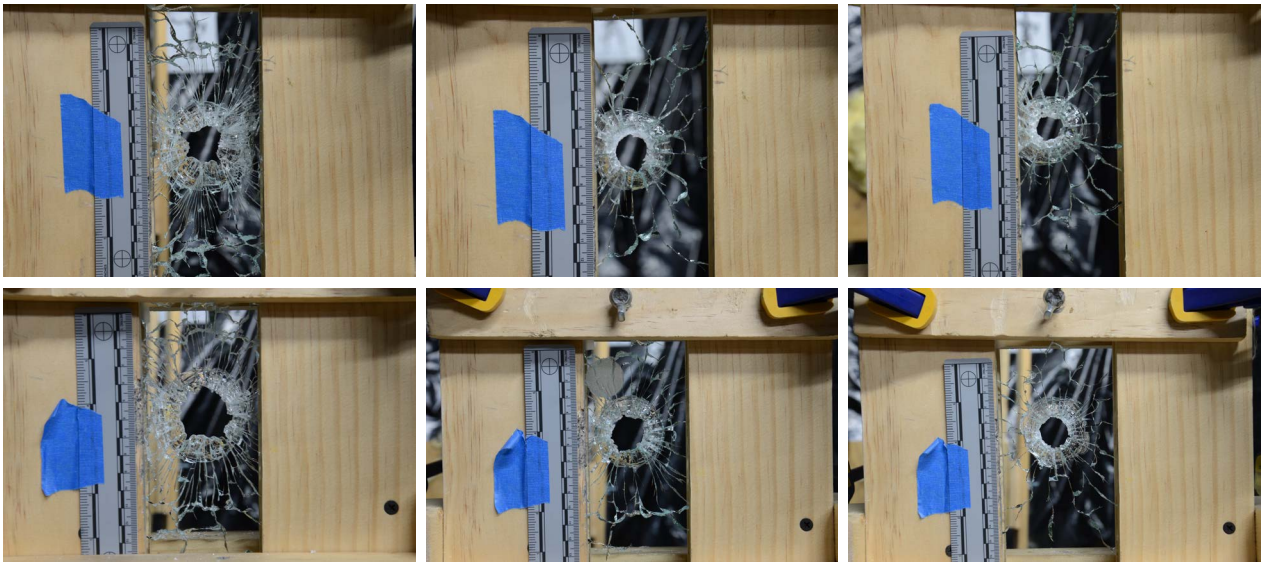

Figure 4.25: 75° lead round nose bullet holes in glass. (Top row): 3W, 3X, 3Z, (Bottom row): 3H, 5P, 5T

Figure 4.26: 90° lead round nose bullet holes in glass. (Top row): 5J, 5K, 5O, (Bottom row): 5S, 5U, 8E

All other pred-res plots, normal Q-Q plots, histograms, and confidence and prediction interval plots for the lead round nose combined methods, as well as for methods inside, outside, and middle can be found in Appendix A.

4.5 Side view bullet deformation

4.5.1 FMJ bullets

Figure 4.27 on the next page displays the model residuals plotted against their corresponding fitted values.There is no recognizable pattern in the data showing non-linearity or non-constant scatter. Overall, the residuals are symmetrically distributed around the zero line, indicating that most errors have constant variance around the line.

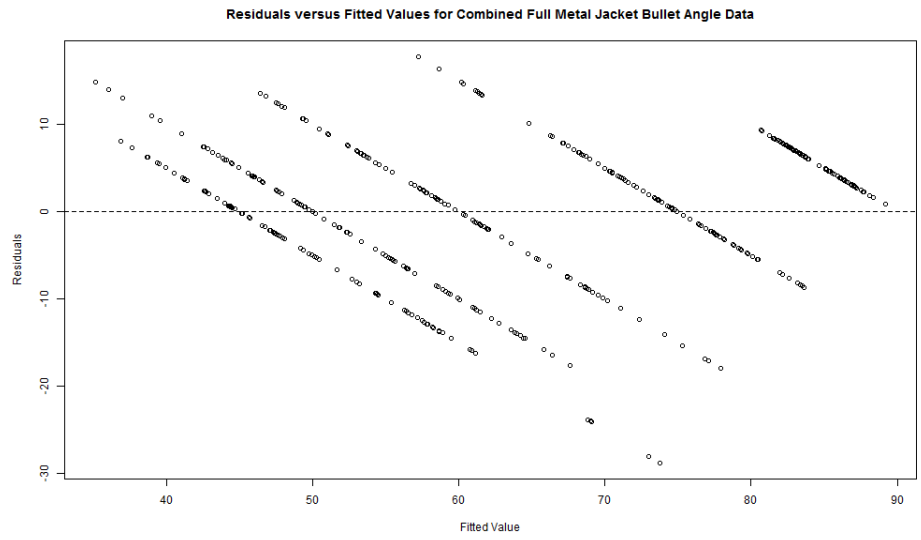

Figure 4.27: Pred-res plot (residual versus fitted values) for combined full metal jacket bullet angle data

Figure 4.28 displays the empirical quantiles obtained from the data against the theoretical quantiles. Although the data does not follow a perfect normal distribution, it does show that most of the points fall on or close to the line demonstrating that the normality assumption is met.

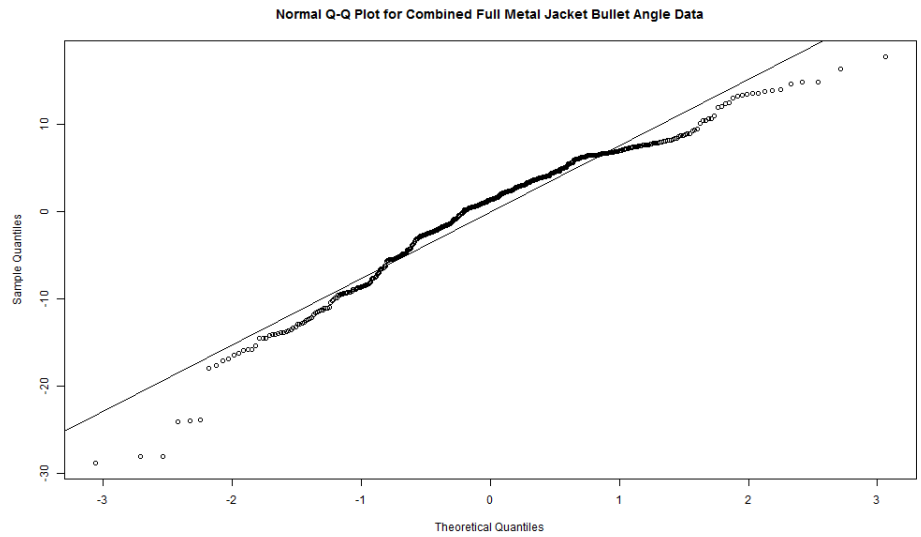

Figure 4.28: Normal Q-Q plot for combined full metal jacket bullet angle data

Figure 4.29 shows a density estimate of the residuals. As displayed in Figure 4.28 on the preceding page, the data does not follow a perfectly normal distribution, although there is no evidence to suggest that the data are skewed.

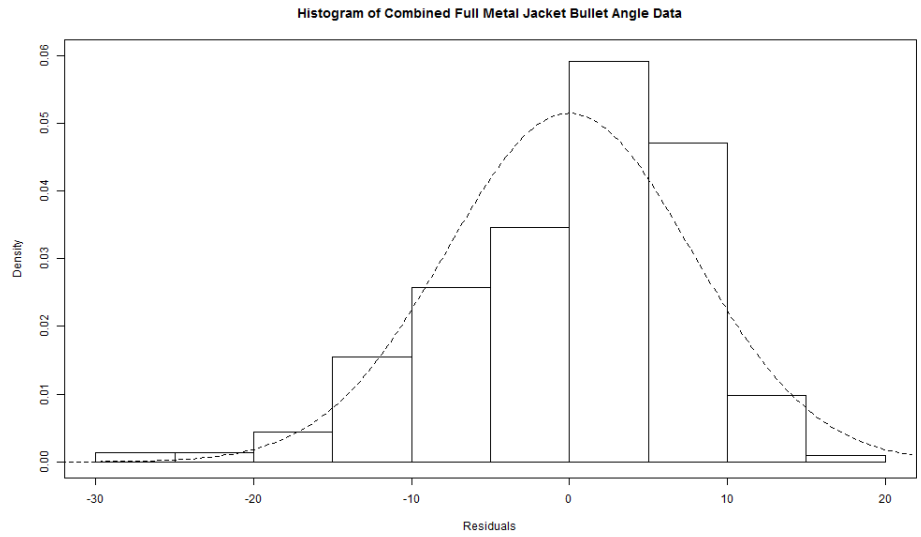

Figure 4.29: Histogram for combined full metal jacket bullet angle data

From Table 4.10, the gradient (or measured degrees) has an extremely low p-value, meaning that there appears to be a significant linear relationship between true angle and measured degrees (calculated values).

Table 4.10: Regression table for combined full metal jacket bullet angle data

Variable	Estimated Coefficient	Standard Error	T-Value	P-Value
Intercept	7.780292935	1.450525351	5.363775911	1.31E-07
Measured Degrees	0.89607084	0.022373886	40.04985227	3.87E-150
Multiple R-Squared	0.78167542		**Adjusted R-Squared**	0.781188089

Based on the R^2 value, the model performs well at explaining the variation in true angle. The estimated regression equation for this model is

$$\hat{y} = 0.8961 \times MeasuredDegrees + 7.7803 \tag{4.9}$$

The standard error (or standard deviation) of the intercept is 1.4505 while the standard error of the slope is 0.0224.

Figure 4.30 displays the linear model for the combined full metal jacket bullet data for all methods and the corresponding confidence and prediction intervals. Bullets fired at 55° cannot be distinguished from bullets fired at 75° but can be distinguished from bullets fired at 90°. Bullets fired from 50° and 45° can be distinguished from bullets fired from 85° and 80°, respectively.

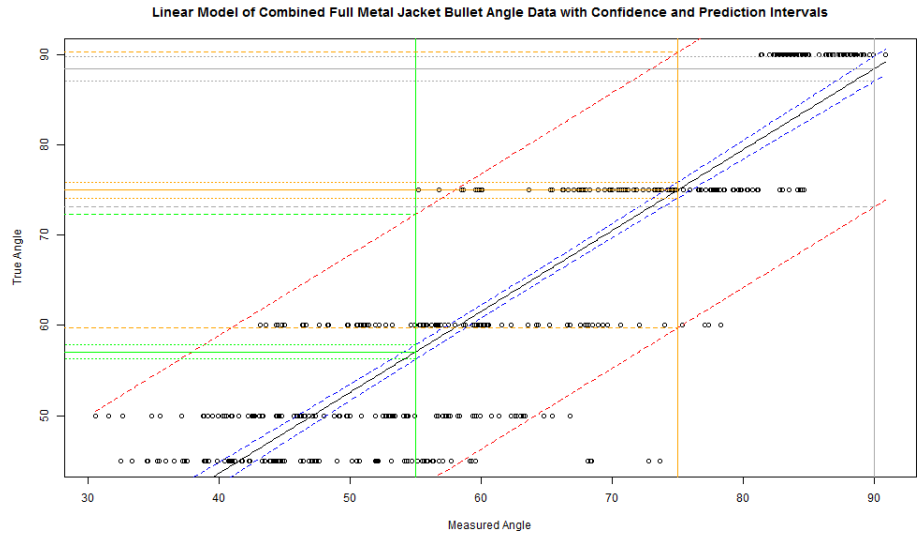

Figure 4.30: Linear model for combined full metal jacket bullet angle data

From Table 4.11, the gradient (or measured degrees) has an extremely low p-value, meaning that there appears to be a significant linear relationship between true angle and measured degrees (calculated values).

Table 4.11: Regression table for method AA using full metal jacket bullet angle data

Variable	Estimated Coefficient	Standard Error	T-Value	P-Value
Intercept	13.23559797	1.494755004	8.854693869	2.39E-15
Measured Degrees	0.89223866	0.025104431	35.54108257	2.35E-74
Multiple R-Squared	0.895122379		**Adjusted R-Squared**	0.894413747

Based on the R^2 value, the model performs great at explaining the variation in true angle. The estimated regression equation for this model is

$$\hat{y} = 0.8922 \times MeasuredDegrees + 13.2356 \tag{4.10}$$

The standard error (or standard deviation) of the intercept is 1.4948 while the standard error of the slope is 0.0251.

Figure 4.31 displays the linear model for method AA and the corresponding confidence and prediction intervals. Bullets fired at 65° cannot be distinguished from bullets fired at 75° but can be distinguished from those fired at 90°. Bullets fired from 75° and 90° are not distinguishable from one another. Bullets fired from 60°, 55°, 50° and 45° can be distinguished from bullets fired from 85°, 80°, 75°, and 70°, respectively.

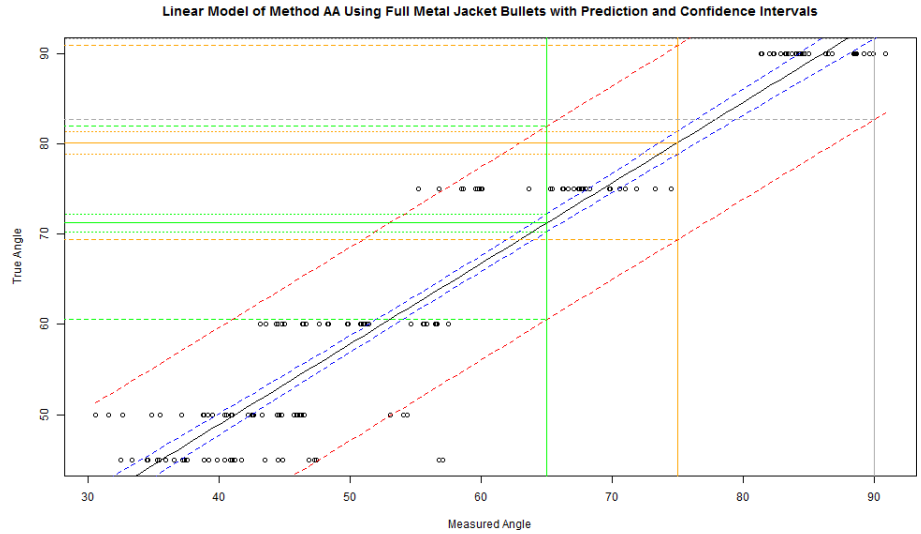

Figure 4.31: Linear model for method AA using full metal jacket bullet angle data

From Table 4.12, the gradient (or measured degrees) has an extremely low p-value, meaning that there appears to be a significant linear relationship between true angle and measured degrees (calculated values).

Table 4.12: Regression table for method HH using full metal jacket bullet angle data

Variable	Estimated Coefficient	Standard Error	T-Value	P-Value
Intercept	0.917854656	2.189936548	0.419123859	0.675733291
Measured Degrees	0.99246379	0.033481605	29.64206162	4.01E-64
Multiple R-Squared	0.855842071		**Adjusted R-Squared**	0.854868031

Based on the R^2 value, the model performs great at explaining the variation in true angle. The estimated regression equation for this model is

$$\hat{y} = 0.9925 \times MeasuredDegrees + 0.9178 \tag{4.11}$$

The standard error (or standard deviation) of the intercept is 2.1900 while the standard error of the slope is 0.0335.

Figure 4.32 displays the linear model for method HH and the corresponding confidence and prediction intervals. Bullets fired at 60° cannot be distinguished from bullets fired at 75° but can be distinguished from those fired at 90°. Bullets fired from 75° and 90° are not distinguishable from one another. Bullets fired from 55°, 50° and 45° can be distinguished from bullets fired from 85°, 80°, and 75°, respectively.

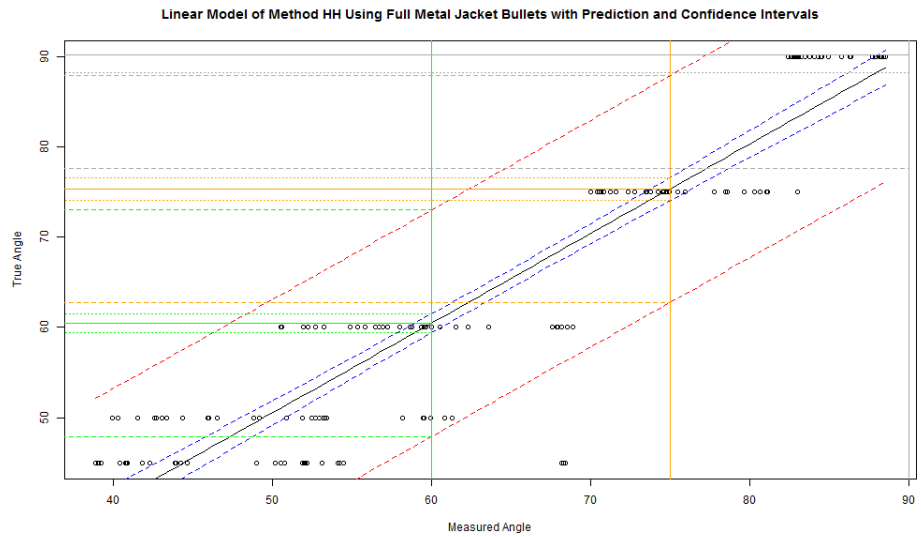

Figure 4.32: Linear model for method HH using full metal jacket bullet angle data

From Table 4.13, the gradient (or measured degrees) has an extremely low p-value, meaning that there appears to be a significant linear relationship between true angle and measured degrees (calculated values).

Table 4.13: Regression table for method VV using full metal jacket bullet angle data

Variable	Estimated Coefficient	Standard Error	T-Value	P-Value
Intercept	-7.920811021	3.040981231	-2.604689217	0.010133872
Measured Degrees	1.061341722	0.043957118	24.14493436	3.43E-53
Multiple R-Squared	0.797531486		**Adjusted R-Squared**	0.796163456

Based on the R^2 value, the model performs well at explaining the variation in true angle. The estimated regression equation for this model is

$$\hat{y} = 1.0613 \times MeasuredDegrees + -7.9208 \tag{4.12}$$

The standard error (or standard deviation) of the intercept is 3.0410 while the standard error of the slope is 0.0440.

Figure 4.33 displays the linear model for method VV and the corresponding confidence and prediction intervals. Bullets fired at 60° cannot be distinguished from bullets fired at 75° but can be distinguished from those fired at 90°. Bullets fired from 75° and 90° are not distinguishable from one another. Bullets fired from 55°, 50° and 45° can be distinguished from bullets fired from 85°, 80°, and 75°, respectively.

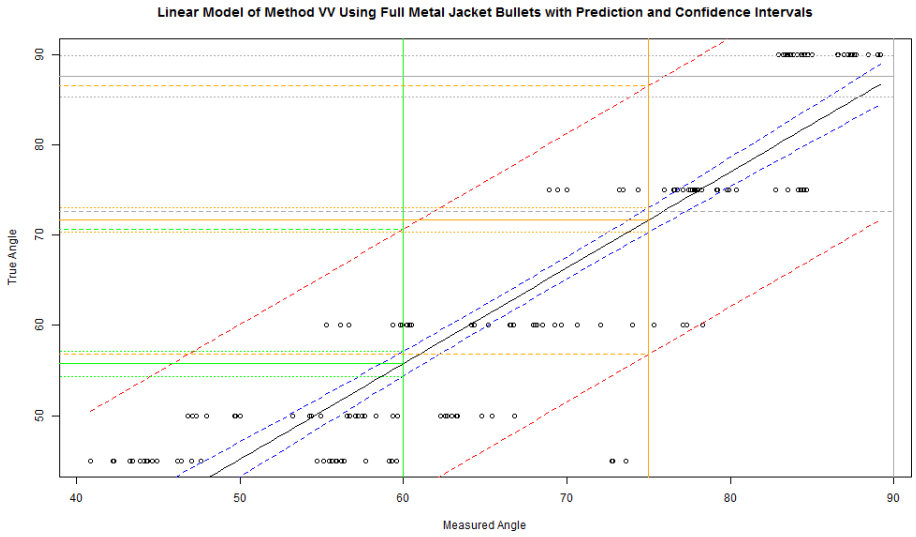

Figure 4.33: Linear model for method VV using full metal jacket bullet angle data

From Table 4.14 on the next page, the gradient (or measured degrees) has an extremely low p-value, meaning that there appears to be a significant linear relationship between true angle and measured degrees (calculated values).

Table 4.14: Regression table for the 5-point method using full metal jacket bullet angle data

Variable	Estimated Coefficient	Standard Error	T-Value	P-Value
Intercept	7.060020078	2.564211451	2.753290909	0.006639381
Measured Degrees	0.906562173	0.039542769	22.92611783	1.47E-50
Multiple R-Squared	0.780287279		**Adjusted R-Squared**	0.778802734

Based on the R^2 value, the model performs well at explaining the variation in true angle. The estimated regression equation for this model is

$$\hat{y} = 0.9066 \times MeasuredDegrees + 7.0600 \tag{4.13}$$

The standard error (or standard deviation) of the intercept is 2.5642 while the standard error of the slope is 0.0395.

Figure 4.34 displays the linear model for the 5-point method and the corresponding confidence and prediction intervals. Bullets fired at 55° cannot be distinguished from bullets fired at 75° but can be distinguished from those fired at 90°. Bullets fired from 75° and 90° are not distinguishable from one another. Bullets fired from 50° and 45° can be distinguished from bullets fired from 85° and 80°, respectively.

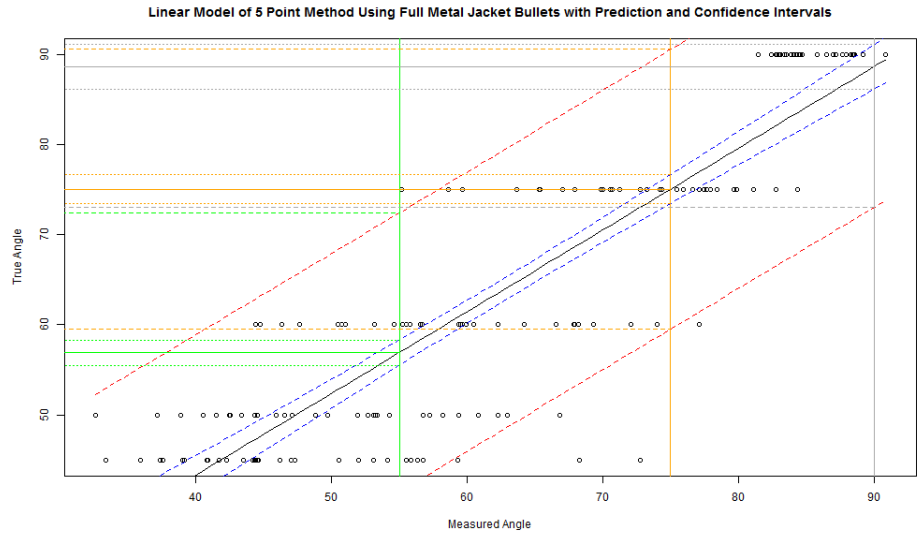

Figure 4.34: Linear model for the 5-point method using full metal jacket bullet angle data

From Table 4.15, the gradient (or measured degrees) has an extremely low p-value, meaning that there appears to be a significant linear relationship between true angle and measured degrees (calculated values).

Table 4.15: Regression table for the 10-point method using full metal jacket bullet angle data

Variable	Estimated Coefficient	Standard Error	T-Value	P-Value
Intercept	7.715492692	2.530086021	3.049498171	0.002716535
Measured Degrees	0.896182821	0.038989348	22.98532473	1.09E-50
Multiple R-Squared	0.781170345		**Adjusted R-Squared**	0.779691766

Based on the R^2 value, the model performs well at explaining the variation in true angle. The estimated regression equation for this model is

$$\hat{y} = 0.8961 \times MeasuredDegrees + 7.7155. \tag{4.14}$$

The standard error (or standard deviation) of the intercept is 2.5300 while the standard error of the slope is 0.0390.

Figure 4.35 on the following page displays the linear model for the 10-point method and the corresponding confidence and prediction intervals. Bullets fired at 55° cannot be distinguished from bullets fired at 75° but can be distinguished from those fired at 90°. Bullets fired from 75° and 90° are not distinguishable from one another. Bullets fired from 50° and 45° can be distinguished from bullets fired from 85° and 80°, respectively.

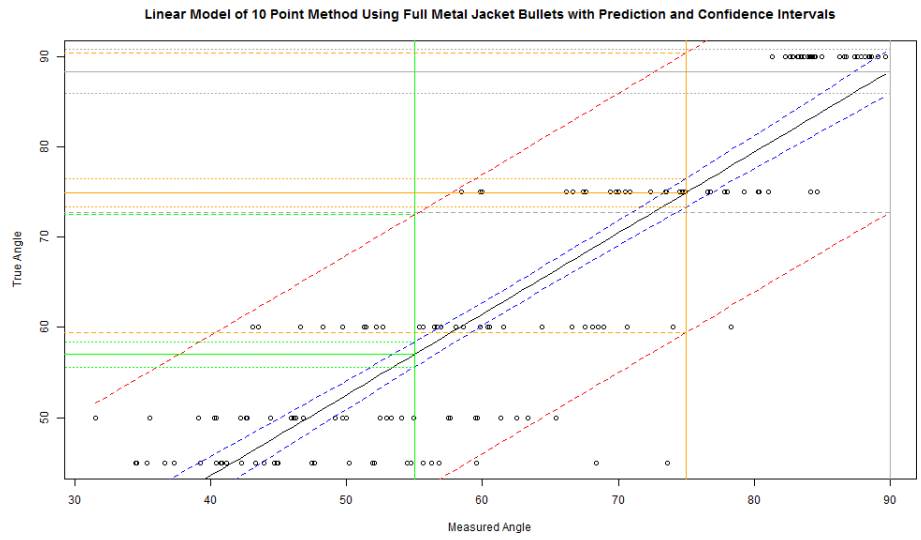

Figure 4.35: Linear model for the 10-point method using full metal jacket bullet angle data

From Table 4.16, the gradient (or measured degrees) has an extremely low p-value, meaning that there appears to be a significant linear relationship between true angle and measured degrees (calculated values).

Table 4.16: Regression table for the 15-point method using full metal jacket bullet angle data

Variable	Estimated Coefficient	Standard Error	T-Value	P-Value
Intercept	8.525406397	2.476697335	3.44224798	0.000750252
Measured Degrees	0.886071691	0.038247083	23.16703947	4.36E-51
Multiple R-Squared	0.783850639		**Adjusted R-Squared**	0.782390171

Based on the R^2 value, the model performs well at explaining the variation in true angle. The estimated regression equation for this model is

$$\hat{y} = 0.8861 \times MeasuredDegrees + 8.5254 \tag{4.15}$$

The standard error (or standard deviation) of the intercept is 2.4767 while the standard error of the slope is 0.0824.

Figure 4.36 on the following page displays the linear model for the 15-point method and the corresponding confidence and prediction intervals. Bullets fired at 55° cannot be distinguished from bullets fired at 75° but can be distinguished from those fired at 90°.

Bullets fired from 75° and 90° are not distinguishable from one another. Bullets fired from 50° and 45° can be distinguished from bullets fired from 85° and 80°, respectively.

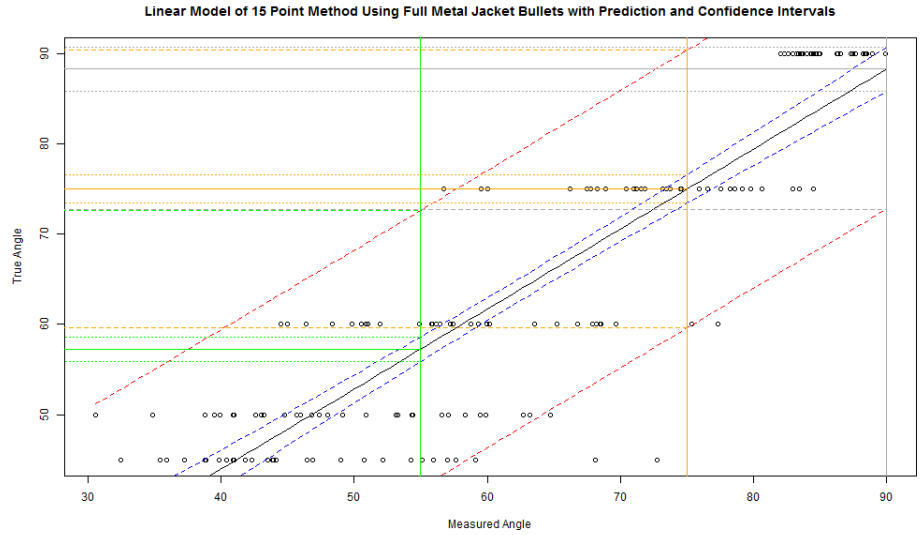

Figure 4.36: Linear model for the 15-point using full metal jacket bullet angle data

4.5.2 Discussion of the FMJ side view bullet deformation analysis

When comparing methods AA, HH, and VV, it can be seen that method AA gave the best results for the full metal jackets using linear regression. Method HH gave better results than did method VV. When comparing the 5-point, 10-point, and 15-point methods, the 15-point method gave the best results followed by the 10-point method. The 5-point method performed the worst of the three. Therefore, a combination of method AA in conjunction with using 15 points would seem to provide the best results for full metal jacket bullets using linear regression.

For the following full metal jacket results as well as for the lead round nose results, all of the point methods (5, 10, and 15) for a specific bullet showed similar higher and lower measured angles as was observed with a specific location method (AA, HH, VV). For example, if a specific bullet had a higher measured angle for the method AA model, similar results would be observed for the 5-point, 10-point, and 15-point model that correspond to the method AA.

45° bullets

For bullets fired at 45°, Sample 1W had high measured angles for all methods. As shown in Figure 4.37, this was a result of the slope on the left side of the bullet not being as steep as other 45° bullets as well as the location of the highest peak, which was not as far to the left as it was on other 45° bullets.

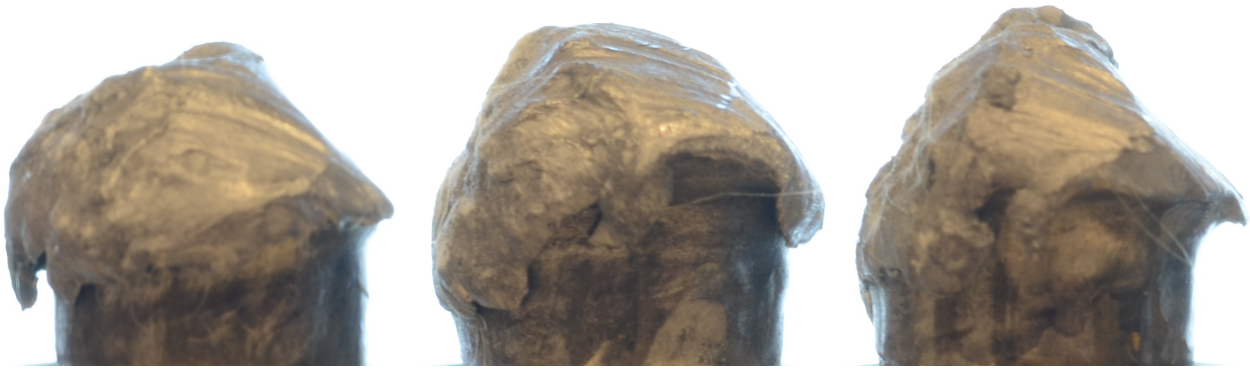

Figure 4.37: 45° problem bullet - Sample 1W (left); other 45° bullets - sample 3A (middle) and sample 1Q (right)

50° bullets

For bullets fired at 50°, samples 3E, 3G, and 6A all presented problems in the data. The problem bullets can be seen in Figure 4.38 on the following page along with other 50° bullets that did not present any problems.

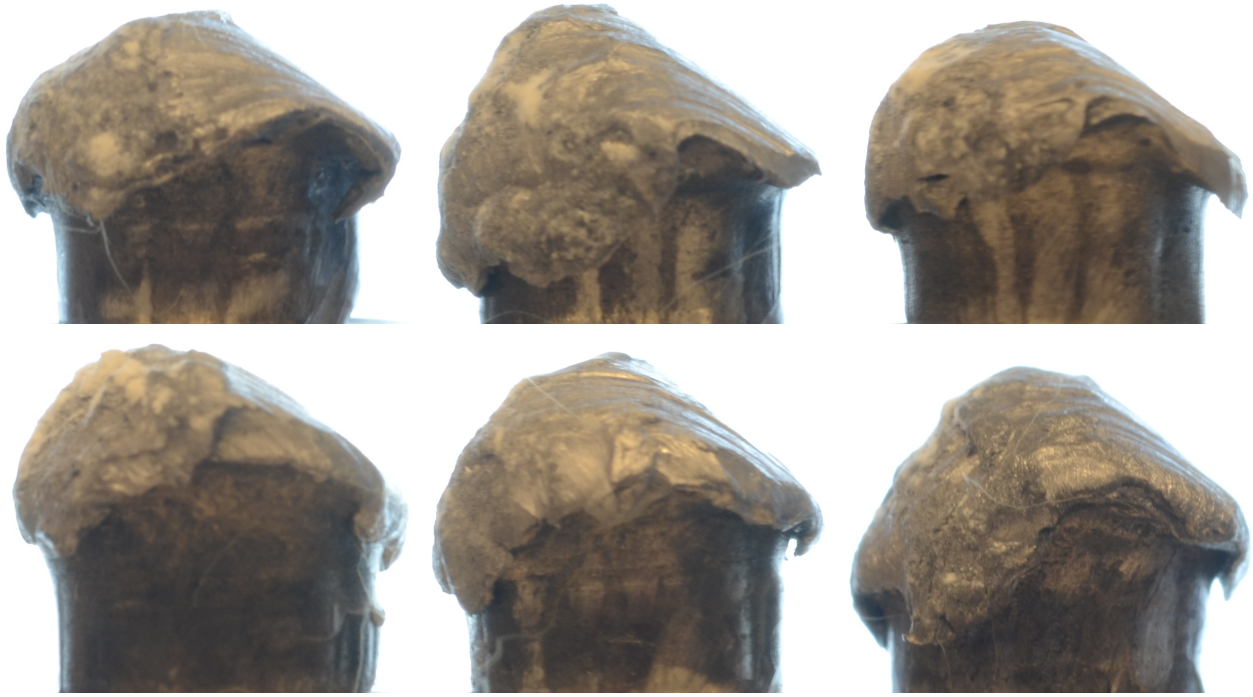

Figure 4.38: 50° problem bullets - Sample 3E (top left) , sample 3G (top middle), and sample 6A (top right); other 50° bullets - Sample 1L (bottom left) , sample 3H (bottom middle), and sample 5B (bottom right)

Sample 3E had higher measured angles for method AA and HH compared to other bullets fired at this angle. This is a result of the slope on the left side of the bullet not being as steep as other 50° bullets as well as the highest peak being more to the right on the top of the bullet.

Sample 3G had lower measured angles for the method AA compared to other bullets fired from this angle. This is a result of the slope on the left side of the bullet being very steep and peeling further down the bearing surface of the bullet. In addition, this would cause the points to be marked further away from each other than they were in other 50° bullets.

Sample 6A had higher measured angles for methods. HH and VV compared to other bullets fired from this angle. This is a result of the slope not being as steep at the location where marking the points would begin (half way point between the highest peak and the left vertical tangent).

60° bullets

For bullets fired at 60°, samples 5D and 4I presented problems in the data. The problem bullets can be seen in Figure 4.39 on the next page along with other 60° bullets that did

not present any problems. Samples 5D and 4I both had higher measured angles for method HH. This is a result of the slope not being as steep at the location where marking the points would begin (half way point between the highest peak and the left vertical tangent).

Figure 4.39: 60° problem bullets - Sample 5D (top left) and sample 4I (top right); other 60° bullets - Sample 1M (bottom left) and sample 5C (bottom right)

75° bullets

For bullets fired at 75°, samples 1D, 1E, and 1J presented problems in the data. The problem bullets can be seen in Figure 4.40 on the following page along with other 75° bullets that did not present any problems. Samples 1D, 1E, and 1J all had lower measured angles for method AA and VV. For method AA, this is a result of a steeper slope on the left side of the bullet. For method VV, it is clear that the slope from the highest peak to above the left vertical is steeper for the problem bullets compared to the other bullets.

Figure 4.40: 75° problem bullets - Sample 1D (top left) , sample 1E (top middle), and sample 1J (top right); other 75° bullets - Sample 1G (bottom left) , sample 4M (bottom middle), and sample 1K (bottom right)

All other pred-res plots, normal Q-Q plots, histograms, and confidence and prediction interval plots for the full metal jacket combined methods, as well as for method AA, HH, VV, 5-point, 10-point, and 15-point can be found in Appendix A.

4.5.3 LRN bullets

From Table 4.17, the gradient (or measured degrees) has an extremely low p-value, meaning that there appears to be a significant linear relationship between true angle and measured degrees (calculated values).

Table 4.17: Regression table for combined lead round nose bullet angle data

Variable	Estimated Coefficient	Standard Error	T-Value	P-Value
Intercept	28.64872007	2.25100901	12.72705704	6.87E-32
Measured Degrees	0.496627414	0.034051521	14.58458831	1.06E-39
Multiple R-Squared	0.32194177		**Adjusted R-Squared**	0.320428247

Based on the R^2 value, the model does not perform well at explaining the variation in true angle. The estimated regression equation for this model is

$$\hat{y} = 0.4966 \times MeasuredDegrees + 28.6487 \tag{4.16}$$

The standard error (or standard deviation) of the intercept is 2.2510 while the standard error of the slope is 0.0341.

Figure 4.41 displays the linear model for the combined methods and the corresponding confidence and prediction intervals. Bullets fired from 45° cannot be distinguished from bullets fired from 90°.

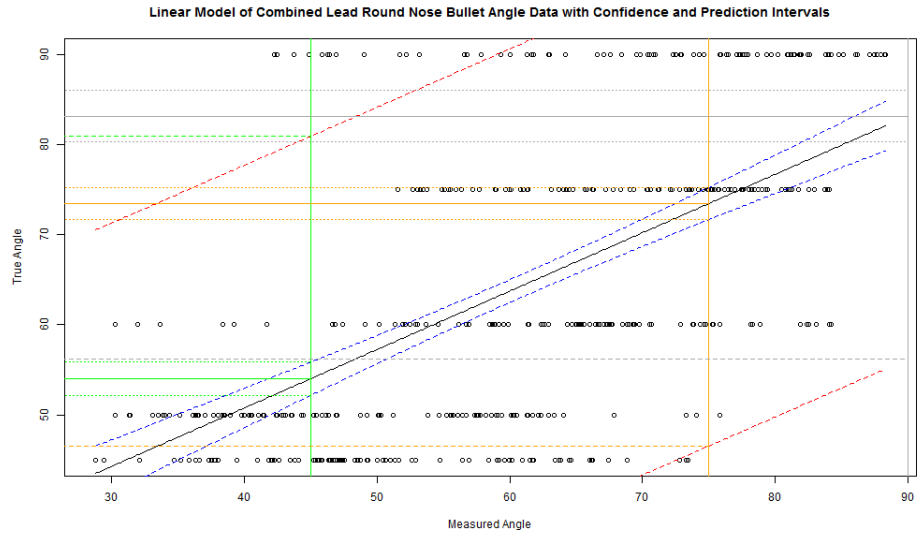

Figure 4.41: Linear model for combined lead round nose bullet angle data

From Table 4.18, the gradient (or measured degrees) has an extremely low p-value, meaning that there appears to be a significant linear relationship between true angle and measured degrees (calculated values).

Table 4.18: Regression table for method AA using lead round nose bullet angle data

Variable	Estimated Coefficient	Standard Error	T-Value	P-Value
Intercept	22.10626142	3.86227266	5.72364081	5.60E-08
Measured Degrees	0.509305869	0.05842547	8.71718914	5.34E-15
Multiple R-Squared	0.339254407		**Adjusted R-Squared**	0.33478991

Based on the R^2 value, the model does not perform well at explaining the variation in true angle. The estimated regression equation for this model is

$$\hat{y} = 0.5093 \times MeasuredDegrees + 22.1062 \tag{4.17}$$

The standard error (or standard deviation) of the intercept is 3.8623 while the standard error of the slope is 0.0584.

Figure 4.42 displays the linear model for method AA and the corresponding confidence and prediction intervals. Bullets fired at 90°, 75°, 60°, 50°, and 45° cannot be distinguished from each other.

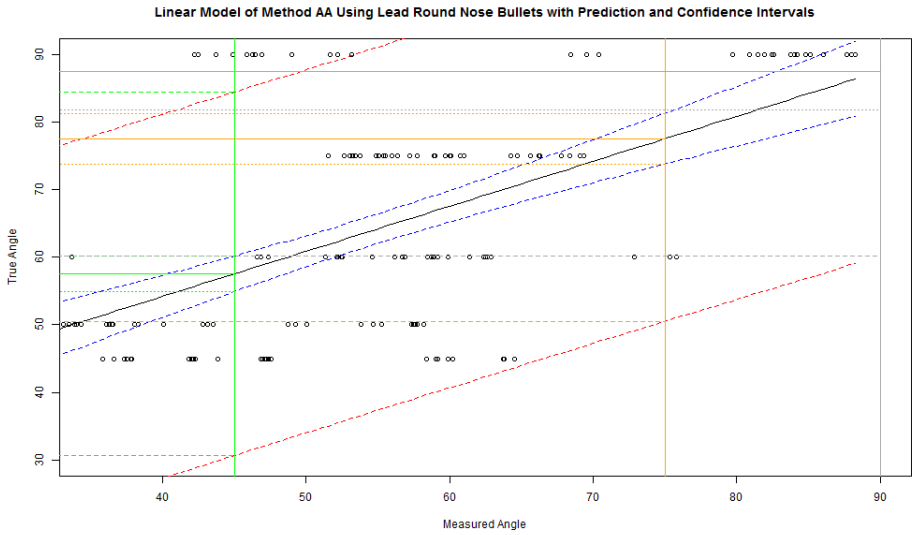

Figure 4.42: Linear model for method AA using lead round nose bullet angle data

From Table 4.19, the gradient (or measured degrees) has an extremely low p-value, meaning that there appears to be a significant linear relationship between true angle and measured degrees (calculated values).

Table 4.19: Regression table for method HH using lead round nose bullet angle data

Variable	Estimated Coefficient	Standard Error	T-Value	P-Value
Intercept	28.91020063	3.500992792	8.25771498	7.62E-14
Measured Degrees	0.509455113	0.052960308	9.619564849	2.58E-17
Multiple R-Squared	0.384707558		**Adjusted R-Squared**	0.380550177

Based on the R^2 value, the model does not perform well at explaining the variation in true angle. The estimated regression equation for this model is

$$\hat{y} = 0.5095 \times MeasuredDegrees + 28.9102 \tag{4.18}$$

The standard error (or standard deviation) of the intercept is 3.5010 while the standard error of the slope is 0.0530.

Figure 4.43 displays the linear model for method HH and the corresponding confidence and prediction intervals. Bullets fired at 90°, 75°, 60°, 50°, and 45° cannot be distinguished from each other.

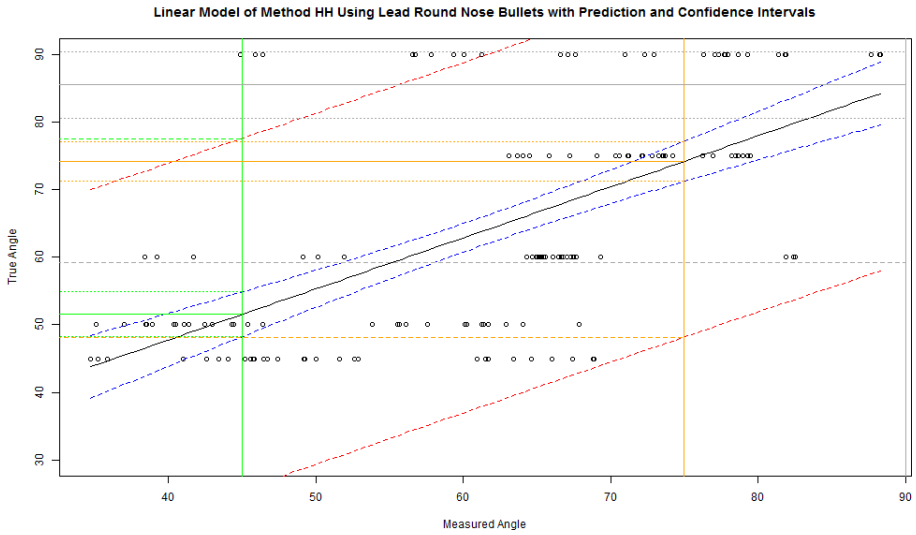

Figure 4.43: Linear model for method HH using lead round nose bullet angle data

From Table 4.20, the gradient (or measured degrees) has an extremely low p-value, meaning that there appears to be a significant linear relationship between true angle and measured degrees (calculated values).

Table 4.20: Regression table for method VV using lead round nose bullet angle data

Variable	Estimated Coefficient	Standard Error	T-Value	P-Value
Intercept	34.92969817	3.580069965	9.756708253	1.13E-17
Measured Degrees	0.471121262	0.054156526	8.699251944	5.93E-15
Multiple R-Squared	0.338331566		**Adjusted R-Squared**	0.333860833

Based on the R^2 value, the model does not perform well at explaining the variation in true angle. The estimated regression equation for this model is

$$\hat{y} = 0.4711 \times MeasuredDegrees + 34.9297 \tag{4.19}$$

The standard error (or standard deviation) of the intercept is 3.5801 while the standard error of the slope is 0.0542.

Figure 4.44 displays the linear model for method VV and the corresponding confidence and prediction intervals. Bullets fired at 90°, 75°, 60°, 50°, and 45° cannot be distinguished from each other.

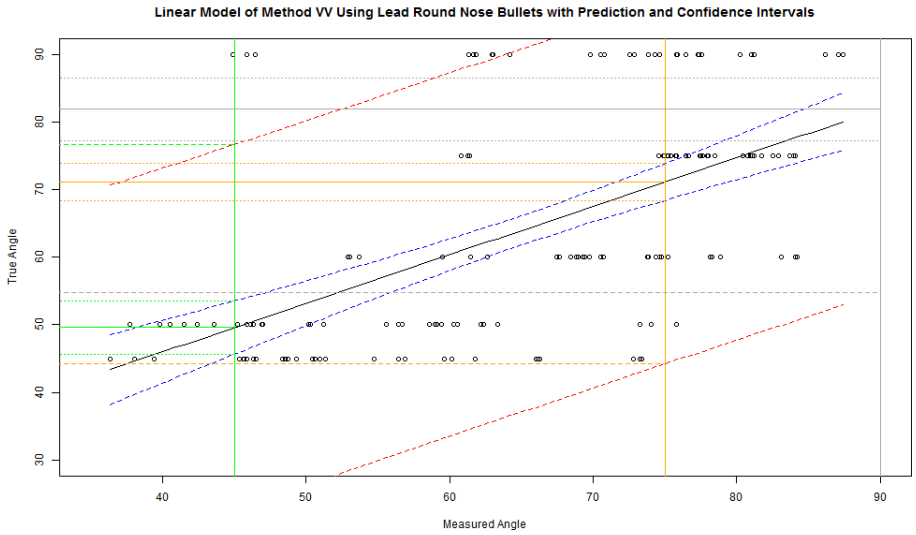

Figure 4.44: Linear model for method VV using lead round nose bullet angle data

From Table 4.21, the gradient (or measured degrees) has an extremely low p-value, meaning that there appears to be a significant linear relationship between true angle and measured degrees (calculated values).

Table 4.21: Regression table for the 5-point method using lead round nose bullet angle data

Variable	Estimated Coefficient	Standard Error	T-Value	P-Value
Intercept	29.24214812	3.827522158	7.639968343	2.51E-12
Measured Degrees	0.487953315	0.057899791	8.427548832	2.87E-14
Multiple R-Squared	0.324273667		**Adjusted R-Squared**	0.319707949

Based on the R^2 value, the model performs well at explaining the variation in true angle. The estimated regression equation for this model is

$$\hat{y} = 0.4880 \times MeasuredDegrees + 29.2421 \tag{4.20}$$

The standard error (or standard deviation) of the intercept is 3.8275 while the standard error of the slope is 0.0579.

Figure 4.45 displays the linear model for the 5-point method and the corresponding confidence and prediction intervals. Bullets fired at 90°, 75°, 60°, 50°, and 45° cannot be distinguished from each other.

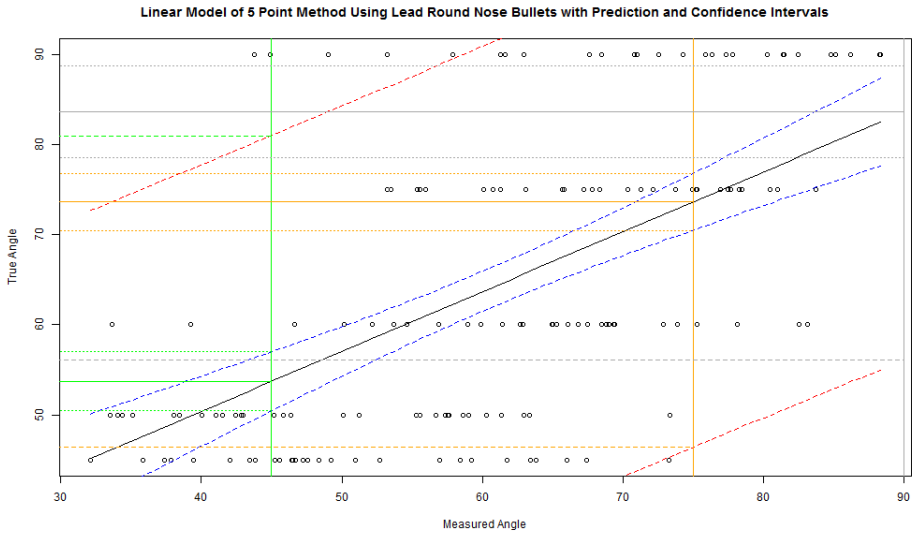

Figure 4.45: Linear model for the 5-point method using lead round nose bullet angle data

From Table 4.22, the gradient (or measured degrees) has an extremely low p-value, meaning that there appears to be a significant linear relationship between true angle and measured degrees (calculated values).

Table 4.22: Regression table for the 10-point method using lead round nose bullet angle data

Variable	Estimated Coefficient	Standard Error	T-Value	P-Value
Intercept	28.40977634	3.925799098	7.236686248	2.31E-11
Measured Degrees	0.500376857	0.059386448	8.425775088	2.90E-14
Multiple R-Squared	0.324181428		**Adjusted R-Squared**	0.319615086

Based on the R^2 value, the model performs well at explaining the variation in true angle. The estimated regression equation for this model is

$$\hat{y} = 0.5004 \times MeasuredDegrees + 28.4098 \tag{4.21}$$

The standard error (or standard deviation) of the intercept is 3.9258 while the standard error of the slope is 0.0594.

Figure 4.46 displays the linear model for the 10-point method and the corresponding confidence and prediction intervals. Bullets fired at 90°, 75°, 60°, 50°, and 45° cannot be distinguished from each other.

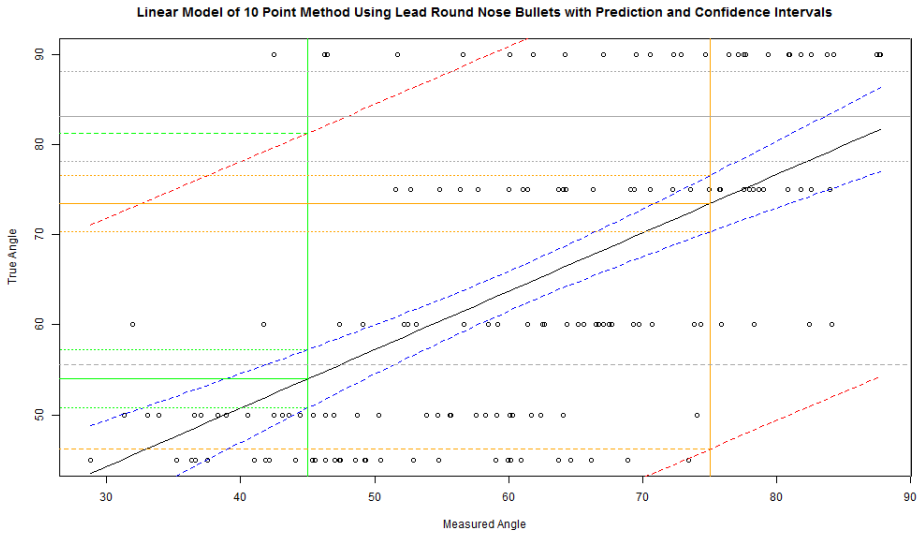

Figure 4.46: Linear model for the 10-point method using lead round nose bullet angle data

From Table 4.23, the gradient (or measured degrees) has an extremely low p-value, meaning that there appears to be a significant linear relationship between true angle and measured degrees (calculated values).

Table 4.23: Regression table for the 15-point method using lead round nose bullet angle data

Variable	Estimated Coefficient	Standard Error	T-Value	P-Value
Intercept	28.29423575	3.99358404	7.084923083	5.25E-11
Measured Degrees	0.501552071	0.060411846	8.302213907	5.91E-14
Multiple R-Squared	0.317742067		**Adjusted R-Squared**	0.313132216

Based on the R^2 value, the model performs well at explaining the variation in true angle. The estimated regression equation for this model is

$$\hat{y} = 0.5016 \times MeasuredDegrees + 28.2942 \tag{4.22}$$

The standard error (or standard deviation) of the intercept is 3.9936 while the standard error of the slope is 0.0604.

Figure 4.47 displays the linear model for the 15-point method and the corresponding confidence and prediction intervals. Bullets fired at 90°, 75°, 60°, 50°, and 45° cannot be distinguished from each other.

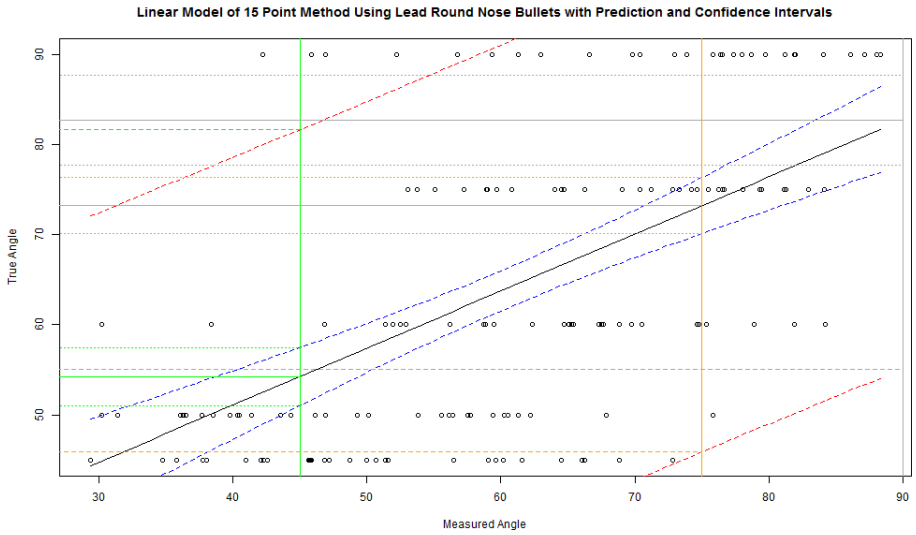

Figure 4.47: Linear model for the 15-point method using lead round nose bullet angle data

4.5.4 Discussion of the LRN side view bullet deformation analysis

Method HH in conjunction with using 15 points performed the best when using linear regression with lead round nose bullets. Method VV performed the second best and AA the worst. Using 10 points performed better than using only 5 points.

None of the methods were able to distinguish between any angles (90°, 75°, 60°, 50°, and 45°).

45° bullets

For bullets fired at 45°, samples 2D, 1Z, and 2A presented problems in the data. The problem bullets can be seen in Figure 4.48 on the next page along with other 45° bullets that did not present any problems. Samples 2D, 1Z, and 2A all had higher measured angles for method

AA, HH, and VV. This is a result of the slope on the left side of the bullet not being as steep as the other 45° bullets.

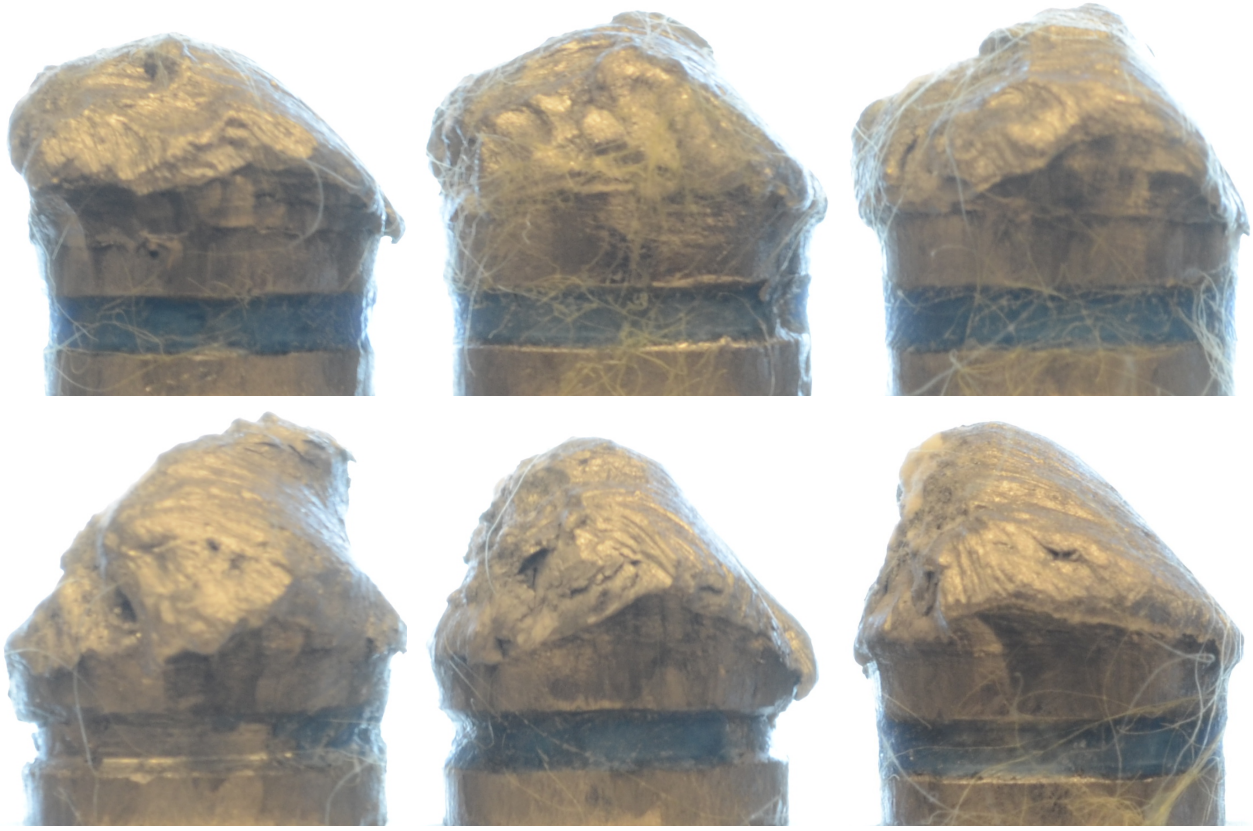

Figure 4.48: 45° problem bullets - Sample 2D (top left) , sample 1Z (top middle), and sample 2A (top right); other 45° bullets - Sample 2C (bottom left) , sample 3F (bottom middle), and sample 1U (bottom right)

60° bullets

For bullets fired at 60°, samples 8X and 3S presented problems in the data. The problem bullets can be seen in Figure 4.49 on the following page along with other 50° bullets that did not present any problems. Sample 8X had higher measured angles for method AA, HH, and VV than other 60° bullets fired at this angle. This is a result of there not being any curve to the left side of the bullet. There is minimal slope on this side.

Sample 3S on the other hand resulted in lower measured angles for method AA, HH, and VV. This is a result of the slope being steeper on the left side of the bullet as compared to other bullets fired from this angle.

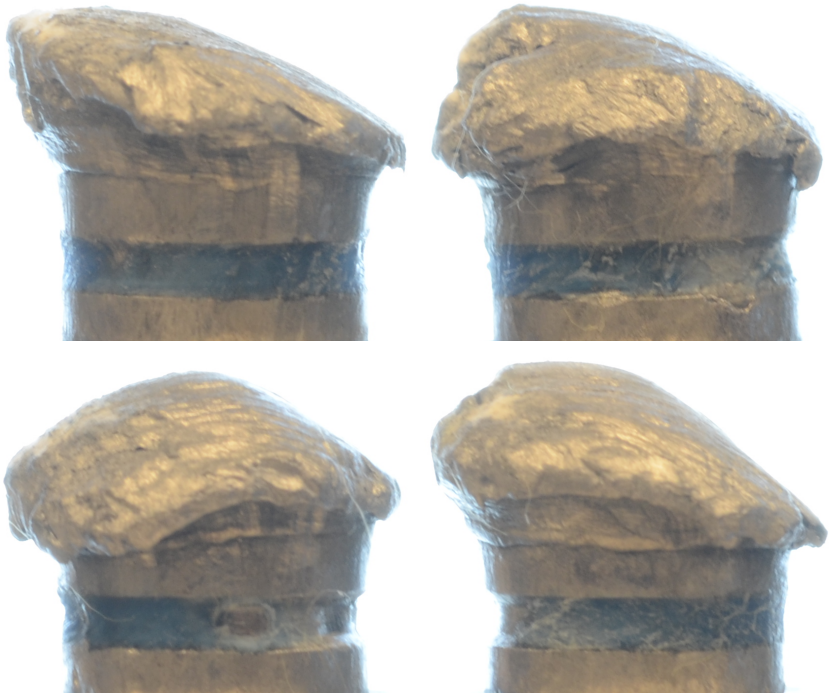

Figure 4.49: 60° problem bullets - Sample 8X (top left) and sample 3S (top right); other 60° bullets - Sample 8U (bottom left) and sample 3R (bottom right)

75° bullets

For bullets fired at 75°, sample 5P presented a major problem in the data. The problem bullet can be seen in Figure 4.49 along with other bullets fired at 75° that did not present any problems. Sample 5P resulted in an extremely lower measured angle for method VV than other bullets fired at 75°. This is a result of the slope being more steep on the top of the bullet compared to the other bullets fired at 75°.

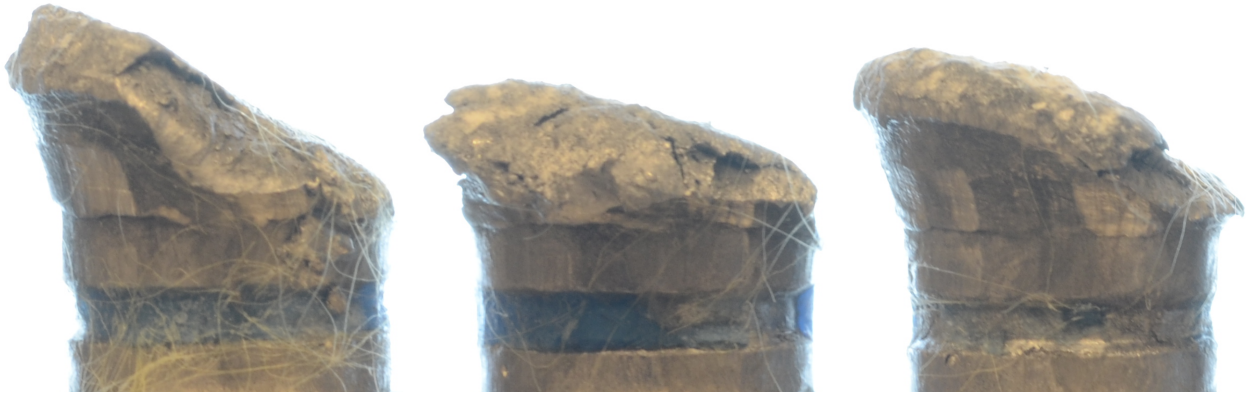

Figure 4.50: 75° problem bullet - Sample 5P (left); other 75° bullets - sample 5C (middle) and sample 3X (right)

90° bullets

For bullets fired at 90°, sample 5V presented a major problem in the data. The problem bullet can be seen in Figure 4.51 along with other bullets fired at 90° that did not present any problems. Sample 5V resulted in an extremely lower measured angle for method HH and VV compared to other bullets fired at 90°. This is a result of the slope being more steep on the left side of the bullet compared to the other bullets fired at 90°.

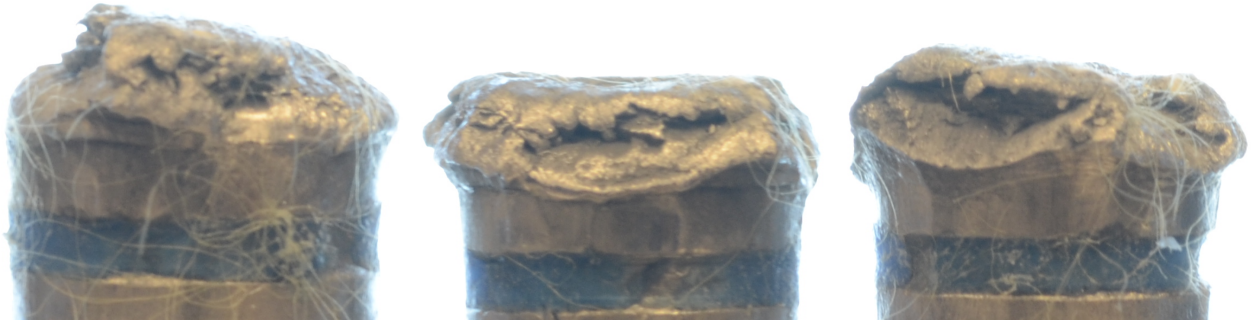

Figure 4.51: 90° problem bullet - Sample 5V (left); other 90° bullets - sample 5S (middle) and sample 5F (right)

A common event observed with the lead round nose bullets is that on some bullets, parts of the lead would break off. This changes the structure of the bullets, thus influencing the results compared to what would be observed if no parts would have broken off.

All other pred-res plots, normal Q-Q plots, histograms, and confidence and prediction interval plots for the lead round nose combined methods, as well as for method AA, HH, VV, 5-point, 10-point, and 15-point can be found in Appendix A.

4.6 Multiple linear regression using $Minor \times X\_Patch$ for FMJ bullets

From Table 4.24, the slope for X_Patch and Minor have a low p-value, meaning that there appears to be a significant linear relationship between each of these variables and the true angle.

Table 4.24: Regression table for $Minor \times X\_Patch$

Variable	Estimated Coefficient	Standard Error	T-Value	P-Value
Intercept	-61.5161006	13.94763154	-4.410505141	6.16E-05
X_Patch	0.048003162	0.011264522	4.261446691	9.96E-05
Minor	0.041629961	0.005046513	8.249252727	1.27E-10
X_Patch:Minor	-1.24E-05	3.75E-06	-3.310561873	0.001816743
Multiple R-Squared	0.922426653		**Adjusted R-Squared**	0.917367522

The slope for X_Patch:Minor has a less significant p-value but still shows there to be a linear relationship between it and the true angle. Based on the R^2 value, the model performs great at explaining the variation in true angle. The estimated regression equation for this model is:

$$\hat{y} = (-1.24 \times 10^5) \times X\_Patch : Minor + 0.042 \times Minor + 0.048 \times X\_Patch - 61.516 \quad (4.23)$$

The standard error (or standard deviation) of the intercept is 13.946 while the standard error for the slope of the three variables are 0.011, 0.005, and 3.75×10^6, respectively.

Figures 4.52 and 4.53 display the linear models for Minor and X_Patch. The measured angles resulting from each individual true angle is grouped well together in the Minor model and are more spread out in the X_Patch model. This would be expected as we see a lower p-value and lower standard error for the Minor model.

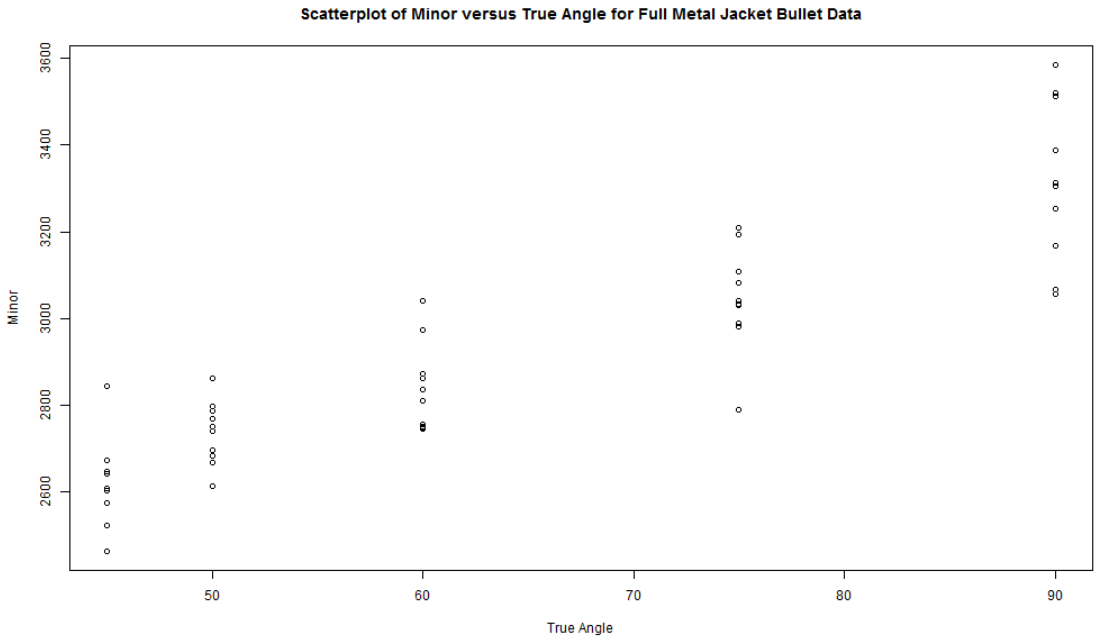

Figure 4.52: Linear model of Minor for FMJ bullet data

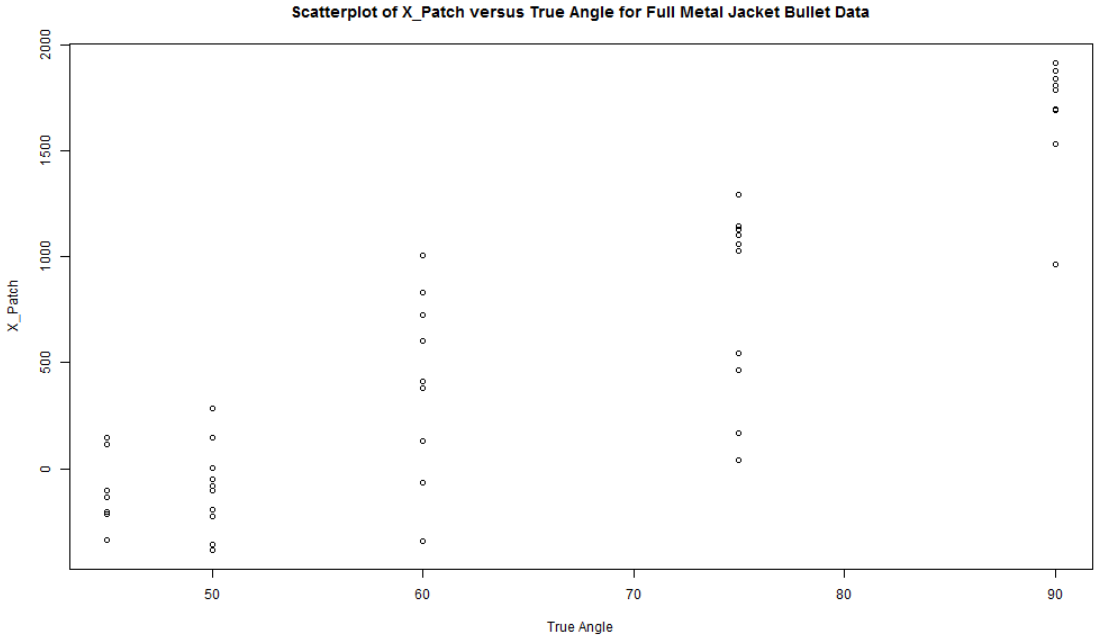

Figure 4.53: Linear model of X_Patch for FMJ bullet data

4.6.1 Description of variables used in multiple linear regression and principal component analysis

The following generalized description will be used to help clarify and describe the following results and figures relating to the distribution of glass on the front of the bullet, bullet outlines, and particle selection. In this description, the term "value" for a specific variable refers to the value of the original data. For example, it would represent the pixel value recorded from ImageJ of a bullet outline.

Area corresponds to the total surface area of the front view of the bullet. A large Area value implies that the nose flattened extensively.

Circularity represents the shape of the front view of the bullet compared to a circle. A low value would indicate that the nose of the bullet flattened in a non-circular fashion (e.g., rough edges, straight lines, etc.). If Circularity is equal to 1, it is a perfect circle. As the value decreases from 1, the shape becomes less circular.

Aspect Ratio (AR) denotes whether the nose of the bullet flattened more into a circular or elliptical shape. It uses the best fitting ellipse of the front view of the bullet (ratio of the major to minor axis). If AR is equal to 1, the shape is a perfect circle. As the value of AR increases above 1, the shape becomes more elliptical. A large value would indicate that the shape of the front view of the bullet is more elliptical.

Minor corresponds to the length of the minor (or secondary) axis of the best fitting ellipse of the front view of the bullet. A larger value would indicate that the nose flattened more following perforation.

Figure 4.54 shows an example of an outlined bullet and where the major and minor axes are located.

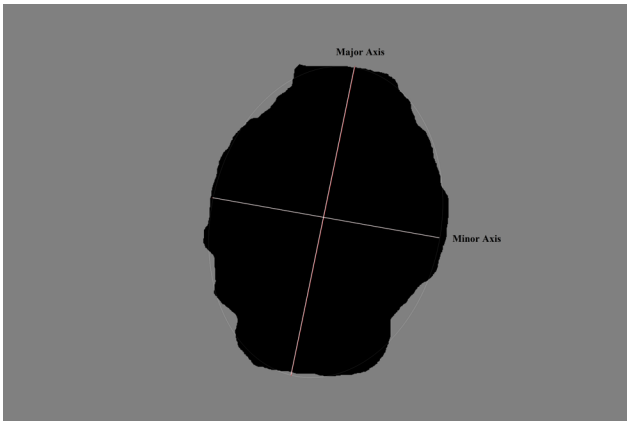

Figure 4.54: Outline of a bullet showing where the major and minor axes are located

Area Largest Particle (ALP) represents how the glass distributes to the front of the bullet and refers to the largest contiguous area of glass deposited onto the front surface of the bullet. A low value would indicate that the largest particle for a particular sample is small.

X_Patch corresponds to the rightmost vertical edge of a distinctive, contiguous area of glass that is located the furthest horizontal distance away from the center of a bullet. X_Patch is determined while viewing the front of the bullet from above.

45° bullets - Minor

Figure 4.55 shows the 45° problem bullet for the Minor model and other 45° bullets. Sample 1T has a large value for Minor compared to other 45° bullets.

Figure 4.55: 45° problem bullet - sample 1T (left); other 45° bullets - samples 1W (middle) and 3K (right)

50° bullets - Minor

Figure 4.56 on the following page shows the 50° problem bullets for the Minor model and other 50° bullets. Sample 3D has a large value for Minor while sample 3I has a low value for Minor than compared to other 50° bullets.

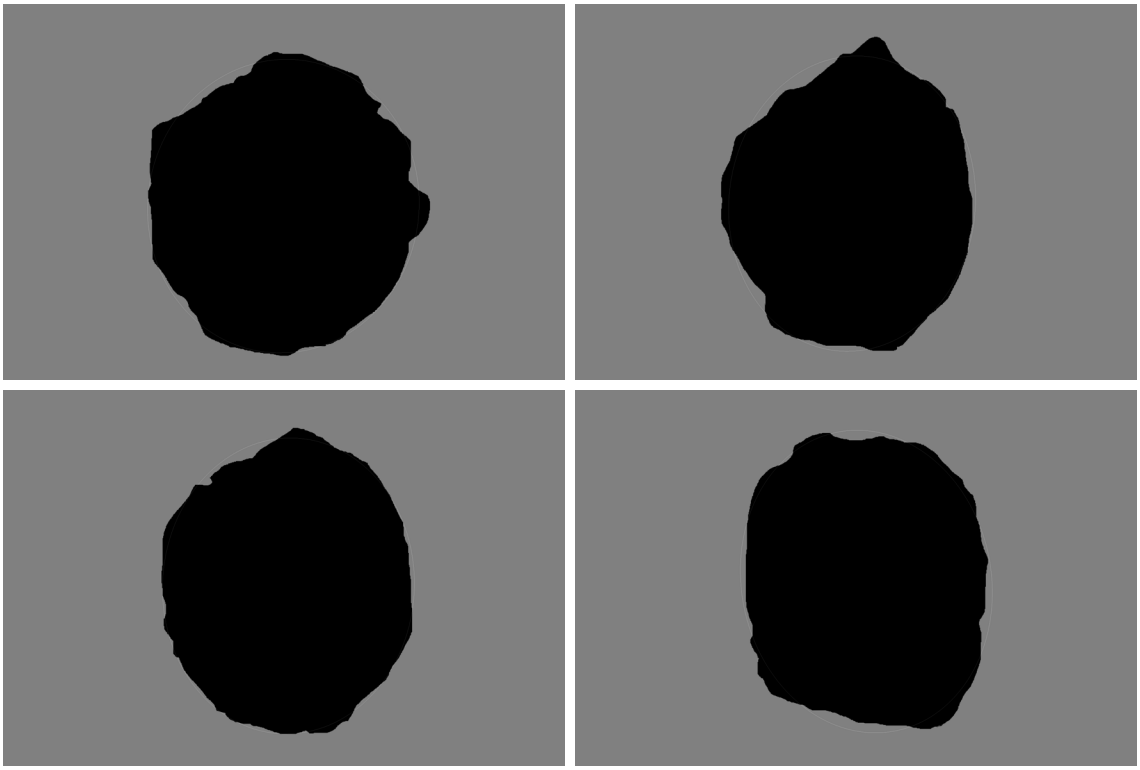

Figure 4.56: 50° problem bullets - samples 3D (top left) and 3I (top right); other 50° bullets - samples 3J (bottom left) and 3L (bottom right)

60° bullets - Minor

Figure 4.57 on the next page shows the 60° problem bullets for the Minor model and other 60° bullets. Samples 4I and 5D have a large value for Minor compared to other 60° bullets.

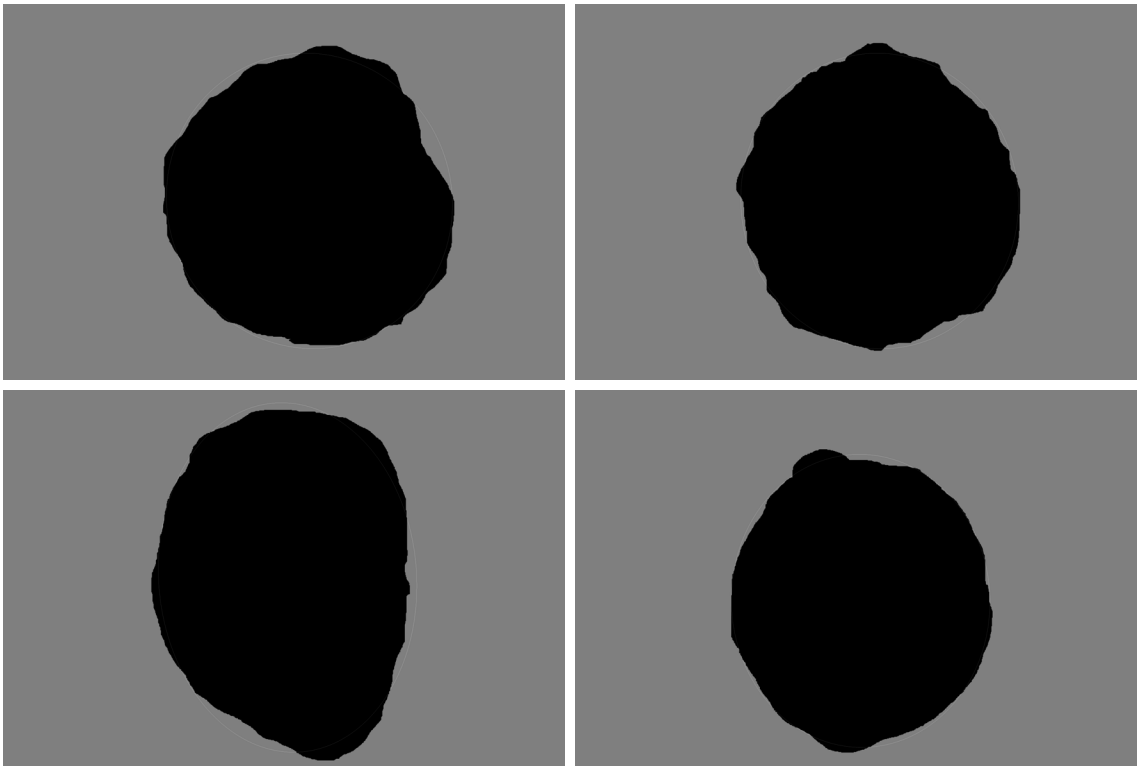

Figure 4.57: 60° problem bullets - samples 4I (top left) and 5D (top right); other 60° bullets - samples 1B (bottom left) and 1M (bottom right)

75° bullets - Minor

Figure 4.58 shows the 75° problem bullets for the Minor model and other 75° bullets. Sample 1H has a low value for Minor compared to other 75° bullets.

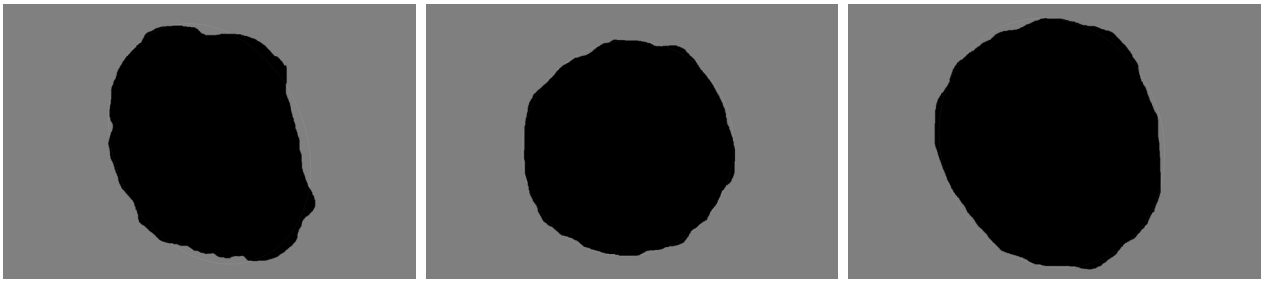

Figure 4.58: 75° problem bullet - sample 1H (left); other 75° bullets - samples 1E (middle) and 4L (right)

90° bullets - Minor

Figure 4.59 on the next page shows the 90° problem bullets for the Minor model and other 90° bullets. Samples 8J, 8G, 8D, and 5A have a low value for Minor compared to other 90° bullets.

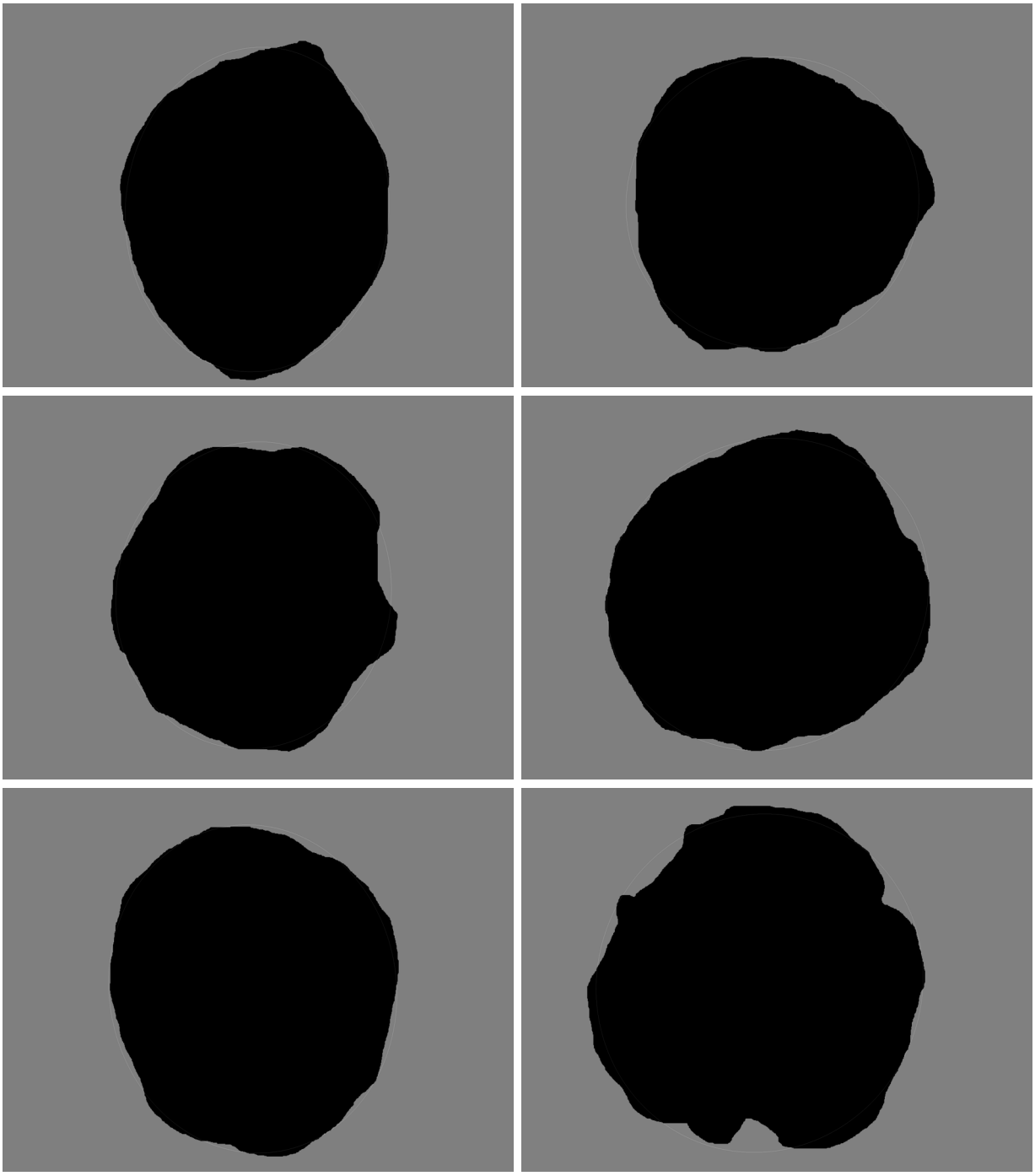

Figure 4.59: 90° problem bullets - samples 8J (top row, left), 8G (top row, right), 8D (middle row, left), and 5A (middle row, right); other 90° bullets - samples 8A (bottom row, left) and 8K (bottom row, right)

45° bullets - X_Patch

Figure 4.60 shows the 45° problem bullets for the X_Patch model and other 45° bullets. Samples 3B, 3K, and 1X have a high value for X_Patch compared to other 45° bullets.

Figure 4.60: 45° problem bullets - samples 3B (top left) and 3K (top right); other 45° bullets - samples 1Q (bottom left) and 1W (bottom right)

50° bullets - X_Patch

Figure 4.61 on the next page shows the 50° problem bullets for the X_Patch model and other 50° bullets. Samples 3L and 6A have a low value for X_Patch compared to other bullets fired from 50°.

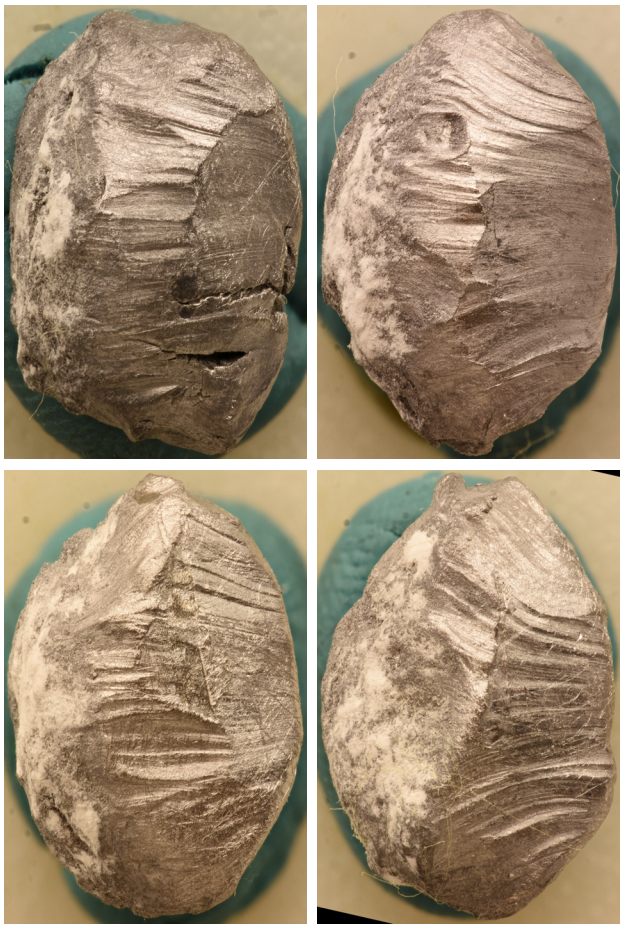

Figure 4.61: 50° problem bullets - samples 3L (top left) and 6A (top right); other 50° bullets - samples 3J (bottom left) and 3E (bottom right)

60° bullets - X_Patch

Figure 4.62 on the following page shows the 60° problem bullets for the X_Patch model and other 60° bullets. Samples 4I, 5E, and 5D have low values for X_Patch compared with other bullets fired from 60°.

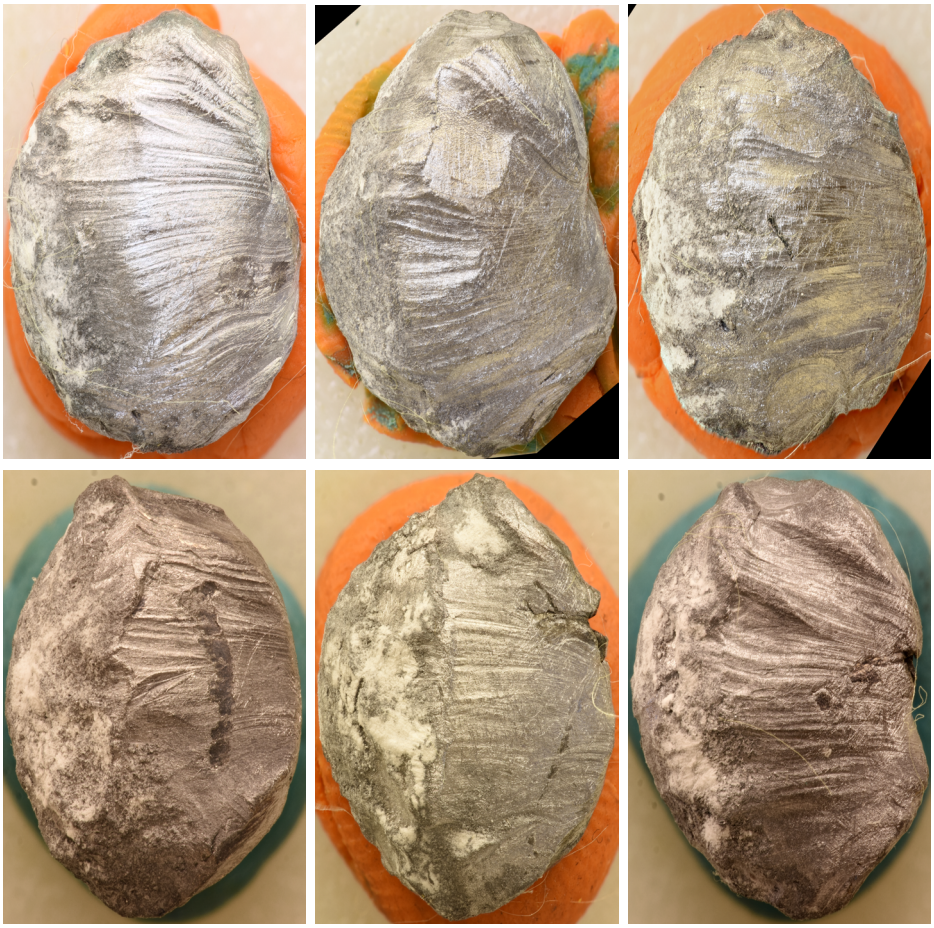

Figure 4.62: 60° problem bullets - samples 4I (top left), 5E (top middle), and 5D (top right); other 60° bullets - samples 1M (bottom left), 5C (bottom middle), and 8H (bottom right)

75° bullets - X_Patch

Figure 4.63 on the next page shows the 75° problem bullets for the X_Patch model and other 75° bullets. Samples 8F, 1E, 1G, and 1D have low values for X_Patch compared with other bullets fired from 75°.

Figure 4.63: 75° problem bullets - samples 8F (top row left), 1E (top row right), 1G (middle row left), and 1D (middle row right); other 75° bullets - samples 1F (bottom row left) and 1J (bottom row right)

90° bullets - X_Patch

Figure 4.64 shows the 90° problem bullet for the X_Patch model and other 90° bullets. Sample 8I has a low value for X_Patch compared with other bullets fired from 90°.

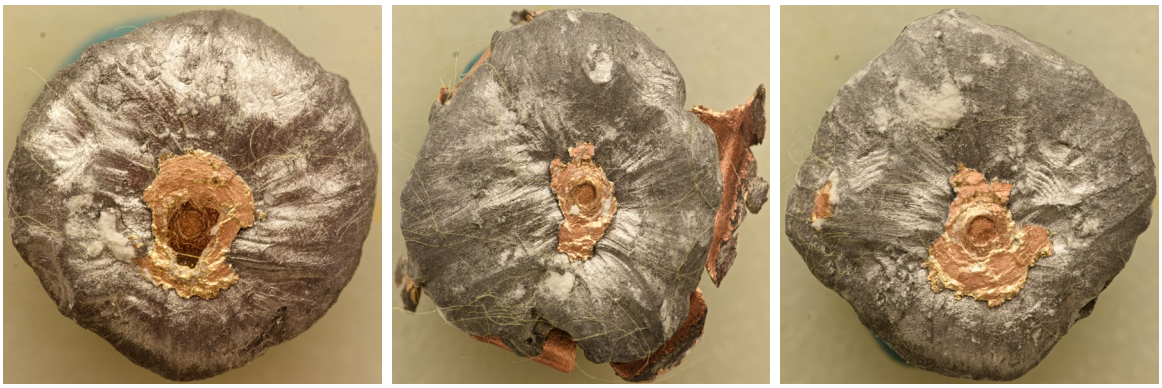

Figure 4.64: 90° problem bullets - sample 8I (left); other 90° bullets - samples 8K (middle) and 8L (right)

Figure 4.65 on the next page displays a $3D$ scatter plot of $Minor \times X\_Patch$. The multiple regression model of $Minor \times X\_Patch$ appears to perform well at providing some separation between individual groups of angles although there is some overlap between the angles.

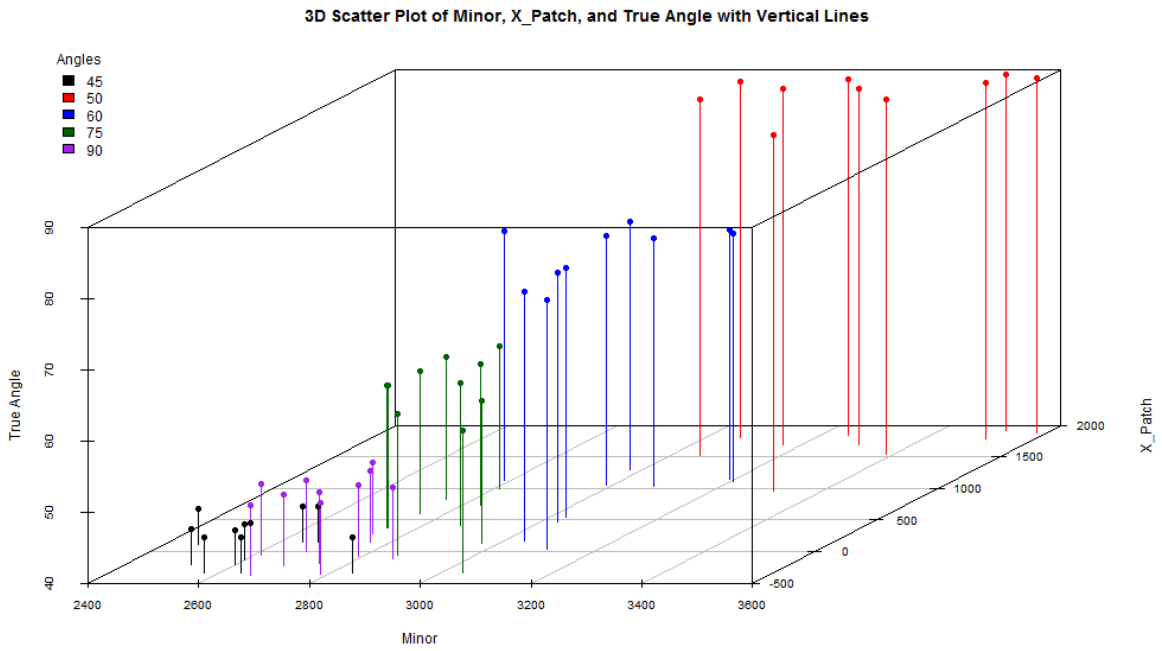

Figure 4.65: 3D Scatter plot of Minor and X_Patch

Figures 4.66 on the following page, 4.67 on page 125, 4.68 on page 126 displays contour plots of the upper, fitted, and lower predictions for $X\_Patch \times Minor$. If a measured bullet was found to have an X_Patch value of -200 and a Minor value of 2700, the fitted value is 47.9° and falls between 38.0° and 57.8°. If the X_Patch value was found to be 400 with a Minor value of 3000, the fitted value is 67.7° and falls between 57.7° and 77.6°. An X_Patch value of 1000 and Minor value of 3300 results in a fitted value of 82.9 and falls between 72.8° and 92.9°. The prediction intervals have an approximate range of 20°-30°.

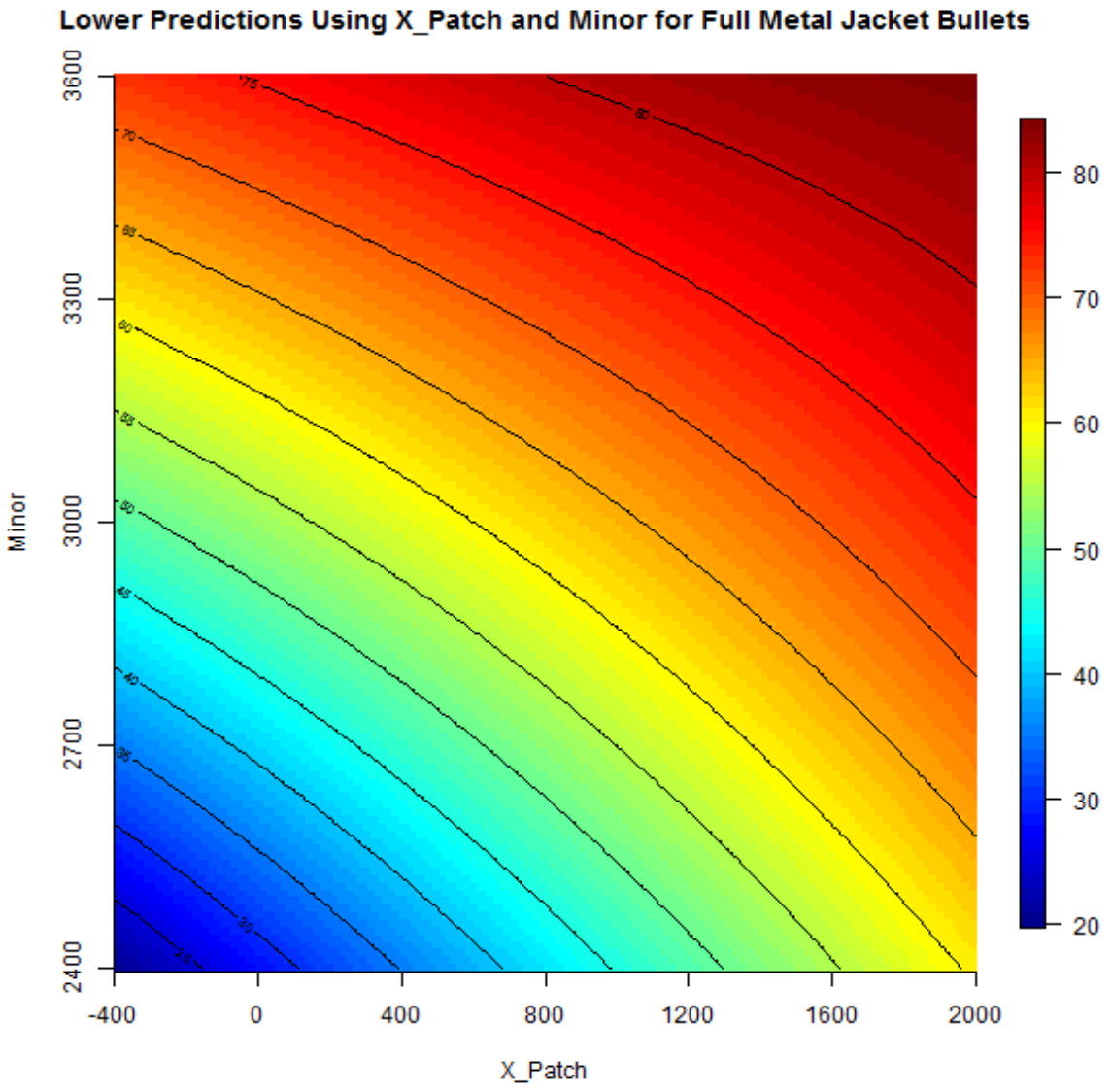

Figure 4.66: Contour plot showing the lower prediction values for Minor × X_Patch

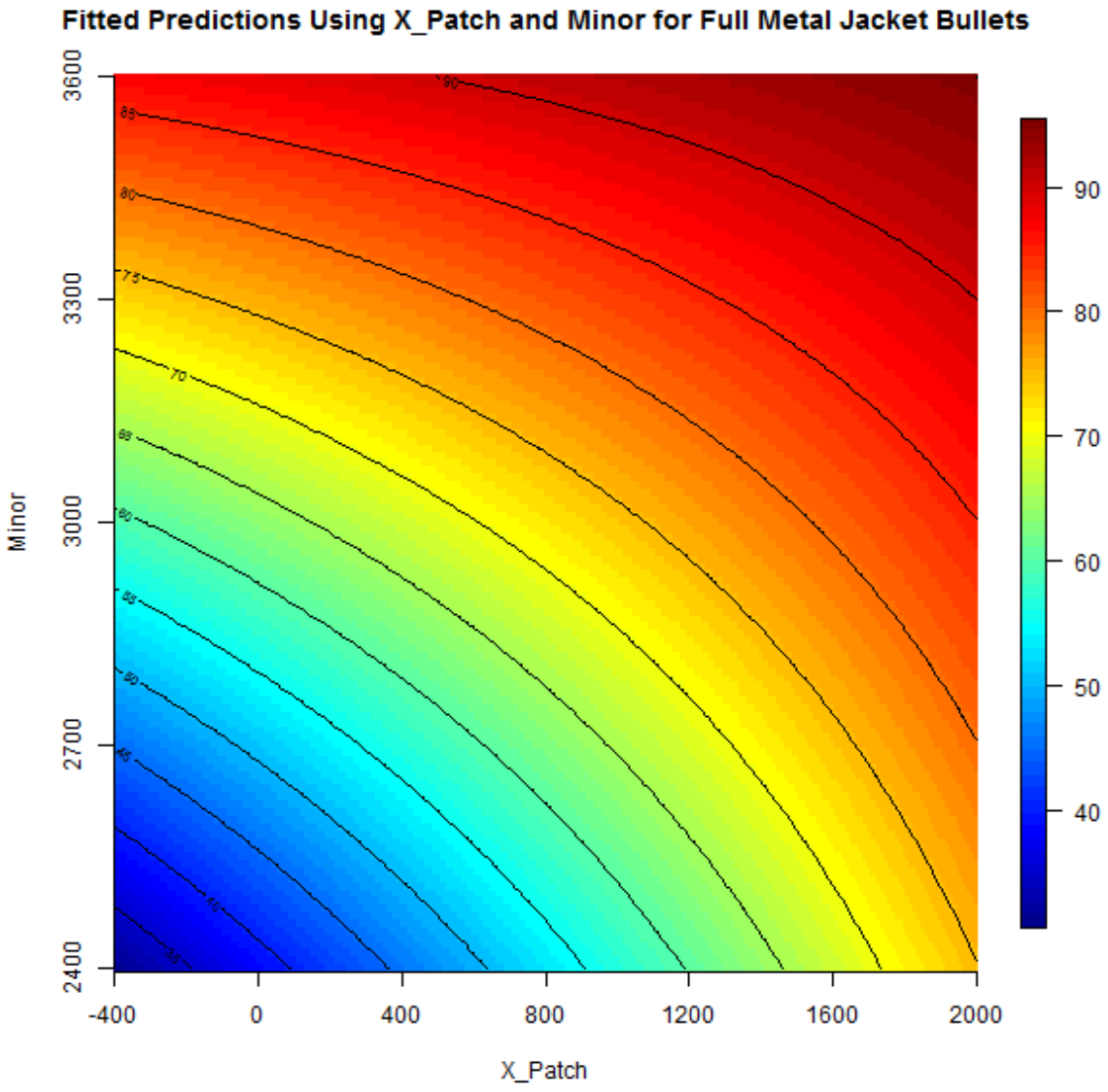

Figure 4.67: Contour plot showing the fitted prediction values for $Minor \times X\_Patch$

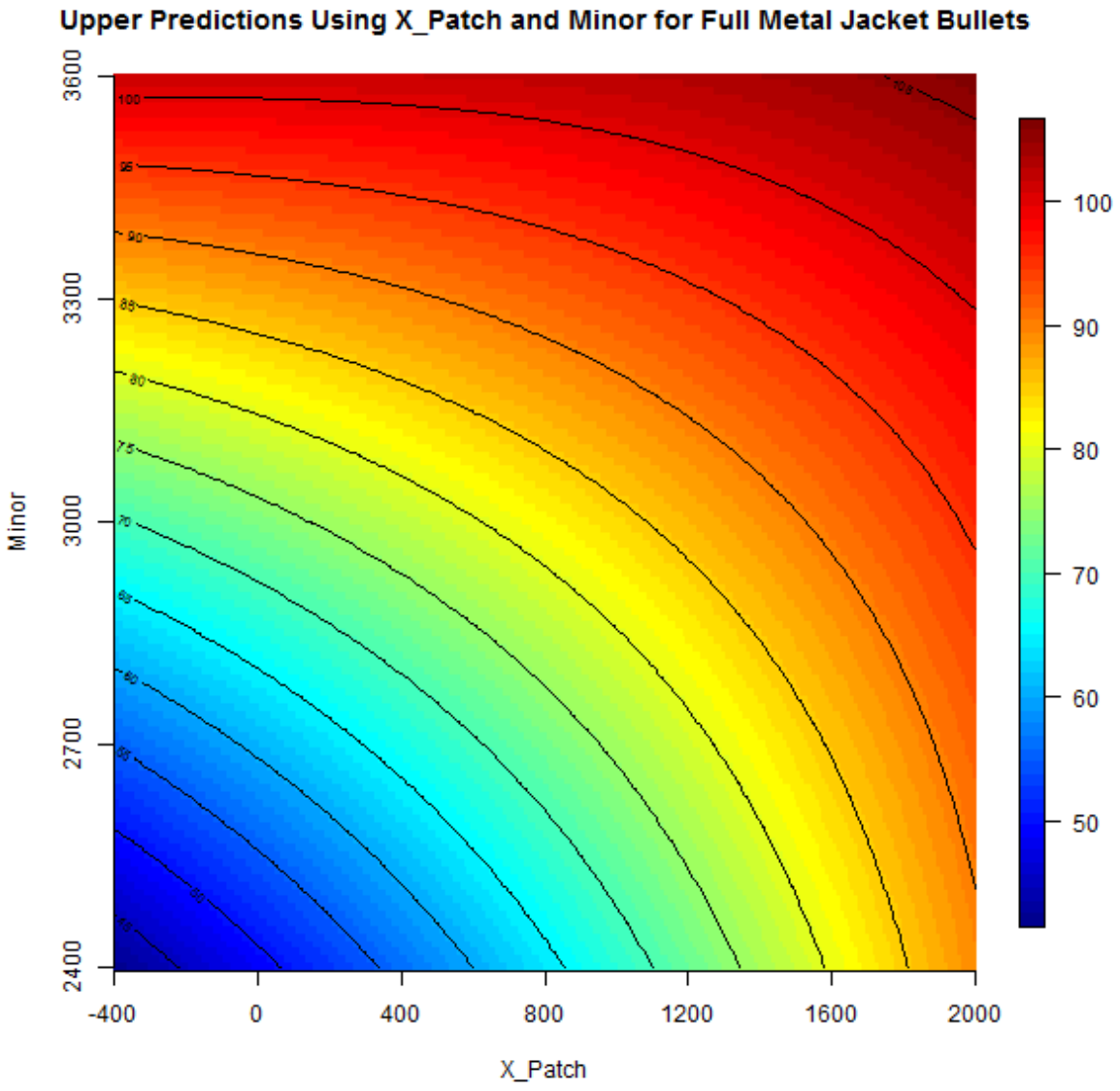

Figure 4.68: Contour plot showing the upper prediction values for $Minor \times X\_Patch$

Figure 4.69 on the next page displays the results of the testing and training performed on $X\_Patch \times Minor$. Bullets fired from 90° cannot be distinguished from bullets fired from 70° but can be distinguished from bullets fired from 60°. Bullets fired from 75° cannot be distinguished from bullets fired from 60° but can be from bullets fired from 50°. Bullets fired from 60° cannot be distinguished from bullets fired from 50° or 45°. There was only one point between the 60° and 45° bullets which resulted in overlap.

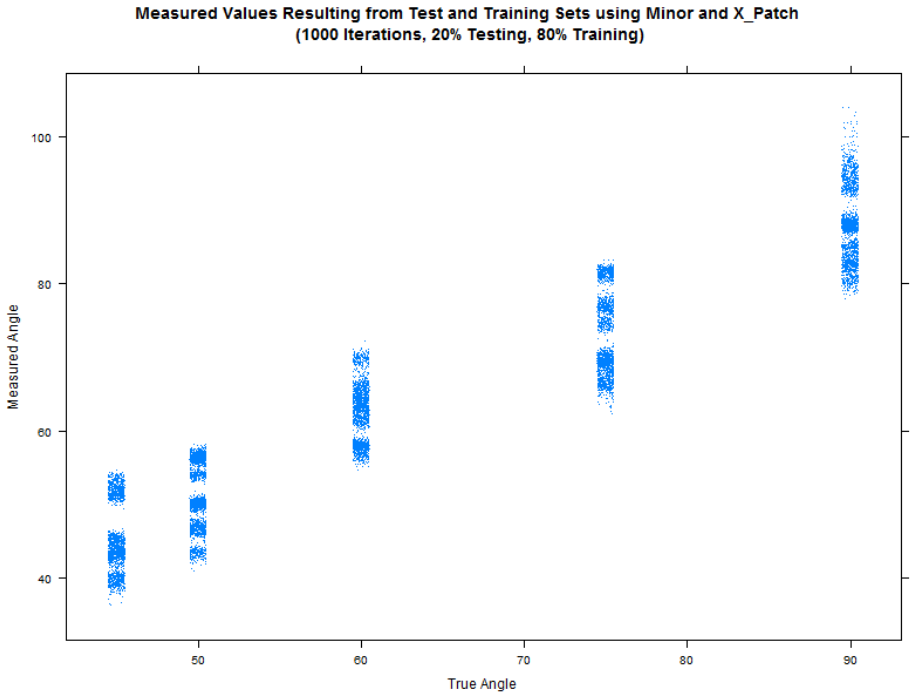

Figure 4.69: Results from testing and training sets performed on full metal jacket data using $Minor \times X\_Patch$

4.7 Principal component analysis

The same information used to describe the multiple linear regression results are used in the following PCA results sections. The phrase "lack of" refers to a small value in the original data for the corresponding variable, and the phrase "abundance of" refers to a large value in the original data for the corresponding variable.

PCA was used on the data in this research since some of the variables are correlated with each other, such as Circularity, Aspect Ratio, and Minor. By using PCA, the transformed data becomes uncorrelated and one particular variable will not have complete influence over the results. In addition, PCA allows one to visualize the contribution of each specific variable to each principal component.

4.7.1 FMJ bullets

Table 4.25 on the following page shows the proportion of variance for the full metal jacket data. PC1 accounts for 63% of the variance, while PC2 accounts for 15%, and PC3 accounts for 12%. Together, they account for 90% of the variance. This means that PC1-PC3 describes

90% of the original variance. 100% of the variance is accounted for by PC6. PC4-PC6 each account for less than 10% of the variance.

Table 4.25: Importance of components for full metal jacket bullet data

Importance of Components	PC1	PC2	PC3	PC4	PC5	PC6
Proportion of Variance	0.63170	0.15331	0.11991	0.05791	0.03689	0.00027
Cumulative Proportion	0.63170	0.78502	0.90493	0.96284	0.99973	1.00000

Figure 4.70 is a graphical representation of Table 4.25. The variance in each feature (PC1-PC6) is defined by its eigenvalues. PC1-PC3 account for a majority of the variance.

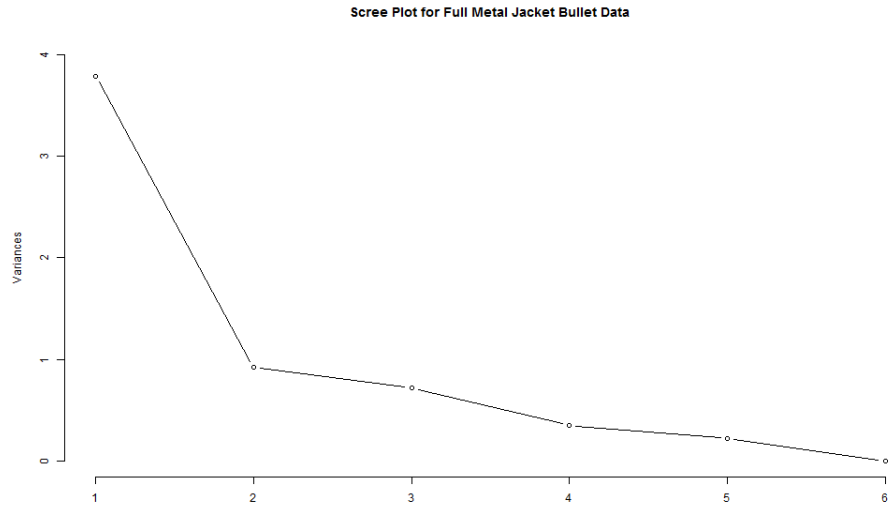

Figure 4.70: Scree plot for full metal jacket data where the variances are the eigenvalues of the PCs

Table 4.26 on the next page displays the standard deviations and rotations (or loadings) for the full metal jacket data. AR and Area Largest Particle are the only two variables that are positively loaded in PC1. Minor has the greatest weight of any variable in PC1 (positive value) while Area Largest Particle has the least weight of any variable in PC1 (positive value).

Table 4.26: Summary of components for full metal jacket bullet data

Summary of Components	PC1	PC2	PC3	PC4	PC5	PC6
Standard Deviation	1.946857318	0.959110567	0.848227744	0.589446123	0.470458263	0.040584723
Rotations:						
Area	-0.45505	-0.38667	0.08473	-0.12704	-0.54767	-0.56583
X_Patch	-0.41617	-0.46295	-0.05987	-0.26784	0.73288	-0.00713
Circ.	-0.34199	0.66078	-0.00835	-0.66771	-0.02157	-0.00698
Area_Largest_Particle	0.32042	-0.14378	0.8791	-0.31888	0.04639	-0.0011
Minor	-0.494	-0.1271	0.22112	0.12578	-0.2893	0.76902
AR	0.39506	-0.40338	-0.4092	-0.59058	-0.27684	0.29721

Circularity is the only variable that is positively loaded in PC2. It also has the greatest weight of any variable (positive value), while Minor has the least weight of any variable (negative value).

Area, Area Largest Particle, and Minor all are positively loaded on PC3. Area Largest Particle has the greatest weight of any variable (positive value), while Circularity has the least weight of any variable (negative value).

Figure 4.71 on the following page displays the biplot for PC1 and PC2 for full metal jacket data. The ellipses represent a contour line (95% confidence) for each group. Bullets fired at 90° can be distinguished from bullets fired at 60°, 50°, and 45°. Bullets fired at 75° can be distinguished from bullets fired at 50° and 45°. Bullets fired at 60° cannot be distinguished from 50° or 45°.

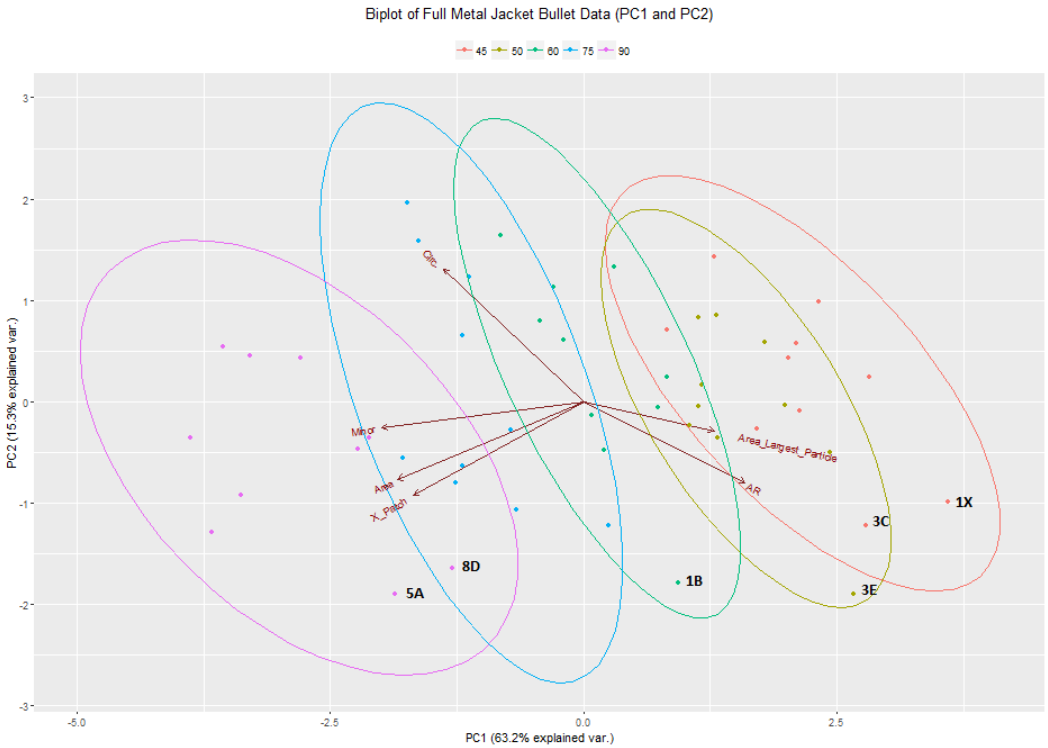

Figure 4.71: Biplot for PC1 and PC2 for full metal jacket data

If the value of PC1 is -2.75 or smaller, the bullet was fired from 90°.

If the value of PC1 is 1.875 or higher, the bullet could have been fired from 50° or 45°. If the PC1 values is 0.625, the bullet could have been fired from 75°, 60°, or 50°. If the PC1 value is -1.25, the bullet could have been fired from 90°, 75°, or 60°.

If the PC2 value is 2, the bullet could have been fired at 75°, 60°, or 45°. If the PC2 value is between 1 and -1.5, then the bullet could have been fired at 90°, 75°, 60°, 50°, or 45°.

Figure 4.72 on the next page displays the 95% confidence bounds of the projected PCs and original data points of PC1 and PC2 for full metal jacket bullets. There were 20,000 test samples (predicted PCs) per individual angle generated. The generated samples take into account the mean and covariance of the original data, thus providing a representation of possible values for bullets fired at a specific angle. The confidence bounds are similar to the normal contour lines (95% probability) of the original data. The original data points for each angle fall into the the corresponding predicted confidence bounds except for sample 3E (50°).

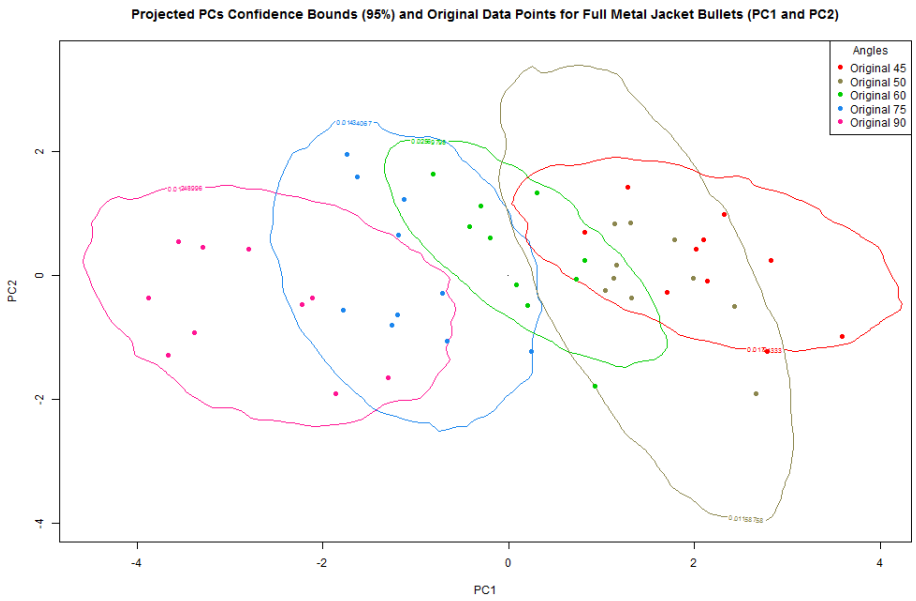

Figure 4.72: Predicted PCs confidence bounds (95%) for full metal jacket bullets (PC1 and PC2)

Figure 4.73 on the following page displays the biplot for PC1 and PC3 for full metal jacket data. The ellipses represent a normal contour line with probability (95% confidence) for each group. Bullets fired at 90°, 75°, 60°, 50°, and 45° cannot be distinguished from one another.

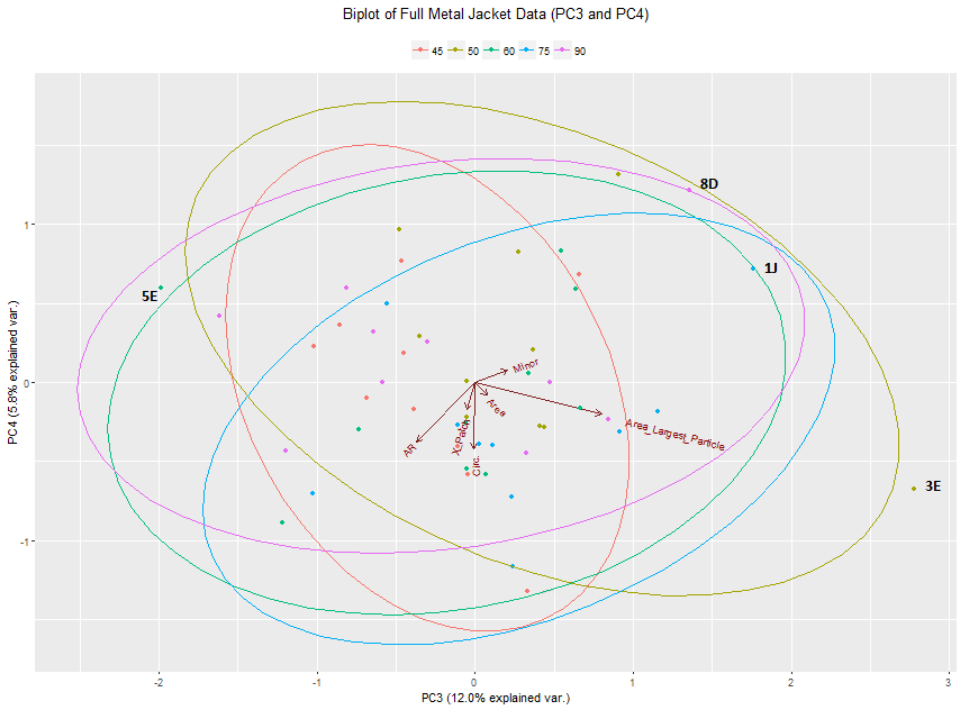

Figure 4.73: Biplot for PC3 and PC4 for full metal jacket data

Figure 4.74 on the next page displays the 95% confidence bounds of the projected PCs and original data points of PC3 and PC4 for full metal jacket bullets. There were 20,000 test samples (predicted PCs) per individual angle generated. The generated samples take into account the mean and covariance of the original data, thus providing a representation of possible values for bullets fired at a specific angle. The confidence bounds are similar to the normal contour lines (95% probability) of the original data. Some original data points for each angle fall outside of the corresponding predicted confidence bounds except for the 45° original samples.

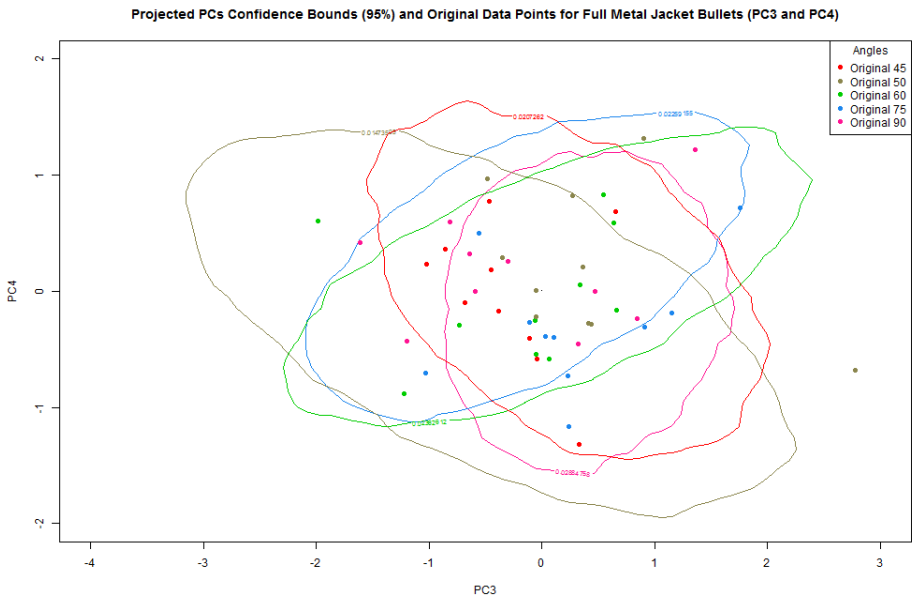

Figure 4.74: Predicted PCs confidence bounds (95%) for full metal jacket bullets (PC3 and PC4)

Figure 4.75 displays a 3D scatterplot of PC1, PC2, and PC3. It is clear that the addition of PC3 does not provide much ability to distinguish between angles.

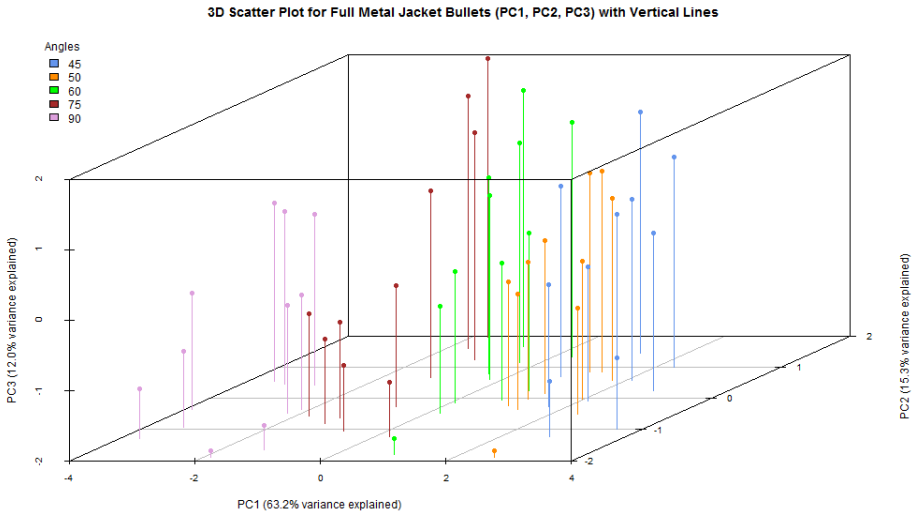

Figure 4.75: 3D scatter plot of PC1, PC2, and PC3 with vertical lines

Discussion of PCs

1. To transform the original data to the transformed values seen in Table 4.27, the original data was centered, scaled, and a Box-Cox transformation was performed.

2. In order to obtain the scores (e.g., PC1_Area) as seen in Table 4.28, the transformed value for a variable, for example Area for sample 5A, was multiplied by the PC1 loading value for Area (-0.45505, Table 4.26 on page 129).

3. Once all the scores were obtained for a sample (Area, X_Patch, Circ, ALP, AR, and Minor), each of them were summed together to obtain the PC1 value (-1.8651, Table 4.28).

4. To understand how much each variable was contributing to the PC1 value of a specific sample (e.g., 5A), the absolute value of each score for a specific variable (e.g., Area) for that sample was calculated and summed together.

5. The absolute value for a specific variable (e.g., 0.7294 for Area, Table 4.28 was then divided by the total sum found in Step 4.

Table 4.27: Data table displaying the original values of each variable ($*_O$) and the transformed values of each variable ($*_T$) for each sample for the full metal jacket problem samples

Sample	True_Angle	Area_O	X_Patch_O	Circ_O	ALP_O	AR_O	Minor_O	Area_T	X_Patch_T	Circ_T	ALP_T	AR_T	Minor_T
5A	90	9675895	1841.1	0.903	59397.5	1.165	3252.5	1.6029	1.7750	-0.3192	0.1061	0.1799	1.2372
8D	90	8238411	1692.5	0.878	88382.2	1.045	3167.9	0.7043	1.5741	-1.4897	0.6691	-1.3930	0.9982
1J	75	8355764	1142.7	0.897	112229.9	1.043	3193.1	0.8015	0.8300	-0.6031	1.0412	-1.4216	1.0714
1B	60	8062778	831.2	0.891	44779.1	1.357	2750.4	0.5586	0.4086	-0.8851	-0.2552	2.2213	-0.5234
5E	60	7995543	-63.7	0.894	8498.8	1.243	2861.7	0.5100	-0.8022	-0.7444	-1.8588	1.0700	-0.0521
3E	50	7770874	-80.5	0.873	436360.4	1.265	2796.2	0.3157	-0.8250	-1.7199	3.7473	1.3050	-0.3227
3C	45	6767034	-104.5	0.861	73918.0	1.269	2605.8	-0.8500	-0.8574	-2.2670	0.4076	1.3471	-1.2280
3B	45	6522922	145.7	0.938	105463.1	1.188	2644.3	-1.2143	-0.5189	1.3748	0.9418	0.4521	-1.0289

Table 4.28: Data table displaying the scores of variables, PC1 values, and percent contributions of variables for each sample for the full metal jacket problem samples

Sample	True_Angle	PC1_Area	PC1_X_Patch	PC1_Circ	PC1_Alp	PC1_AR	PC1_Minor	PC1	PC1_Area	PC1_X_Patch	PC1_Circ	PC1_Alp	PC1_AR	PC1_Minor
5A	90	-0.7294	-0.7387	0.1092	0.0340	0.0711	-0.6112	-1.8651	31.8%	32.2%	4.8%	1.5%	3.1%	26.6%
8D	90	-0.3205	-0.6551	0.5095	0.2144	-0.5503	-0.4931	-1.2951	11.7%	23.9%	18.6%	7.8%	20.1%	18.0%
1J	75	-0.3647	-0.3454	0.2063	0.3336	-0.5616	-0.5293	-1.2611	15.6%	14.8%	8.8%	14.3%	24.0%	22.6%
1B	60	-0.2542	-0.1701	0.3027	-0.0818	0.8775	0.2586	0.9328	13.1%	8.7%	15.6%	4.2%	45.1%	13.3%
5E	60	-0.2321	0.3339	0.2546	-0.5956	0.4227	0.0257	0.2092	12.4%	17.9%	13.7%	31.9%	22.7%	1.4%
3E	50	-0.1437	0.3433	0.5882	1.2007	0.5156	0.1594	2.6635	4.9%	11.6%	19.9%	40.7%	17.5%	5.4%
3C	45	0.3868	0.3568	0.7753	0.1306	0.5322	0.6066	2.7883	13.9%	12.8%	27.8%	4.7%	19.1%	21.8%
3B	45	0.5526	0.2159	-0.4702	0.3018	0.1786	0.5083	1.2870	24.8%	9.7%	21.1%	13.5%	8.0%	22.8%

If a specific sample (e.g., 5A for 90°) was causing a problem in the data, the average of all the 90° scores for each variable was calculated as shown in Table 4.29. The average of each variable (e.g., -0.6123 for 8D) was then subtracted from the individual problem sample scores corresponding to those variables (e.g., -0.03205 for 8D). This provided the distance that each variable for a specific sample was away from the average of all 90° samples of that variable (e.g., -0.2918 for 8D, Area). The absolute value of these distances provided information as to which variables were causing problems. Using the same table, Circularity and ALP are the major contributors to this sample. This can be confirmed by viewing Figure 4.71 on page 130.

Table 4.29: Data table displaying the scores of each variable, averages of variables, and distances away from the average for sample 8D for 90°

Sample	True_Angle	PC1_Area	PC1_X_Patch	PC1_Circ	PC1_Alp	PC1_AR	PC1_Minor
6C	90	-0.8289	-0.7096	-0.3024	-0.5960	-0.5166	-0.9231
8K	90	-0.9615	-0.7579	-0.0050	-0.6118	-0.3363	-0.9984
6G	90	-0.5305	-0.6567	-0.5378	-0.5486	-0.6015	-0.6800
8L	90	-0.8510	-0.7804	-0.1860	-0.1707	-0.4665	-0.9309
8A	90	-0.6078	-0.5654	-0.5378	-0.0933	-0.7061	-0.7833
8I	90	-0.5968	-0.2445	-0.3693	-0.4242	-0.4720	-0.6886
8G	90	-0.3868	-0.7198	-0.2524	-0.4911	-0.0399	-0.3365
8J	90	-0.3094	-0.5634	-0.0706	-0.6918	-0.1596	-0.3196
5A	90	-0.7294	-0.7387	0.1092	0.0340	0.0711	-0.6112
8D	90	-0.3205	-0.6551	0.5095	0.2144	-0.5503	-0.4931
	Average	-0.6123	-0.6392	-0.1643	-0.3379	-0.3778	-0.6765
	Distance	-0.2918	0.0159	-0.6737	-0.5523	0.1725	-0.1834

All other PC tables for both full metal jacket and lead round nose bullets can be seen in Appendix A.

The samples described in the results below can be observed in Figures 4.71 on page 130 and 4.73 on page 132

90° bullets (PC1 through PC3)

The following results for 90° full metal jacket bullets can be inspected visually and compared with other 90° bullets in Figures 4.71 on page 130, 4.73 on page 132, and 4.76 on page 137.

Circularity ranges from 0.878 (sample 8D) to 0.942 (samples 6G and 8A). Normalization of these values results in 8D having a z-score of -2.14 and a z-score of 1.16 for samples 6G and 8A. It is clear that sample 8D is in the negative tail of the distribution. The lack of Circularity for sample 8D contributes significantly to its PC1 and PC2 values. It has a value of 0.878, whilst the average value for Circularity to PC1 is 0.920.

The contributions of Circularity (18.6%) and then ALP (7.8%) to the PC1 value and the contributions of Circularity (35.5%) to the PC2 value of sample 8D result in it being located away from the other 90° samples.

The abundance of ALP and lack of Circularity for sample 8D contributes significantly to its PC3 value, respectively. It has a value of 88382 for ALP (average is 28803) and a value of 0.878 for Circularity (average is 0.920).

The contribution of ALP (38.1%) to the PC3 value and Circularity (37.3%) to the PC4 value result in it being located away from the other 90° samples.

AR ranges from 1.02 (sample 8A) to 1.17 (sample 5A). Normalization of these values results in 5A having a z-score of 1.80 and a z-score of -1.23 for samples 8A. The abundance of AR for sample 5A contributes significantly to its PC1 value. It has a value of 1.17, whilst the average value for AR to PC1 is 1.08.

Normalization of the Circularity values results in sample 5A having a z-score of -0.85. It has a value of 0.903 for Circularity. The lack of Circularity for sample 5A contributes significantly to its PC2 value.

The contributions of AR (3.1%) and then ALP (1.5%) to the PC1 value and the contributions of Circularity (11.1%) and then AR (3.8%) to the PC2 value of sample 5A result in it being located away from the other 90° samples.

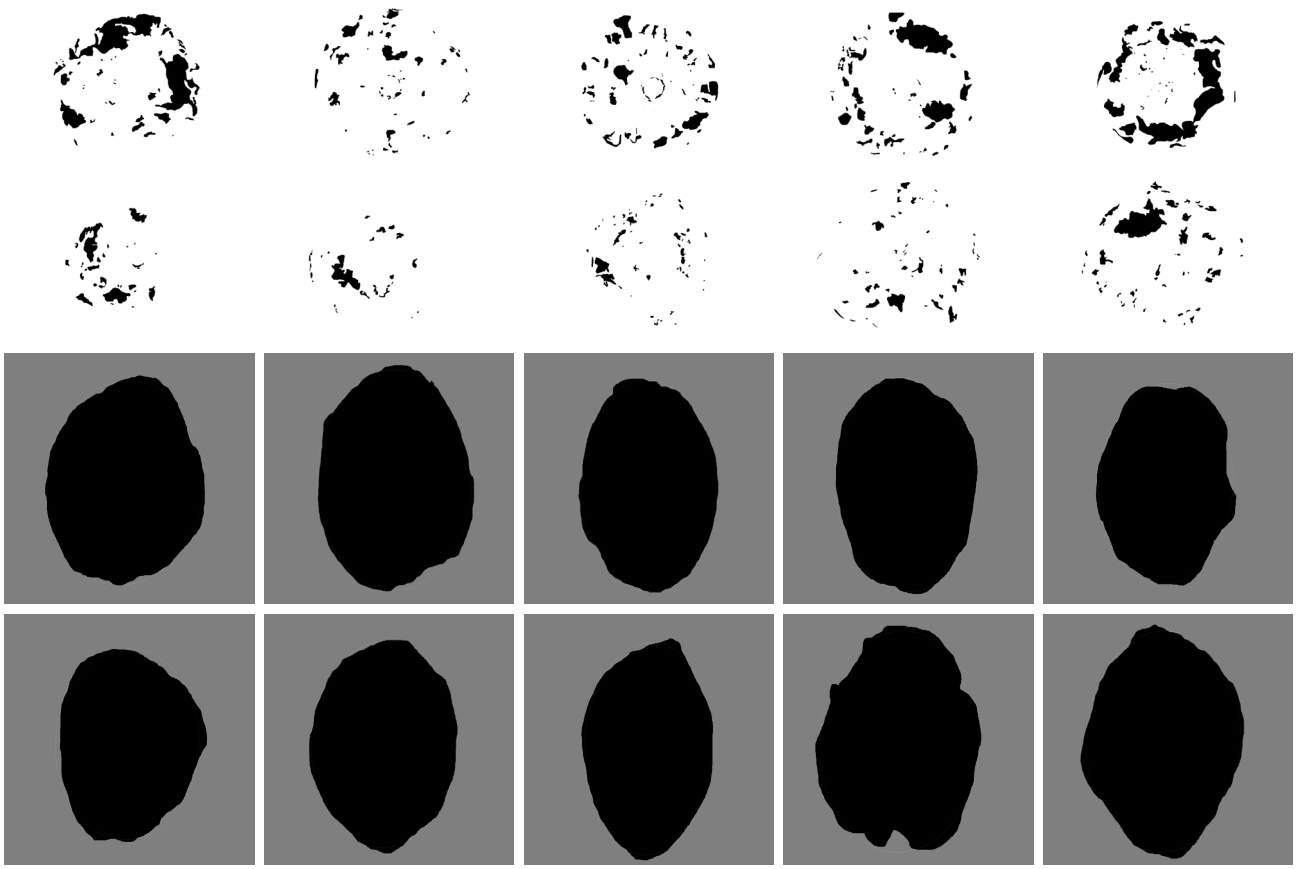

Figure 4.76: Particle selection (top two rows) and bullet outline (bottom two rows) images for 90° lead round nose bullets. Samples 5A, 6C, 6G, 8A, 8D (first and third rows) and samples 8G, 8I, 8J, 8K, 8L (second and forth rows)

75° bullets (PC1 through PC3)

The following results for 75° full metal jacket bullets can be inspected visually and compared with other 75° bullets in Figures 4.71 on page 130, 4.73 on page 132, and 4.76.

ALP ranges from 13272 (sample 1E) to 112229 (sample 1J). Normalization of these values results in 1J having a z-score of 1.74 and a z-score of -1.48 for sample 1E. The abundance of ALP for sample 1J contributes significantly to its PC3 value. It has a value of 102842, whilst the average value for ALP is 58707.

The contribution of ALP (49.3%) to the PC3 value result in it being located away from the other 75° samples.

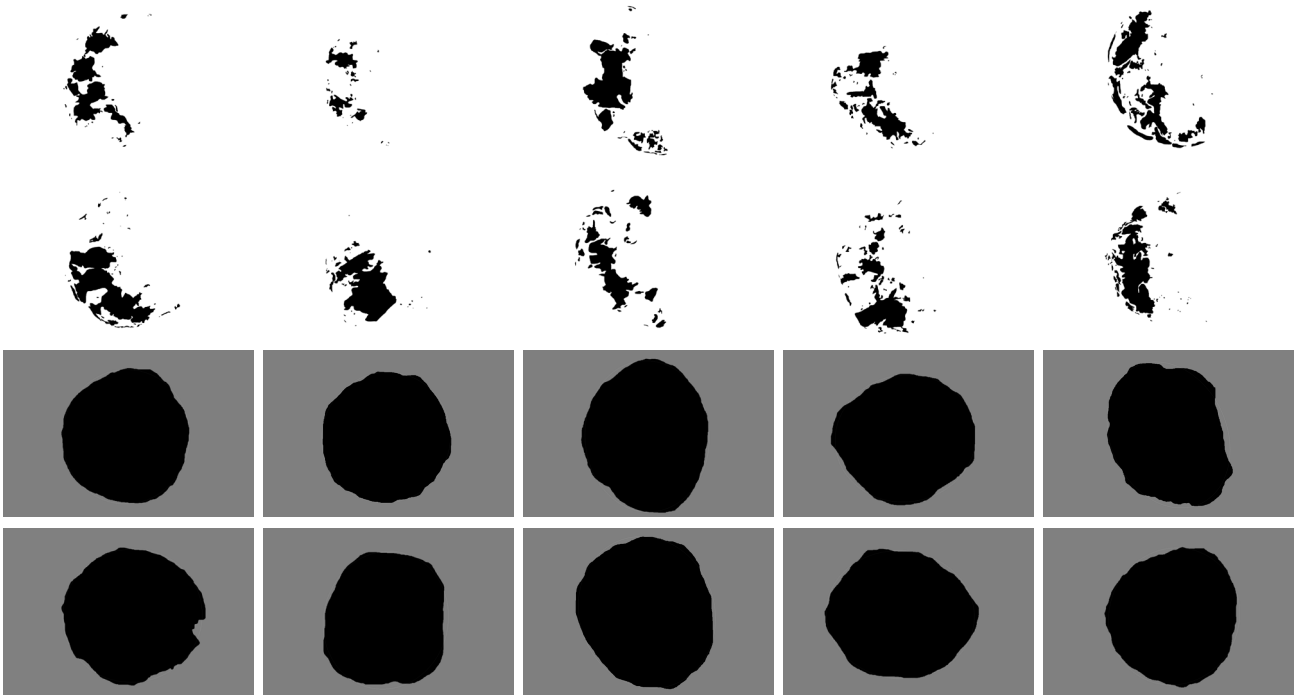

Figure 4.77: Particle selection (top two rows) and bullet outline (bottom two rows) images for 90° lead round nose bullets. Samples 1D, 1E, 1F, 1G, 1H (first and third rows) and samples 1J, 1K, 4L, 4M, 8F (second and forth rows)

60° bullets (PC1 through PC3)

The following results for 60° full metal jacket bullets can be inspected visually and compared with other 60° bullets in Figures 4.71 on page 130, 4.73 on page 132, and 4.76 on the preceding page.

AR ranges from 1.05 (sample 4I) to 1.36 (sample 1B). Normalization of these values results in 1B having a z-score of 2.09 and a z-score of -1.18 for samples 4I. The abundance of AR for sample 1B contributes significantly to its PC1 and PC2 values. It has a value of 1.36, whilst the average value for AR is 1.16.

The contributions of AR (45.1%) and then Circularity (15.6%) to the PC1 value and of AR (45%) and then Circularity (29.4%) to the PC2 value of sample 1B result in it being located further away from other 60° samples.

ALP ranges from 8498 (sample 5E) to 102842 (sample 4J). Normalization of these values results in 5E having a z-score of -1.91 and a z-score of 2.09 for samples 4J. The lack of ALP for sample 5E contributes significantly to its PC3 value. It has a value of 8498, whilst the average value for ALP is 53487.

The contribution of ALP (74.9%) to the PC3 value result in it being located away from the other 60° samples.

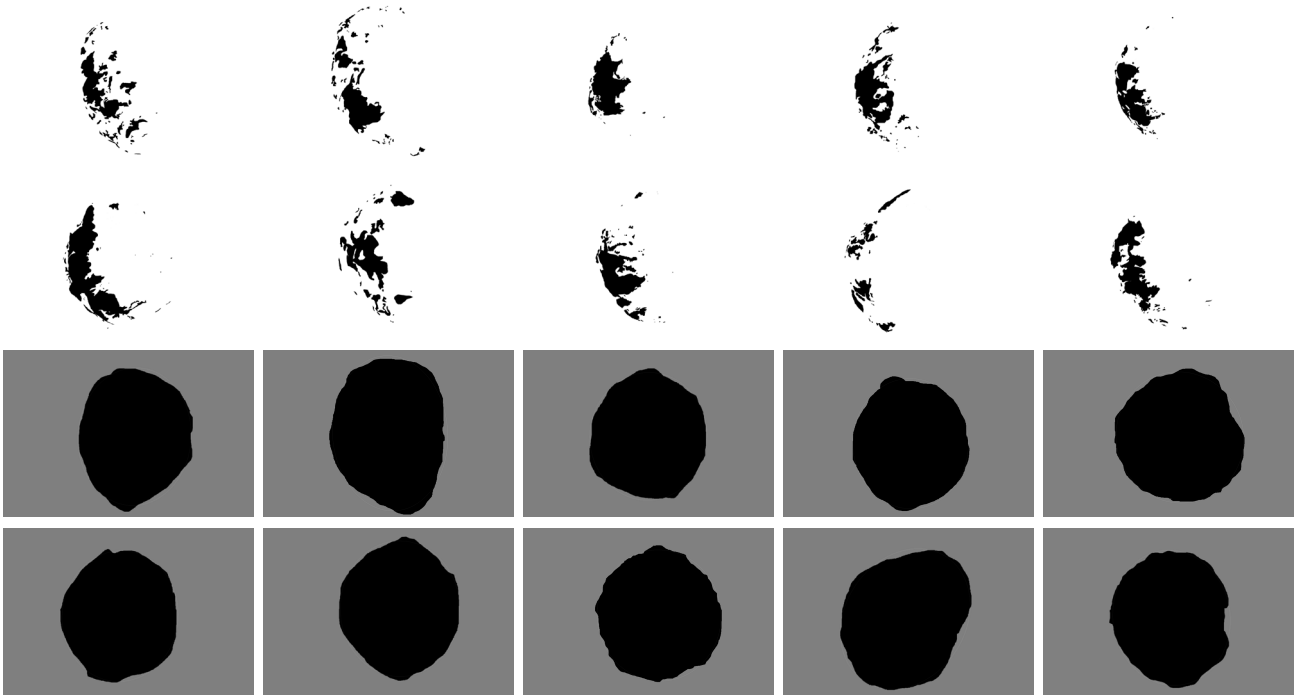

Figure 4.78: Particle selection (top two rows) and bullet outline (bottom two rows) images for 90° lead round nose bullets. Samples 1A, 1B, 1C, 1M, 4I (first and third rows) and samples 4J, 5C, 5D, 5E, 8H (second and forth rows)

50° bullets (PC1 through PC3)

The following results for 50° full metal jacket bullets can be inspected visually and compared with other 50° bullets in Figures 4.71 on page 130, 4.73 on page 132, and 4.76 on page 137.

ALP ranges from 58261 (sample 3L) to 436360 (sample 3E). Normalization of these values results in 3E having a z-score of 2.82 and a z-score of -0.50 for samples 3L. The abundance of ALP for sample 3E contributes significantly to its PC1 value. It has a value of 436360, whilst the average value for ALP to PC1 is 115139. Circularity ranges from 0.871 (sample 3I) to 0.917 (sample 5B). The abundance of ALP for sample 3E also contributes significantly to its PC3 value. It has a value of 436360, whilst the average value for ALP is 115139.

The contribution of ALP (82.6%) to the PC3 value result in it being located away from the other 50° samples.

Normalization of the ALP values results in 3I having a z-score of -1.40 and a z-score of 1.39 for sample 5B. Sample 3E (behind sample 3I) has a value of 0.873 for Circularity and

z-score of -1.27. The lack of Circularity for sample 3E contributes significantly to its PC2 value.

The contributions of ALP (40.7%) then Area (4.9%) to the PC1 value and the contributions of Circularity (41.4%) and then ALP (19.6%) to the value of PC2 of sample 3E result in it being located further away from other 50° samples.

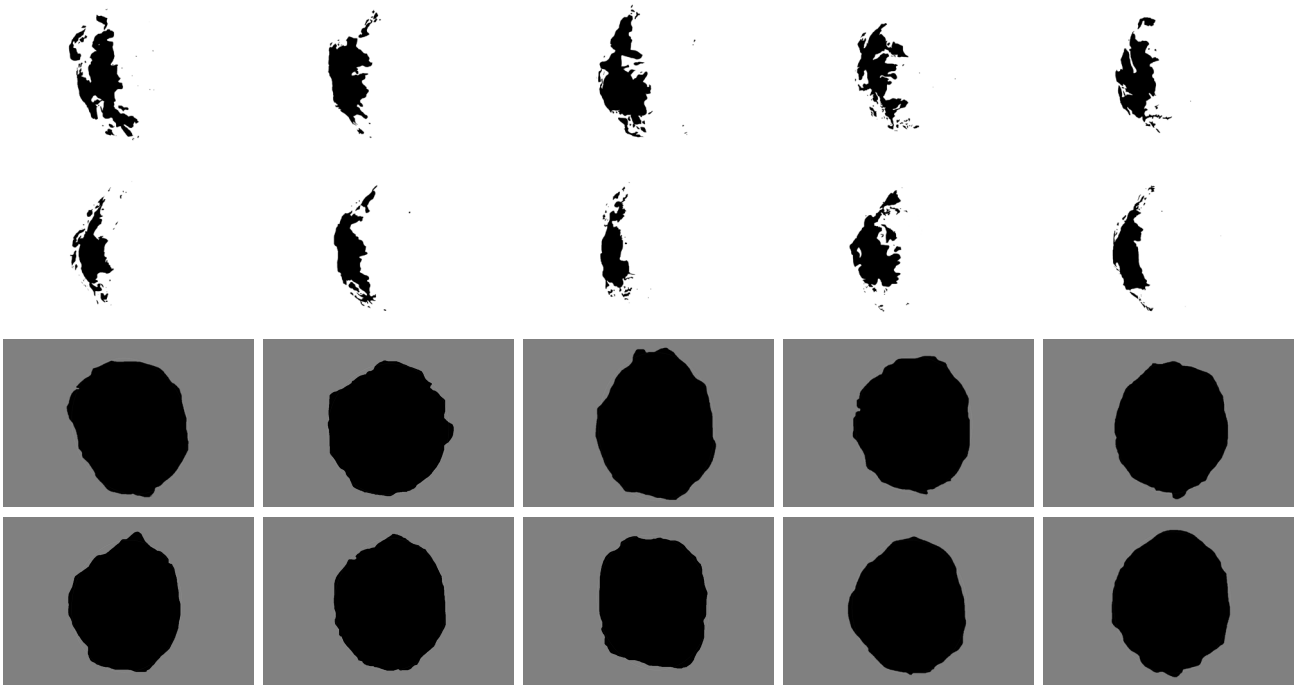

Figure 4.79: Particle selection (top two rows) and bullet outline (bottom two rows) images for 90° lead round nose bullets. Samples 1L, 3D, 3E, 3G, 3H (first and third rows) and samples 3I, 3J, 3L, 5B, 6A (second and forth rows)

45° bullets (PC1 through PC3)

The following results for 45° full metal jacket bullets can be inspected visually and compared with other 45° bullets in Figures 4.71 on page 130, 4.73 on page 132, and 4.76 on page 137.

Circularity ranges from 0.861 (sample 3C) to 0.938 (sample 3B). Normalization of these values results in 3C having a z-score of -1.62 and a z-score of 1.86 for samples 3B. The lack of Circularity for both samples 3C and 1X (z-score = -1.49) contributes significantly to their PC1 and PC2 values. Sample 3C has a value of 0.861, and sample 1X has a value of 0.864, whilst the average value for Circularity to PC1 is 0.897.

The contributions of Circularity (27.8%) to the PC1 value and Circularity (50.2%) to the PC2 value of sample 3C result in it being located further away from other 45° samples.

The contributions of Circularity (20.3%) and then Minor (28.3%) to the PC1 value and Circularity (41.9%) to the PC2 value of sample 1X result in it being located further away from other 45° samples.

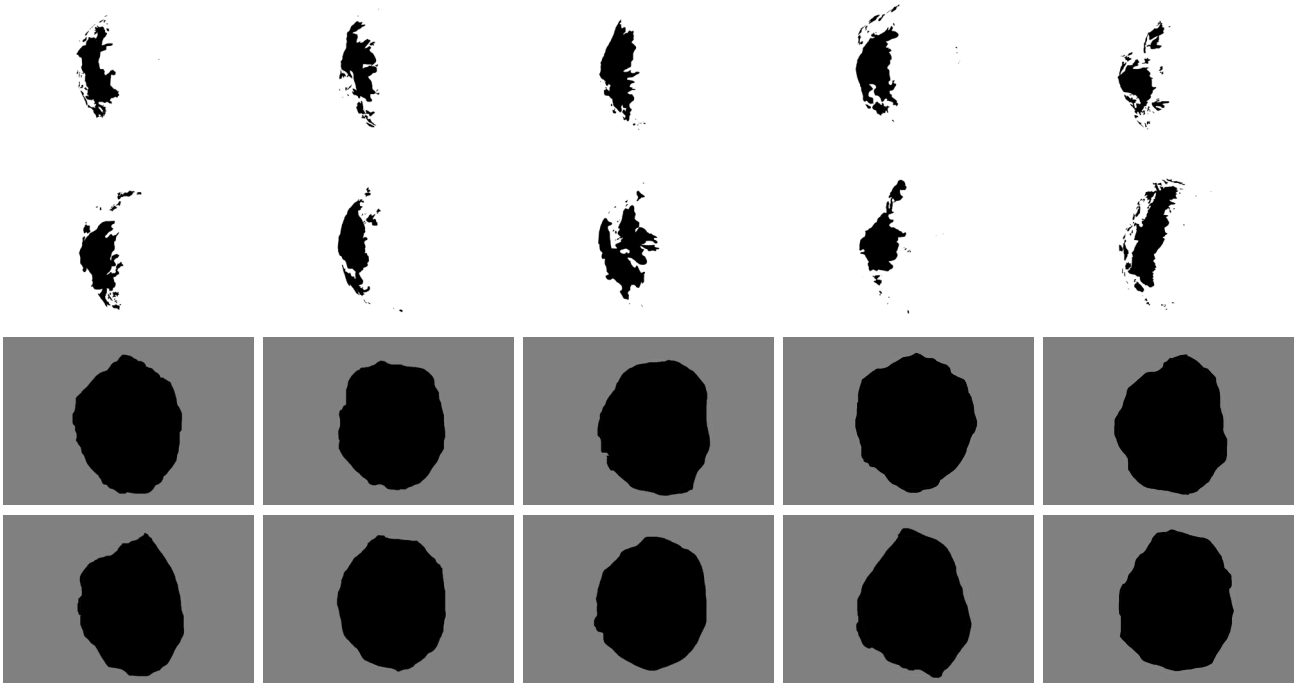

Figure 4.80: Particle selection (top two rows) and bullet outline (bottom two rows) images for 90° lead round nose bullets. Samples 1Q, 1R, 1S, 1T, 1W (first and third rows) and samples 1X, 3A, 3B, 3C, 3K (second and forth rows)

4.7.2 LRN bullets

Table 4.30 on the next page shows the proportion of variance explained for the lead round nose bullet data. PC1 accounts for approximately 35% of the variance, while PC2 accounts for approximately 26%, PC3 approximately 21%, and PC4 approximately 11%. Together, they account for approximately 93% of the variance explained. 100% of the variance is accounted for by PC6. PC5 and PC6 each account for less than 10% of the variance. This means that PC1-PC4 describes 93% of the original variance.

Table 4.30: Importance of components for lead round nose bullet data (proportion of variance explained by PCs

Importance of Components	PC1	PC2	PC3	PC4	PC5	PC6
Proportion of Variance	0.35384	0.25582	0.20700	0.11307	0.06999	0.00027
Cumulative Proportion	0.35384	0.60966	0.81666	0.92973	0.99973	1.00000

Figure 4.81 is a graphical representation of Table 4.30. The variance in each feature (PC1-PC6) is defined by its eigenvalues. PC1-PC4 account for a majority of the variance.

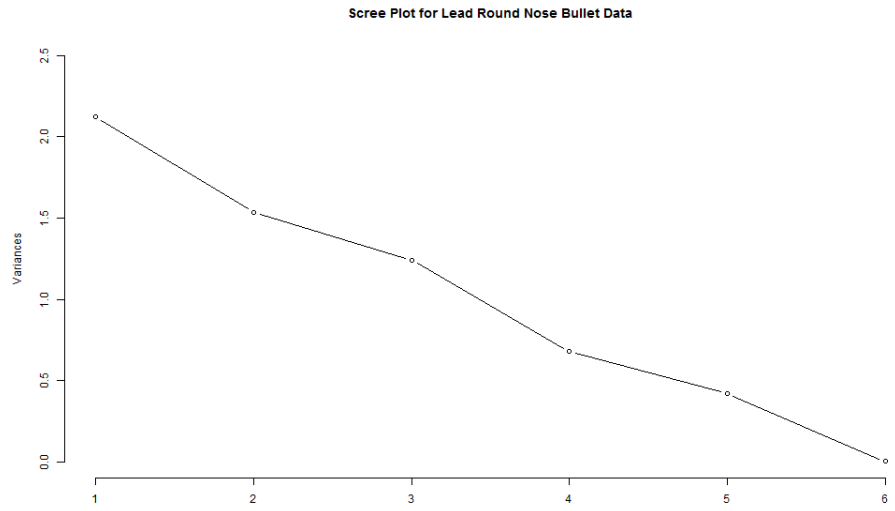

Figure 4.81: Scree plot for lead round nose bullet data where the variances are the eigenvalues of the PCs

Table 4.31 on the following page displays the standard deviations and rotations (or loadings) for the lead round nose data. Aspect ratio (AR) is the only variable that is negatively loaded in PC1. Minor has the greatest weight of any variable in PC1 (positive value) while X_Patch has the lowest weight of any variable in PC1 (positive value).

Table 4.31: Summary of components for lead round nose bullet data

Summary of Components	PC1	PC2	PC3	PC4	PC5	PC6
Standard Deviation	1.45707	1.23893	1.11445	0.82367	0.64803	0.04053
Rotations:						
Area	0.52498	0.43503	-0.16990	0.24288	0.33800	-0.57710
Circ.	0.29662	-0.37310	0.53161	-0.40641	0.57010	-0.00508
AR	-0.38935	0.59359	0.05000	0.02227	0.56402	0.41826
Minor	0.66648	0.00333	-0.15552	0.19085	-0.05727	0.70136
Area_Largest_Particle	0.20142	0.55571	0.29878	-0.60062	-0.44789	-0.00092
X_Patch	0.00734	-0.10183	-0.75668	-0.61496	0.19683	0.00914

Circularity and X_Patch are the only variables that that are negatively loaded in PC2. AR has the greatest weight of any variable (positive value), while Minor has the least weight of any variable (positive value).

Area, Minor, and X_Patch are all negatively loaded on PC3. X_Patch has the greatest weight of any variable (negative value), while AR has the least weight of any variable (positive value).

Circularity, Area Largest Particle, and X_Patch are all negatively loaded in PC4. X_Patch has the greatest weight of any variable (negative value), while AR has the least weight (positive value).

Figure 4.82 on the next page displays the biplot for PC1 and PC2 for lead round nose data. The ellipses represent a contour line (95% confidence) for each group. Bullets fired at angles of 90°, 75°, 60°, 50°, and 45° cannot be distinguished from each other.

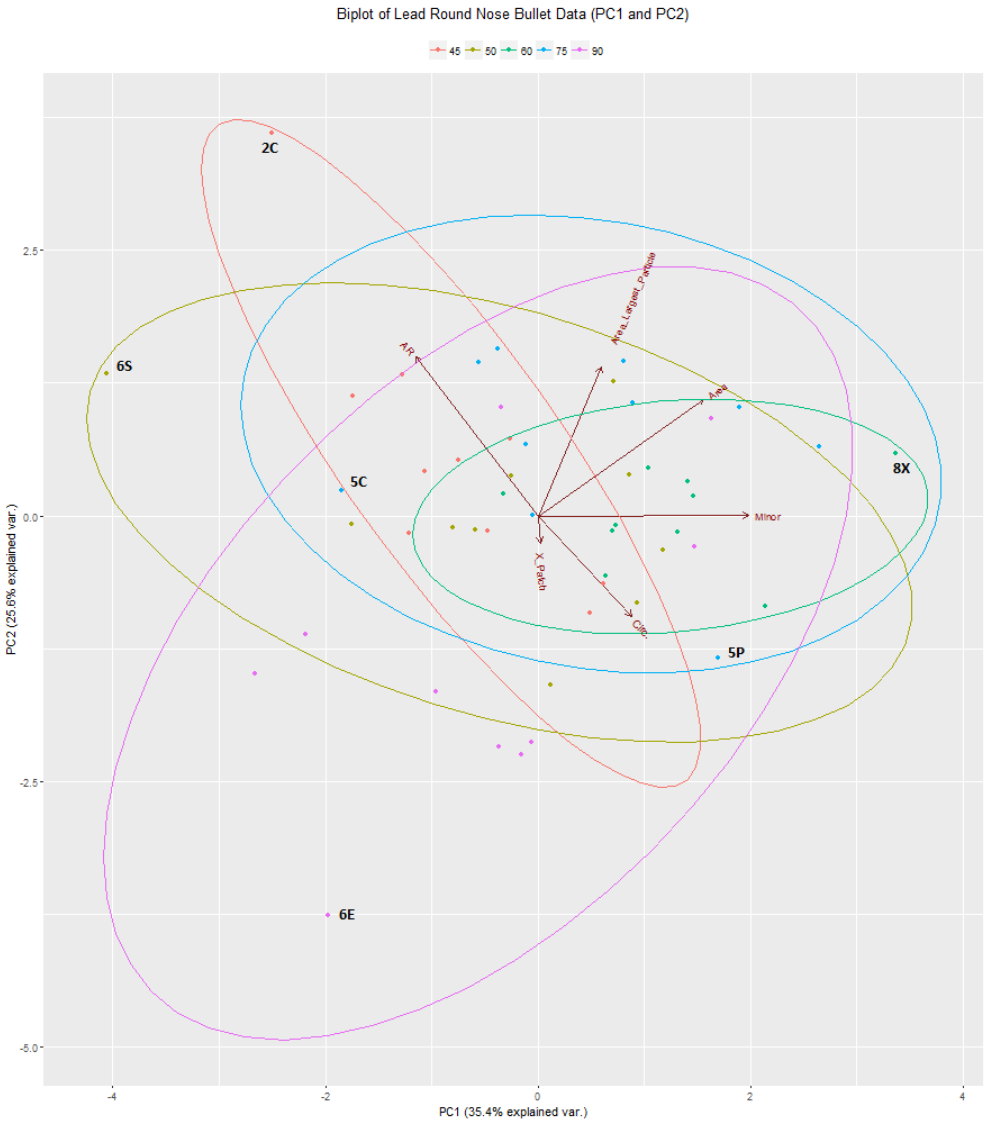

Figure 4.82: Biplot for PC1 and PC2 for lead round nose bullet data

Figure 4.83 on the following page displays the 95% confidence bounds of the projected PCs and original data points of PC1 and PC2 for lead round nose bullets. There were 20,000 test samples (predicted PCs) per individual angle generated. The generated samples take into account the mean and covariance of the original data, thus providing a representation of possible values for bullets fired at a specific angle. The confidence bounds are similar to the normal contour lines (95% probability) of the original data. Some of the original data points for each angle fall outside of the predicted confidence bounds, except for 50°.

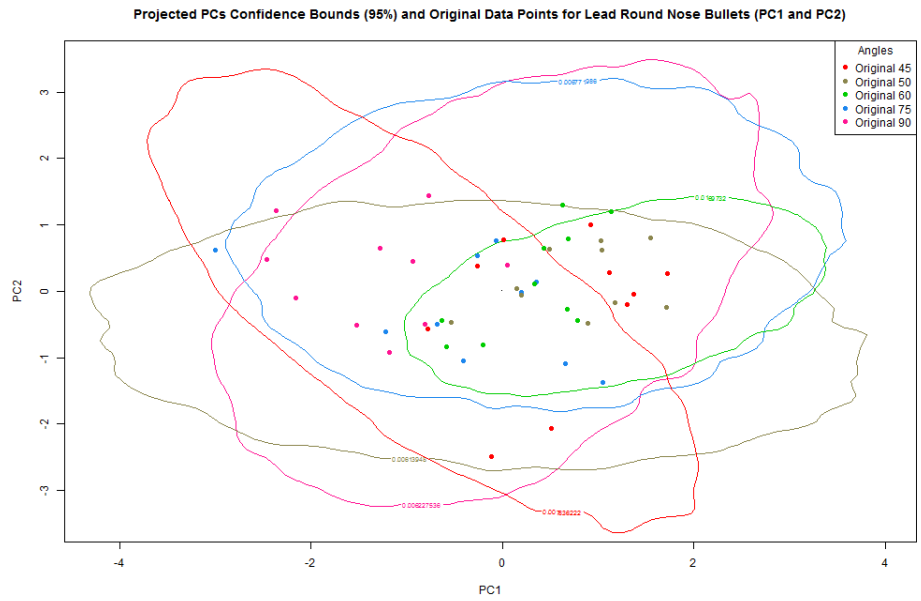

Figure 4.83: Predicted PCs confidence bounds (95%) for lead round nose bullets (PC1 and PC2)

Figure 4.84 on the next page displays the biplot for PC3 and PC4 for lead round nose bullet data. The ellipses represent a normal contour line with probability (95% confidence) for each group. Bullets fired at angles of 90°, 75°, 60°, 50°, and 45° cannot be distinguished from each other.

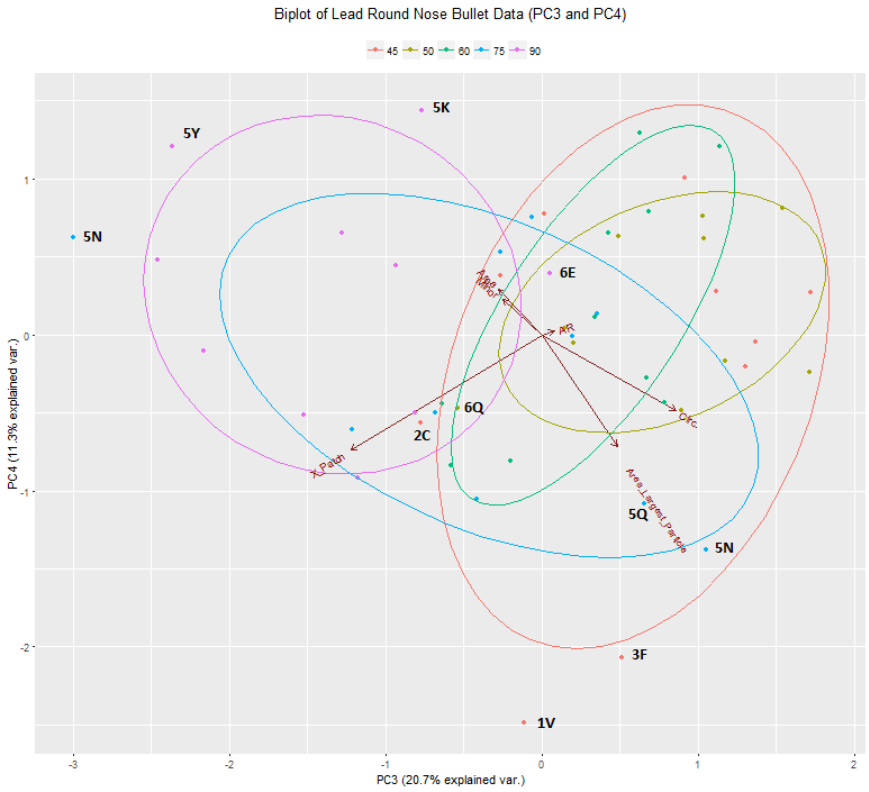

Figure 4.84: Biplot for PC3 and PC4 for lead round nose bullet data

If the value of PC3 is -1 or lower, the bullet could have been fired at 90° or 75°. If the value of PC3 is 0, the bullet could have been fired at 75°, 60°, 50°, or 45°. If the PC3 value is 1.5, the bullet could have been fired at 50° or 45°.

If the PC4 value is -1.5 or lower, the bullet was fired at 45°. If the PC4 value is -1, the bullet could have been fired at 60° or 45°. If the PC4 value is 1, the bullet could have been fired at 90°, 60°, or 45°.

Figure 4.85 on the following page displays the 95% confidence bounds of the projected PCs and original data points of PC3 and PC4 for lead round nose bullets. There were 20,000 test samples (predicted PCs) per individual angle generated. The generated samples take into account the mean and covariance of the original data, thus providing a representation of possible values for bullets fired at a specific angle. The confidence bounds are similar to the normal contour lines (95% probability) of the original data. Original data points from each of the five angles fall outside the predicted confidence bounds.

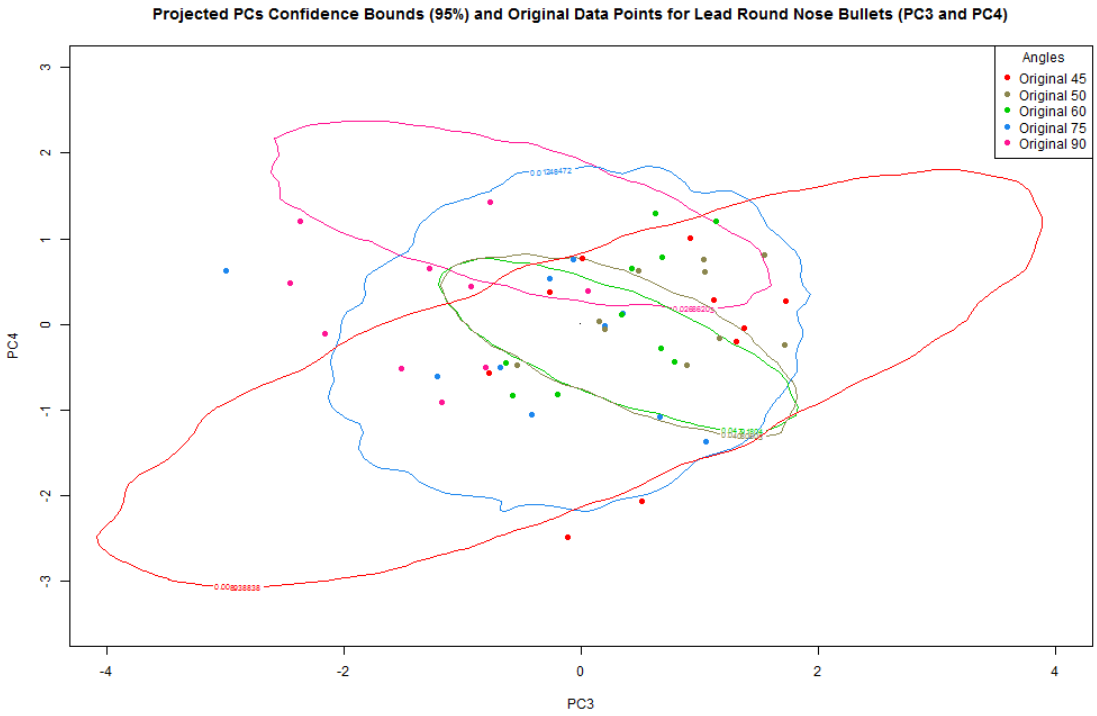

Figure 4.85: Predicted PCs confidence bounds (95%) for lead round nose bullets (PC3 and PC4)

Figure 4.69 displays a 3D scatterplot of PC1, PC2, and PC3. It is clear that the addition of PC3 does not provide much ability to distinguish between angles.

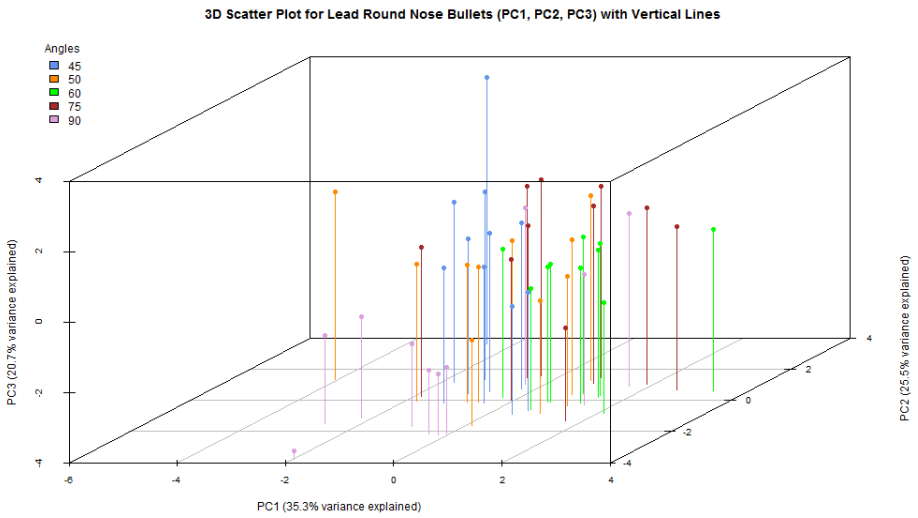

Figure 4.86: 3D scatter plot of PC1, PC2, and PC3 with vertical lines for lead round nose bullet data

Discussion of PCs

The samples described in the results below can be observed in Figures 4.82 on page 144 and 4.84 on page 146.

90° bullets (PC1 through PC4)

The following results for 90° lead round nose bullets can be inspected visually and compared with other 90° bullets in Figure 4.87 on page 150.

ALP ranges from 6124 (sample 6E) to 187297 (sample 5Y). Normalization of these values results in 6E having a z-score of -1.21 and a z-score of 2.08 for sample 5Y. The lack of ALP for sample 6E contributes significantly to its PC2 value. It has a value of 6124, whilst the average value for ALP is 72724.

The contribution of ALP (45.9%) and then Area (26.1%) to the PC2 value result in it being located away from the other 90° samples.

The abundance of ALP for sample 5Y contributes significantly to its PC4. It has a value of 187297, whilst the average value for ALP is 72723.

The contribution of Circularity (44.2%) to the PC3 value and the contributions of ALP (8.26%), Circularity (35.2%), then Area (18.4%) to the PC4 value result in it being located outside the 90° ellipse.

Circularity ranges from 0.749 (sample 5Y) to 0.869 (sample 6E). Normalization of these values results in 6E having a z-score of 1.55 and a z-score of -1.31 for sample 5Y. The abundance of Circularity for sample 6E contributes significantly to its PC3 value. It has a value of 0.869, whilst the average value for Circularity is 0.804.

The contribution of Circularity (26.5%) then X_Patch (8.2%) to the PC3 value result in it being outside the 90° ellipse.

X_Patch ranges from 11 (sample 5K) to 1201 (sample 8E). Normalization of these values results in 5K having a z-score of -1.83 and a z-score of 1.18 for sample 8E. The lack of X_Patch for sample 5K contributes significantly to its PC4 value. It has a value of 11, whilst the average value for X_Patch is 735.

The contribution of X_Patch (14.5%) to the PC4 value result in it being located outside the 90° ellipse.

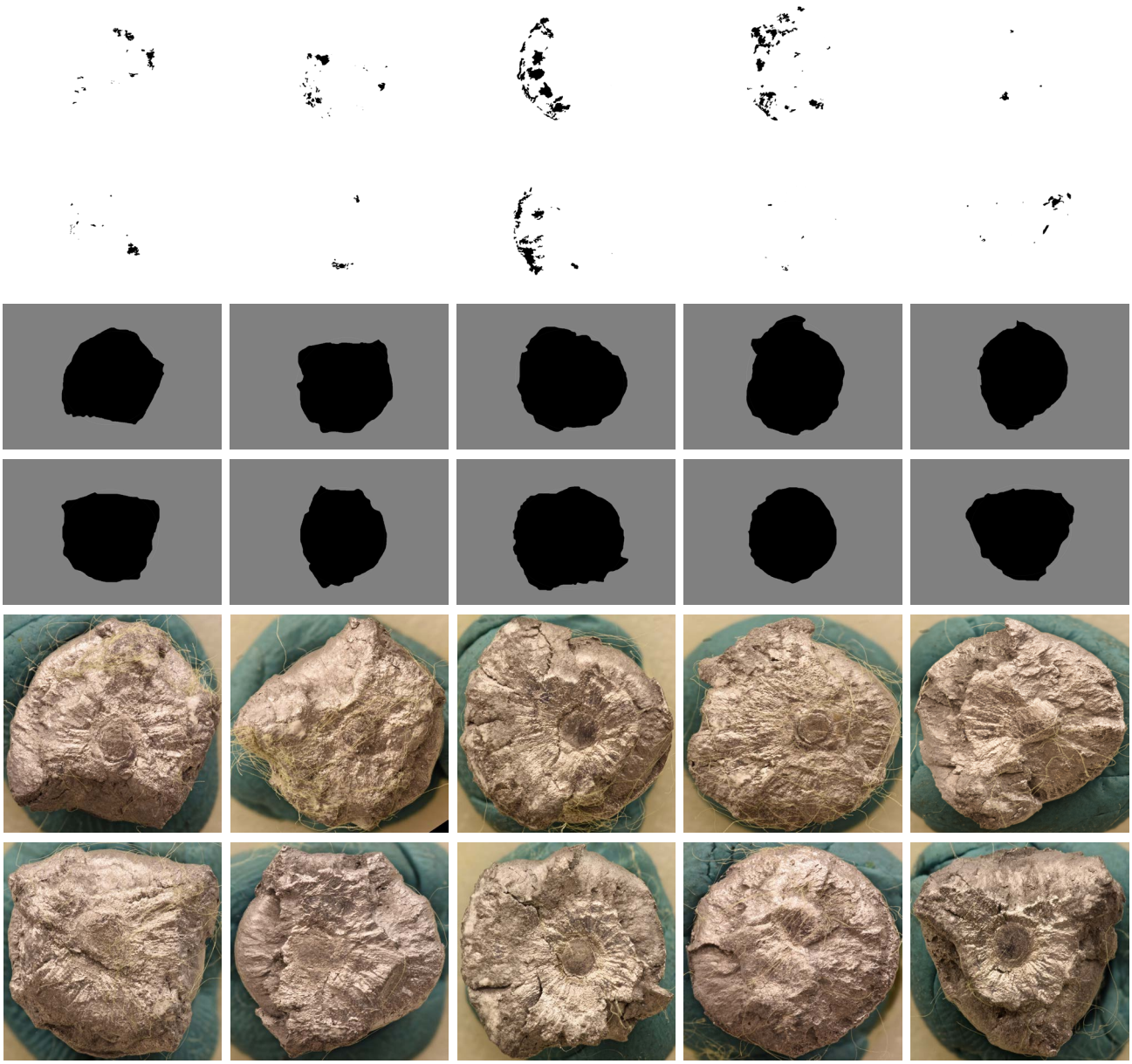

Figure 4.87: Particle selection (top two rows), bullet outline (middle two rows), and glass distribution (bottom two rows) images for 90° lead round nose bullets. Samples 5F, 5J, 5K, 5M, 5O (first, third, and fifth rows) and samples 5S, 5V, 5Y, 6E, 8E (second, fourth, and sixth rows)

75° bullets (PC1 through PC4)

The following results for 75° lead round nose bullets can be inspected visually and compared with other 75° bullets in Figure 4.88 on page 152.

Minor ranges from 2379 (sample 5C) to 2774 (sample 5H). Normalization of these values results in 5C having a z-score of -1.67 and a z-score of 1.49 for sample 5H. The lack of Minor for sample 5C contributes significantly to its PC1 value. It has a value of 2379, whilst the average value for Minor is 2588.

The contribution of Minor (40.7%) then Area (11.2%) to the PC3 value result in it being located away from the other 75° samples.

AR ranges from 1.10 (sample 5P) to 1.29 (sample 5C). Normalization of these values results in 5P having a z-score of -1.44 and a z-score of 1.52 for sample 5C. The lack of AR for sample 5P contributes significantly to its PC2 value. It has a value of 1.10, whilst the average value for AR is 1.19.

The contribution of AR(32.0%), ALP (20.9%) and then Circularity (26.9%) to the PC3 value result in it being located away from the other 75° samples.

Circularity ranges from 0.724 (sample 5N) to 0.874 (sample 5P). Normalization of these values results in 5N having a z-score of -2.10 and a z-score of 1.18 for sample 5P. The lack of Circularity for sample 5N contributes significantly to its PC3 and PC4 values. It has a value of 0.724, whilst the average value for Circularity is 0.820.

The contribution of Circularity (44.2%) then X_Patch (42.3%) to the PC3 value and the contribution of Circularity (37.95%) and then X_Patch (38.63%) to the PC4 value result in it being located outside the 75° ellipse.

ALP ranges from 76190 (sample 5C) to 1722200 (sample 5Q). Normalization of these values results in 5Q having a z-score of 1.47 and a z-score of -1.14 for sample 5C. The abundance of ALP for sample 5Q contributes significantly to its PC3 value.

The contribution of ALP (37.28%), X_Patch (24.55%) and then Circularity (15.38%) result in it being located away from the other 75° samples.

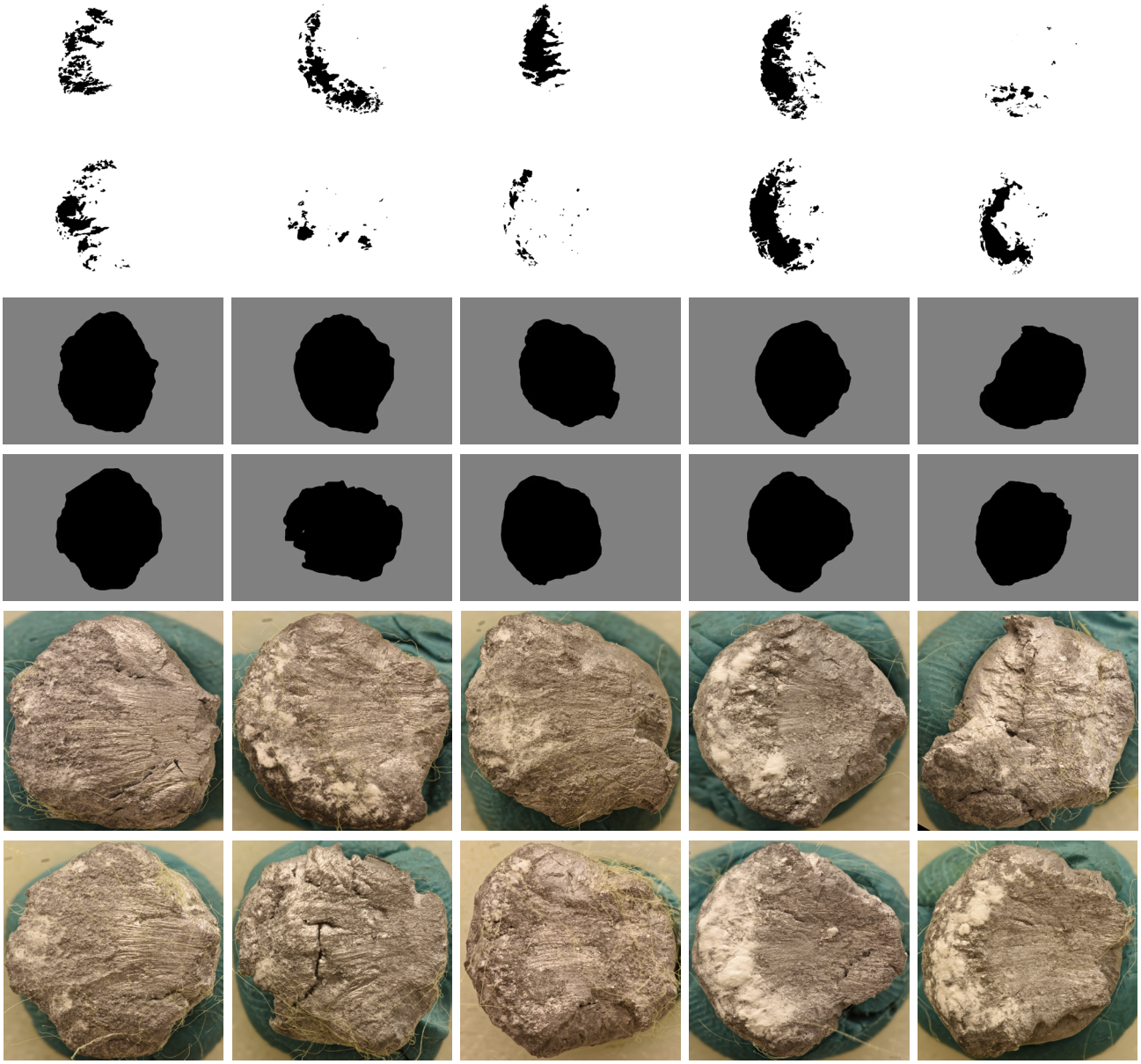

Figure 4.88: Particle selection (top two rows), bullet outline (middle two rows), and glass distribution (bottom two rows) images for 75° lead round nose bullets. Samples 3W, 3X, 3Y, 3Z, 5C (first, third, and firth rows) and samples 5H, 5N, 5P, 5Q, 5T (second, fourth, and sixth rows)

60° bullets (PC1 through PC4)

The following results for 60° lead round nose bullets can be inspected visually and compared with other 60° bullets in Figure 4.89 on the next page.

Minor ranges from 2534 (sample 3R) to 2842 (sample 8X). Normalization of these values results in 8X having a z-score of 2.18 and a z-score of -1.37 for sample 3R. The abundance of Minor for sample 8X contributes significantly to its PC1 value. It has a value of 2842, whilst the average value for Minor is 2653.

The contribution of Minor (44.2%) then Area (35.6%) to the PC1 value result in it being located away from the other 60° samples.

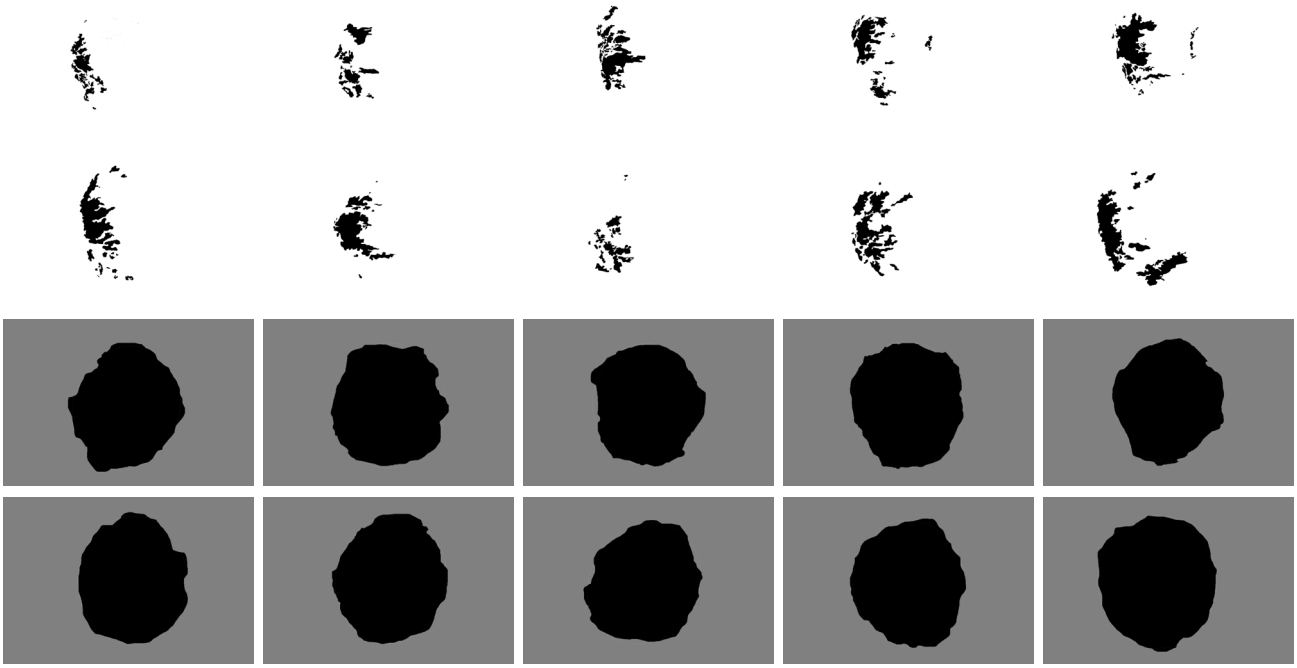

Figure 4.89: Particle selection (top two rows) and bullet outline (bottom two rows) images for 60° lead round nose bullets. Samples 3R, 3S, 3T, 8R, 8S (first and third rows) and samples 8T, 8U, 8V, 8W, 8X (second and forth rows)

50° bullets (PC1 through PC4)

The following results for 50° lead round nose bullets can be inspected visually and compared with other 50° bullets in Figure 4.90 on page 155.

AR ranges from 1.05 (sample 8Z) to 1.45 (sample 6S). Normalization of these values results in 6S having a z-score of 2.36 and a z-score of -1.29 for sample 8Z. The abundance of AR for sample 6S contributes significantly to its PC1 value. It has a value of 1.45, whilst the average value for AR is 1.19.

The contribution of AR (25.3%) then Area (19.3%) to the PC1 value result in it being located away from the other 50° samples.

X_Patch ranges from -674 (sample 6R) to 634 (sample 6Q). Normalization of these values results in 6Q having a z-score of 2.12 and a z-score of -1.25 for sample 6R. The abundance of X_Patch for sample 6Q contributes significantly to its PC3 value. It has a value of 634, whilst the average value for X_Patch is -188.

The contribution of X_Patch (54.7%) to the PC3 value result in it being located outside the 50° ellipse.

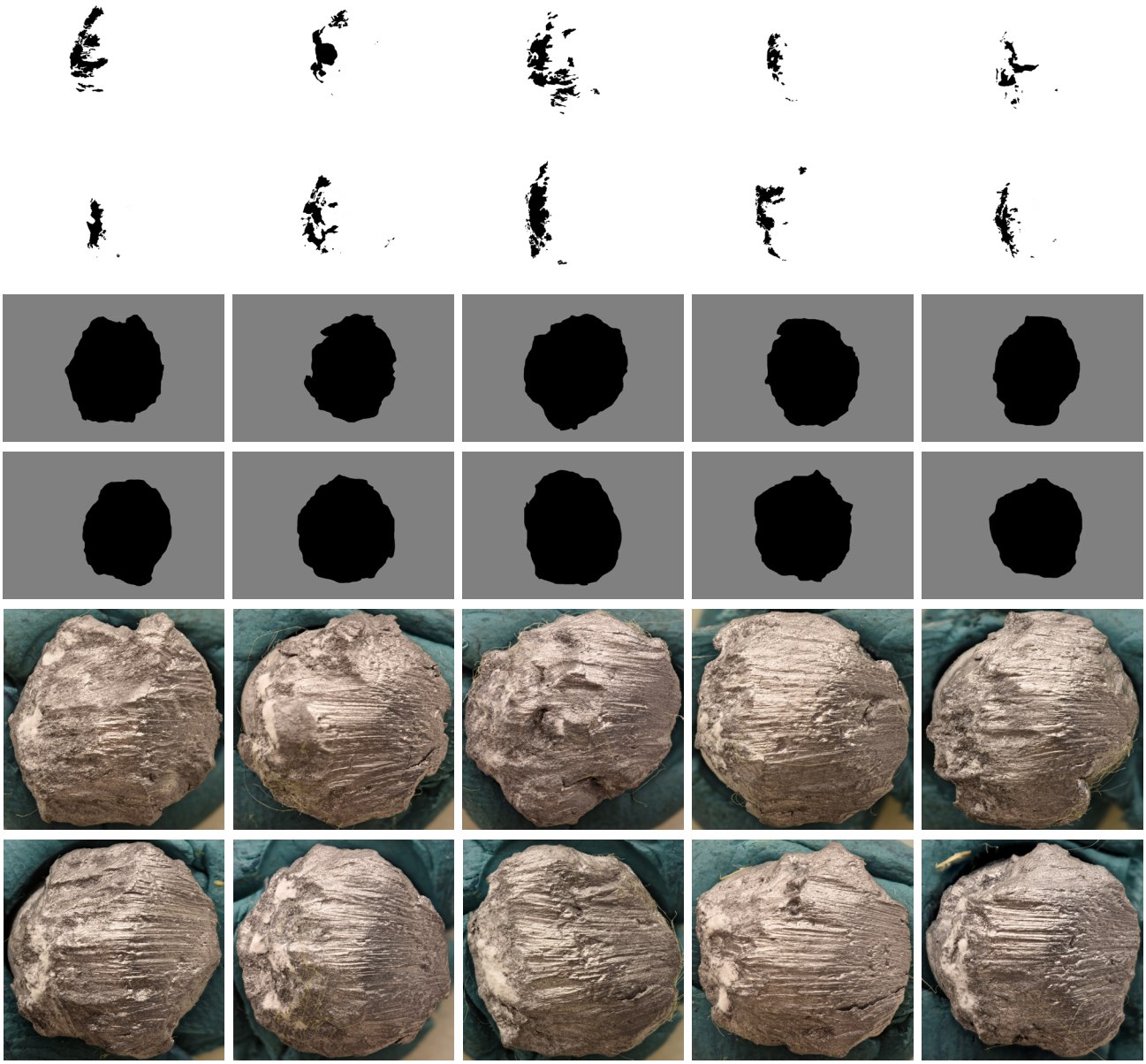

Figure 4.90: Particle selection (top two rows), bullet outline (middle two rows), and glass distribution (bottom two rows) images for 50° lead round nose bullets. Samples 3U, 6P, 6Q, 6R, 6S (first, third, and firth rows) and samples 6T, 6U, 6V, 8Y, 8Z (second, fourth, and sixth rows)

45° bullets (PC1 through PC4)

The following results for 45° lead round nose bullets can be inspected visually and compared with other 45° bullets in Figure 4.91 on page 157.

AR ranges from 1.11 (sample 2D) to 1.51 (sample 2C). Normalization of these values results in 2C having a z-score of 2.32 and a z-score of -1.08 for sample 2D. The abundance of AR for sample 2C contributes significantly to its PC1 and PC2 value. It has a value of 1.51, whilst the average value for AR is 1.24.

The contribution of AR (48.5%) to the PC1 value and the contributions of AR (33.5%) , Minor (33.3%), and then Circularity (18.6%) to the PC2 value result in it being located away from the other 45° samples.

X_Patch ranges from -701 (sample 3M) to 895 (sample 1V). Normalization of these values results in 1V having a z-score of 1.53 and a z-score of -1.24 for sample 6R. Sample 3F (behind sample 1V) has a z-score of 1.39. The abundance of X_Patch for sample 3F contributes significantly to its PC4 value. It has a value of 814, whilst the average value for X_Patch is 14.

The contribution of X_Patch (32.5%) then Circularity (32.0%) to the PC4 value result in it being located outside the 45° ellipse.

ALP ranges from 104313 (sample 2A) to 5478486 (sample 1V). Normalization of these values results in 1V having a z-score of 2.71 and a z-score of -0.57 for sample 2A. The abundance of ALP for sample 1V contributes significantly to its PC4 value. It has a value of 5478486, whilst the average value for ALP is 1037530. The contribution of ALP (55.3%), then X_Patch (29.4%) to the PC4 value result in it being located outside the 45° ellipse. The abundance of X_Patch for sample 1V contributes significantly to its PC3 value. It has a value of 895, whilst the average value for X_Patch is 14.

The contribution of X_Patch (46.5%) in the value of PC3 is also causing sample 1V to be outside the 45° ellipse.

Circularity ranges from 0.739 (sample 2C) to 0.885 (sample 3F). Normalization of these values results in 2C having a z-score of -1.98 and a z-score of 1.46 for sample 3F. The lack of Circularity for sample 2C contributes significantly to its PC3 value. It has a value of 0.739, whilst the average value for Circularity is 0.823.

The contribution of Circularity (45.9%) then X_Patch (16.8%) to the PC3 value result in it being located outside the 45° ellipse.

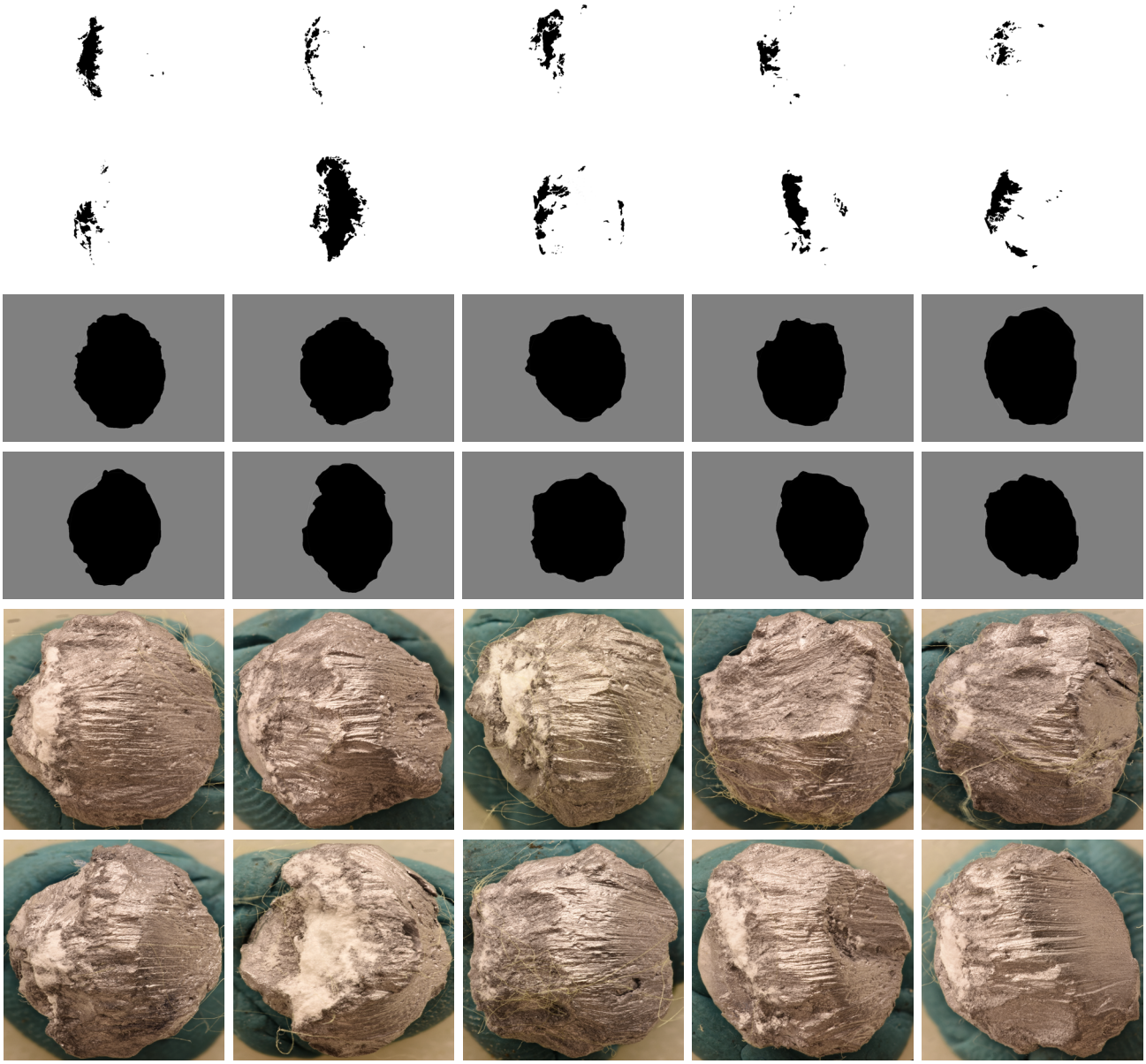

Figure 4.91: Particle selection (top two rows), bullet outline (middle two rows), and glass distribution (bottom two rows) images for 50° lead round nose bullets. Samples 1U, 1V, 1Y, 1Z, 2A (first, third, and firth rows) and samples 2B, 2C, 2D, 3F, 3M (second, fourth, and sixth rows)

5. Limitations and Future Directions

This study has many limitations. The following limitations are ranked in order of importance:

1. The bullet came to rest in a "soft" location (fiber trap). In real casework, once the bullet perforates glass, it may end up impacting a harder material such as a wall. This could change the structure of the bullet even more as well as cause material to be lost or gained by the bullet.

2. Only one distance (80 inches) was used in this study. Shorter and longer distances could be studied. The distance fired from the target would influence the velocity at which the bullet perforates the glass target. This could significantly change the structure of the bullet. Lead round nose bullets may not break apart from further distances.

3. The glass targets were similar in dimensions (width, length, and thickness). Glass targets of significantly different dimensions could be used. Longer dimensions and less thickness could have a significant impact on the structure of a bullet following perforation. The jackets of full metal jacket bullets may not separate as much if different dimensions are used.

4. Only plate glass was used. In actual casework, tempered and laminated glass are also encountered. This would allow observations to be made about how glass distributes to a bullet depending on the type of material involved in a shooting incident and how that particular bullet may deform.

5. Only two types of bullets were studied (full metal jacket and lead round nose). Other bullets types could include hollow-point and semi jacketed. This would allow for a better understanding of how different bullets deform and how glass deposits on those bullets.

6. Only five angles were studied (90°, 75°, 60°, 50°, and 45°). More angles in between these five angles could be studied to observe any characteristics that would be specific to those angles. This could prove useful in determining the angle of impact.

7. One firearm (Ruger® SR9®) was used. Performing this research with different firearms will help to understand how muzzle velocity could play a part in the structure of a bullet following perforation with a glass target.

All of the above limitations provide means for future research in this area of forensic science. Using different variables in this research would help examiners to understand how the bullet structure changes when there is a specific combination of the above variables. The more variables used in this type of research will allow examiners to better answer the question of where the shooter was positioned when they fired the shot during a shooting incident reconstruction.

6. Conclusion

The hypothesis of this research was that the angle of impact can be determined by examining and analyzing bullet structure and the glass distribution on bullets following perforation with glass.

The side view bullet deformation method using simple linear regression for full metal jacket bullets proved to be a viable method for distinguishing between possible directions that a shot was fired. However, this method does not work for lead round nose bullets.

Using simple linear regression and HemoSpat, only one method (FMJ middle) could be used to distinguish between a bullet fired at 90° and 45°. No other angles could be distinguished from each other. It is important to realize that the middle method has some bias associated with it since it would be the examiners choice as to where the best fitting ellipse is located. Therefore, the examination of bullet holes in glass from both full metal jacket and lead round nose bullets proved not to be a viable method to distinguish between between possible directions that a shot was fired.

Multiple linear regression using $Minor \times X\_Patch$ proved to be a viable method to distinguish between possible directions that a shot was fired. No variables proved to be significant when testing multiple linear regression on lead round nose bullets.

Principal component analysis can be used with the variables Area, X_Patch, Circularity, Area Largest Particle, AR, and Minor for full metal jacket bullets for distinguishing between possible directions that a shot was fired. It cannot be used with lead round nose bullets.

Although some methods could only distinguish between select angles, other methods were determined to not be viable. The results are intriguing and could eventually prove to be beneficial to not only those reconstructing the shooting incident but also to defense attorneys.

In forensic science, it is imperative that an examiner keep both the prosecutorial and the defense hypotheses in mind when examining the evidence. From a prosecutorial perspective, given that a crime has occurred, the defendant is the person who committed the crime. From a defense prospective, another person, other than the defendant, committed the crime.

For example, suppose that there was a shooting incident and the investigators on scene photographed the bullet hole in a kitchen window. Furthermore, they used software to

measure the bullet hole and calculated the angle at which the bullet perforated the glass. If this evidence is eventually brought to trial, the research performed in this study could prove beneficial to the defense. The prosecution could state that based on the calculations, person X must have been the person who fired the shot that killed person Y due to their position at the scene. However, the defense could counter by saying that there is too much variability in bullet holes in glass to exclude any other persons present at the scene.

Variability plays a huge role in forensic science and oftentimes this key factor is forgotten by those involved in the investigation. This research provides a perfect example of the importance of understanding variability and its effect on expert testimony. For example, bullets which were fired at the same angle under the same controlled conditions all presented differences in the measurable outcomes. This variation is a classic example of variability in controlled experiments. Such variability needs to be considered when developing hypotheses of what occurred during the commissioning of a crime. The big question is: "How well does the investigator understand the crime scene to conduct further analyses on a particular piece of evidence?" All variables and conditions need to be taken into account when the examiner is performing the analyses, interpreting the results, and testifying in the courtroom.

7. Appendix A - Tables and Figures

7.1 Data for all FMJ and LRN bullets

Table 7.1: All samples used for the full metal jacket bullet analysis

Sample Name	Angle (°)	Average Thickness of all 4 sides (inches)	Standard Deviation of Thickness (inches)	Length (inches)	Width (inches)
5A	90	0.1873	0.00050	8.625	4.500
6C	90	0.1853	0.00050	8.750	4.500
6G	90	0.1850	0.00000	8.625	4.500
8A	90	0.1863	0.00050	8.375	4.500
8D	90	0.1838	0.00050	8.500	4.500
8G	90	0.1833	0.00050	8.500	4.500
8I	90	0.1855	0.00058	8.500	4.500
8J	90	0.1835	0.00058	8.500	4.500
8K	90	0.1840	0.00000	8.500	4.500
8L	90	0.1853	0.00050	8.500	4.500
1D	75	0.1888	0.00050	9.125	4.375
1E	75	0.1878	0.00050	9.000	4.375
1F	75	0.1863	0.00050	8.875	4.625
1G	75	0.1840	0.00000	8.625	4.375
1H	75	0.1880	0.00000	9.000	4.375
1J	75	0.1873	0.00050	9.000	4.375
1K	75	0.1875	0.00058	8.875	4.375
4L	75	0.1923	0.00050	16.000	4.500
4M	75	0.1920	0.00000	16.000	4.375
8F	75	0.1843	0.00050	8.375	4.500
1A	60	0.1885	0.00058	9.000	4.375
1B	60	0.1888	0.00096	9.000	4.375
1C	60	0.1890	0.00000	9.125	4.375
1M	60	0.1910	0.00115	9.500	4.500
4I	60	0.1883	0.00050	16.000	4.500
4J	60	0.1885	0.00058	16.000	4.500
5C	60	0.1880	0.00000	8.500	4.500
5D	60	0.1850	0.00000	8.500	4.500
5E	60	0.1870	0.00000	8.500	4.500
8H	60	0.1860	0.00000	9.250	4.500
1L	50	0.1853	0.00050	9.500	5.000
3D	50	0.1908	0.00050	10.500	4.875
3E	50	0.1900	0.00000	10.500	4.875
3G	50	0.1890	0.00000	10.500	4.875
3H	50	0.1823	0.00050	10.500	5.000
3I	50	0.1893	0.00050	10.500	5.000
3J	50	0.1900	0.00000	10.500	5.000
3L	50	0.1893	0.00050	9.000	5.000
5B	50	0.1890	0.00000	8.500	4.500
6A	50	0.1910	0.00000	8.625	5.000
1Q	45	0.1870	0.00082	10.500	4.875
1R	45	0.1893	0.00050	10.625	5.000
1S	45	0.1893	0.00050	10.500	4.875
1T	45	0.1885	0.00100	10.500	4.875
1W	45	0.1855	0.00058	10.375	5.000
1X	45	0.1890	0.00000	10.500	5.125
3A	45	0.1900	0.00000	10.500	5.000
3B	45	0.1913	0.00050	10.500	5.000
3C	45	0.1908	0.00050	10.500	4.875
3K	45	0.1905	0.00058	10.500	4.750

Table 7.2: All samples used for the lead round nose bullet analysis

Sample Name	Angle (°)	Average Thickness of all 4 sides (inches)	Standard Deviation of Thickness (inches)	Length (inches)	Width (inches)
5I	90	0.1920	0.00000	7.875	4.000
5J	90	0.1920	0.00000	7.875	4.000
5K	90	0.1900	0.00000	7.875	4.000
5M	90	0.1893	0.00050	7.875	4.000
5O	90	0.1913	0.00050	8.000	4.000
5S	90	0.1883	0.00050	8.500	4.000
5U	90	0.1880	0.00000	7.875	4.000
5V	90	0.1880	0.00000	8.000	4.000
6E	90	0.1910	0.00000	9.000	4.875
8E	90	0.1875	0.00058	8.000	4.000
3W	75	0.1888	0.00050	10.500	4.125
3X	75	0.1890	0.00000	10.500	3.750
3Y	75	0.1893	0.00050	10.500	3.750
3Z	75	0.1900	0.00000	10.500	3.875
5H	75	0.1913	0.00050	8.000	4.000
5L	75	0.1900	0.00000	8.000	4.000
5N	75	0.1895	0.00058	7.375	4.000
5P	75	0.1865	0.00058	8.000	4.000
5Q	75	0.1860	0.00000	7.750	4.500
5T	75	0.1840	0.00000	8.500	4.800
3R	60	0.1880	0.00000	10.625	4.000
3S	60	0.1895	0.00058	10.625	4.250
3T	60	0.1895	0.00058	10.500	4.250
8R	60	0.1908	0.00050	11.875	4.000
8S	60	0.1903	0.00050	11.875	4.000
8T	60	0.1900	0.00000	11.875	4.000
8U	60	0.1895	0.00058	11.875	4.000
8V	60	0.1893	0.00050	11.875	4.000
8W	60	0.1900	0.00000	11.875	4.000
8X	60	0.1898	0.00050	11.875	4.000
3U	50	0.1893	0.00050	10.500	4.375
6P	50	0.1860	0.00000	10.500	4.250
6Q	50	0.1878	0.00050	9.500	4.625
6R	50	0.1905	0.00058	11.875	4.000
6S	50	0.1903	0.00050	11.875	4.000
6T	50	0.1830	0.00000	12.125	4.500
6U	50	0.1835	0.00058	12.000	4.500
6V	50	0.1903	0.00050	11.875	4.000
8Y	50	0.1888	0.00050	12.125	4.500
8Z	50	0.1860	0.00000	12.125	5.000
1U	45	0.1883	0.00050	10.500	5.000
1V	45	0.1885	0.00058	10.500	4.875
1Y	45	0.1828	0.00050	10.500	4.875
1Z	45	0.1850	0.00000	10.250	5.000
2A	45	0.1890	0.00000	10.500	5.000
2B	45	0.1873	0.00050	10.500	5.000
2C	45	0.1870	0.00000	10.500	5.000
2D	45	0.1880	0.00000	10.500	5.000
3M	45	0.1898	0.00050	9.125	6.000
3F	45	0.1868	0.00050	10.500	5.000

7.2 Bullet deformation plots for the FMJ bullet data

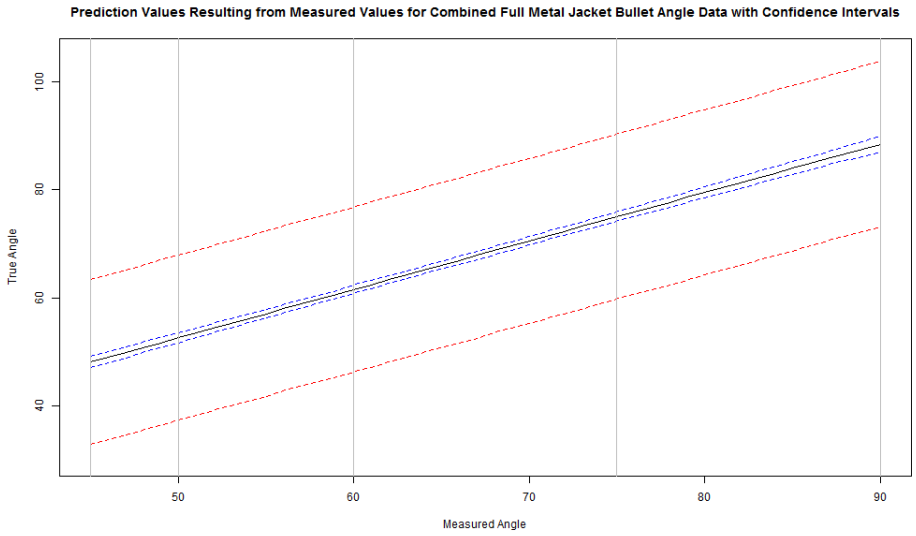

Figure 7.1: Prediction values for combined full metal jacket bullet angle data

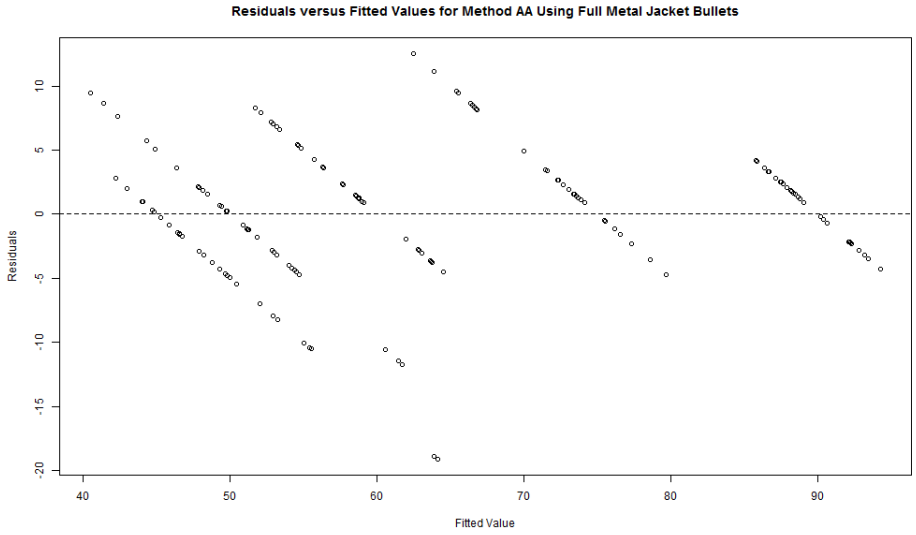

Figure 7.2: Pred-res plot (residual versus fitted values) for method AA using full metal jacket bullet angle data

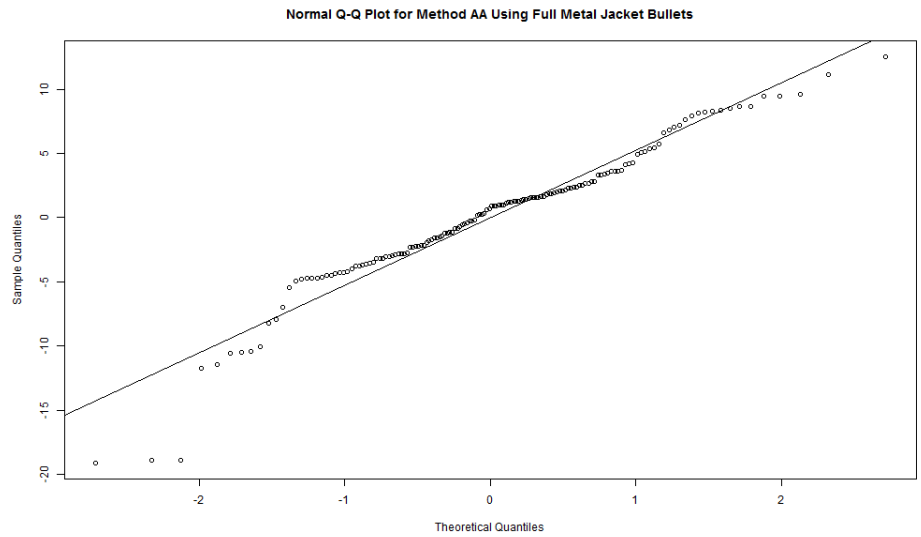

Figure 7.3: Normal Q-Q plot for method AA using full metal jacket bullet angle data

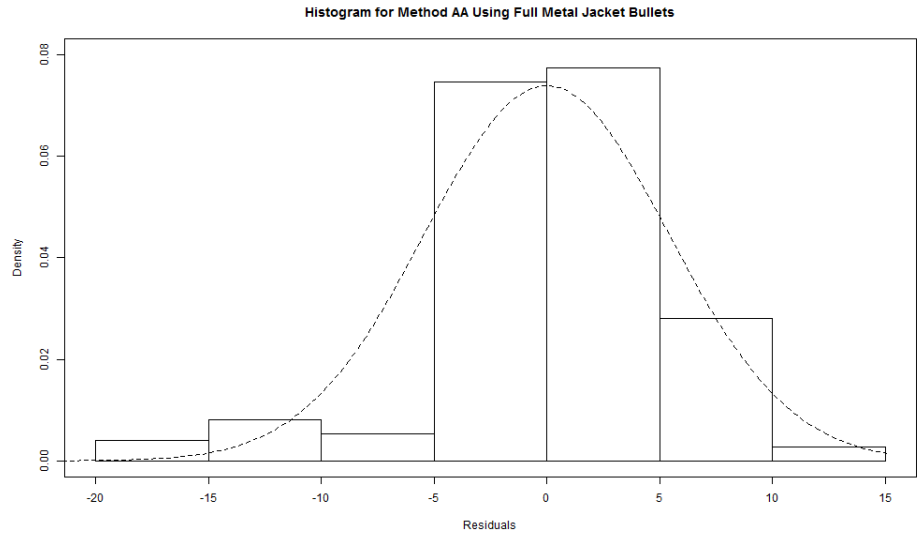

Figure 7.4: Histogram for method AA using full metal jacket bullet angle data

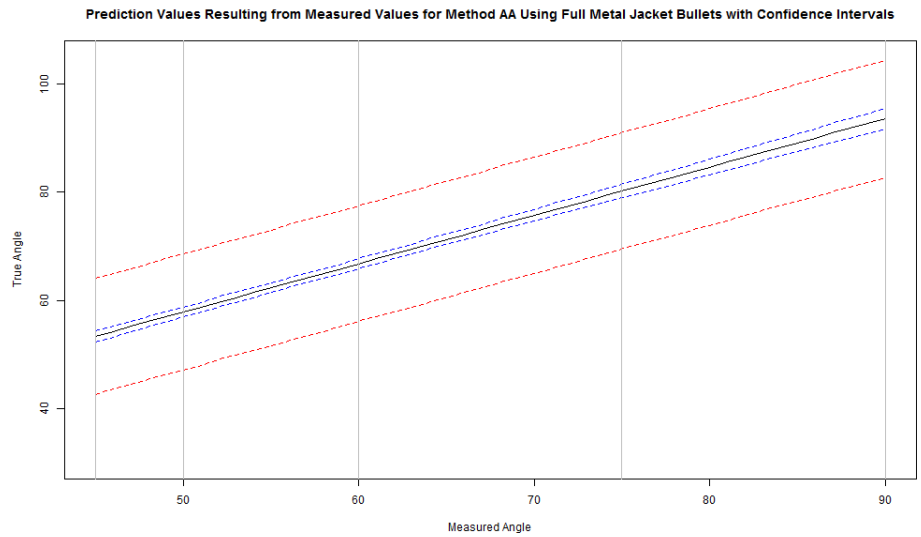

Figure 7.5: Prediction values for method AA using full metal jacket bullet angle data

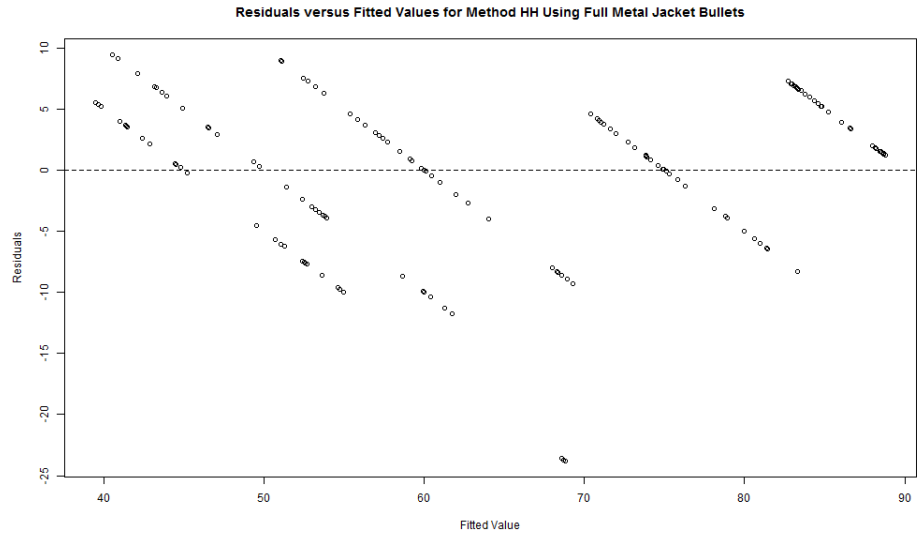

Figure 7.6: Pred-res plot (residual versus fitted values) for method HH using full metal jacket bullet angle data

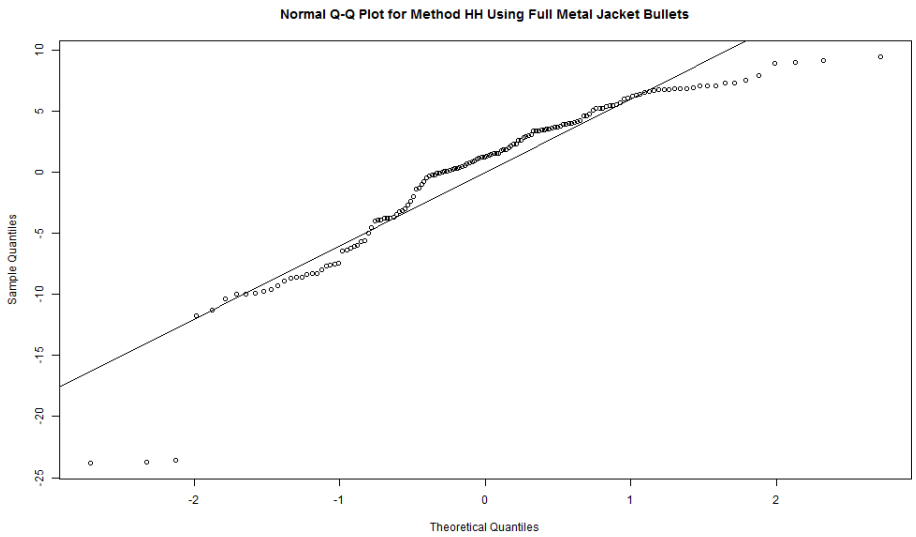

Figure 7.7: Normal Q-Q plot for method HH using full metal jacket bullet angle data

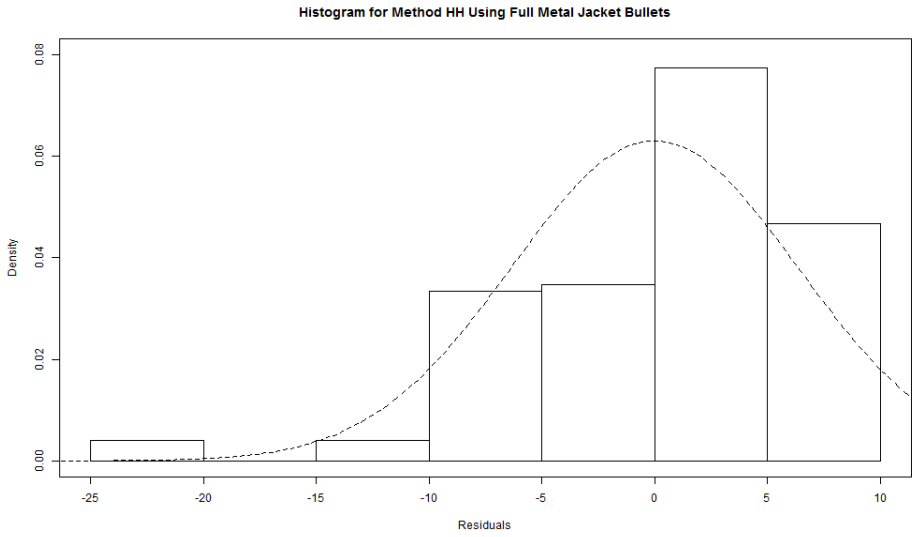

Figure 7.8: Histogram for method HH using full metal jacket bullet angle data

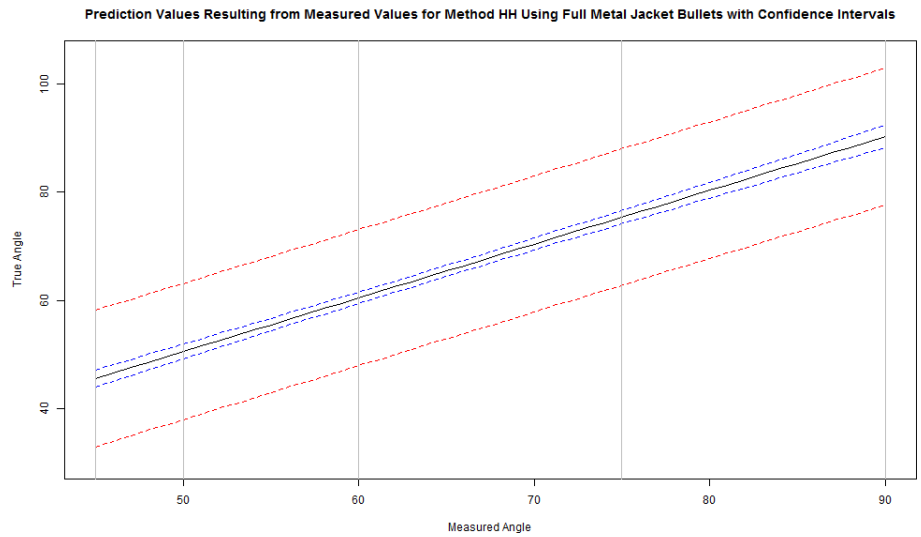

Figure 7.9: Prediction values for method HH using full metal jacket bullet angle data

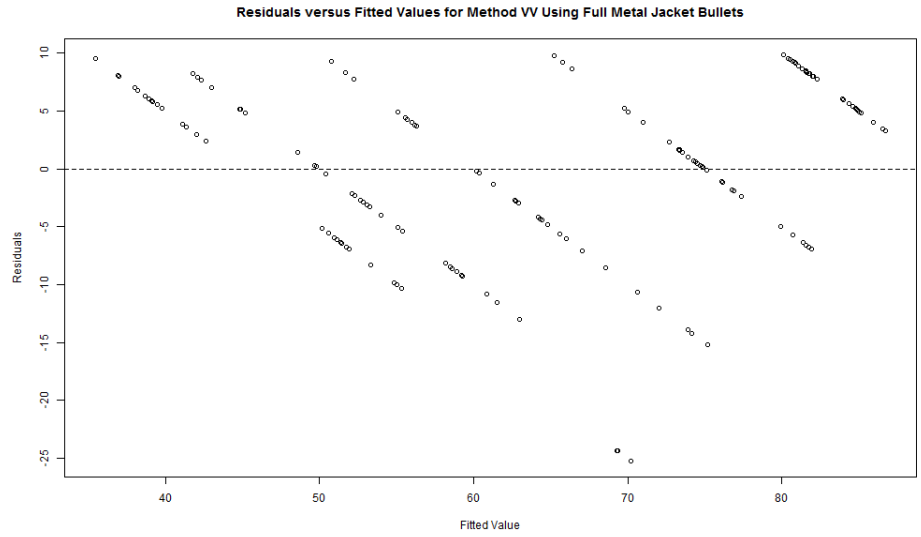

Figure 7.10: Pred-res plot (residual versus fitted values) for method VV using full metal jacket bullet angle data

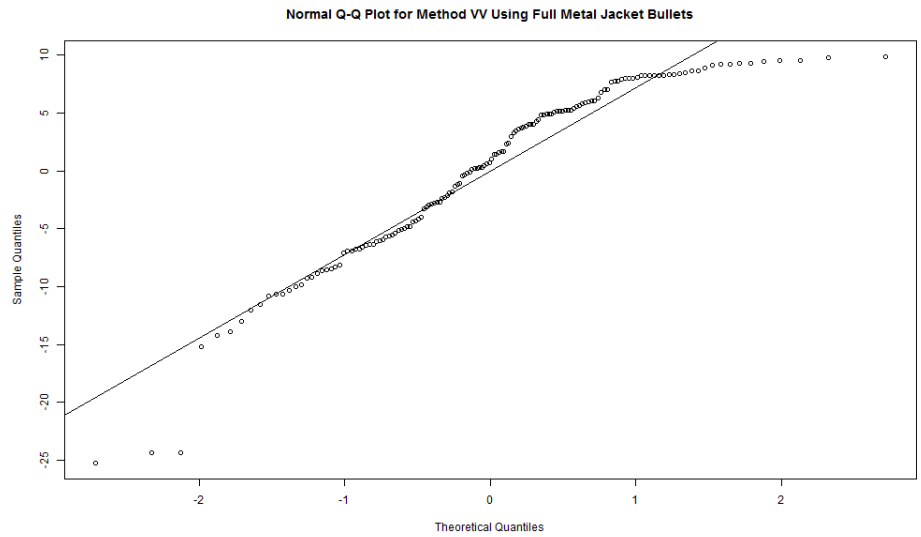

Figure 7.11: Normal Q-Q plot for method VV using full metal jacket bullet angle data

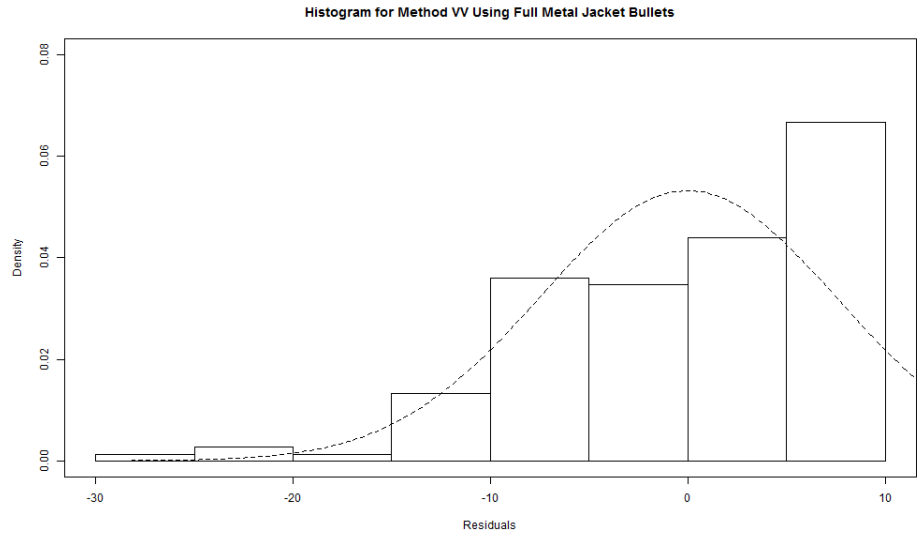

Figure 7.12: Histogram for method VV using full metal jacket bullet angle data

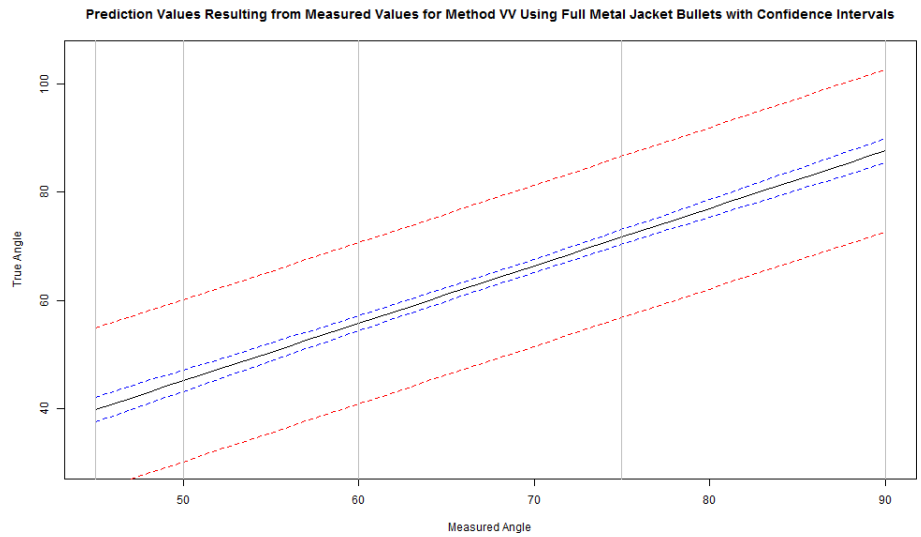

Figure 7.13: Prediction values for method VV using full metal jacket bullet angle data

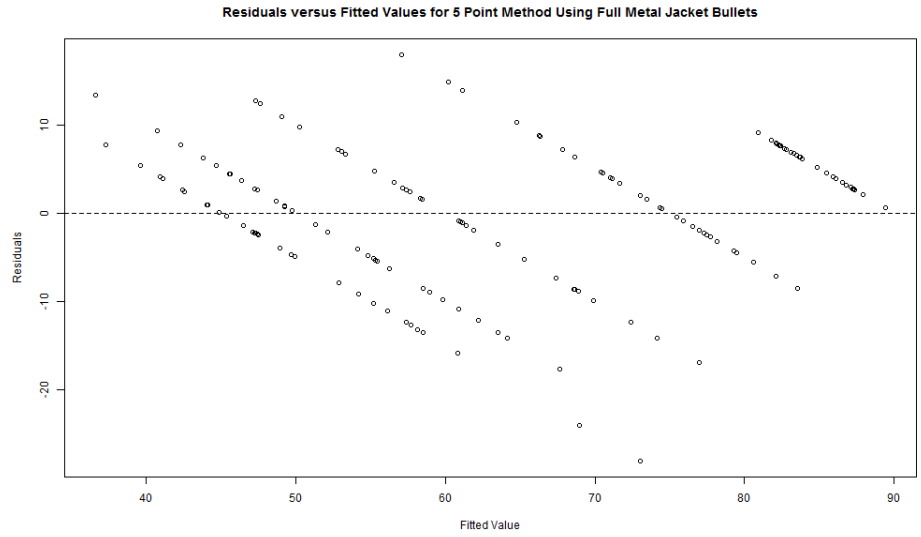

Figure 7.14: Pred-res plot (residual versus fitted values) for 5 points using full metal jacket bullet angle data

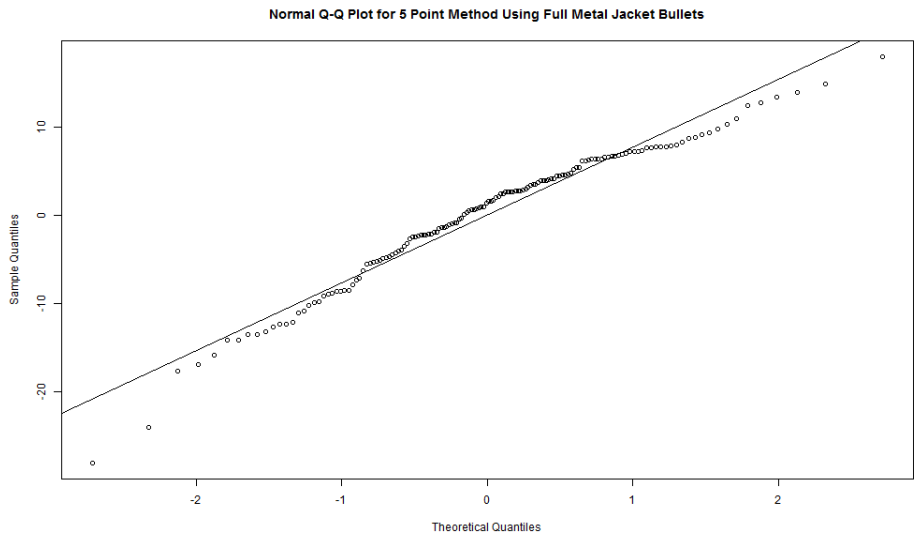

Figure 7.15: Normal Q-Q plot for 5 points using full metal jacket bullet angle data

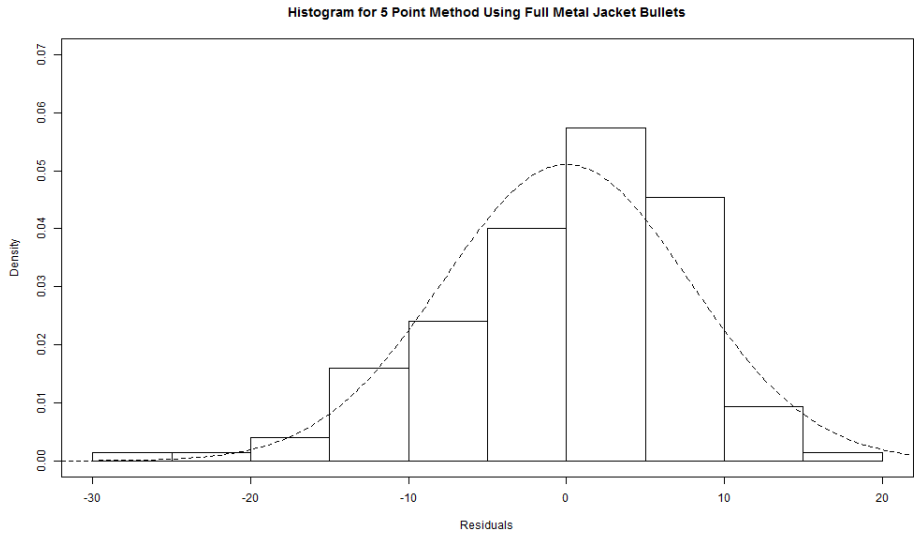

Figure 7.16: Histogram for 5 points using full metal jacket bullet angle data

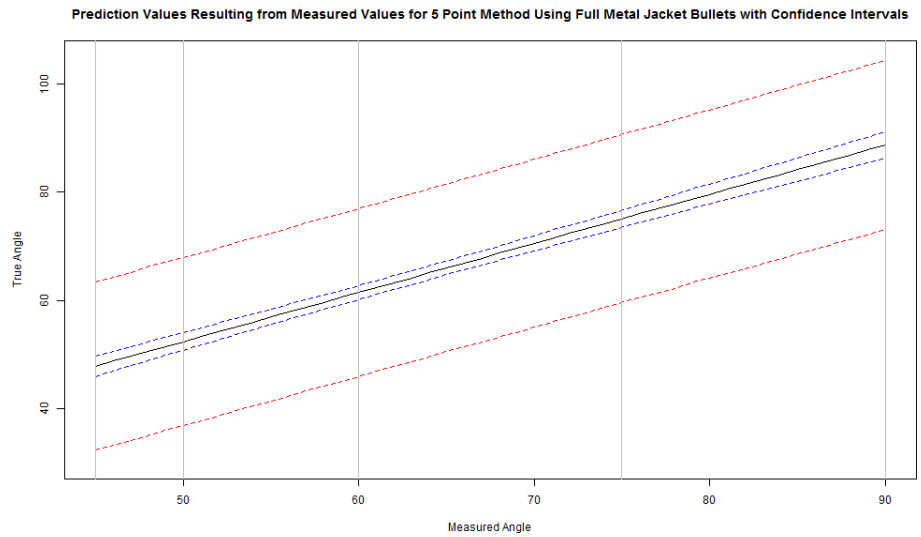

Figure 7.17: Prediction values for 5 points using full metal jacket bullet angle data

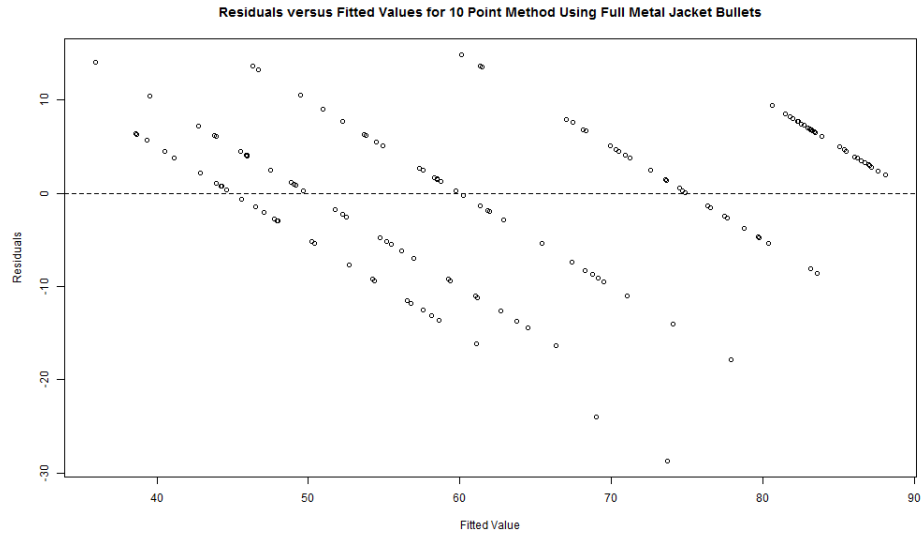

Figure 7.18: Pred-res plot (residual versus fitted values) for 10 points using full metal jacket bullet angle data

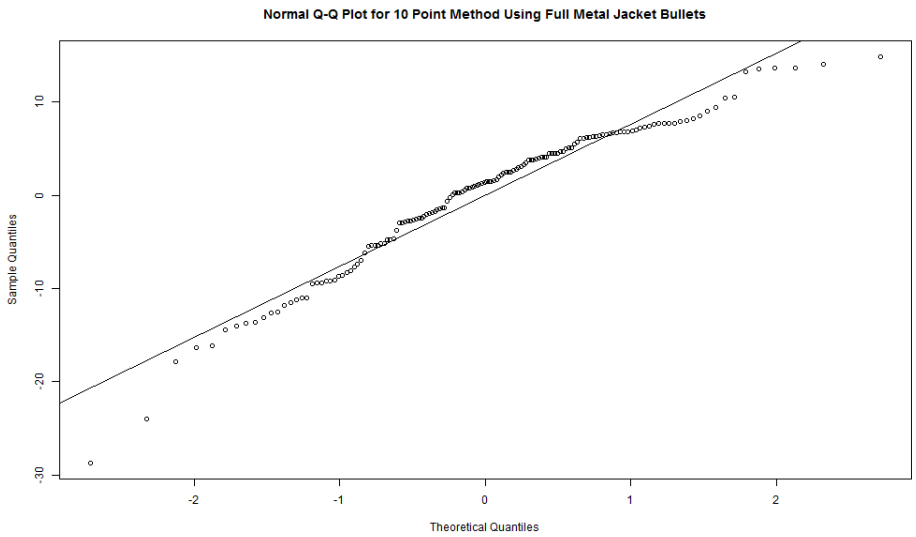

Figure 7.19: Normal Q-Q plot for 10 points using full metal jacket bullet angle data

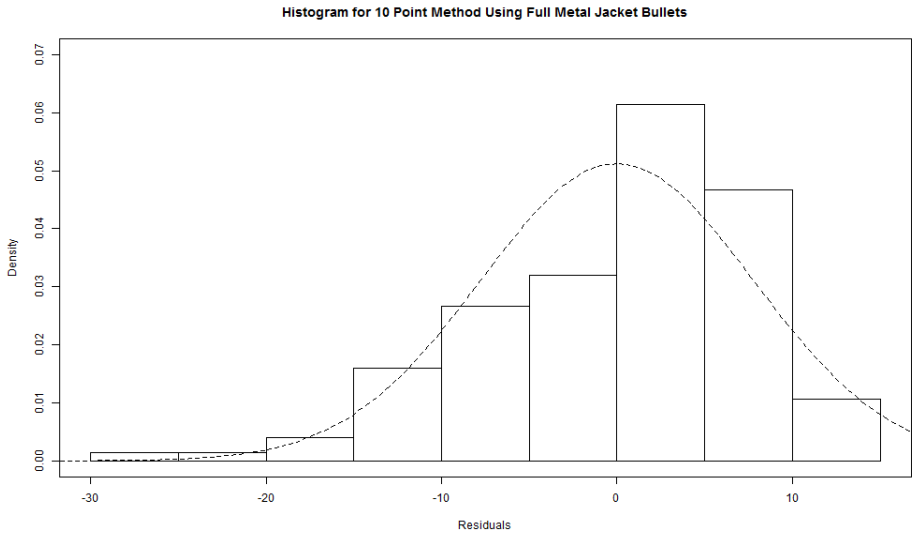

Figure 7.20: Histogram for 10 points using full metal jacket bullet angle data

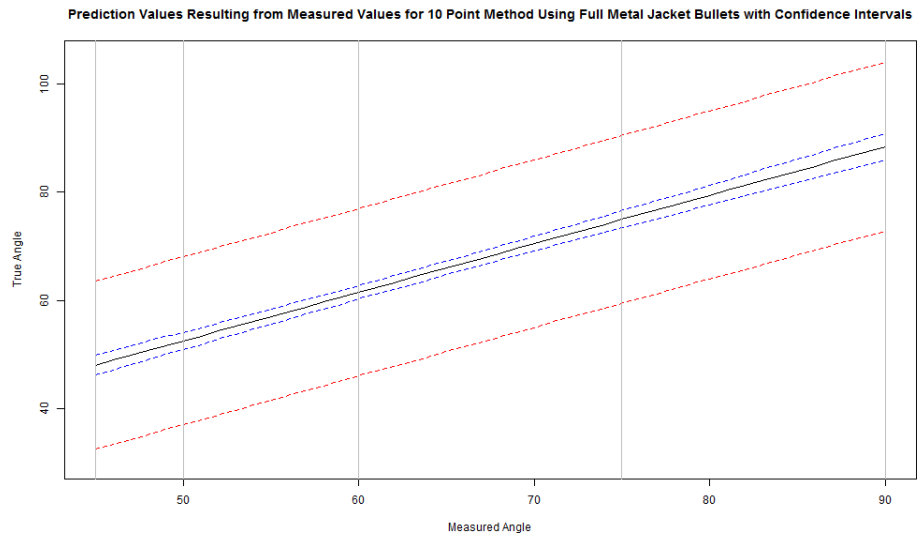

Figure 7.21: Prediction values for 10 points using full metal jacket bullet angle data

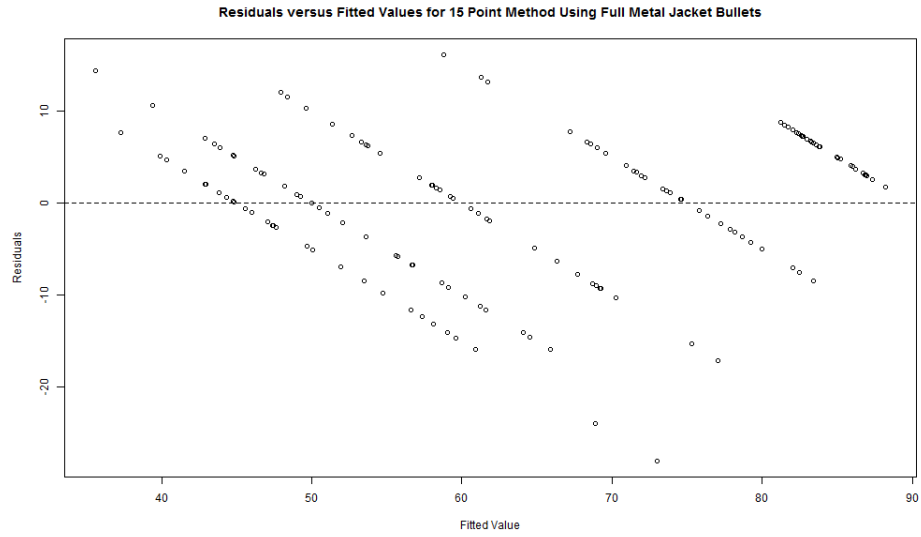

Figure 7.22: Pred-res plot (residual versus fitted values) for 15 points using full metal jacket bullet angle data

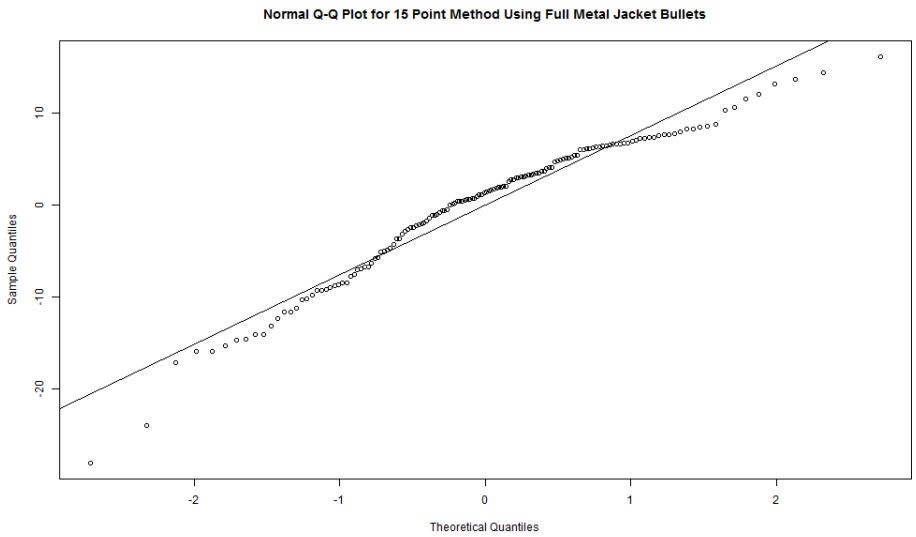

Figure 7.23: Normal Q-Q plot for 15 points using full metal jacket bullet angle data

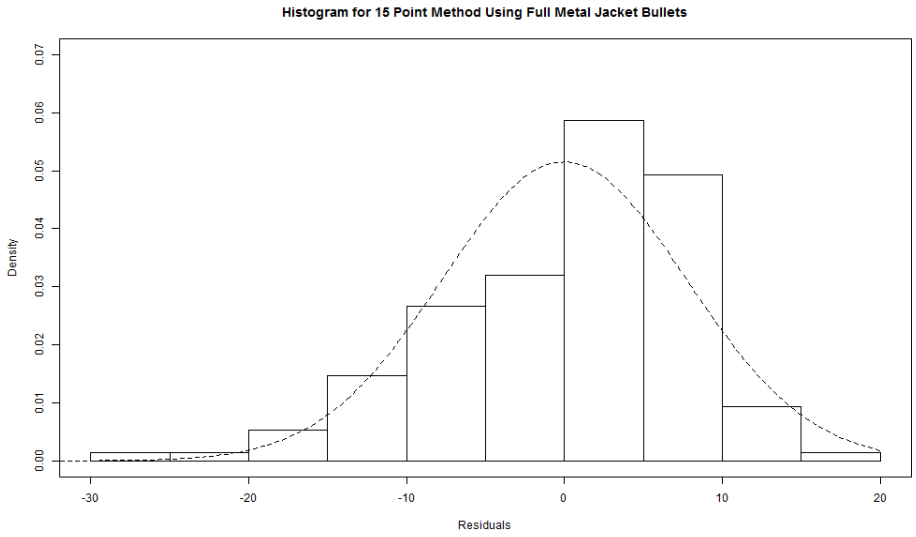

Figure 7.24: Histogram for 15 points using full metal jacket bullet angle data

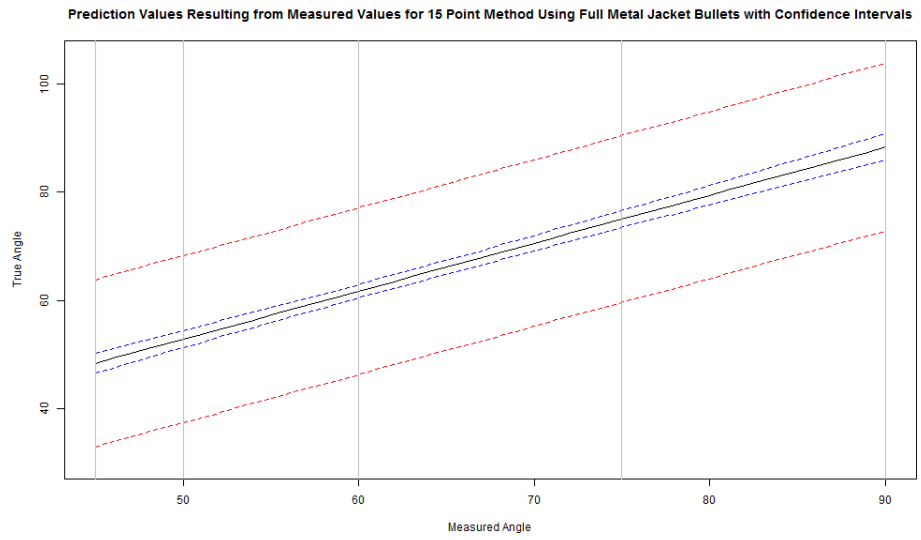

Figure 7.25: Prediction values for 15 points using full metal jacket bullet angle data

7.3 Bullet deformation plots for the LRN bullet data

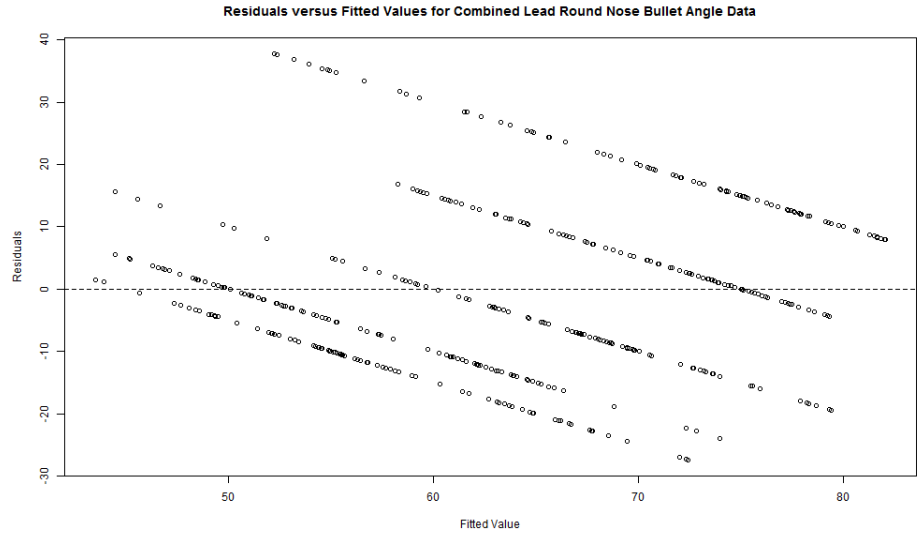

Figure 7.26: Pred-res plot (residual versus fitted values) for combined lead round nose bullet angle data

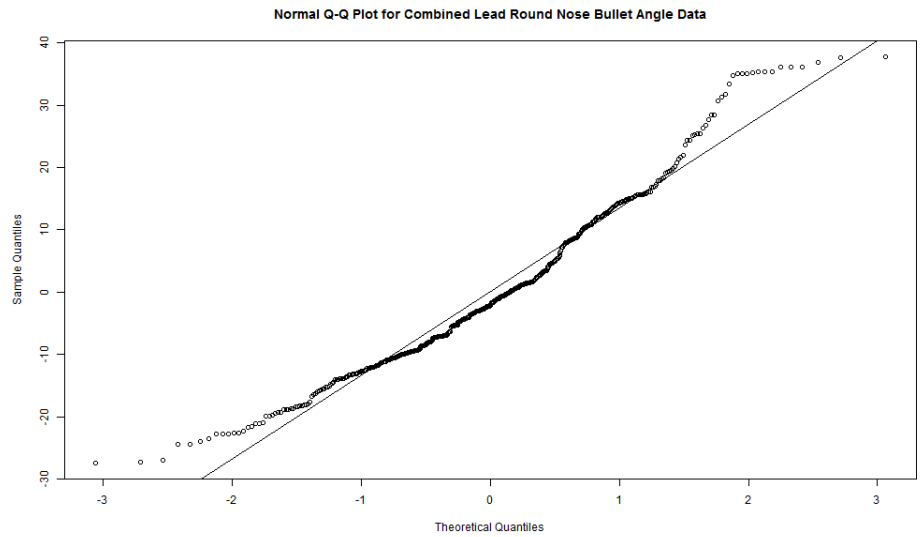

Figure 7.27: Normal Q-Q plot for combined lead round nose bullet angle data

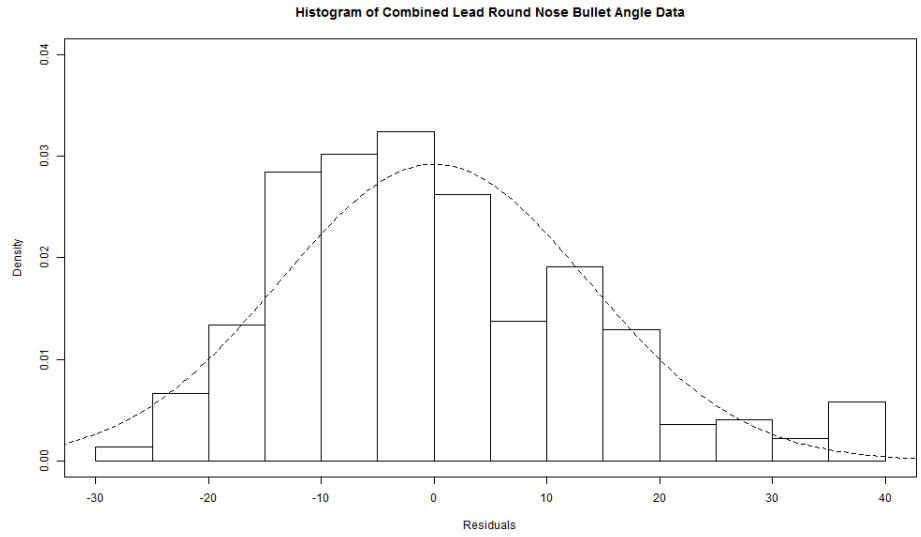

Figure 7.28: Histogram for combined lead round nose bullet angle data

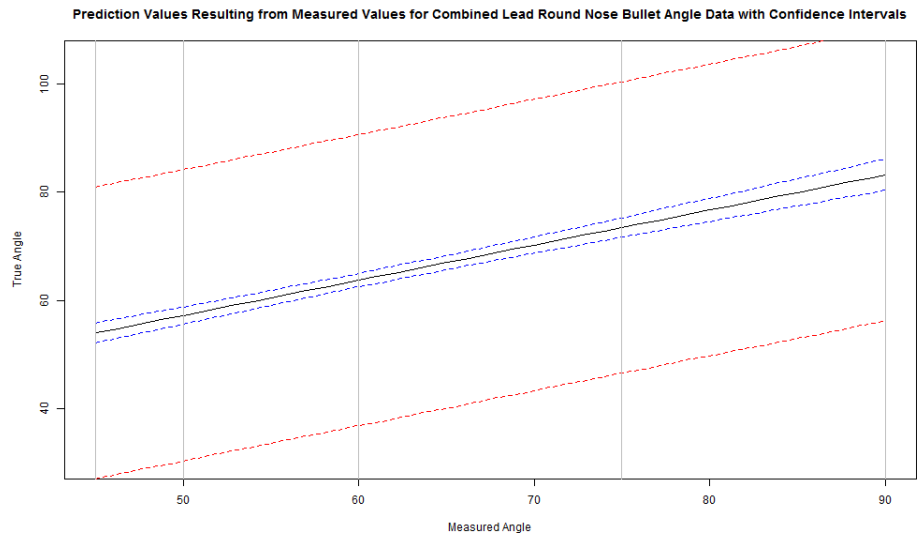

Figure 7.29: Prediction values for combined lead round nose bullet angle data

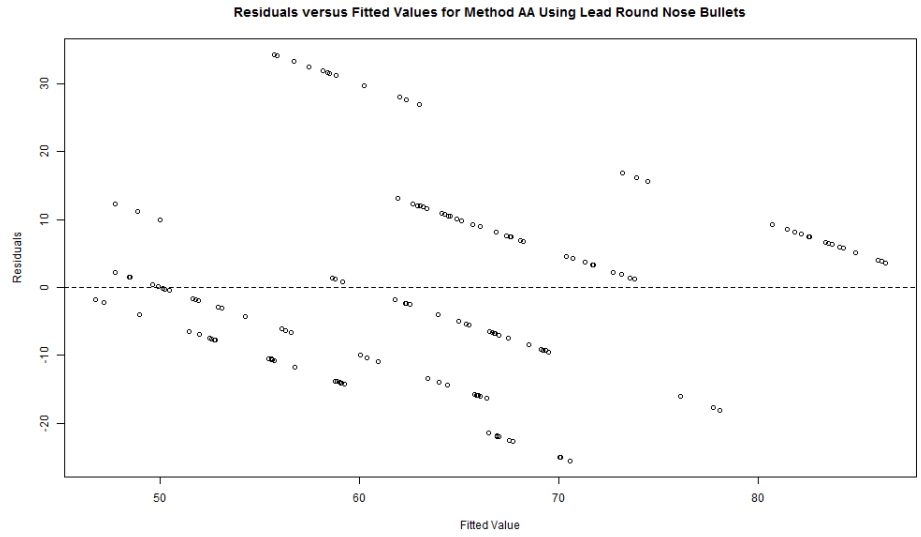

Figure 7.30: Pred-res plot (residual versus fitted values) for method AA using lead round nose bullet angle data

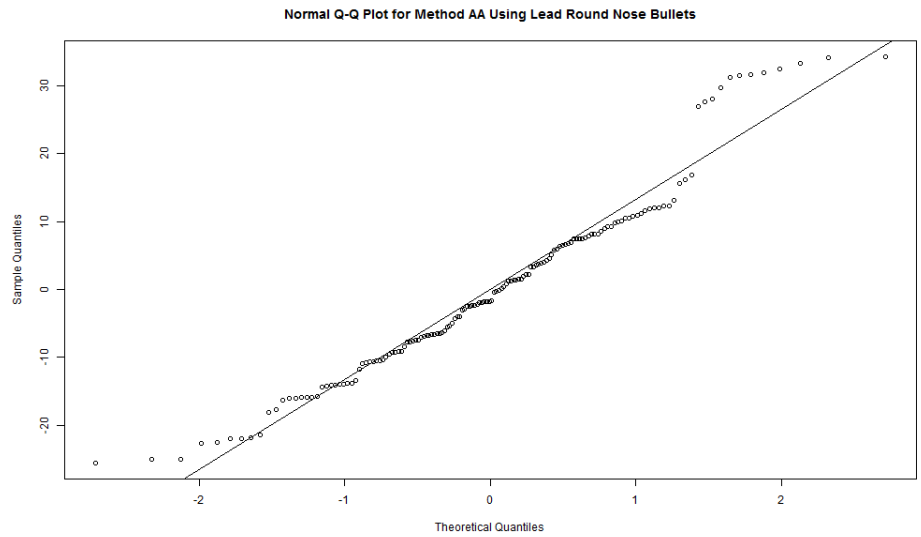

Figure 7.31: Normal Q-Q plot for method AA using lead round nose bullet angle data

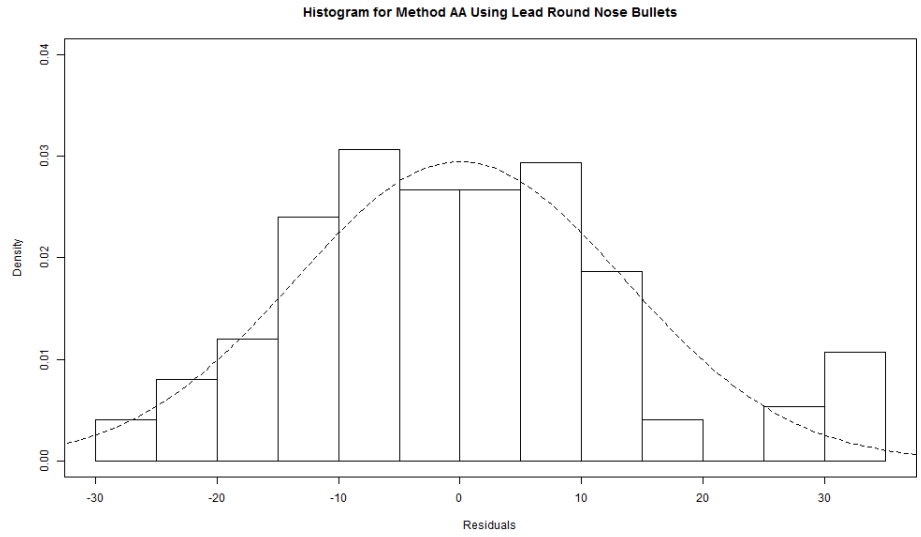

Figure 7.32: Histogram for method AA using lead round nose bullet angle data

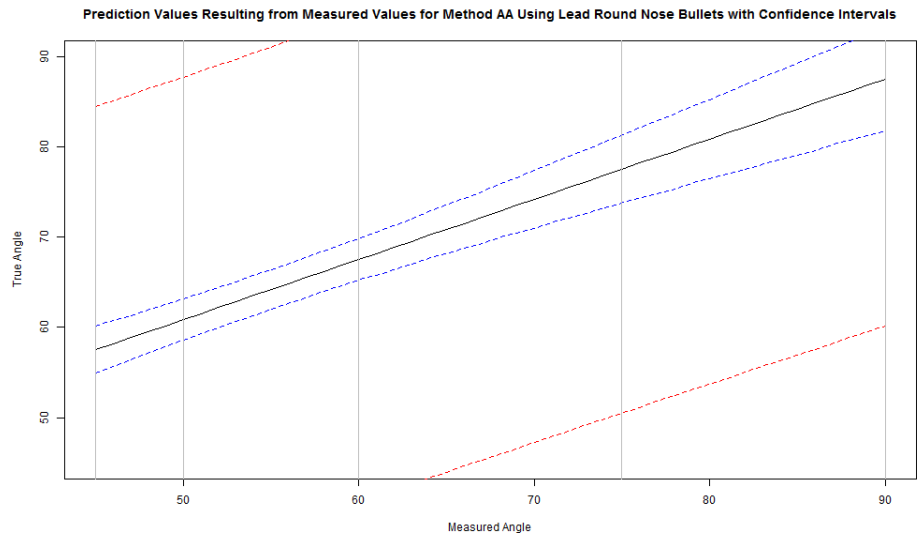

Figure 7.33: Prediction values for method AA using lead round nose bullet angle data

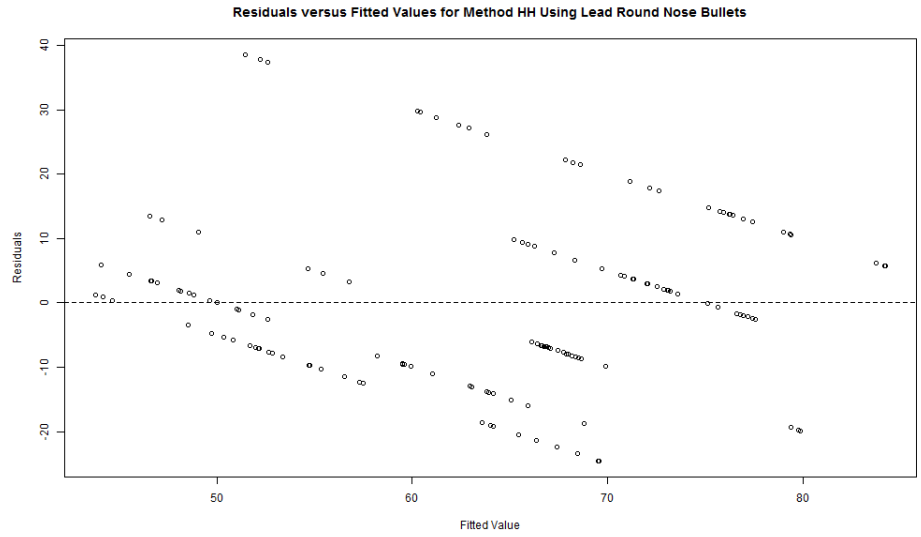

Figure 7.34: Pred-res plot (residual versus fitted values) for method HH using lead round nose bullet angle data

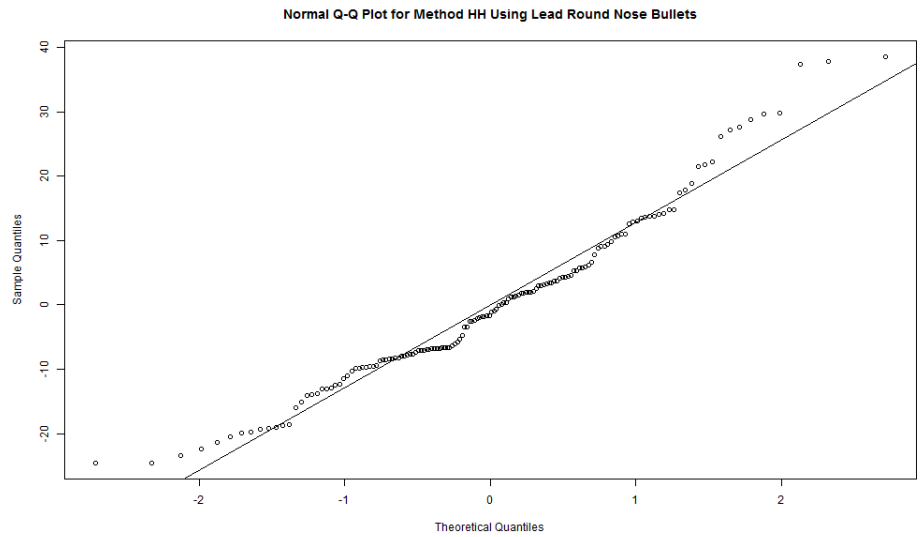

Figure 7.35: Normal Q-Q plot for method HH using lead round nose bullet angle data

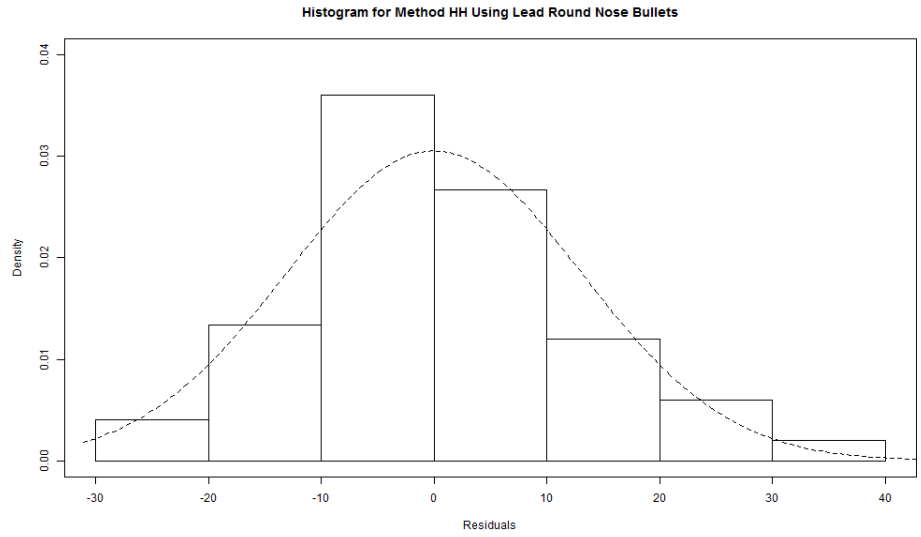

Figure 7.36: Histogram for method HH using lead round nose bullet angle data

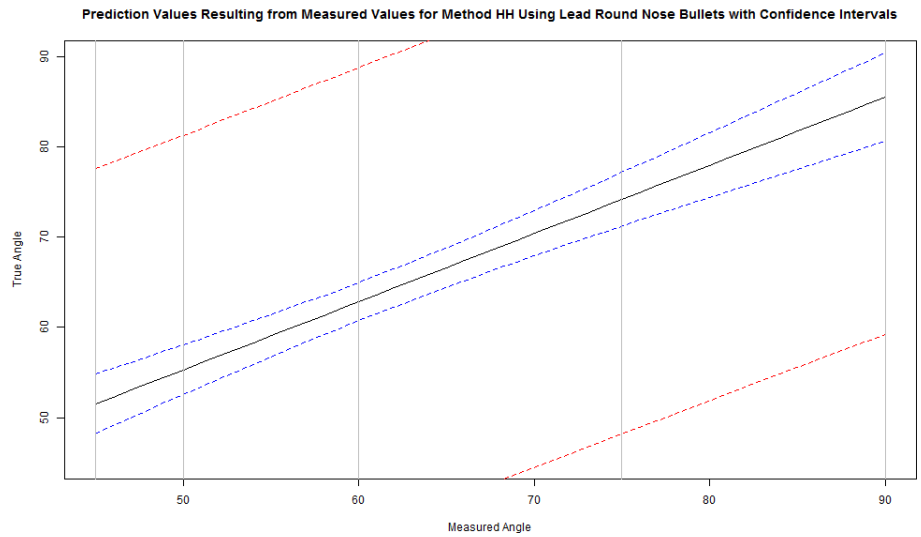

Figure 7.37: Prediction values for method HH using lead round nose bullet angle data

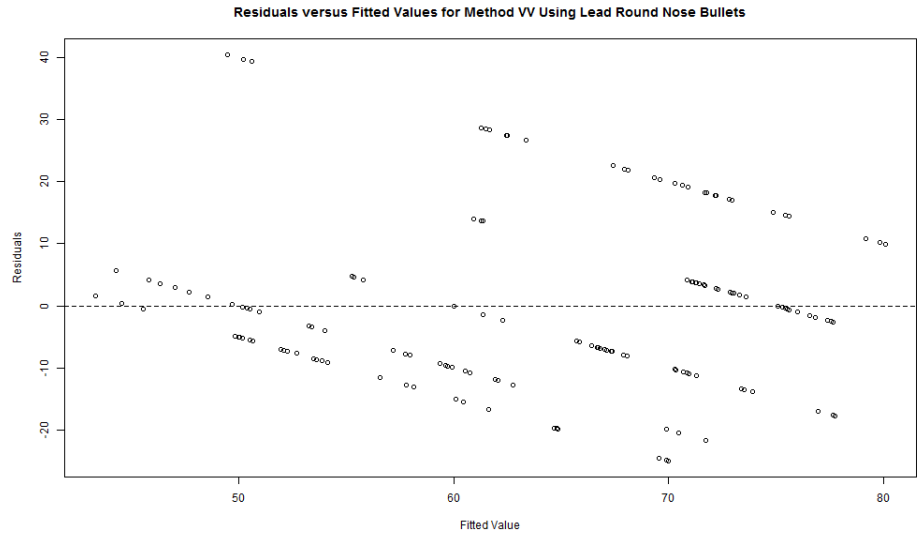

Figure 7.38: Pred-res plot (residual versus fitted values) for method VV using lead round nose bullet angle data

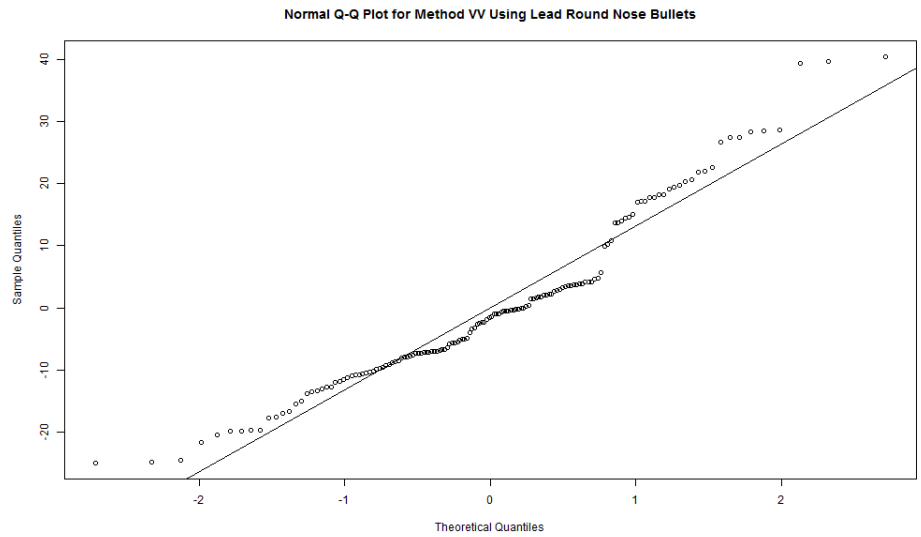

Figure 7.39: Normal Q-Q plot for method VV using lead round nose bullet angle data

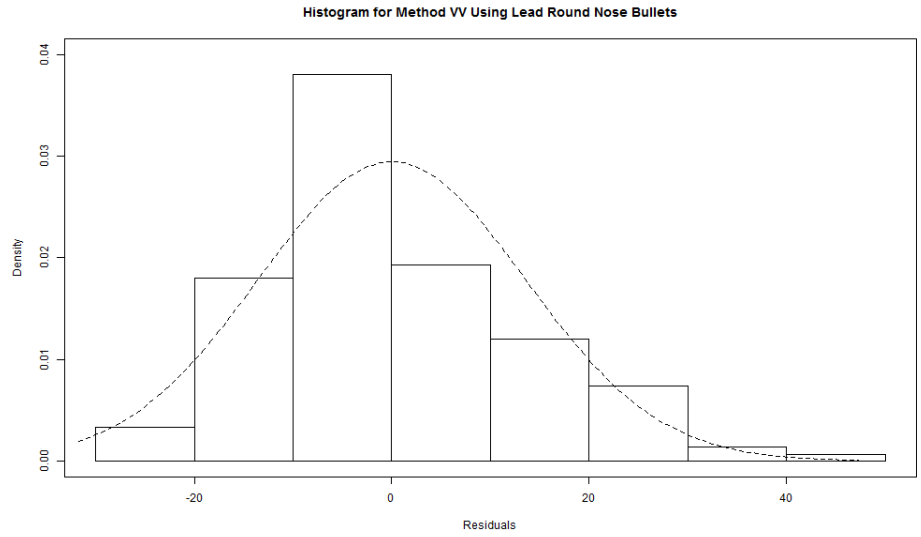

Figure 7.40: Histogram for method VV using lead round nose bullet angle data

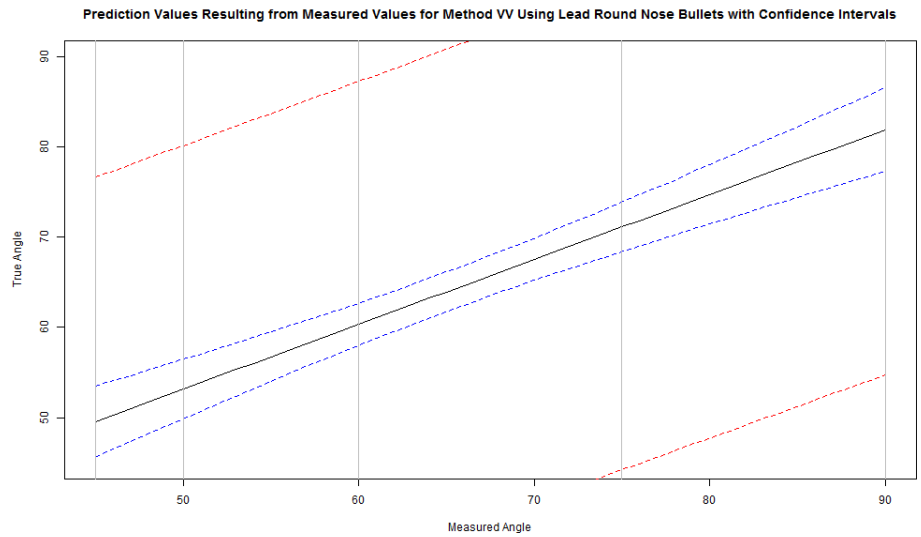

Figure 7.41: Prediction values for method VV using lead round nose bullet angle data

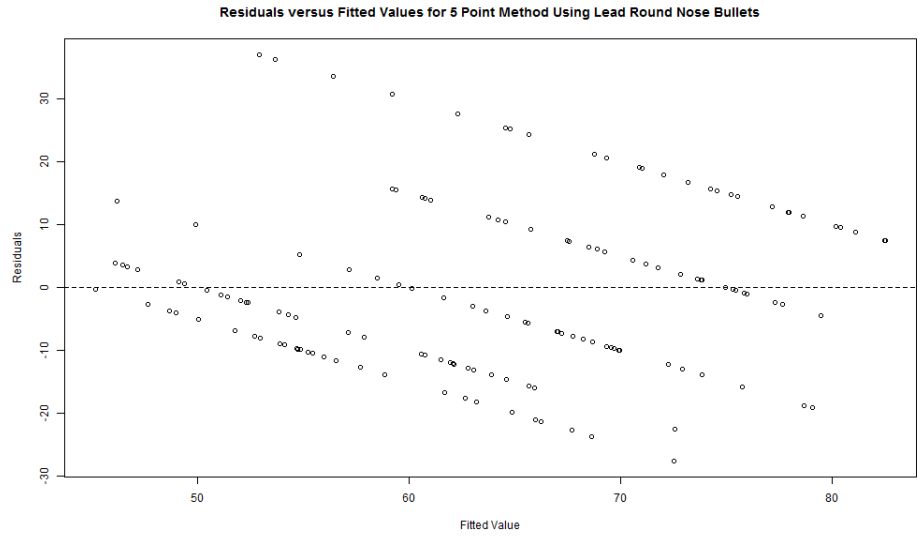

Figure 7.42: Pred-res plot (residual versus fitted values) for 5 points using lead round nose bullet angle data

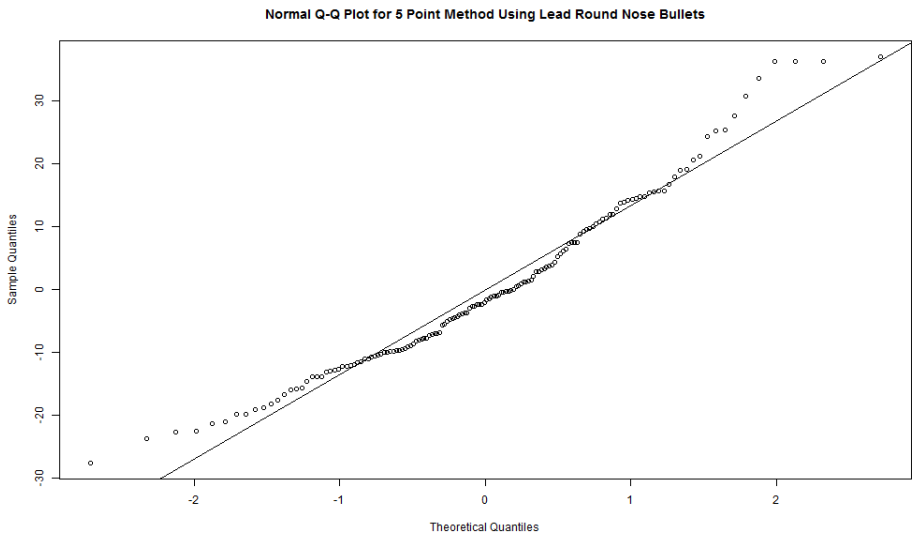

Figure 7.43: Normal Q-Q plot for 5 points using lead round nose bullet angle data

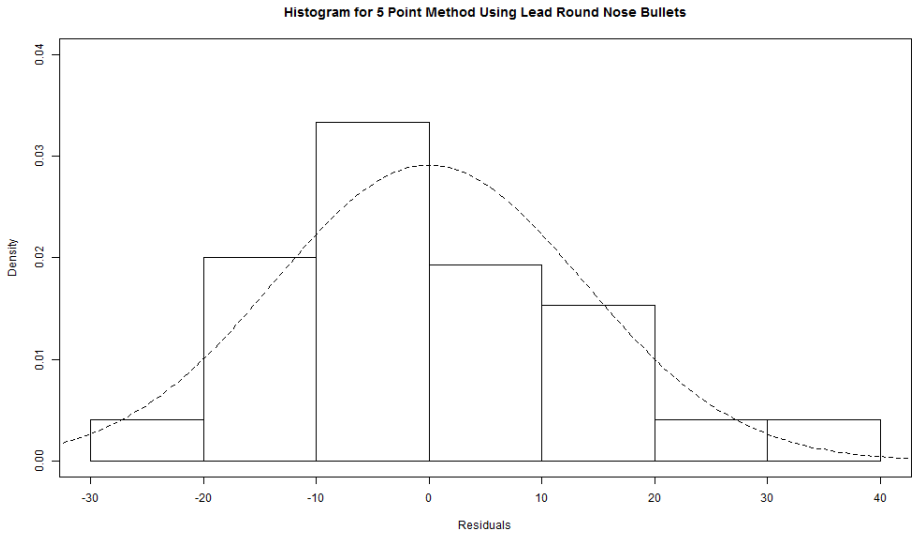

Figure 7.44: Histogram for 5 points using lead round nose bullet angle data

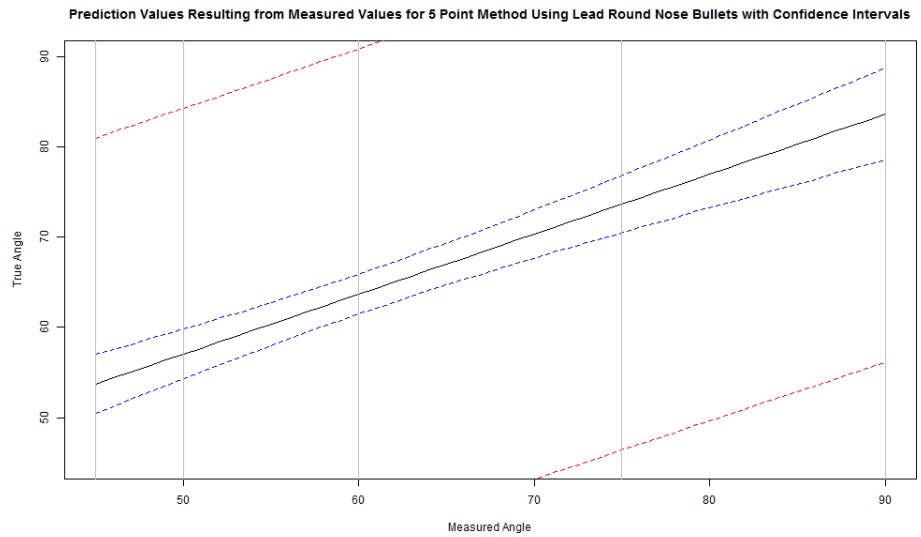

Figure 7.45: Prediction values for 5 points using lead round nose bullet angle data

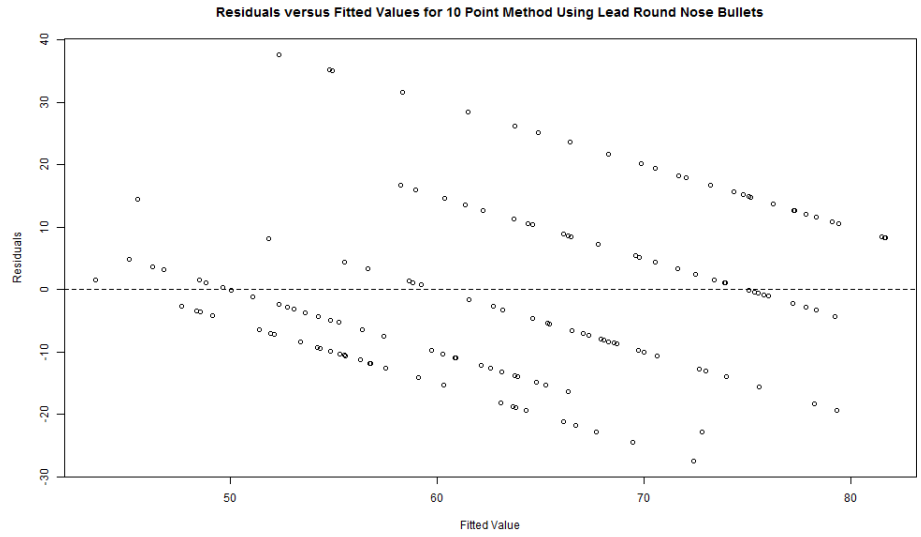

Figure 7.46: Pred-res plot (residual versus fitted values) for 10 points using lead round nose bullet angle data

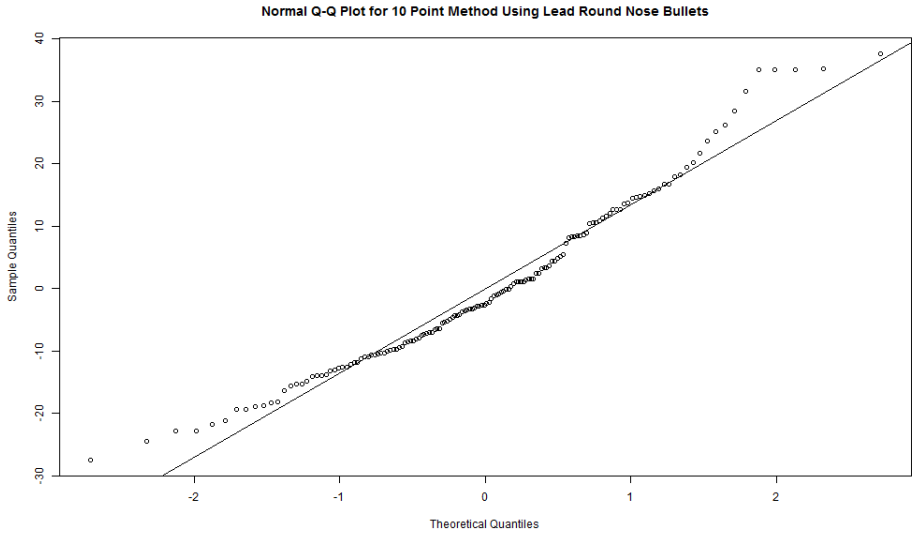

Figure 7.47: Normal Q-Q plot for 10 points using lead round nose bullet angle data

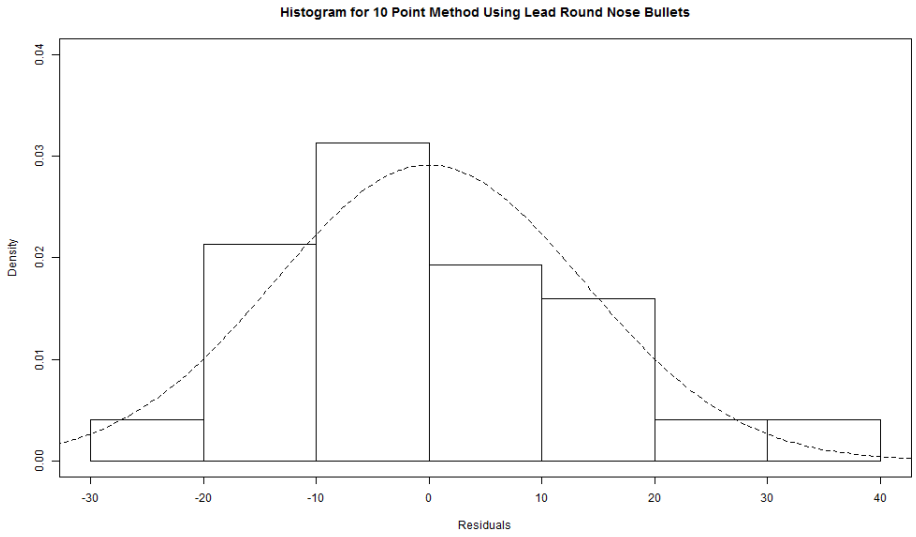

Figure 7.48: Histogram for 10 points using lead round nose bullet angle data

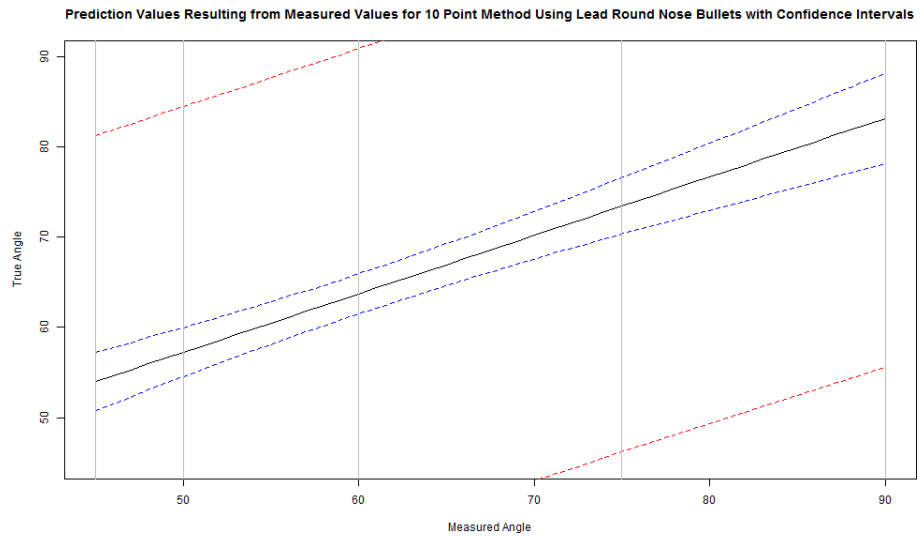

Figure 7.49: Prediction values for 10 points using lead round nose bullet angle data

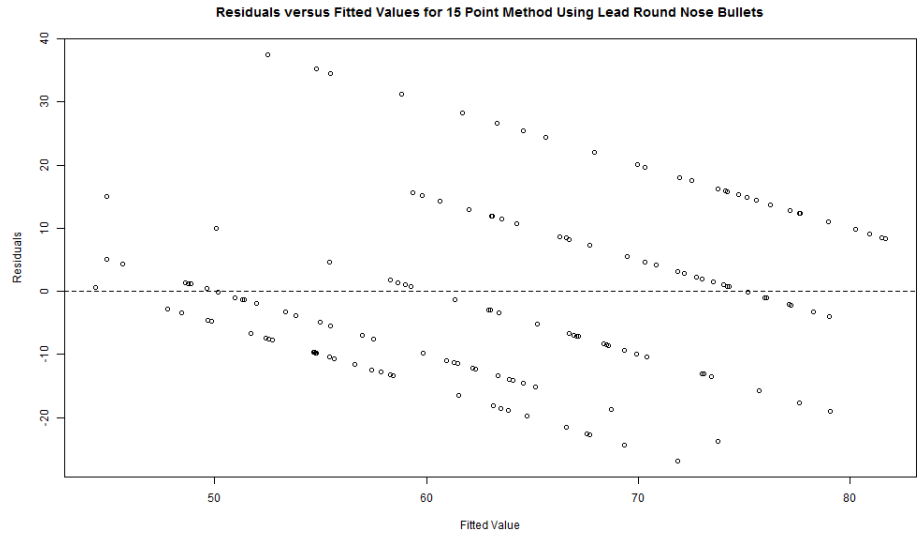

Figure 7.50: Pred-res plot (residual versus fitted values) for 15 points using lead round nose bullet angle data

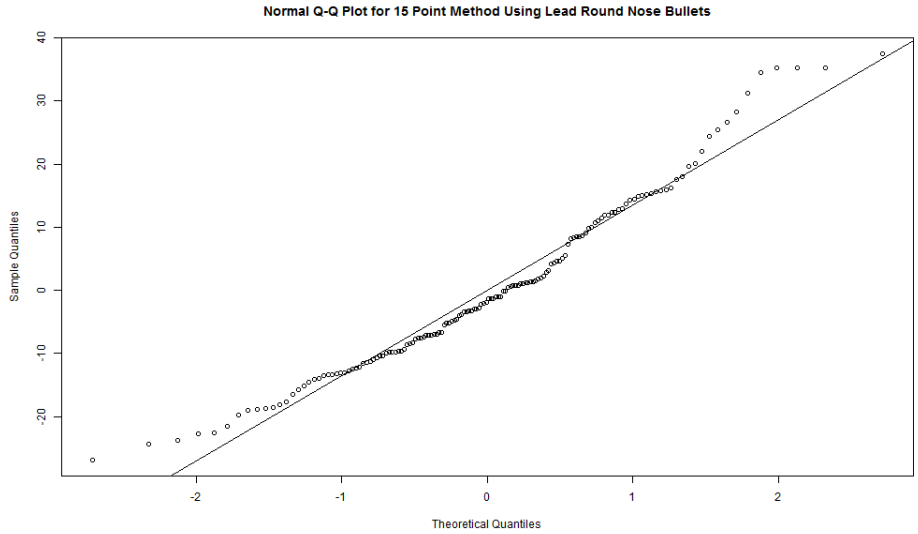

Figure 7.51: Normal Q-Q plot for 15 points using lead round nose bullet angle data

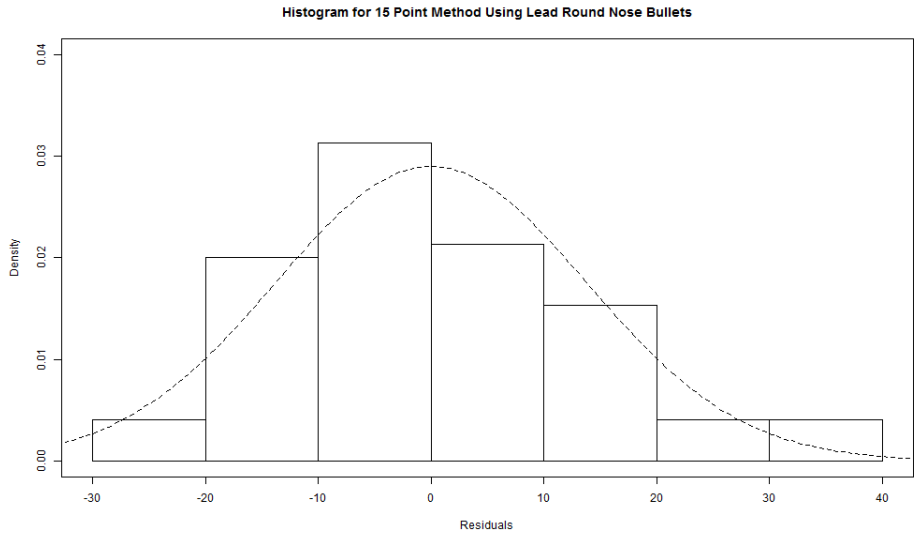

Figure 7.52: Histogram for 15 points using lead round nose bullet angle data

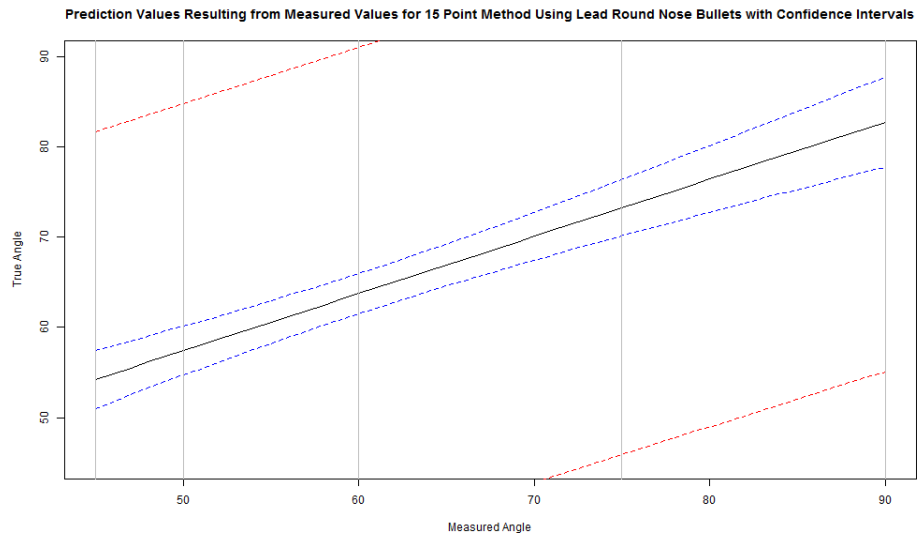

Figure 7.53: Prediction values for 15 points using lead round nose bullet angle data

7.4 HemoSpat plots for the FMJ bullet data

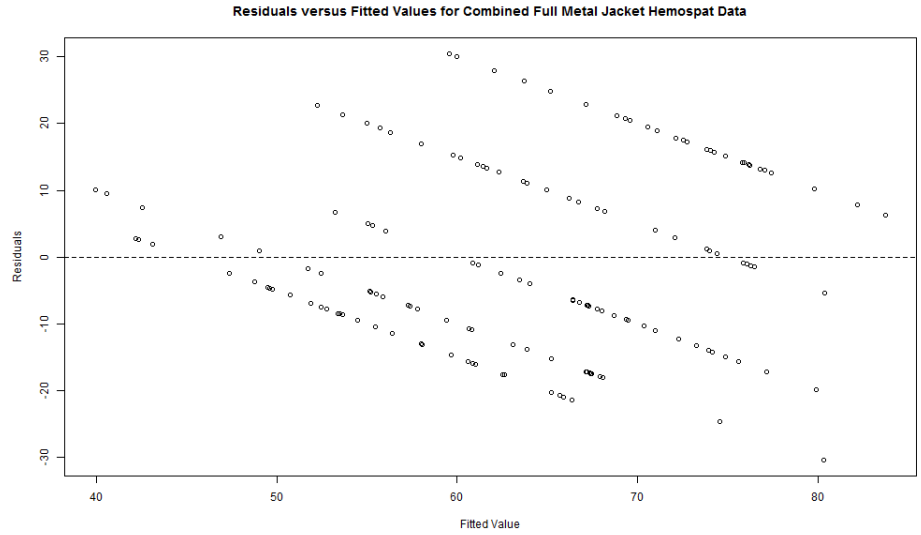

Figure 7.54: Pred-res plot (residual versus fitted values) for combined full metal jacket bullet HemoSpat data

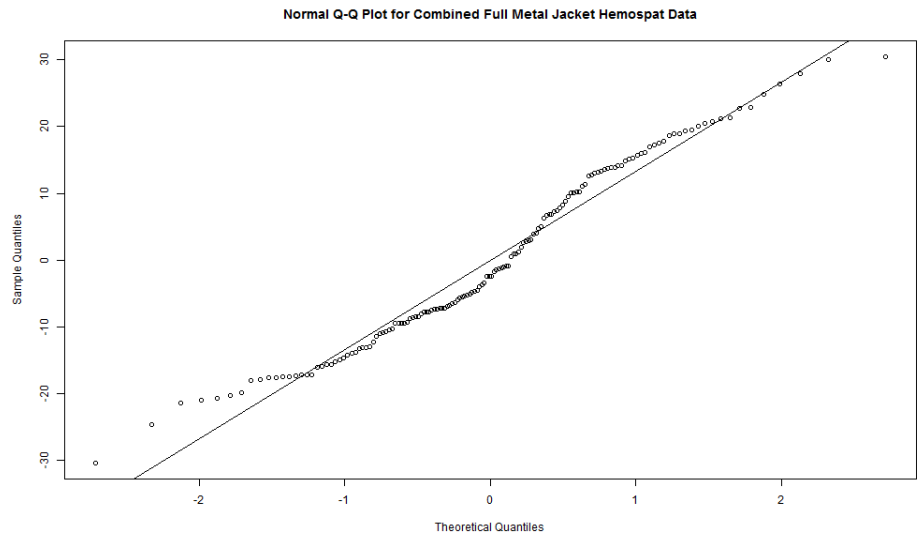

Figure 7.55: Normal Q-Q plot for combined full metal jacket bullet HemoSpat data

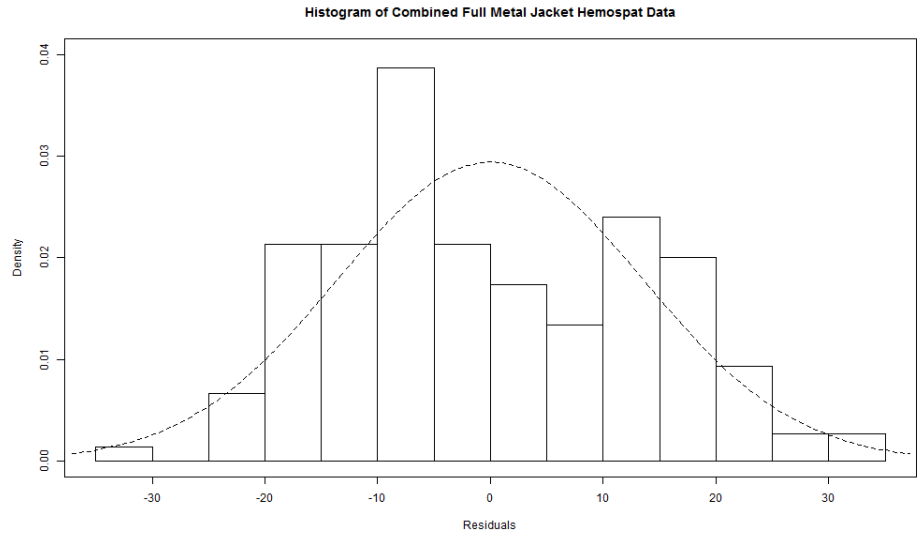

Figure 7.56: Histogram for combined full metal jacket bullet HemoSpat data

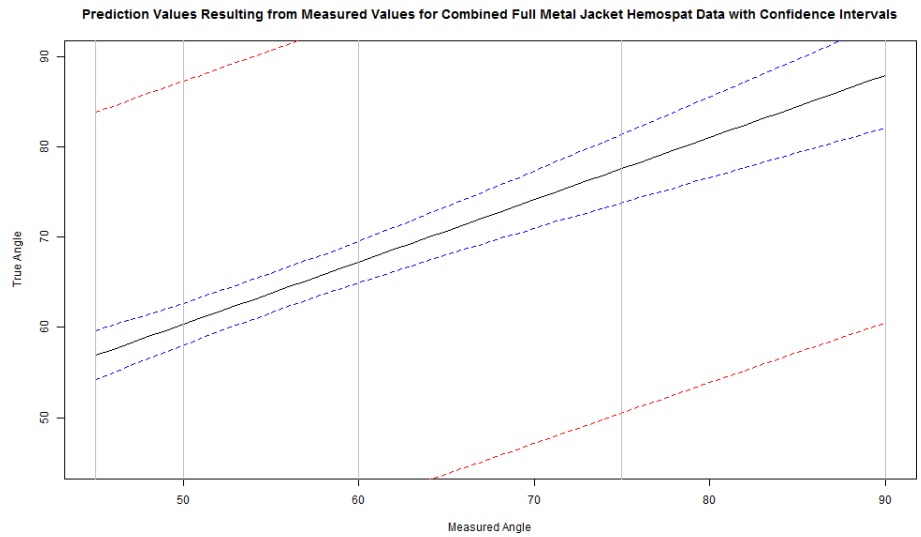

Figure 7.57: Prediction values for combined full metal jacket bullet HemoSpat data

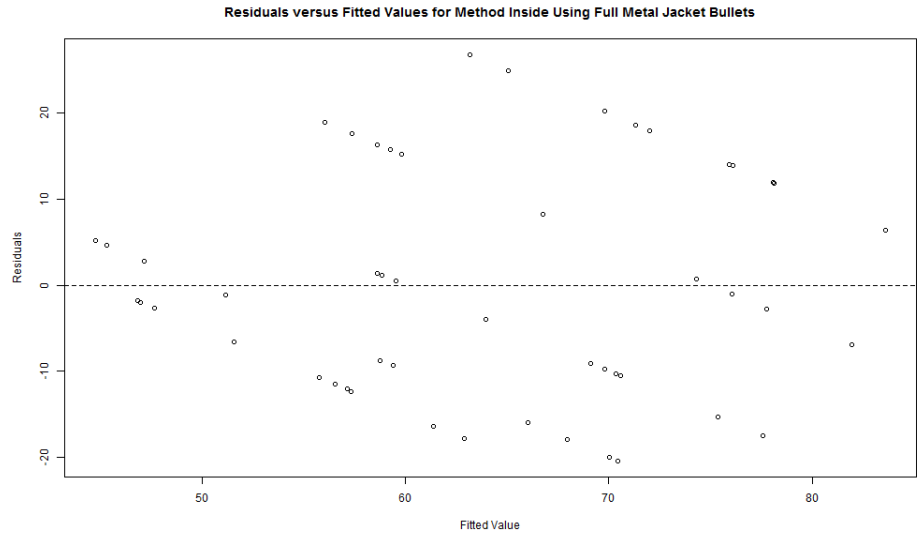

Figure 7.58: Pred-res plot (residual versus fitted values) for inside full metal jacket bullet HemoSpat data

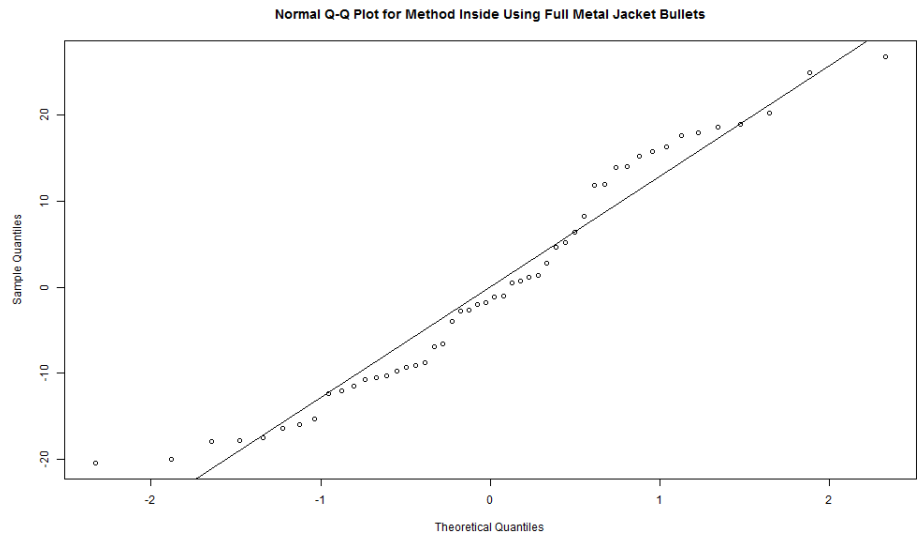

Figure 7.59: Normal Q-Q plot for inside full metal jacket bullet HemoSpat data

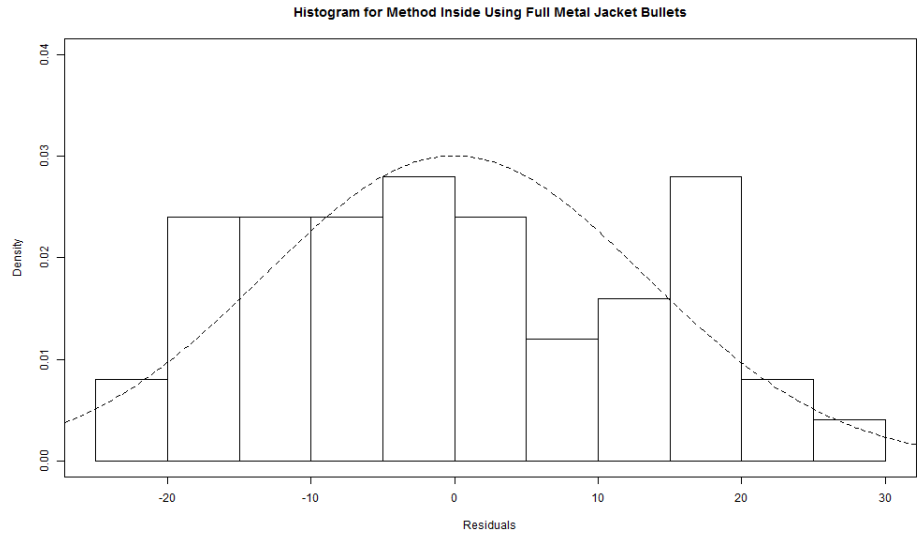

Figure 7.60: Histogram for inside full metal jacket bullet HemoSpat data

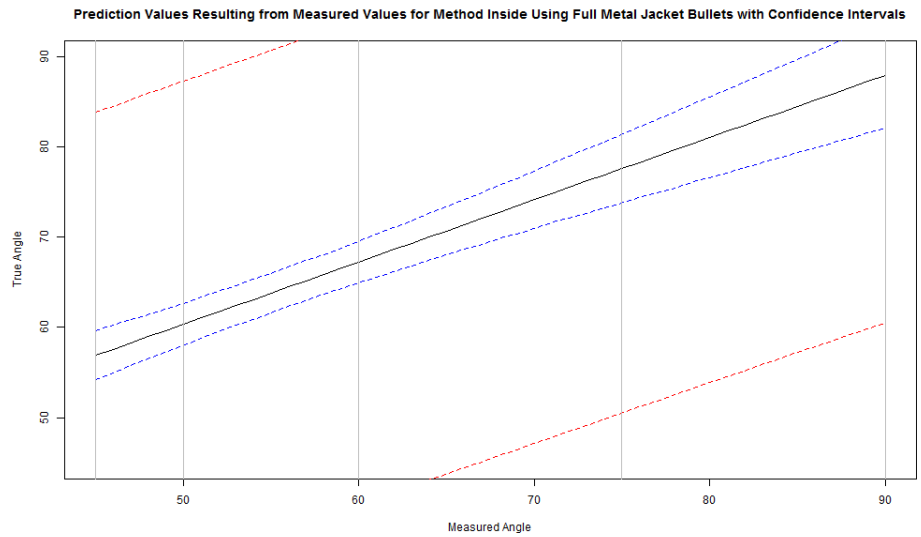

Figure 7.61: Prediction values for inside full metal jacket bullet HemoSpat data

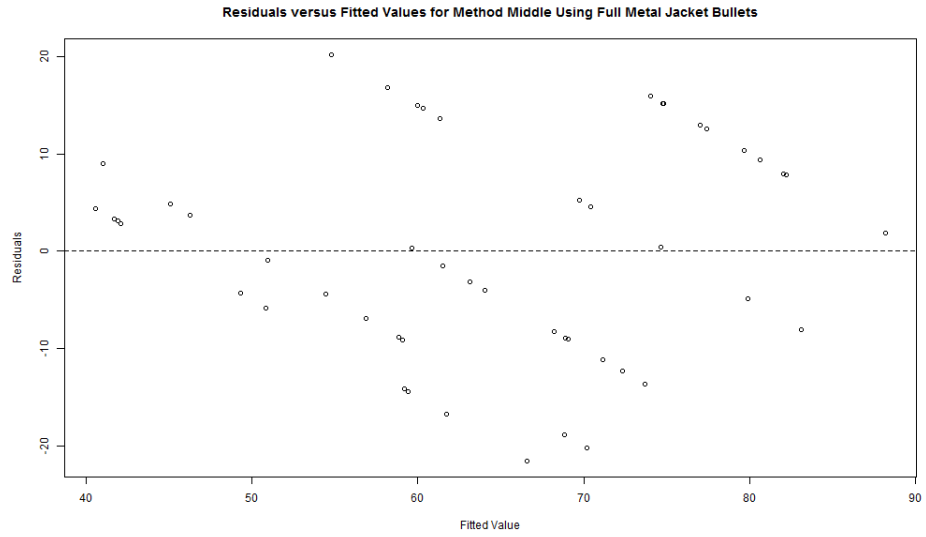

Figure 7.62: Pred-res plot (residual versus fitted values) for middle full metal jacket bullet HemoSpat data

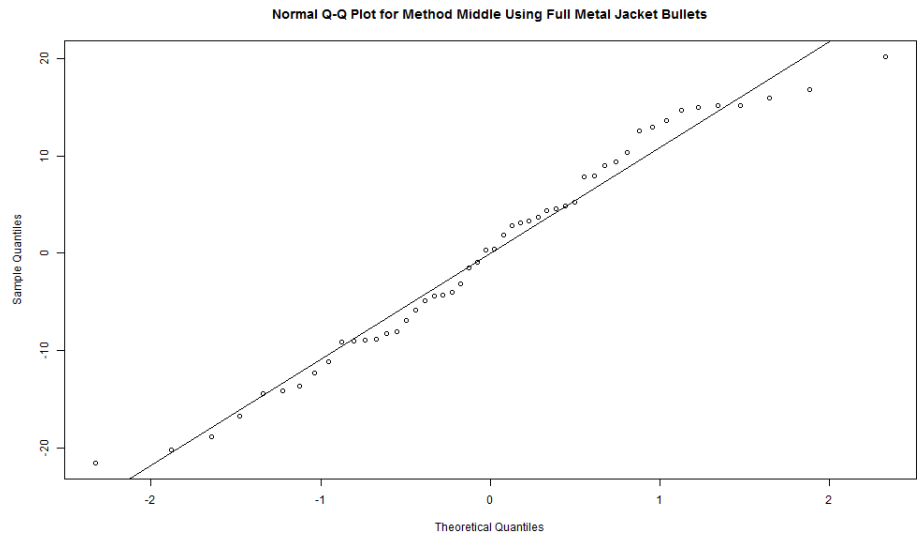

Figure 7.63: Normal Q-Q plot for middle full metal jacket bullet HemoSpat data

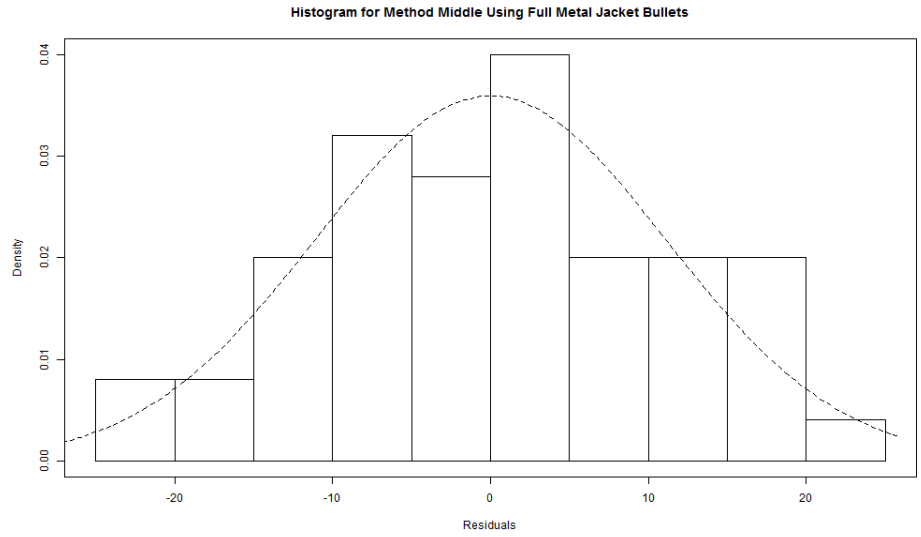

Figure 7.64: Histogram for middle full metal jacket bullet HemoSpat data

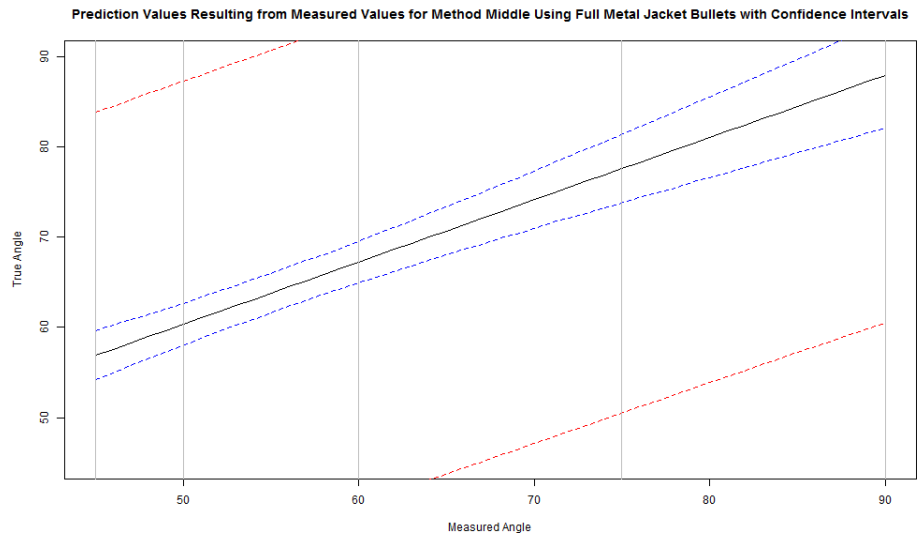

Figure 7.65: Prediction values for middle full metal jacket bullet HemoSpat data

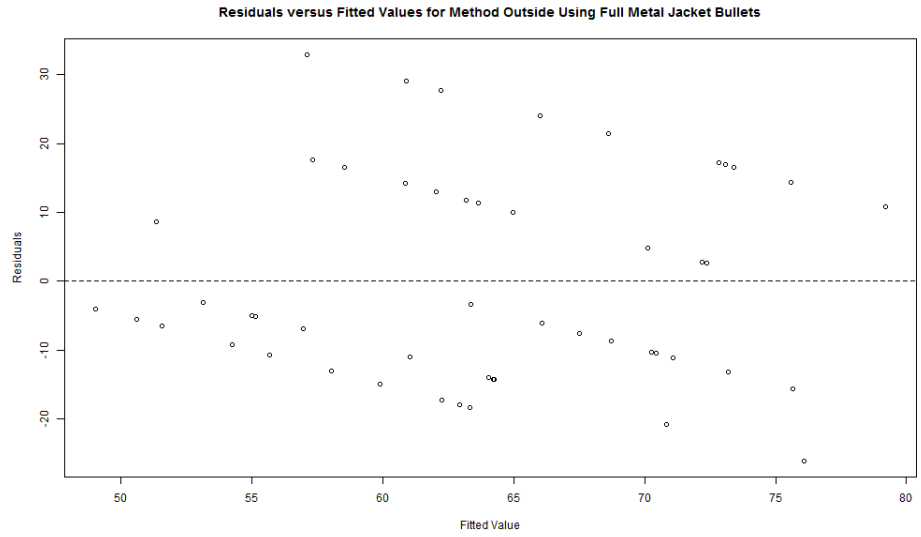

Figure 7.66: Pred-res plot (residual versus fitted values) for outside full metal jacket bullet HemoSpat data

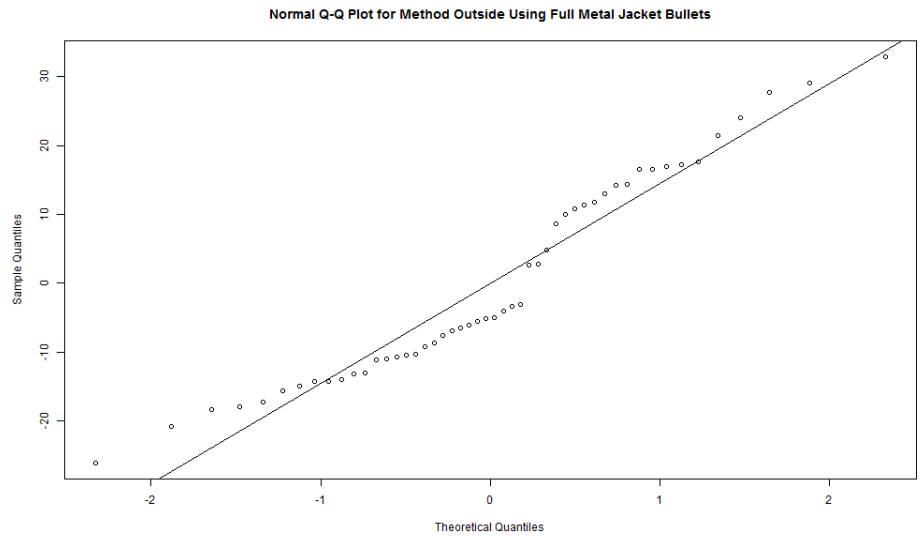

Figure 7.67: Normal Q-Q plot for outside full metal jacket bullet HemoSpat data

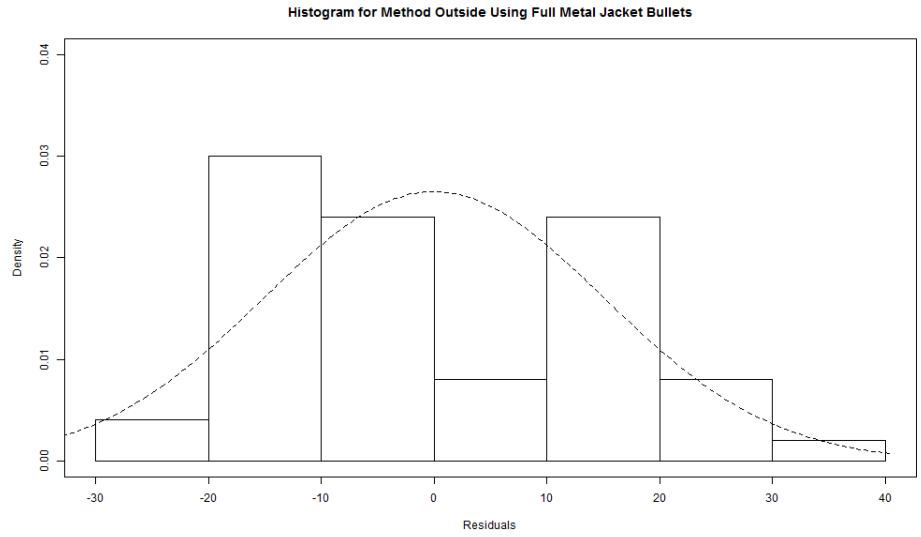

Figure 7.68: Histogram for outside full metal jacket bullet HemoSpat data

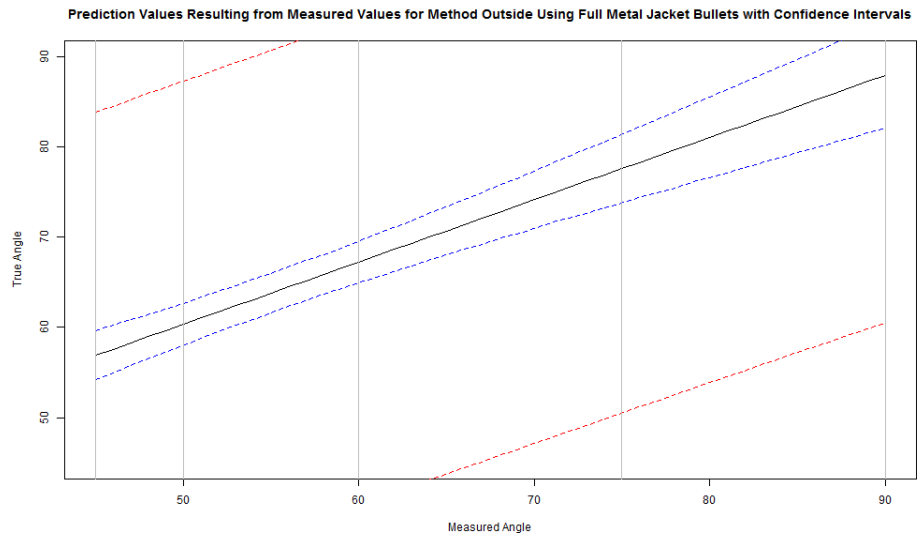

Figure 7.69: Prediction values for outside full metal jacket bullet HemoSpat data

7.5 HemoSpat plots for the LRN bullet data

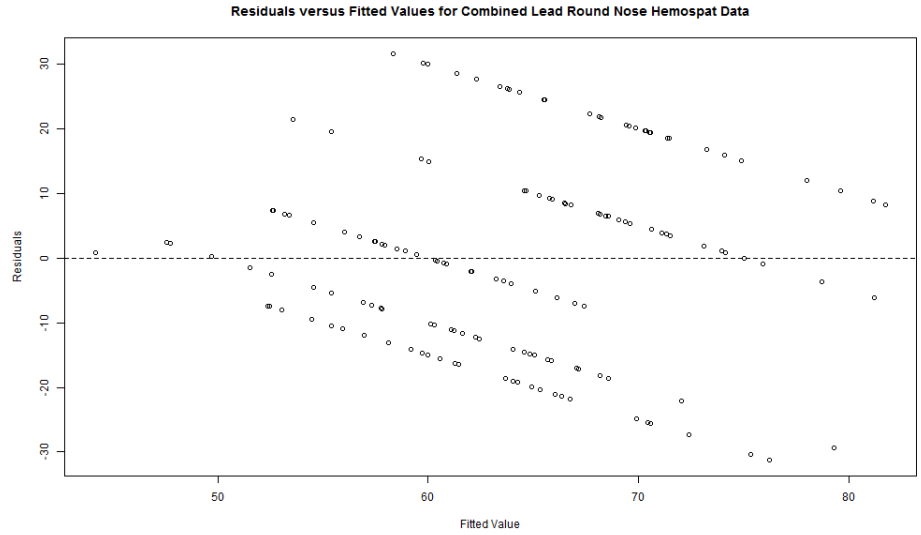

Figure 7.70: Pred-res plot (residual versus fitted values) for combined lead round nose bullet HemoSpat data

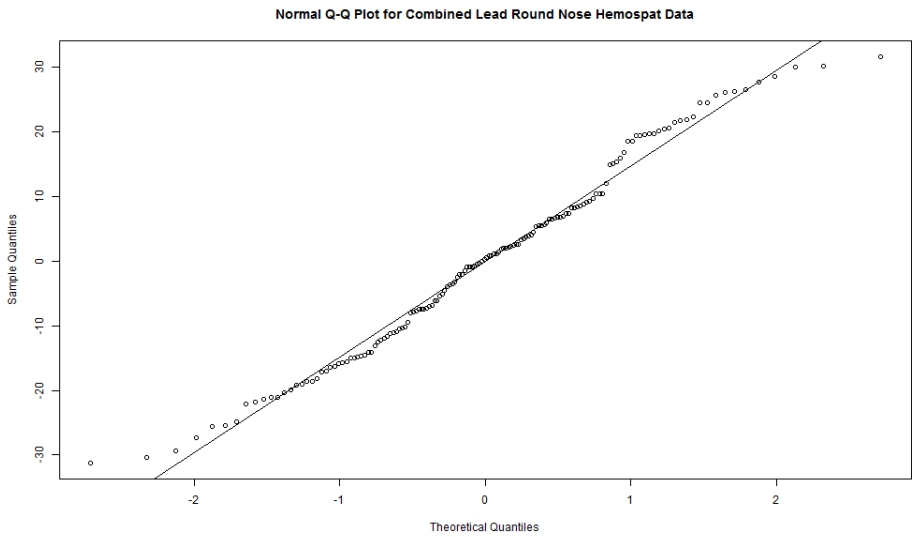

Figure 7.71: Normal Q-Q plot for combined lead round nose bullet HemoSpat data

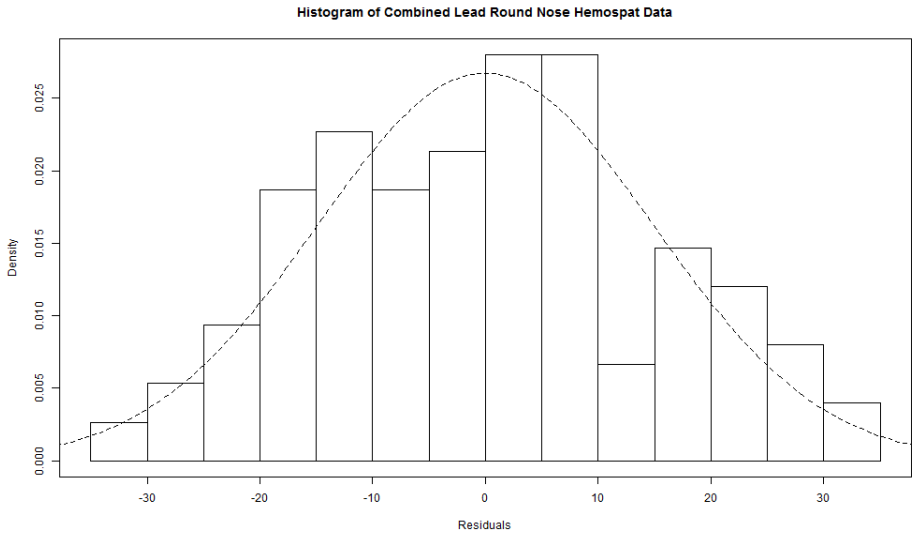

Figure 7.72: Histogram for combined lead round nose bullet HemoSpat data

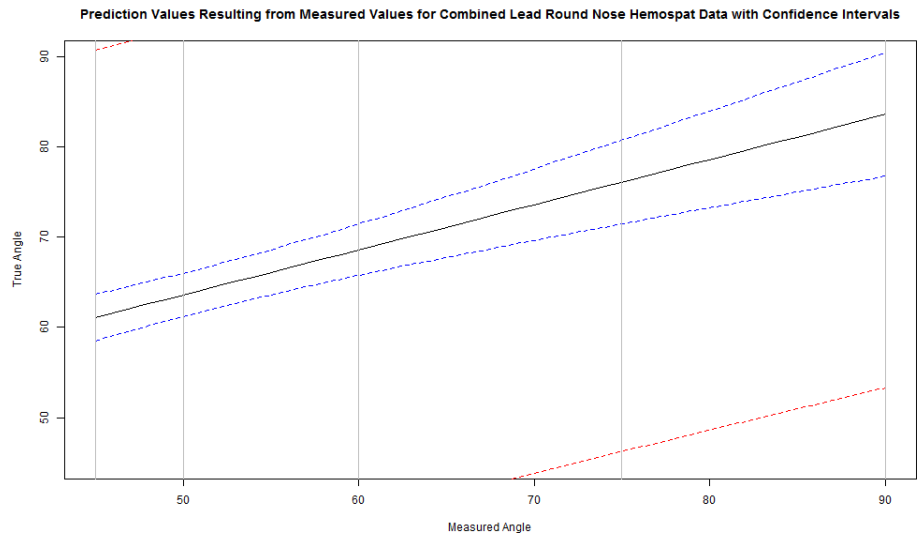

Figure 7.73: Prediction values for combined lead round nose bullet HemoSpat data

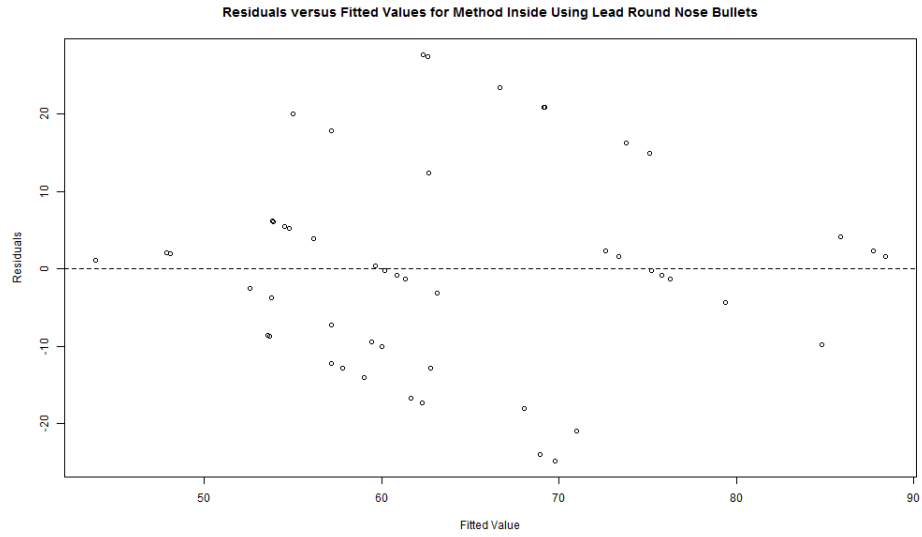

Figure 7.74: Pred-res plot (residual versus fitted values) for inside lead round nose bullet HemoSpat data

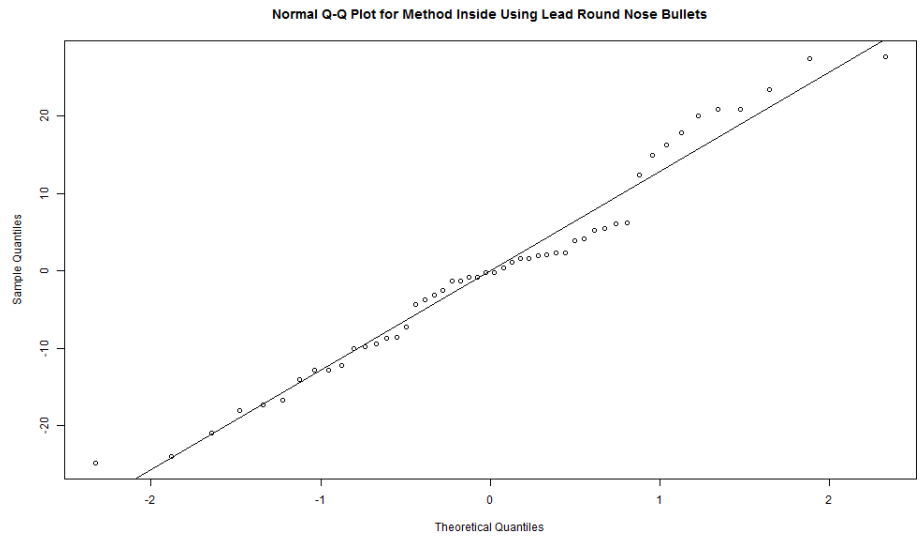

Figure 7.75: Normal Q-Q plot for inside lead round nose bullet HemoSpat data

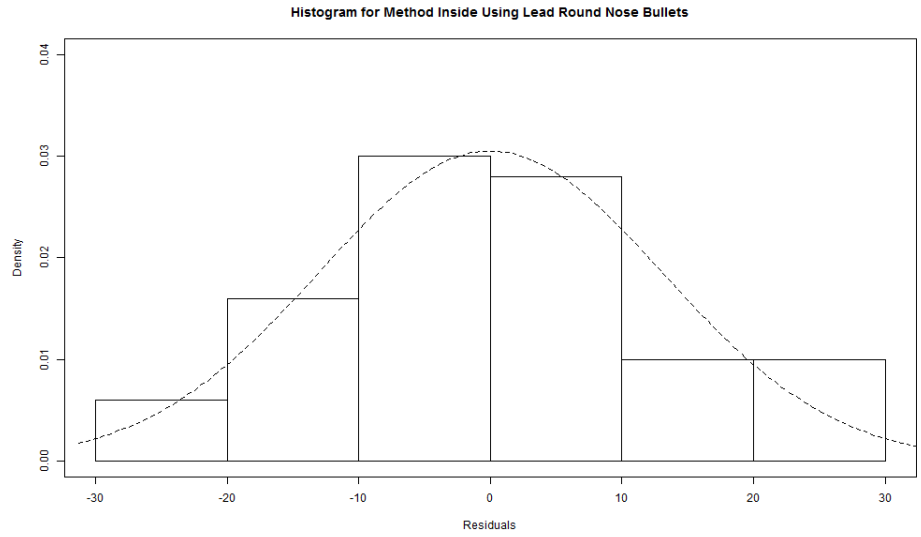

Figure 7.76: Histogram for inside lead round nose bullet HemoSpat data

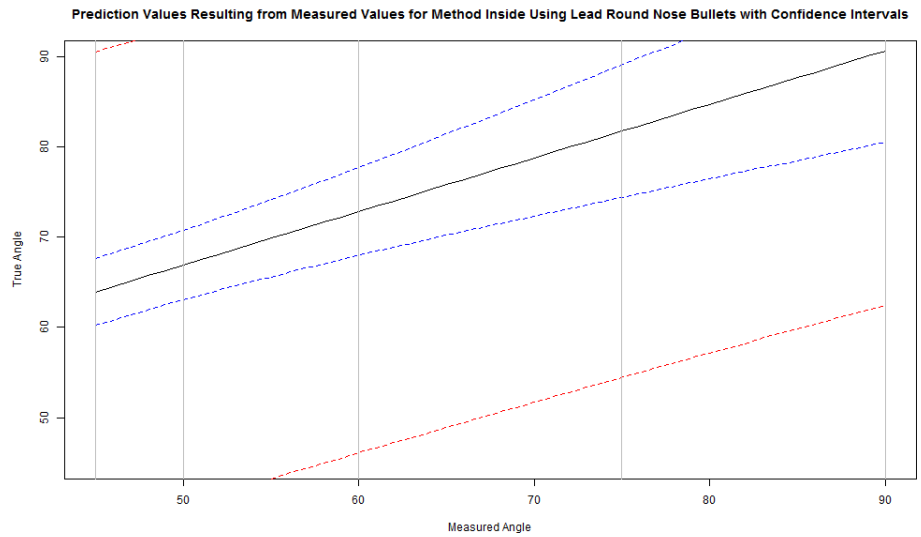

Figure 7.77: Prediction values for inside lead round nose bullet HemoSpat data

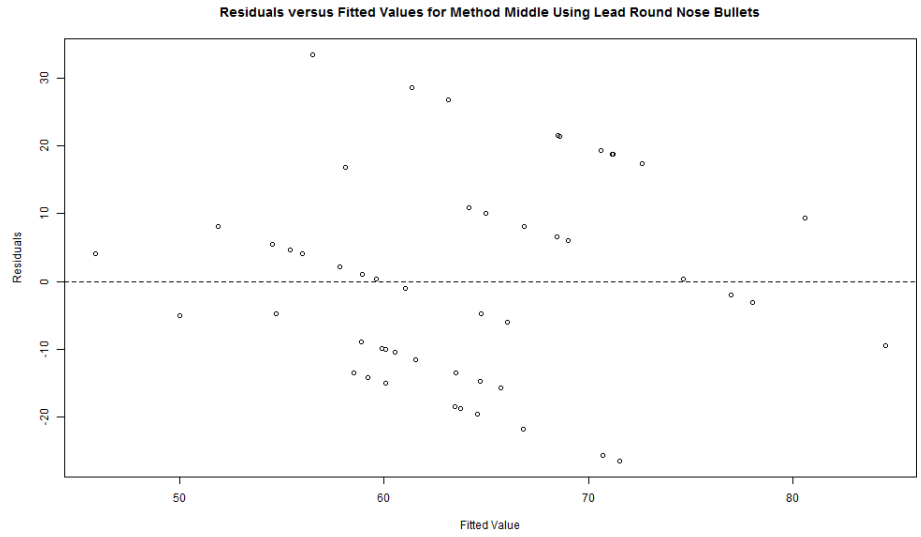

Figure 7.78: Pred-res plot (residual versus fitted values) for middle lead round nose bullet HemoSpat data

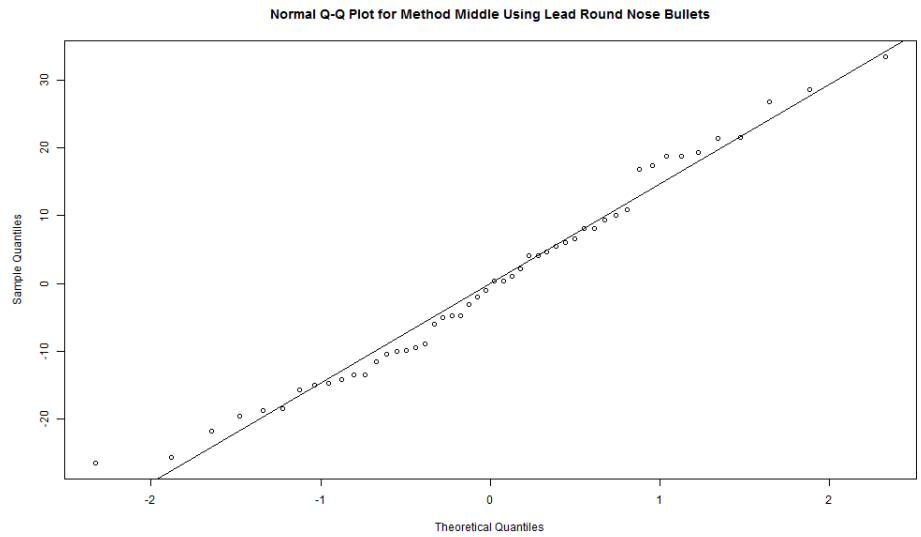

Figure 7.79: Normal Q-Q plot for middle lead round nose bullet HemoSpat data

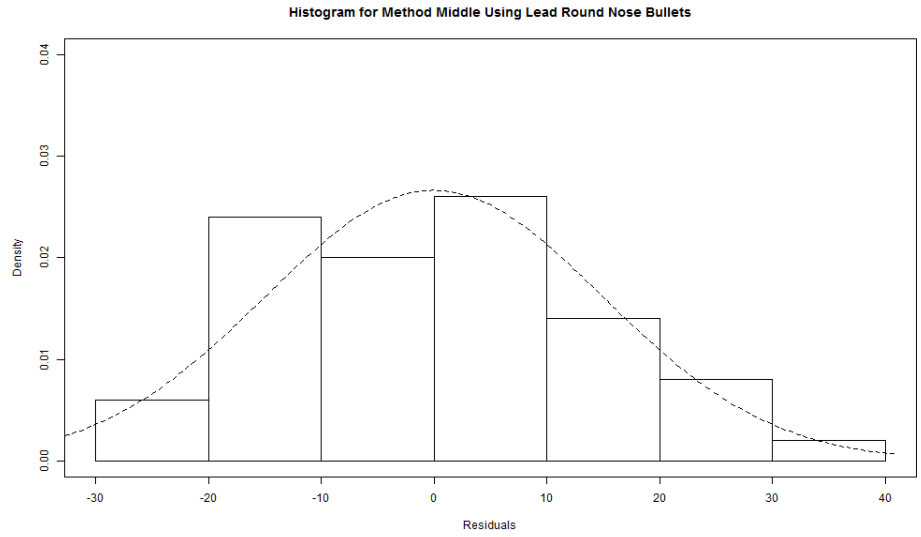

Figure 7.80: Histogram for middle lead round nose bullet HemoSpat data

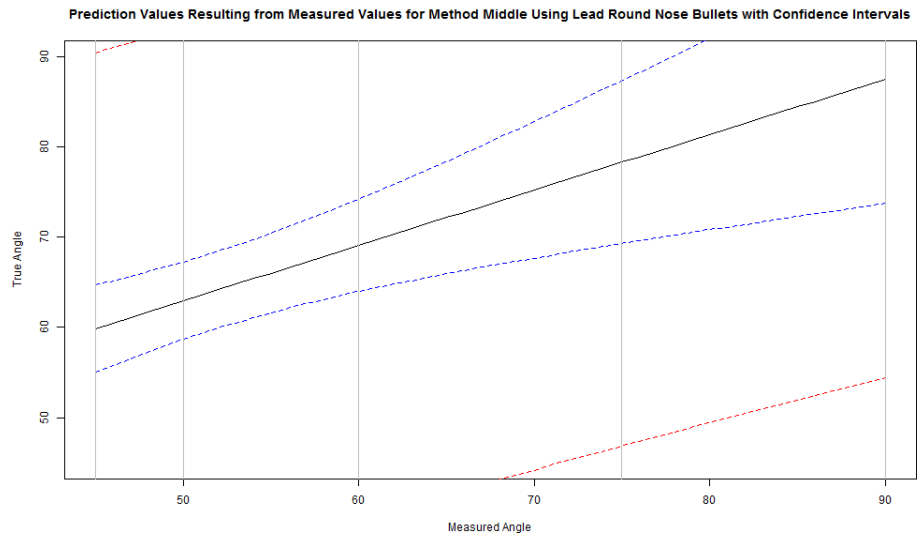

Figure 7.81: Prediction values for middle lead round nose bullet HemoSpat data

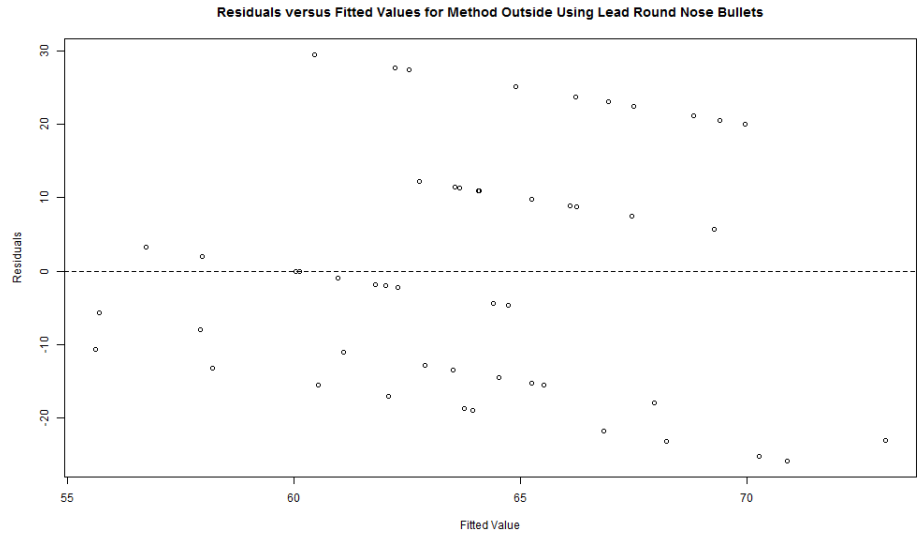

Figure 7.82: Pred-res plot (residual versus fitted values) for outside lead round nose bullet HemoSpat data

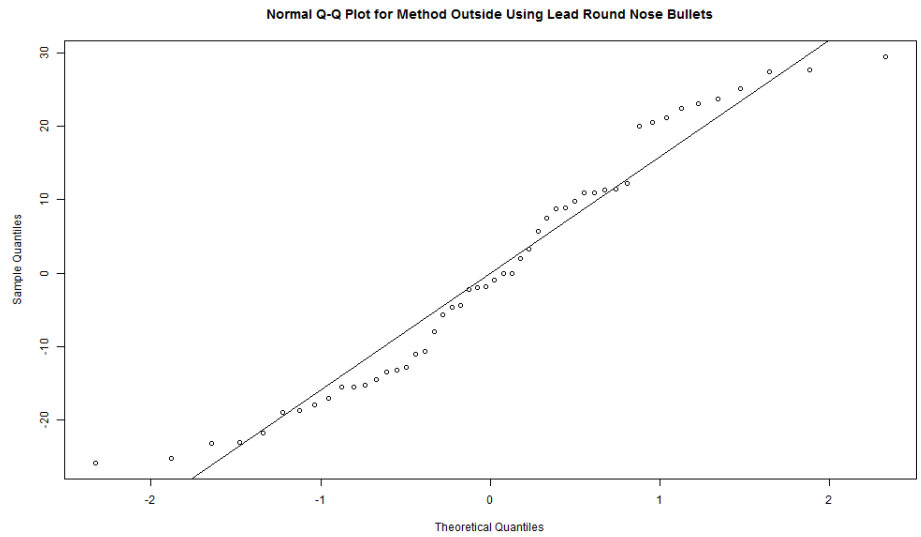

Figure 7.83: Normal Q-Q plot for outside lead round nose bullet HemoSpat data

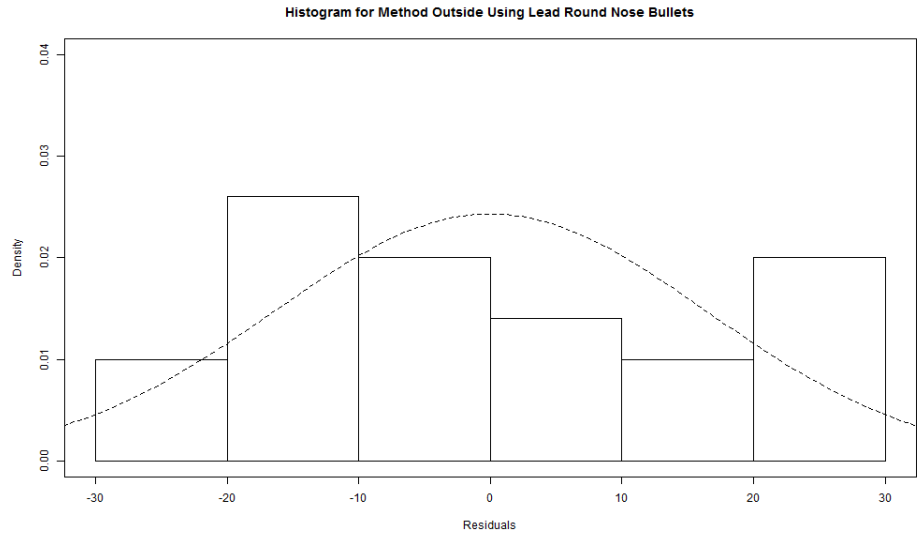

Figure 7.84: Histogram for outside lead round nose bullet HemoSpat data

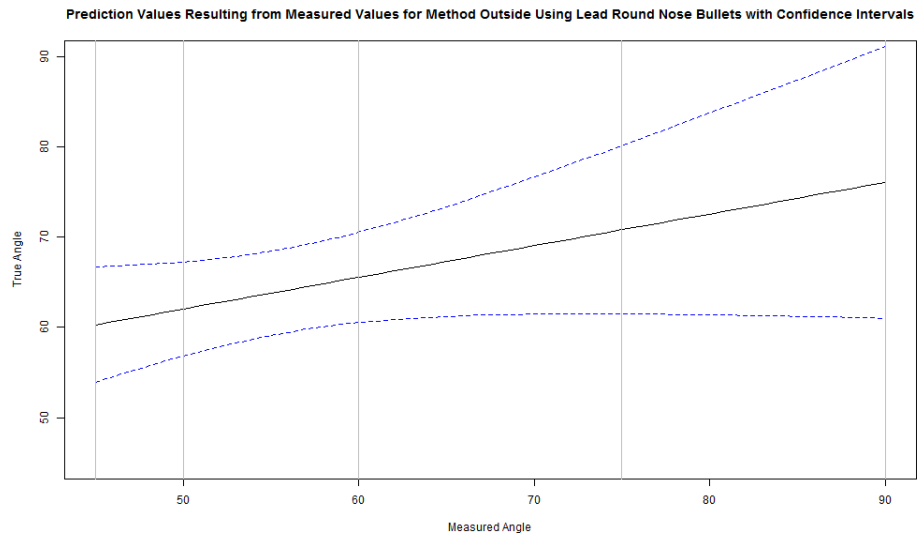

Figure 7.85: Prediction values for outside lead round nose bullet HemoSpat data

7.6 Multiple linear regression plots for the FMJ bullet data using $Minor \times X\_Patch$

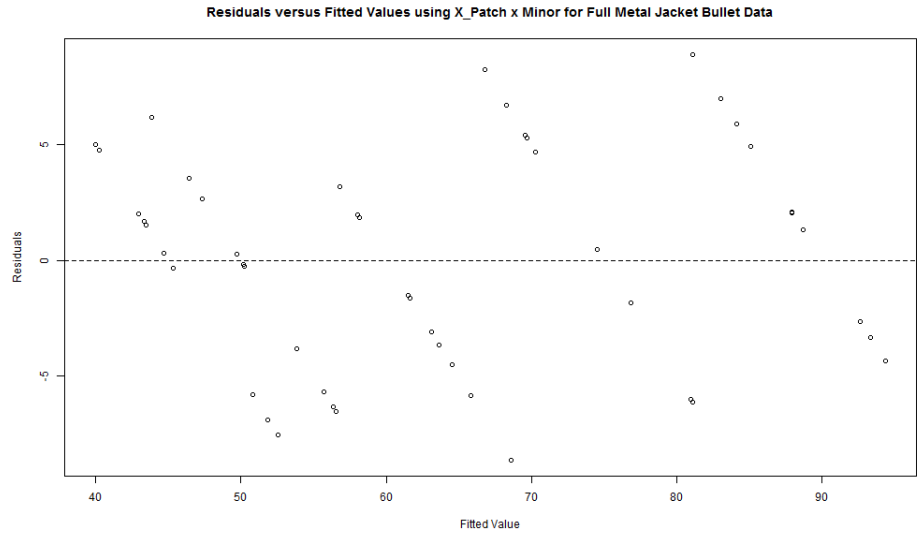

Figure 7.86: Pred-res plot (residual versus fitted values) for $Minor \times X\_Patch$ using full metal jacket bullet data

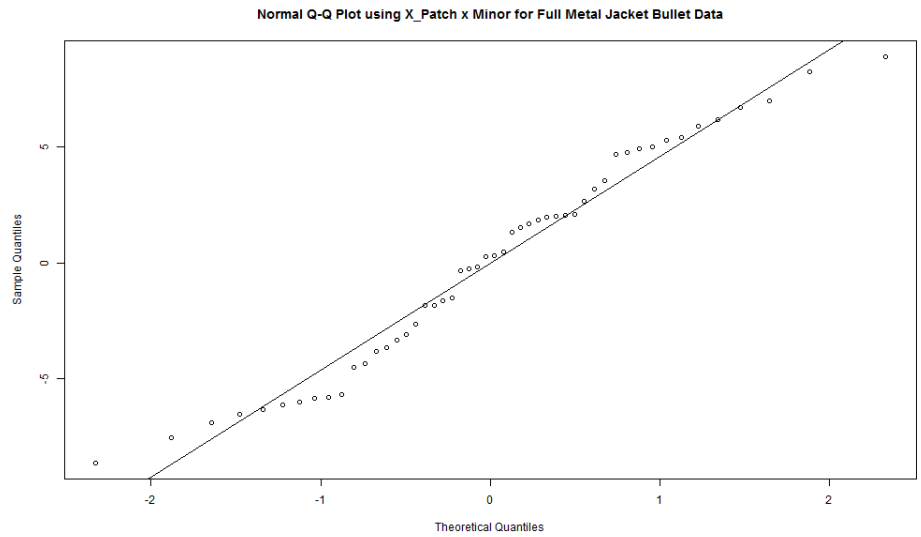

Figure 7.87: Normal Q-Q plot for Minor × X_Patch using full metal jacket bullet data

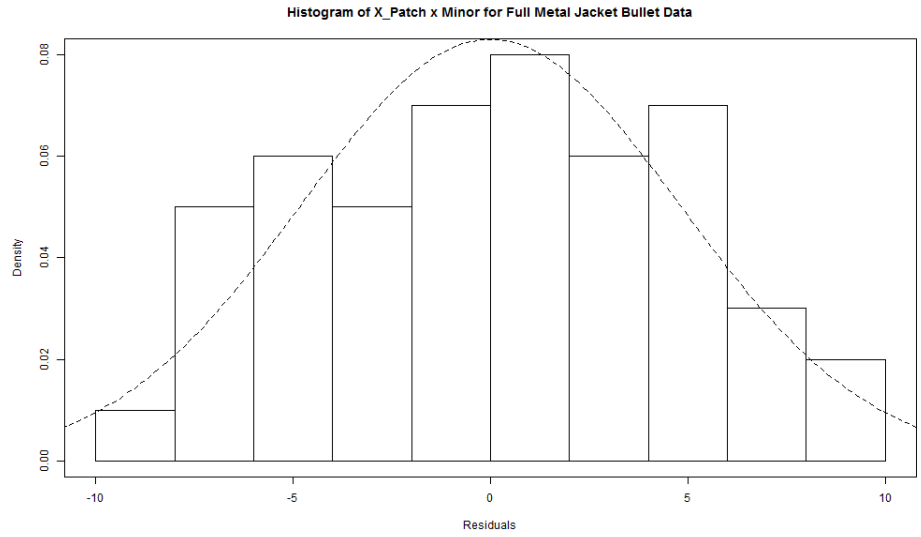

Figure 7.88: Histogram for Minor × X_Patch using full metal jacket bullet data

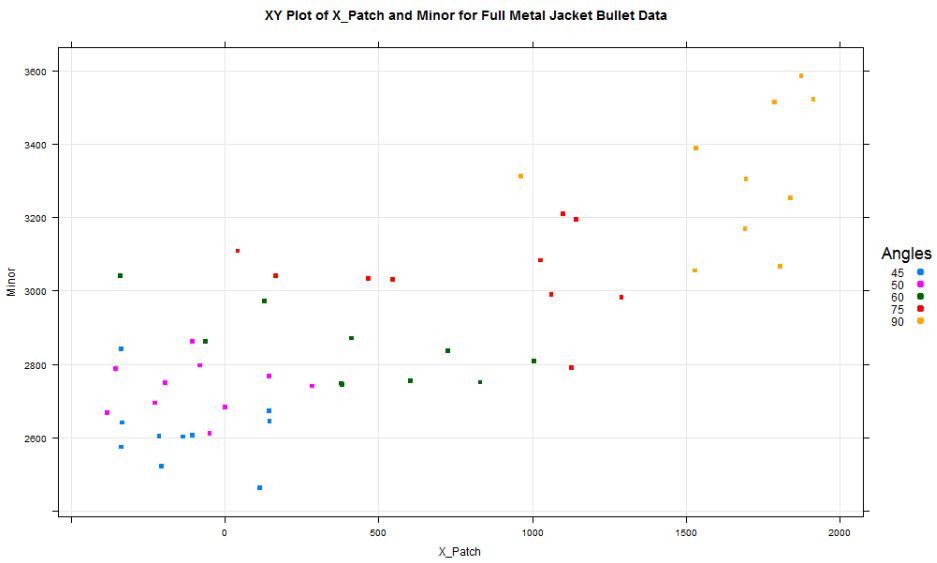

Figure 7.89: XY scatter plot for Minor and X_Patch using full metal jacket bullet data

7.7 Principal component analysis tables

Table 7.3: PCA table for full metal jacket bullets (PC1)

Sample	True_Angle	PC1_Area	PC1_X_Patch	PC1_Circ.	PC1_Area_Largest_Particle	PC1_AR	PC1_Minor	PC1
6C	90	-0.82886	-0.70962	-0.30241	-0.59599	-0.51656	-0.92314	-3.87659
8K	90	-0.96148	-0.75792	-0.00495	-0.61180	-0.33631	-0.99837	-3.67084
6G	90	-0.53047	-0.65672	-0.53779	-0.54857	-0.60151	-0.68000	-3.55508
8L	90	-0.85097	-0.78035	-0.18604	-0.17069	-0.46651	-0.93090	-3.38546
8A	90	-0.60783	-0.56543	-0.53779	-0.09329	-0.70609	-0.78332	-3.29376
8I	90	-0.59678	-0.24446	-0.36930	-0.42422	-0.47203	-0.68859	-2.79539
8G	90	-0.38680	-0.71983	-0.25243	-0.49106	-0.03989	-0.33653	-2.22654
8J	90	-0.30944	-0.56342	-0.07055	-0.69180	-0.15956	-0.31965	-2.11442
5A	90	-0.72940	-0.73871	0.10915	0.03401	0.07108	-0.61119	-1.86506
8D	90	-0.32049	-0.65508	0.50948	0.21440	-0.55030	-0.49312	-1.29513
1H	75	-0.14367	-0.33696	0.14159	-0.13375	0.54458	0.17373	0.24552
1F	75	-0.40891	-0.42890	-0.10346	0.16656	0.30508	-0.19658	-0.66620
4M	75	-0.45311	-0.28007	-0.08700	-0.05011	0.03768	-0.36408	-1.19668
4L	75	-0.64099	-0.32145	-0.25243	-0.02569	0.00880	-0.55351	-1.78527
1G	75	-0.26524	0.03472	-0.35255	-0.16288	-0.15956	-0.28347	-1.18898
1K	75	-0.16577	-0.30011	-0.08700	0.23334	-0.18501	-0.21025	-0.71479
1D	75	-0.09946	-0.00953	-0.63975	-0.16981	-0.43352	-0.27852	-1.63059
8F	75	-0.26524	0.27416	-0.45332	0.16108	-0.43900	-0.40394	-1.12626
1J	75	-0.36470	-0.34543	0.20625	0.33364	-0.56162	-0.52927	-1.26114
1E	75	-0.04421	0.20443	-0.53779	-0.48183	-0.58436	-0.29588	-1.73964
1B	60	-0.25419	-0.17007	0.30271	-0.08176	0.87753	0.25856	0.93279
4J	60	0.37575	-0.04259	0.01140	0.28904	-0.05955	0.24972	0.82377
1A	60	0.13262	0.08268	0.02774	-0.09880	0.31394	0.27444	0.73263
1M	60	0.40891	0.08463	-0.38607	0.01974	-0.08429	0.26460	0.30752
5E	60	-0.23208	0.33387	0.25456	-0.59559	0.42271	0.02571	0.20918
8H	60	0.11052	-0.26833	-0.08700	0.10281	0.09002	0.13452	0.08254
5C	60	0.04421	0.06524	-0.21920	-0.03849	-0.05462	0.00870	-0.19417
1C	60	0.37575	-0.11016	-0.26907	0.02155	-0.39540	0.07726	-0.30007
5D	60	0.04421	0.22538	-0.03772	-0.01411	-0.46099	-0.18044	-0.42366
4I	60	-0.06631	0.48971	-0.33582	-0.05104	-0.55030	-0.29798	-0.81173
3E	50	-0.14367	0.34333	0.58819	1.20070	0.51557	0.15940	2.66352
3I	50	0.57468	0.32552	0.61955	0.04340	0.27837	0.59100	2.43253
3D	50	0.17682	0.35692	0.47786	0.23659	-0.23128	0.02528	1.04219
1L	50	0.17682	0.13805	0.17396	0.29779	0.26045	0.28109	1.32817
3J	50	0.47522	0.29657	-0.08700	0.10671	0.10886	0.41579	1.31615
6A	50	0.05526	0.49845	0.09291	0.08365	0.25595	0.17868	1.16490
5B	50	0.29839	0.40652	-0.11994	0.22717	0.06633	0.26120	1.13967
3H	50	0.46416	0.42536	0.43031	0.19854	0.08057	0.38821	1.98715
3G	50	0.23208	0.21598	0.19012	0.20097	0.07583	0.22110	1.13608
3L	50	0.45311	0.51352	0.14159	0.02578	0.20153	0.45148	1.78702
1X	45	0.78466	0.23362	0.72875	0.14653	0.68587	1.01584	3.59527
1Q	45	0.71835	0.41382	0.25456	0.10164	0.49888	0.83911	2.82635
3C	45	0.38680	0.35684	0.77528	0.13061	0.53218	0.60664	2.78835
1R	45	0.79571	0.48812	0.09291	0.05351	0.20153	0.69155	2.32333
1W	45	0.45311	0.37412	0.31872	-0.08830	0.46101	0.61752	2.13619
3A	45	0.56363	0.41824	0.07664	0.09955	0.32718	0.61522	2.10046
1S	45	0.38680	0.48620	0.04406	0.19337	0.39261	0.51858	2.02162
3K	45	0.23208	0.21635	0.12538	0.23358	0.46101	0.44059	1.70899
3B	45	0.55258	0.21593	-0.47018	0.30177	0.17860	0.50830	1.28699
1T	45	0.22103	0.48687	0.09291	0.16154	-0.20550	0.06491	0.82176

Table 7.4: PCA table for full metal jacket bullets (PC2)

Sample	True_Angle	PC2_Area	PC2_X_Patch	PC2_Circ.	PC2_Area_Largest_Particle	PC2_AR	PC2_Minor	PC2
6C	90	-0.70431	-0.78939	0.58431	0.26744	0.52743	-0.23751	-0.35204
8K	90	-0.81700	-0.84312	0.00957	0.27453	0.34339	-0.25687	-1.28950
6G	90	-0.45076	-0.73054	1.03911	0.24616	0.61418	-0.17496	0.54318
8L	90	-0.72309	-0.86807	0.35946	0.07659	0.47633	-0.23951	-0.91829
8A	90	-0.51650	-0.62899	1.03911	0.04186	0.72096	-0.20154	0.45491
8I	90	-0.50710	-0.27194	0.71355	0.19036	0.48198	-0.17717	0.42967
8G	90	-0.32868	-0.80074	0.48773	0.22035	0.04073	-0.08659	-0.46719
8J	90	-0.26294	-0.62675	0.13632	0.31043	0.16292	-0.08224	-0.36227
5A	90	-0.61979	-0.82174	-0.21090	-0.01526	-0.07258	-0.15725	-1.89753
8D	90	-0.27233	-0.72872	-0.98439	-0.09620	0.56189	-0.12687	-1.64662
1H	75	-0.12208	-0.37484	-0.27358	0.06002	-0.55605	0.04470	-1.22183
1F	75	-0.34746	-0.47712	0.19990	-0.07474	-0.31151	-0.05058	-1.06150
4M	75	-0.38502	-0.31155	0.16809	0.02248	-0.03848	-0.09367	-0.63815
4L	75	-0.54467	-0.35759	0.48773	0.01153	-0.00898	-0.14241	-0.55439
1G	75	-0.22538	0.03862	0.68119	0.07309	0.16292	-0.07293	0.65751
1K	75	-0.14086	-0.33384	0.16809	-0.10470	0.18890	-0.05409	-0.27651
1D	75	-0.08452	-0.01060	1.23610	0.07620	0.44265	-0.07166	1.58817
8F	75	-0.22538	0.30498	0.87590	-0.07228	0.44824	-0.10393	1.22753
1J	75	-0.30990	-0.38426	-0.39852	-0.14971	0.57345	-0.13618	-0.80511
1E	75	-0.03756	0.22741	1.03911	0.21621	0.59667	-0.07613	1.96570
1B	60	-0.21599	-0.18918	-0.58488	0.03669	-0.89601	0.06652	-1.78286
4J	60	0.31929	-0.04738	-0.02203	-0.12970	0.06080	0.06425	0.24523
1A	60	0.11269	0.09198	-0.05360	0.04433	-0.32055	0.07061	-0.05453
1M	60	0.34746	0.09414	0.74595	-0.00886	0.08606	0.06808	1.33284
5E	60	-0.19721	0.37140	-0.49186	0.26726	-0.43161	0.00662	-0.47540
8H	60	0.09391	-0.29849	0.16809	-0.04613	-0.09192	0.03461	-0.13994
5C	60	0.03756	0.07257	0.42353	0.01727	0.05577	0.00224	0.60894
1C	60	0.31929	-0.12254	0.51989	-0.00967	0.40373	0.01988	1.13058
5D	60	0.03756	0.25071	0.07287	0.00633	0.47070	-0.04642	0.79175
4I	60	-0.05634	0.54476	0.64886	0.02290	0.56189	-0.07667	1.64540
3E	50	-0.12208	0.38192	-1.13648	-0.53878	-0.52643	0.04101	-1.90084
3I	50	0.48832	0.36211	-1.19707	-0.01948	-0.28423	0.15206	-0.49830
3D	50	0.15025	0.39704	-0.92331	-0.10616	0.23615	0.00650	-0.23952
1L	50	0.15025	0.15357	-0.33612	-0.13363	-0.26593	0.07232	-0.35953
3J	50	0.40381	0.32991	0.16809	-0.04788	-0.11116	0.10698	0.84974
6A	50	0.04695	0.55447	-0.17951	-0.03754	-0.26134	0.04597	0.16901
5B	50	0.25355	0.45221	0.23174	-0.10194	-0.06773	0.06720	0.83504
3H	50	0.39441	0.47318	-0.83143	-0.08909	-0.08226	0.09988	-0.03531
3G	50	0.19721	0.24026	-0.36733	-0.09018	-0.07742	0.05689	-0.04059
3L	50	0.38502	0.57125	-0.27358	-0.01157	-0.20578	0.11616	0.58151
1X	45	0.66675	0.25988	-1.40806	-0.06575	-0.70031	0.26136	-0.98613
1Q	45	0.61040	0.46033	-0.49186	-0.04561	-0.50938	0.21589	0.23978
3C	45	0.32868	0.39695	-1.49796	-0.05861	-0.54338	0.15608	-1.21824
1R	45	0.67614	0.54299	-0.17951	-0.02401	-0.20578	0.17793	0.98776
1W	45	0.38502	0.41617	-0.61582	0.03962	-0.47072	0.15888	-0.08685
3A	45	0.47893	0.46525	-0.14808	-0.04467	-0.33407	0.15829	0.57565
1S	45	0.32868	0.54085	-0.08513	-0.08677	-0.40087	0.13342	0.43018
3K	45	0.19721	0.24067	-0.24226	-0.10481	-0.47072	0.11336	-0.26655
3B	45	0.46954	0.24021	0.90847	-0.13541	-0.18236	0.13078	1.43122
1T	45	0.18782	0.54160	-0.17951	-0.07249	0.20983	0.01670	0.70395

Table 7.5: PCA table for full metal jacket bullets (PC3)

Sample	True_Angle	PC3_Area	PC3_X_Patch	PC3_Circ.	PC3_Area_Largest_Particle	PC3_AR	PC3_Minor	PC3
6C	90	0.15433	-0.10209	-0.00738	-1.63516	0.53504	0.41321	-0.64204
8K	90	0.17903	-0.10903	-0.00012	-1.67852	0.34835	0.44688	-0.81342
6G	90	0.09877	-0.09448	-0.01313	-1.50506	0.62304	0.30438	-0.58647
8L	90	0.15845	-0.11226	-0.00454	-0.46831	0.48320	0.41668	0.47322
8A	90	0.11318	-0.08134	-0.01313	-0.25595	0.73136	0.35062	0.84474
8I	90	0.11112	-0.03517	-0.00902	-1.16388	0.48893	0.30822	-0.29979
8G	90	0.07202	-0.10355	-0.00616	-1.34727	0.04131	0.15064	-1.19302
8J	90	0.05762	-0.08105	-0.00172	-1.89801	0.16527	0.14308	-1.61482
5A	90	0.13581	-0.10627	0.00267	0.09330	-0.07363	0.27357	0.32545
8D	90	0.05968	-0.09424	0.01244	0.58821	0.57000	0.22073	1.35682
1H	75	0.02675	-0.04848	0.00346	-0.36695	-0.56407	-0.07776	-1.02705
1F	75	0.07614	-0.06170	-0.00253	0.45698	-0.31600	0.08799	0.24088
4M	75	0.08437	-0.04029	-0.00212	-0.13747	-0.03903	0.16296	0.02841
4L	75	0.11935	-0.04624	-0.00616	-0.07047	-0.00911	0.24776	0.23512
1G	75	0.04939	0.00500	-0.00861	-0.44687	0.16527	0.12689	-0.10894
1K	75	0.03087	-0.04317	-0.00212	0.64019	0.19163	0.09411	0.91149
1D	75	0.01852	-0.00137	-0.01562	-0.46588	0.44903	0.12467	0.10936
8F	75	0.04939	0.03944	-0.01107	0.44193	0.45471	0.18081	1.15520
1J	75	0.06791	-0.04969	0.00504	0.91536	0.58172	0.23691	1.75724
1E	75	0.00823	0.02941	-0.01313	-1.32195	0.60528	0.13244	-0.55972
1B	60	0.04733	-0.02447	0.00739	-0.22431	-0.90894	-0.11573	-1.21873
4J	60	-0.06996	-0.00613	0.00028	0.79301	0.06168	-0.11178	0.66710
1A	60	-0.02469	0.01189	0.00068	-0.27105	-0.32517	-0.12284	-0.73119
1M	60	-0.07614	0.01217	-0.00943	0.05416	0.08730	-0.11844	-0.05037
5E	60	0.04321	0.04803	0.00622	-1.63406	-0.43784	-0.01151	-1.98595
8H	60	-0.02058	-0.03860	-0.00212	0.28206	-0.09325	-0.06021	0.06730
5C	60	-0.00823	0.00938	-0.00535	-0.10559	0.05658	-0.00389	-0.05711
1C	60	-0.06996	-0.01585	-0.00657	0.05913	0.40956	-0.03458	0.34172
5D	60	-0.00823	0.03242	-0.00092	-0.03870	0.47749	0.08077	0.54282
4I	60	0.01235	0.07045	-0.00820	-0.14002	0.57000	0.13338	0.63795
3E	50	0.02675	0.04939	0.01436	3.29423	-0.53402	-0.07135	2.77936
3I	50	-0.10700	0.04683	0.01513	0.11908	-0.28834	-0.26454	-0.47884
3D	50	-0.03292	0.05135	0.01167	0.64911	0.23956	-0.01131	0.90744
1L	50	-0.03292	0.01986	0.00425	0.81701	-0.26977	-0.12582	0.41260
3J	50	-0.08848	0.04266	-0.00212	0.29276	-0.11276	-0.18611	-0.05405
6A	50	-0.01029	0.07171	0.00227	0.22951	-0.26511	-0.07998	-0.05190
5B	50	-0.05556	0.05848	-0.00293	0.62327	-0.06871	-0.11692	0.43764
3H	50	-0.08643	0.06119	0.01051	0.54470	-0.08345	-0.17377	0.27275
3G	50	-0.04321	0.03107	0.00464	0.55139	-0.07854	-0.09897	0.36638
3L	50	-0.08437	0.07388	0.00346	0.07072	-0.20875	-0.20209	-0.34715
1X	45	-0.14610	0.03361	0.01779	0.40202	-0.71042	-0.45470	-0.85780
1Q	45	-0.13376	0.05953	0.00622	0.27885	-0.51673	-0.37560	-0.68149
3C	45	-0.07202	0.05134	0.01893	0.35834	-0.55122	-0.27154	-0.46618
1R	45	-0.14816	0.07022	0.00227	0.14681	-0.20875	-0.30954	-0.44715
1W	45	-0.08437	0.05382	0.00778	-0.24225	-0.47751	-0.27641	-1.01894
3A	45	-0.10495	0.06017	0.00187	0.27313	-0.33889	-0.27538	-0.38404
1S	45	-0.07202	0.06994	0.00108	0.53053	-0.40666	-0.23212	-0.10925
3K	45	-0.04321	0.03112	0.00306	0.64084	-0.47751	-0.19721	-0.04291
3B	45	-0.10289	0.03106	-0.01148	0.82792	-0.18499	-0.22752	0.33211
1T	45	-0.04116	0.07004	0.00227	0.44321	0.21285	-0.02905	0.65816

Table 7.6: PCA table for lead round nose bullets (PC1)

Sample	True_Angle	PC1_Area	PC1_X_Patch	PC1_Circ.	PC1_Area_Largest_Particle	PC1_AR	PC1_Minor	PC1
5Y	90	0.90006	0.00619	-0.58389	-0.06288	0.20193	1.16890	1.63032
5K	90	0.50199	-0.00256	-0.20977	-0.15168	0.38933	0.94263	1.46994
5J	90	-0.49448	0.01172	-0.02161	-0.22979	0.62069	0.05526	-0.05822
5S	90	-0.52835	0.00845	0.17212	-0.24822	0.51500	-0.07200	-0.15299
5M	90	0.44520	0.01092	-0.56213	-0.12012	-0.27943	0.15864	-0.34691
5F	90	-0.52856	0.01289	0.20495	-0.25684	0.38322	-0.18682	-0.37116
8E	90	-0.50726	0.01330	-0.27126	-0.31995	0.33498	-0.20654	-0.95674
6E	90	-1.18244	0.00190	0.35460	-0.62567	0.37714	-0.90385	-1.97832
5O	90	-0.68988	0.00477	-0.36232	-0.36305	-0.04614	-0.73362	-2.19024
5V	90	-1.04581	0.00329	-0.36985	-0.33126	0.07675	-0.99723	-2.66410
5P	75	0.30525	0.00842	0.39672	-0.14017	0.38933	0.73190	1.69145
5H	75	0.98963	-0.00188	0.32107	0.12153	0.08734	1.13289	2.65059
3Z	75	-0.12689	0.00004	0.27107	0.28800	-0.21246	-0.33156	-0.11179
3X	75	0.51885	0.00729	0.13944	0.19522	-0.24402	0.27112	0.88791
5T	75	-0.35691	0.00003	0.09072	0.24395	0.16854	-0.19571	-0.04938
3W	75	0.79416	-0.00313	-0.07707	0.03968	-0.35662	0.40791	0.80494
5C	75	-0.20798	0.00011	-0.13986	-0.21089	-0.53946	-0.75299	-1.85107
5Q	75	0.55666	0.00708	-0.27126	0.30217	0.34095	0.95627	1.89188
3Y	75	0.07735	-0.00352	-0.32455	0.25457	-0.23056	-0.14919	-0.37590
5N	75	0.51806	0.01268	-0.76189	-0.11509	-0.35662	0.14324	-0.55963
3R	60	0.06753	-0.00949	-0.10854	-0.10934	-0.12399	-0.04320	-0.32703
8T	60	0.37124	-0.00180	0.32107	0.13791	-0.09032	0.29944	1.03755
8U	60	0.42532	-0.00194	0.32107	0.11468	0.07148	0.53023	1.46082
8V	60	0.18952	-0.00403	0.20495	-0.14264	0.08734	0.29858	0.63372
8R	60	0.33786	0.00578	0.29603	0.07106	0.11944	0.48840	1.31855
8W	60	0.43778	-0.00803	0.04235	0.07078	0.19633	0.67481	1.41401
8X	60	1.19695	0.00646	0.32107	0.14510	0.20755	1.48964	3.36676
3T	60	0.08873	-0.00289	0.04235	0.06454	0.21318	0.32216	0.72806
8S	60	-0.01119	0.00621	-0.02161	0.13648	0.29361	0.29389	0.69739
3S	60	0.45098	-0.01097	0.32107	-0.08858	0.48293	0.98105	2.13648
6S	50	-0.78044	-0.00167	-0.42226	-0.04448	-1.02446	-1.77921	-4.05252
6T	50	-0.65569	-0.00812	0.19673	0.03082	-0.33976	-0.97268	-1.74871
6V	50	0.53535	-0.00980	0.02630	0.12278	-0.24848	0.28661	0.71276
6R	50	-0.17036	-0.01169	0.16394	-0.07273	-0.16642	-0.32813	-0.58539
6Q	50	0.42005	0.00575	0.10692	0.04763	-0.08059	0.35637	0.85614
6P	50	-0.43978	-0.00313	0.09882	0.09006	-0.05604	-0.48951	-0.79958
3U	50	-0.07869	-0.00691	-0.18656	0.05195	0.01948	-0.04626	-0.24698
8Y	50	0.15035	-0.00117	0.10692	0.06796	0.34095	0.50996	1.17498
6U	50	-0.02338	-0.00860	0.18031	-0.02132	0.41391	0.39508	0.93600
8Z	50	-0.68754	-0.00672	0.13944	0.05175	0.71014	-0.09062	0.11644
2C	45	0.19675	0.00416	-0.65582	0.31460	-1.18385	-1.17753	-2.50170
2B	45	-0.16139	-0.00476	-0.39985	-0.02043	-0.49366	-0.65936	-1.73944
1U	45	-0.12017	-0.00858	-0.12422	0.13367	-0.51672	-0.64366	-1.27969
1Z	45	-0.50179	-0.00609	0.16394	0.02441	-0.20334	-0.68958	-1.21247
3M	45	-0.43538	-0.01205	-0.00568	0.13051	-0.16175	-0.58577	-1.07012
2A	45	0.24625	0.00136	0.02630	-0.15918	-0.53569	-0.32306	-0.74402
3F	45	-0.29035	0.00814	0.49025	0.14711	-0.27504	-0.55544	-0.47534
1V	45	-0.47272	0.00923	-0.06127	0.49258	0.12484	-0.35671	-0.26406
1Y	45	-0.21898	-0.00689	0.34620	0.01565	0.28777	0.06150	0.48526
2D	45	-0.00545	-0.00975	0.07456	-0.07286	0.31125	0.31380	0.61155

Table 7.7: PCA table for lead round nose bullets (PC2)

Sample	True_Angle	PC2_Area	PC2_X_Patch	PC2_Circ.	PC2_Area_Largest_Particle	PC2_AR	PC2_Minor	PC2
5Y	90	0.74585	-0.08595	0.73444	-0.17348	-0.30785	0.00584	0.91885
5K	90	0.41598	0.03547	0.26386	-0.41849	-0.59355	0.00471	-0.29202
5J	90	-0.40976	-0.16265	0.02718	-0.63400	-0.94627	0.00028	-2.12522
5S	90	-0.43783	-0.11732	-0.21650	-0.68484	-0.78515	-0.00036	-2.24199
5M	90	0.36892	-0.15162	0.70706	-0.33141	0.42600	0.00079	1.01975
5F	90	-0.43800	-0.17888	-0.25779	-0.70861	-0.58424	-0.00093	-2.16846
8E	90	-0.42035	-0.18453	0.34119	-0.88275	-0.51069	-0.00103	-1.65815
6E	90	-0.97985	-0.02643	-0.44602	-1.72620	-0.57496	-0.00451	-3.75798
5O	90	-0.57168	-0.06622	0.45574	-1.00164	0.07034	-0.00366	-1.11713
5V	90	-0.86663	-0.04569	0.46520	-0.91394	-0.11701	-0.00498	-1.48304
5P	75	0.25295	-0.11684	-0.49901	-0.38672	-0.59355	0.00365	-1.33952
5H	75	0.82008	0.02615	-0.40385	0.33531	-0.13315	0.00566	0.65019
3Z	75	-0.10515	-0.00060	-0.34096	0.79460	0.32391	-0.00166	0.67013
3X	75	0.42996	-0.10115	-0.17540	0.53862	0.37202	0.00135	1.06541
5T	75	-0.29576	-0.00040	-0.11411	0.67305	-0.25695	-0.00098	0.00484
3W	75	0.65810	0.04339	0.09694	0.10948	0.54369	0.00204	1.45363
5C	75	-0.17234	-0.00149	0.17593	-0.58185	0.82243	-0.00376	0.23891
5Q	75	0.46129	-0.09825	0.34119	0.83369	-0.51980	0.00477	1.02289
3Y	75	0.06410	0.04884	0.40822	0.70237	0.35150	-0.00074	1.57428
5N	75	0.42930	-0.17598	0.95832	-0.31752	0.54369	0.00072	1.43853
3R	60	0.05596	0.13170	0.13653	-0.30167	0.18902	-0.00022	0.21133
8T	60	0.30764	0.02502	-0.40385	0.38050	0.13769	0.00150	0.44849
8U	60	0.35244	0.02692	-0.40385	0.31639	-0.10897	0.00265	0.18559
8V	60	0.15705	0.05591	-0.25779	-0.39353	-0.13315	0.00149	-0.57002
8R	60	0.27997	-0.08015	-0.37235	0.19605	-0.18209	0.00244	-0.15613
8W	60	0.36277	0.11147	-0.05326	0.19529	-0.29931	0.00337	0.32032
8X	60	0.99187	-0.08964	-0.40385	0.40034	-0.31642	0.00744	0.58974
3T	60	0.07353	0.04018	-0.05326	0.17806	-0.32500	0.00161	-0.08489
8S	60	-0.00928	-0.08625	0.02718	0.37654	-0.44763	0.00147	-0.13796
3S	60	0.37371	0.15228	-0.40385	-0.24438	-0.73625	0.00490	-0.85360
6S	50	-0.64673	0.02319	0.53113	-0.12271	1.56184	-0.00888	1.33784
6T	50	-0.54335	0.11266	-0.24745	0.08502	0.51798	-0.00486	-0.07999
6V	50	0.44362	0.13594	-0.03308	0.33876	0.37883	0.00143	1.26550
6R	50	-0.14117	0.16228	-0.20620	-0.20066	0.25371	-0.00164	-0.13368
6Q	50	0.34808	-0.07981	-0.13449	0.13140	0.12286	0.00178	0.38981
6P	50	-0.36443	0.04339	-0.12430	0.24846	0.08544	-0.00244	-0.11388
3U	50	-0.06521	0.09587	0.23466	0.14333	-0.02970	-0.00023	0.37872
8Y	50	0.12459	0.01628	-0.13449	0.18751	-0.51980	0.00255	-0.32337
6U	50	-0.01937	0.11934	-0.22680	-0.05883	-0.63103	0.00197	-0.81473
8Z	50	-0.56974	0.09329	-0.17540	0.14277	-1.08264	-0.00045	-1.59217
2C	45	0.16304	-0.05776	0.82490	0.86796	1.80484	-0.00588	3.59711
2B	45	-0.13374	0.06613	0.50295	-0.05636	0.75260	-0.00329	1.12829
1U	45	-0.09958	0.11912	0.15625	0.36879	0.78776	-0.00321	1.32913
1Z	45	-0.41582	0.08457	-0.20620	0.06734	0.31001	-0.00344	-0.16355
3M	45	-0.36078	0.16717	0.00714	0.36007	0.24659	-0.00292	0.41726
2A	45	0.20406	-0.01882	-0.03308	-0.43917	0.81669	-0.00161	0.52806
3F	45	-0.24061	-0.11295	-0.61664	0.40588	0.41931	-0.00277	-0.14777
1V	45	-0.39173	-0.12806	0.07707	1.35901	-0.19032	-0.00178	0.72419
1Y	45	-0.18146	0.09559	-0.43546	0.04319	-0.43872	0.00031	-0.91655
2D	45	-0.00452	0.13530	-0.09378	-0.20102	-0.47451	0.00157	-0.63696

Table 7.8: PCA table for lead round nose bullets (PC3)

Sample	True_Angle	PC3_Area	PC3_X_Patch	PC3_Circ.	PC3_Area_Largest_Particle	PC3_AR	PC3_Minor	PC3
5Y	90	-0.29129	-0.63862	-1.04646	-0.09327	-0.02593	-0.27276	-2.36834
5K	90	-0.16246	0.26355	-0.37596	-0.22500	-0.05000	-0.21996	-0.76982
5J	90	0.16003	-1.20858	-0.03873	-0.34087	-0.07971	-0.01290	-1.52075
5S	90	0.17099	-0.87173	0.30848	-0.36820	-0.06614	0.01680	-0.80980
5M	90	-0.14408	-1.12661	-1.00746	-0.17818	0.03588	-0.03702	-2.45747
5F	90	0.17106	-1.32919	0.36731	-0.38099	-0.04921	0.04359	-1.17742
8E	90	0.16417	-1.37116	-0.48615	-0.47461	-0.04302	0.04820	-2.16258
6E	90	0.38268	-0.19638	0.63552	-0.92809	-0.04843	0.21091	0.05619
5O	90	0.22327	-0.49209	-0.64936	-0.53853	0.00593	0.17119	-1.27960
5V	90	0.33846	-0.33952	-0.66285	-0.49138	-0.00986	0.23270	-0.93245
5P	75	-0.09879	-0.86823	0.71101	-0.20792	-0.05000	-0.17079	-0.68471
5H	75	-0.32028	0.19434	0.57543	0.18028	-0.01122	-0.26436	0.35420
3Z	75	0.04107	-0.00447	0.48582	0.42722	0.02728	0.07737	1.05428
3X	75	-0.16792	-0.75157	0.24991	0.28959	0.03134	-0.06326	-0.41192
5T	75	0.11551	-0.00300	0.16259	0.36186	-0.02164	0.04567	0.66099
3W	75	-0.25702	0.32238	-0.13812	0.05886	0.04580	-0.09518	-0.06328
5C	75	0.06731	-0.01110	-0.25067	-0.31283	0.06928	0.17571	-0.26231
5Q	75	-0.18015	-0.73009	-0.48615	0.44823	-0.04378	-0.22314	-1.21509
3Y	75	-0.02503	0.36290	-0.58166	0.37763	0.02961	0.03481	0.19826
5N	75	-0.16766	-1.30762	-1.36547	-0.17071	0.04580	-0.03342	-2.99909
3R	60	-0.02186	0.97863	-0.19453	-0.16219	0.01592	0.01008	0.62605
8T	60	-0.12015	0.18591	0.57543	0.20457	0.01160	-0.06987	0.78749
8U	60	-0.13765	0.20007	0.57543	0.17011	-0.00918	-0.12373	0.67505
8V	60	-0.06134	0.41547	0.36731	-0.21158	-0.01122	-0.06967	0.42897
8R	60	-0.10934	-0.59557	0.53055	0.10541	-0.01534	-0.11397	-0.19826
8W	60	-0.14168	0.82829	0.07589	0.10500	-0.02521	-0.15746	0.68483
8X	60	-0.38737	-0.66607	0.57543	0.21524	-0.02665	-0.34760	-0.63702
3T	60	-0.02872	0.29854	0.07589	0.09573	-0.02738	-0.07518	0.33890
8S	60	0.00362	-0.64089	-0.03873	0.20245	-0.03771	-0.06858	-0.57984
3S	60	-0.14595	1.13150	0.57543	-0.13139	-0.06202	-0.22892	1.13864
6S	50	0.25258	0.17234	-0.75678	-0.06597	0.13156	0.41517	0.14890
6T	50	0.21220	0.83714	0.35258	0.04571	0.04363	0.22697	1.71823
6V	50	-0.17326	1.01013	0.04713	0.18213	0.03191	-0.06688	1.03117
6R	50	0.05513	1.20581	0.29381	-0.10788	0.02137	0.07657	1.54481
6Q	50	-0.13594	-0.59305	0.19163	0.07065	0.01035	-0.08316	-0.53952
6P	50	0.14233	0.32239	0.17710	0.13359	0.00720	0.11422	0.89683
3U	50	0.02547	0.71240	-0.33435	0.07706	-0.00250	0.01079	0.48887
8Y	50	-0.04866	0.12094	0.19163	0.10081	-0.04378	-0.11900	0.20195
6U	50	0.00757	0.88676	0.32316	-0.03163	-0.05315	-0.09219	1.04050
8Z	50	0.22251	0.69319	0.24991	0.07676	-0.09119	0.02115	1.17232
2C	45	-0.06367	-0.42916	-1.17537	0.46666	0.15203	0.27477	-0.77474
2B	45	0.05223	0.49139	-0.71663	-0.03030	0.06339	0.15386	0.01395
1U	45	0.03889	0.88516	-0.22264	0.19828	0.06636	0.15020	1.11625
1Z	45	0.16240	0.62839	0.29381	0.03621	0.02611	0.16091	1.30783
3M	45	0.14090	1.24215	-0.01018	0.19359	0.02077	0.13669	1.72392
2A	45	-0.07970	-0.13985	0.04713	-0.23612	0.06879	0.07538	-0.26435
3F	45	0.09397	-0.83926	0.87863	0.21822	0.03532	0.12961	0.51649
1V	45	0.15299	-0.95157	-0.10981	0.73067	-0.01603	0.08324	-0.11052
1Y	45	0.07087	0.71030	0.62047	0.02322	-0.03695	-0.01435	1.37355
2D	45	0.00176	1.00534	0.13362	-0.10808	-0.03997	-0.07322	0.91946

Table 7.9: PCA table for lead round nose bullets (PC4)

Sample	True_Angle	PC4_Area	PC4_X_Patch	PC4_Circ.	PC4_Area_Largest_Particle	PC4_AR	PC4_Minor	PC4
5Y	90	0.41641	-0.51901	0.80001	0.18749	-0.01155	0.33472	1.20807
5K	90	0.23225	0.21419	0.28742	0.45231	-0.02227	0.26993	1.43382
5J	90	-0.22877	-0.98222	0.02961	0.68523	-0.03550	0.01583	-0.51583
5S	90	-0.24444	-0.70846	-0.23583	0.74018	-0.02946	-0.02062	-0.49863
5M	90	0.20597	-0.91561	0.77019	0.35819	0.01598	0.04543	0.48015
5F	90	-0.24454	-1.08024	-0.28081	0.76587	-0.02192	-0.05350	-0.91513
8E	90	-0.23468	-1.11436	0.37166	0.95408	-0.01916	-0.05915	-0.10161
6E	90	-0.54705	-0.15960	-0.48584	1.86569	-0.02157	-0.25882	0.39280
5O	90	-0.31917	-0.39992	0.49643	1.08258	0.00264	-0.21008	0.65248
5V	90	-0.48384	-0.27593	0.50674	0.98779	-0.00439	-0.28556	0.44480
5P	75	0.14122	-0.70562	-0.54356	0.41797	-0.02227	0.20958	-0.50267
5H	75	0.45785	0.15794	-0.43991	-0.36241	-0.00500	0.32441	0.13289
3Z	75	-0.05871	-0.00364	-0.37140	-0.85881	0.01215	-0.09494	-1.37535
3X	75	0.24005	-0.61081	-0.19106	-0.58215	0.01396	0.07764	-1.05237
5T	75	-0.16513	-0.00244	-0.12430	-0.72743	-0.00964	-0.05604	-1.08498
3W	75	0.36742	0.26200	0.10559	-0.11833	0.02040	0.11681	0.75389
5C	75	-0.09622	-0.00902	0.19163	0.62887	0.03086	-0.21562	0.53049
5Q	75	0.25754	-0.59335	0.37166	-0.90105	-0.01950	0.27383	-0.61088
3Y	75	0.03579	0.29494	0.44467	-0.75912	0.01319	-0.04272	-0.01326
5N	75	0.23968	-1.06271	1.04389	0.34318	0.02040	0.04102	0.62544
3R	60	0.03124	0.79534	0.14872	0.32605	0.00709	-0.01237	1.29607
8T	60	0.17176	0.15109	-0.43991	-0.41124	0.00517	0.08575	-0.43739
8U	60	0.19677	0.16260	-0.43991	-0.34196	-0.00409	0.15183	-0.27475
8V	60	0.08768	0.33765	-0.28081	0.42533	-0.00500	0.08550	0.65037
8R	60	0.15631	-0.48402	-0.40560	-0.21189	-0.00683	0.13985	-0.81218
8W	60	0.20254	0.67316	-0.05802	-0.21107	-0.01123	0.19323	0.78861
8X	60	0.55377	-0.54132	-0.43991	-0.43269	-0.01187	0.42656	-0.44545
3T	60	0.04105	0.24262	-0.05802	-0.19245	-0.01219	0.09225	0.11327
8S	60	-0.00518	-0.52086	0.02961	-0.40697	-0.01679	0.08416	-0.83603
3S	60	0.20864	0.91958	-0.43991	0.26413	-0.02762	0.28093	1.20574
6S	50	-0.36107	0.14006	0.57855	0.13262	0.05860	-0.50949	0.03927
6T	50	-0.30335	0.68035	-0.26954	-0.09189	0.01943	-0.27853	-0.24354
6V	50	0.24768	0.82094	-0.03603	-0.36613	0.01421	0.08207	0.76273
6R	50	-0.07882	0.97997	-0.22461	0.21687	0.00952	-0.09396	0.80897
6Q	50	0.19434	-0.48198	-0.14650	-0.14202	0.00461	0.10205	-0.46950
6P	50	-0.20346	0.26201	-0.13539	-0.26854	0.00321	-0.14017	-0.48235
3U	50	-0.03640	0.57898	0.25561	-0.15491	-0.00111	-0.01325	0.62891
8Y	50	0.06956	0.09829	-0.14650	-0.20266	-0.01950	0.14603	-0.05478
6U	50	-0.01081	0.72067	-0.24705	0.06359	-0.02367	0.11313	0.61586
8Z	50	-0.31809	0.56336	-0.19106	-0.15430	-0.04062	-0.02595	-0.16666
2C	45	0.09102	-0.34879	0.89856	-0.93810	0.06771	-0.33719	-0.56679
2B	45	-0.07467	0.39936	0.54785	0.06091	0.02824	-0.18881	0.77288
1U	45	-0.05560	0.71937	0.17020	-0.39859	0.02955	-0.18432	0.28062
1Z	45	-0.23215	0.51070	-0.22461	-0.07278	0.01163	-0.19747	-0.20468
3M	45	-0.20143	1.00950	0.00778	-0.38916	0.00925	-0.16774	0.26821
2A	45	0.11393	-0.11366	-0.03603	0.47466	0.03064	-0.09251	0.37703
3F	45	-0.13433	-0.68208	-0.67170	-0.43868	0.01573	-0.15905	-2.07011
1V	45	-0.21870	-0.77335	0.08395	-1.46883	-0.00714	-0.10215	-2.48622
1Y	45	-0.10131	0.57727	-0.47434	-0.04668	-0.01646	0.01761	-0.04391
2D	45	-0.00252	0.81705	-0.10215	0.21726	-0.01780	0.08986	1.00169

8. Appendix B

8.1 Script for HemoSpat

FMJ bullets

```
###begin FMJ Hemospat script
setwd("C:/Users/Jefferys/Desktop/Thesis_Jefferys/Hemospat/FMJ")

linmod <- read.table("Hemo_Original.csv",header=TRUE, sep=",",
    ↪ stringsAsFactors=FALSE)

hemo <- lm(True_Angle ~ Calculated_Degrees, data = linmod)
summary(hemo)

# range <- range(linmod$Calculated_Degrees)
# xrange <-seq(20.43,83.89,0.1)

#ycalculated <- predict(linmod, list(Calculated_Degrees =
    ↪ ycalculated,type="response"))

normrsq<- c()
gradients1 <- c()
intercepts1 <- c()
adjrsq <- c()
pvalueint <- c()
pvaluevar <- c()
sterrorint <- c()
sterrorvar <- c()

gradients1 <- as.numeric(hemo$coefficients[2])
```

```
intercepts1 <- as.numeric(hemo$coefficients[1])
normrsq <- summary(hemo)$r.squared
adjrsq <- summary(hemo)$adj.r.squared
pvalueint <- summary(hemo)$coefficients[1,4]
pvaluevar <- summary(hemo)$coefficients[2,4]
sterrorint <- summary(hemo)$coefficients[1,2]
sterrorvar <- summary(hemo)$coefficients[2,2]
tvalueint <- summary(hemo)$coefficients[1,3]
tvaluevar <- summary(hemo)$coefficients[2,3]

output.df1 <-cbind(intercepts1,sterrorint,tvalueint,pvalueint,
    ↪ normrsq)
output.df2 <- cbind(gradients1,sterrorvar,tvaluevar,pvaluevar,
    ↪ adjrsq)

final.output <- rbind(output.df1,output.df2)
write.csv(final.output,file="Combined_Data_Hemospat_FMJ.csv",row.
    ↪ names=FALSE)

#stats
res = residuals(hemo)
pred = fitted(hemo)
png(file = "Residual_Combined_Hemo.png", width = 1000, height =
    ↪ 600)
plot(pred,res,xlab = "Fitted Value", ylab= "Residuals", main ="
    ↪ Residuals versus Fitted Values for Combined Full Metal
    ↪ Jacket Hemospat Data")
abline(h=0,lty=2)
#qqnorm(res)
dev.off()

res = sort(residuals(hemo))
n = length(res)
z = qnorm(ppoints(n))
png(file = "QQplot_Combined_Hemo.png", width = 1000, height = 600)
```

```
plot(z,res,xlab="Theoretical Quantiles",ylab="Sample Quantiles",
    ↪ main="Normal Q-Q Plot for Combined Full Metal Jacket
    ↪ Hemospat Data")
abline(lm(res~z))
dev.off()

res = residuals(hemo)
mx = mean(res)
##Note the residual standard error
#not the simple SD of the residuals
#is the estimate of the SD of the residuals
#residual SE is the best estimate for sigma (estimating SD of
    ↪ residuals)
sx = summary(hemo)$sigma
png(file = "Histogram Combined Hemo.png", width = 1000, height =
    ↪ 600)
hist(res, prob=TRUE, xlab="Residuals",ylim=c(0,0.040),main="
    ↪ Histogram of Combined Full Metal Jacket Hemospat Data")
x = seq(min(res)-0.5*sx, max(res)+0.5*sx, length=200)
y = dnorm(x, mx, sx)
lines(x,y,lty=2)
box()
dev.off()

png(file = "Linear Model of Combined Hemospat Data.png", width =
    ↪ 1000, height = 600)
plot(True_Angle ~ Calculated_Degrees, data = linmod,ylim=c(40,90),
    ↪ xlim=c(30,90), main="Linear Model of Combined Full Metal
    ↪ Jacket Hemospat Data with Prediction and Confidence
    ↪ Intervals",xlab="Measured Angle",ylab="True Angle")
new.Calculated_Degrees = seq(min(linmod$Calculated_Degrees), max(
    ↪ linmod$Calculated_Degrees),length = 420)
True_Angle.pred.ci = predict(hemo, data.frame(Calculated_Degrees =
    ↪  new.Calculated_Degrees),interval = "confidence")
True_Angle.pred.pred = predict(hemo, data.frame(Calculated_Degrees
    ↪  = new.Calculated_Degrees),interval = "prediction")
```

```
lines(new.Calculated_Degrees, True_Angle.pred.ci[, 1])
lines(new.Calculated_Degrees,True_Angle.pred.ci[, 2] , lty = 2,
   ↪ col = "blue")
lines( new.Calculated_Degrees, True_Angle.pred.ci[, 3] , lty = 2,
   ↪ col = "blue")
lines( new.Calculated_Degrees,True_Angle.pred.pred[, 2], lty = 2,
   ↪ col = "red")
lines( new.Calculated_Degrees, True_Angle.pred.pred[, 3] , lty =
   ↪ 2, col = "red")

testval <- c(45,75,90)
l.colors <- c("green","orange","darkgrey")
for (i in 1:length(testval)){
  abline(v=testval[i],col=l.colors[i])
  new.Calculated_Degrees <- c(testval[i])

  xmax1 <- predict(hemo,data.frame(Calculated_Degrees =new.
     ↪ Calculated_Degrees),interval="prediction")
  xg1 <- c(0,testval[i])
  yg1 <- c(xmax1[,3],xmax1[,3])
  lines(xg1,yg1,lty=2,col=l.colors[i])
  xg2 <- c(0,testval[i])
  yg2 <- c(xmax1[,2],xmax1[,2])
  lines(xg2,yg2,lty=2,col=l.colors[i])
  xg3 <- c(0,testval[i])
  yg3 <- c(xmax1[,1],xmax1[,1])
  lines(xg3,yg3,lty=1,col=l.colors[i])
  xmax2 <- predict(hemo,data.frame(Calculated_Degrees =new.
     ↪ Calculated_Degrees),interval="confidence")
  xg4 <- c(0,testval[i])
  yg4 <- c(xmax2[,2],xmax2[,2])
  lines(xg4,yg4,lty=3,col=l.colors[i])
  xg5 <- c(0,testval[i])
  yg5 <- c(xmax2[,3],xmax2[,3])
  lines(xg5,yg5,lty=3,col=l.colors[i])
}
```

```
dev.off()

#prediction code for model
outers<-c()
inners<-c()
angle <- c()
TA.pred.fit <- c()
TA.pred.lwr <- c()
TA.pred.upr <- c()
angle.pred.fit <- c()
angle.pred.lwr <- c()
angle.pred.upr <- c()

for (jj in 45:90) {

angle[jj] <- jj
CD <- c(jj)
TA.pred = predict(hemo, data.frame(Calculated_Degrees=CD),interval
   ↪ = "confidence")
angle.pred = predict(hemo, data.frame(Calculated_Degrees=CD),
   ↪ interval = "prediction")
TA.pred.fit[jj] <- angle.pred[1]
TA.pred.lwr[jj] <- angle.pred[2]
TA.pred.upr[jj] <- angle.pred[3]
angle.pred.fit[jj] <- TA.pred[1]
angle.pred.lwr[jj] <- TA.pred[2]
angle.pred.upr[jj] <- TA.pred[3]
inners <-cbind(angle[jj], TA.pred.fit[jj], TA.pred.lwr[jj], TA.
   ↪ pred.upr[jj],
                angle.pred.fit[jj], angle.pred.lwr[jj],angle.pred.
                   ↪ upr[jj])
outers<-rbind(outers, inners)
}

outers<- data.frame(outers)
write.csv(outers,file = "Combined_Outers.csv",row.names=FALSE)
```

```
outer.cols <-c("Angle","Pred.fit","Pred.lower","Pred.upper","CI.
    ↪ fit","CI.lower","CI.upper")
colnames(outers)<-outer.cols

old.output <- output
output <- outers

ymin<-min(output$Angle)
ymax<-max(output$Angle)

mypath <- file.path("C:/Users/Jefferys/Desktop/Thesis_Jefferys/
    ↪ Hemospat/FMJ",paste("Combined_Prediction", ".png", sep = "")
    ↪ )
png(file = mypath, width = 1000, height = 600)
#mytitle = paste("Prediction Values for Combined Hemospat Data")
plot(output$Angle, output$CI.fit , type="l", ylim=c(ymin,ymax),
    ↪ ylab="True Angle", xlab="Measured Angle", main="Prediction
    ↪ Values Resulting from Measured Values for Combined Full
    ↪ Metal Jacket Hemospat Data with Confidence Intervals")
lines( output$Angle,output$CI.upper , lty=2, col="blue")
lines(output$Angle,output$CI.lower , lty=2, col="blue")
#for (i in 1:length(output$Angle)){
#  x.temp <- c(output$Angle[i],output$Angle[i])
#  y.temp <- c(output$CI.lower[i],output$CI.upper[i])
#  lines(x.temp,y.temp)
#}
lines(output$Angle,output$Pred.upper , lty=2, col="red")
lines(output$Angle,output$Pred.lower , lty=2, col="red")
#for (i in 1:length(output$Angle)){
#  x.temp <- c(output$Angle[i],output$Angle[i])
#  y.temp <- c(output$Pred.lower[i],output$Pred.upper[i])
#  lines(x.temp,y.temp)
#}
abline(v=45, col="grey")
abline(v=50, col="grey")
```

```
abline(v=60, col="grey")
abline(v=75, col="grey")
abline(v=90, col="grey")
dev.off()
#output <- old.output

#start of methods loop
method_type <- as.character(unique(linmod$Method))

##########################################Methods
#adjust the current method being used here
i <- "Outside"
#for(i in method_type){
  linmodsub <- subset(linmod, linmod$Method == as.character(i))

  hemo1 <- lm(True_Angle ~ Calculated_Degrees, data = linmodsub)
  summary(hemo1)

  normrsq<- c()
  gradients1 <- c()
  intercepts1 <- c()
  adjrsq <- c()
  pvalueint <- c()
  pvaluevar <- c()
  sterrorint <- c()
  sterrorvar <- c()

  gradients1[i] <- as.numeric(hemo1$coefficients[2])
  intercepts1[i] <- as.numeric(hemo1$coefficients[1])
  normrsq[i] <- summary(hemo1)$r.squared
  adjrsq[i] <- summary(hemo1)$adj.r.squared
  pvalueint[i] <- summary(hemo1)$coefficients[1,4]
  pvaluevar[i] <- summary(hemo1)$coefficients[2,4]
  sterrorint[i] <- summary(hemo1)$coefficients[1,2]
  sterrorvar[i] <- summary(hemo1)$coefficients[2,2]
  tvalueint[i] <- summary(hemo1)$coefficients[1,3]
```

```
tvaluevar[i] <- summary(hemo1)$coefficients[2,3]

output.df1 <-cbind(intercepts1[i],sterrorint[i],tvalueint[i],
    ↪ pvalueint[i],normrsq[i])
output.df2 <- cbind(gradients1[i],sterrorvar[i],tvaluevar[i],
    ↪ pvaluevar[i],adjrsq[i])

finaloutput2 <- rbind(output.df1,output.df2)
write.csv(finaloutput2,file = paste(as.character(i),"_Data_Model
    ↪ .csv"),row.names=FALSE)

# plot(linmodsub$Calculated_Degrees,linmodsub$True_Angle, main =
    ↪  mytitle, ylab ="Calculated Angle", xlab = "True Angle")
# abline(coef = c(intercepts[i],gradients[i]))
# dev.off()

#residuals plots
res = residuals(hemo1)
pred = fitted(hemo1)
mypath <- file.path("C:/Users/Jefferys/Desktop/Thesis_Jefferys/
    ↪ Hemospat/FMJ",paste("Residuals_for", as.character(i), ".
    ↪ png", sep = ""))
png(file = mypath, width = 1000, height = 600)
mytitle = paste("Residuals_versus_Fitted_Values_for_Method", as.
    ↪ character(i), "Using_Full_Metal_Jacket_Bullets")
plot(pred,res,xlab = "Fitted_Value", ylab= "Residuals", main =
    ↪ mytitle)
abline(h=0,lty=2)
dev.off()

# res = residuals(hemo1)
# qqnorm(res)
# qqline(res)

res = sort(residuals(hemo1))
n = length(res)
```

```
z = qnorm(ppoints(n))
mypath <- file.path("C:/Users/Jefferys/Desktop/Thesis_Jefferys/
    ↪ Hemospat/FMJ",paste("Normal_QQ_Plot", as.character(i), ".
    ↪ png", sep = ""))
png(file = mypath, width = 1000, height = 600)
mytitle = paste("Normal_Q-Q_Plot_for_Method", as.character(i),"
    ↪ Using_Full_Metal_Jacket_Bullets")
plot(z,res,xlab="Theoretical_Quantiles",ylab="Sample_Quantiles",
    ↪  main = mytitle)
abline(lm(res~z))
dev.off()

res = residuals(hemo1)
mx = mean(res)
##Note the residual standard error
#not the simple SD of the residuals
#is the estimate of the SD of the residuals
#residual SE is the best estimate for sigma (estimating SD of
    ↪ residuals)
sx = summary(hemo1)$sigma
mypath <- file.path("C:/Users/Jefferys/Desktop/Thesis_Jefferys/
    ↪ Hemospat/FMJ",paste("Histogram_for", as.character(i), ".
    ↪ png", sep = ""))
png(file = mypath, width = 1000, height = 600)
mytitle = paste("Histogram_for_Method", as.character(i), "Using_
    ↪ Full_Metal_Jacket_Bullets")
hist(res, prob=TRUE, xlab="Residuals", main =mytitle, ylim=c
    ↪ (0,0.04))
x = seq(min(res)-0.5*sx, max(res)+0.5*sx, length=200)
y = dnorm(x, mx, sx)
lines(x,y,lty=2)
box()
dev.off()
```

```
mypath <- file.path("C:/Users/Jefferys/Desktop/Thesis_Jefferys/
    ↪ Hemospat/FMJ",paste("Linear_Model_of", as.character(i), ".
    ↪ png", sep = ""))
png(file = mypath, width = 1000, height = 600)
mytitle = paste("Linear_Model_of_Method", as.character(i), "
    ↪ Using_Full_Metal_Jacket_Bullets_with_Prediction_and_
    ↪ Confidence_Intervals")
plot(True_Angle ~ Calculated_Degrees, data = linmodsub, main=
    ↪ mytitle, xlab="Measured_Angle",ylab="True_Angle",xlim=c
    ↪ (30,90))
new.Calculated_Degrees = seq(min(linmodsub$Calculated_Degrees),
    ↪ max(linmodsub$Calculated_Degrees),length = 90)
True_Angle.pred.ci = predict(hemo1,data.frame(Calculated_Degrees
    ↪  =new.Calculated_Degrees),interval = "confidence")
True_Angle.pred.pred = predict(hemo1,data.frame(Calculated_
    ↪ Degrees = new.Calculated_Degrees),interval = "prediction")
lines(new.Calculated_Degrees, True_Angle.pred.ci[, 1])
lines(new.Calculated_Degrees,True_Angle.pred.ci[, 2] , lty = 2,
    ↪ col = "blue")
lines( new.Calculated_Degrees, True_Angle.pred.ci[, 3] , lty =
    ↪ 2, col = "blue")
lines( new.Calculated_Degrees,True_Angle.pred.pred[, 2], lty =
    ↪ 2, col = "red")
lines( new.Calculated_Degrees, True_Angle.pred.pred[, 3] , lty =
    ↪  2, col = "red")

testval <- c(45,75,90)
l.colors <- c("green","orange","darkgrey")
for (i in 1:length(testval)){
  abline(v=testval[i],col=l.colors[i])
  new.Calculated_Degrees <- c(testval[i])

  xmax1 <- predict(hemo1,data.frame(Calculated_Degrees =new.
      ↪ Calculated_Degrees),interval="prediction")
  xg1 <- c(0,testval[i])
  yg1 <- c(xmax1[,3],xmax1[,3])
```

```
  lines(xg1,yg1,lty=2,col=l.colors[i])
  xg2 <- c(0,testval[i])
  yg2 <- c(xmax1[,2],xmax1[,2])
  lines(xg2,yg2,lty=2,col=l.colors[i])
  xg3 <- c(0,testval[i])
  yg3 <- c(xmax1[,1],xmax1[,1])
  lines(xg3,yg3,lty=1,col=l.colors[i])
  xmax2 <- predict(hemo1,data.frame(Calculated_Degrees =new.
    ↪ Calculated_Degrees),interval="confidence")
  xg4 <- c(0,testval[i])
  yg4 <- c(xmax2[,2],xmax2[,2])
  lines(xg4,yg4,lty=3,col=l.colors[i])
  xg5 <- c(0,testval[i])
  yg5 <- c(xmax2[,3],xmax2[,3])
  lines(xg5,yg5,lty=3,col=l.colors[i])
}
dev.off()
#adjust what i is for the method being used
i <- "Outside"

outers<-c()
inners<-c()
angle <- c()
TA.pred.fit <- c()
TA.pred.lwr <- c()
TA.pred.upr <- c()
angle.pred.fit <- c()
angle.pred.lwr <- c()
angle.pred.upr <- c()

for (jj in 45:90) {

angle[jj] <- jj
CD <- c(jj)
  TA.pred = predict(hemo1, data.frame(Calculated_Degrees=CD),
    ↪ interval = "confidence")
```

```
  angle.pred = predict(hemo1, data.frame(Calculated_Degrees=CD),
    ↪  interval = "prediction")
  TA.pred.fit[jj] <- angle.pred[1]
  TA.pred.lwr[jj] <- angle.pred[2]
  TA.pred.upr[jj] <- angle.pred[3]
  angle.pred.fit[jj] <- TA.pred[1]
  angle.pred.lwr[jj] <- TA.pred[2]
  angle.pred.upr[jj] <- TA.pred[3]
  inners <-cbind(angle[jj], TA.pred.fit[jj], TA.pred.lwr[jj], TA
    ↪ .pred.upr[jj],
                 angle.pred.fit[jj], angle.pred.lwr[jj],angle.
                   ↪ pred.upr[jj])
  outers<-rbind(outers, inners)
}

outers<- data.frame(outers)
write.csv(outers,file = paste(as.character(i),"_Outers.csv"),row
  ↪ .names=FALSE)

outer.cols <-c("Angle","Pred.fit","Pred.lower","Pred.upper","CI.
  ↪ fit","CI.lower","CI.upper")
colnames(outers)<-outer.cols

old.output <- output
# output <- outers

ymin<-min(output$Angle)
ymax<-max(output$Angle)

mypath <- file.path("C:/Users/Jefferys/Desktop/Thesis_Jefferys/
  ↪ Hemospat/FMJ",paste("Final_Model_of", as.character(i), ".
  ↪ png", sep = ""))
png(file = mypath, width = 1000, height = 600)
mytitle = paste("Prediction_Values_Resulting_from_Measured_
  ↪ Values_for_Method", as.character(i),"Using_Full_Metal_
  ↪ Jacket_Bullets_with_Confidence_Intervals")
```

```
  plot(output$Angle, output$CI.fit, type="l",xlim=c(45,90), ylim=c
    ↪ (ymin,ymax), ylab="True Angle", xlab="Measured Angle",
    ↪ main=mytitle)
  lines( output$Angle,output$CI.upper , lty=2, col="blue")
  lines(output$Angle,output$CI.lower , lty=2, col="blue")
  #for (i in 1:length(output$Angle)){
  #  x.temp <- c(output$Angle[i],output$Angle[i])
  #  y.temp <- c(output$CI.lower[i],output$CI.upper[i])
  #  lines(x.temp,y.temp)
  #}
  lines(output$Angle,output$Pred.upper , lty=2, col="red")
  lines(output$Angle,output$Pred.lower , lty=2, col="red")
  #for (i in 1:length(output$Angle)){
  #  x.temp <- c(output$Angle[i],output$Angle[i])
  #  y.temp <- c(output$Pred.lower[i],output$Pred.upper[i])
  #  lines(x.temp,y.temp)
  #}
  abline(v=45, col="grey")
  abline(v=50, col="grey")
  abline(v=60, col="grey")
  abline(v=75, col="grey")
  abline(v=90, col="grey")
  dev.off()

  #output <- old.output

  #write.csv(output_final,file = paste(substr(linmodsub$Method[i
    ↪ ],1,2),"_Data_Methods.csv"),row.names=FALSE)
#}
####end of FMJ Hemospat script
```

LRN bullets

```
###begin script for LRN Hemospat
setwd("C:/Users/Jefferys/Desktop/Thesis_Jefferys/Hemospat/LRN")
```

```
linmod <- read.table("Hemo_LRN_Data.csv",header=TRUE, sep=",",
    ↪ stringsAsFactors=FALSE)

hemo <- lm(True_Angle ~ Calculated_Degrees, data = linmod)
summary(hemo)

# range <- range(linmod$Calculated_Degrees)
# xrange <-seq(20.43,83.89,0.1)

#ycalculated <- predict(linmod, list(Calculated_Degrees =
    ↪ ycalculated,type="response"))

normrsq<- c()
gradients1 <- c()
intercepts1 <- c()
adjrsq <- c()
pvalueint <- c()
pvaluevar <- c()
sterrorint <- c()
sterrorvar <- c()

gradients1 <- as.numeric(hemo$coefficients[2])
intercepts1 <- as.numeric(hemo$coefficients[1])
normrsq <- summary(hemo)$r.squared
adjrsq <- summary(hemo)$adj.r.squared
pvalueint <- summary(hemo)$coefficients[1,4]
pvaluevar <- summary(hemo)$coefficients[2,4]
sterrorint <- summary(hemo)$coefficients[1,2]
sterrorvar <- summary(hemo)$coefficients[2,2]
tvalueint <- summary(hemo)$coefficients[1,3]
tvaluevar <- summary(hemo)$coefficients[2,3]

output.df1 <-cbind(intercepts1,sterrorint,tvalueint,pvalueint,
    ↪ normrsq)
output.df2 <- cbind(gradients1,sterrorvar,tvaluevar,pvaluevar,
    ↪ adjrsq)
```

```
final.output <- rbind(output.df1,output.df2)
write.csv(final.output,file ="Combined_Data_Hemospat_LRN.csv",row.
    ↪ names=FALSE)

#stats
res = residuals(hemo)
pred = fitted(hemo)
png(file = "Residual_Combined_Hemo.png", width = 1000, height =
    ↪ 600)
plot(pred,res,xlab = "Fitted_Value", ylab= "Residuals", main ="
    ↪ Residuals_versus_Fitted_Values_for_Combined_Lead_Round_Nose_
    ↪ Hemospat_Data")
abline(h=0,lty=2)
#qqnorm(res)
dev.off()

res = sort(residuals(hemo))
n = length(res)
z = qnorm(ppoints(n))
png(file = "QQplot_Combined_Hemo.png", width = 1000, height = 600)
plot(z,res,xlab="Theoretical_Quantiles",ylab="Sample_Quantiles",
    ↪ main="Normal_Q-Q_Plot_for_Combined_Lead_Round_Nose_Hemospat_
    ↪ Data")
abline(lm(res~z))
dev.off()

res = residuals(hemo)
mx = mean(res)
##Note the residual standard error
#not the simple SD of the residuals
#is the estimate of the SD of the residuals
#residual SE is the best estimate for sigma (estimating SD of
    ↪ residuals)
sx = summary(hemo)$sigma
```

```
png(file = "Histogram_Combined_Hemo.png", width = 1000, height =
    ↪ 600)
hist(res, prob=TRUE, xlab="Residuals",main="Histogram of Combined
    ↪ Lead Round Nose Hemospat Data")
x = seq(min(res)-0.5*sx, max(res)+0.5*sx, length=200)
y = dnorm(x, mx, sx)
lines(x,y,lty=2)
box()
dev.off()

png(file = "Linear Model of Combined Hemospat Data.png", width =
    ↪ 1000, height = 600)
plot(True_Angle ~ Calculated_Degrees, data = linmod, xlim=c(30,90)
    ↪ , main="Linear Model of Combined Lead Round Nose Hemospat
    ↪ Data with Prediction and Confidence Intervals",xlab="
    ↪ Measured Angle",ylab="True Angle")
new.Calculated_Degrees = seq(min(linmod$Calculated_Degrees), max(
    ↪ linmod$Calculated_Degrees),length = 420)
True_Angle.pred.ci = predict(hemo, data.frame(Calculated_Degrees =
    ↪  new.Calculated_Degrees),interval = "confidence")
True_Angle.pred.pred = predict(hemo, data.frame(Calculated_Degrees
    ↪  = new.Calculated_Degrees),interval = "prediction")
lines(new.Calculated_Degrees, True_Angle.pred.ci[, 1])
lines(new.Calculated_Degrees,True_Angle.pred.ci[, 2] , lty = 2,
    ↪ col = "blue")
lines( new.Calculated_Degrees, True_Angle.pred.ci[, 3] , lty = 2,
    ↪ col = "blue")
lines( new.Calculated_Degrees,True_Angle.pred.pred[, 2], lty = 2,
    ↪ col = "red")
lines( new.Calculated_Degrees, True_Angle.pred.pred[, 3] , lty =
    ↪ 2, col = "red")

testval <- c(45,75,90)
l.colors <- c("green","orange","darkgrey")
for (i in 1:length(testval)){
  abline(v=testval[i],col=l.colors[i])
```

```
  new.Calculated_Degrees <- c(testval[i])

  xmax1 <- predict(hemo,data.frame(Calculated_Degrees =new.
     ↪ Calculated_Degrees),interval="prediction")
  xg1 <- c(0,testval[i])
  yg1 <- c(xmax1[,3],xmax1[,3])
  lines(xg1,yg1,lty=2,col=l.colors[i])
  xg2 <- c(0,testval[i])
  yg2 <- c(xmax1[,2],xmax1[,2])
  lines(xg2,yg2,lty=2,col=l.colors[i])
  xg3 <- c(0,testval[i])
  yg3 <- c(xmax1[,1],xmax1[,1])
  lines(xg3,yg3,lty=1,col=l.colors[i])
  xmax2 <- predict(hemo,data.frame(Calculated_Degrees =new.
     ↪ Calculated_Degrees),interval="confidence")
  xg4 <- c(0,testval[i])
  yg4 <- c(xmax2[,2],xmax2[,2])
  lines(xg4,yg4,lty=3,col=l.colors[i])
  xg5 <- c(0,testval[i])
  yg5 <- c(xmax2[,3],xmax2[,3])
  lines(xg5,yg5,lty=3,col=l.colors[i])
}
dev.off()
#prediction code for model
outers<-c()
inners<-c()
angle <- c()
TA.pred.fit <- c()
TA.pred.lwr <- c()
TA.pred.upr <- c()
angle.pred.fit <- c()
angle.pred.lwr <- c()
angle.pred.upr <- c()


for (jj in 45:90) {
```

```
angle[jj] <- jj
CD <- c(jj)
TA.pred = predict(hemo, data.frame(Calculated_Degrees=CD),interval
   ↪ = "confidence")
angle.pred = predict(hemo, data.frame(Calculated_Degrees=CD),
   ↪ interval = "prediction")
TA.pred.fit[jj] <- angle.pred[1]
TA.pred.lwr[jj] <- angle.pred[2]
TA.pred.upr[jj] <- angle.pred[3]
angle.pred.fit[jj] <- TA.pred[1]
angle.pred.lwr[jj] <- TA.pred[2]
angle.pred.upr[jj] <- TA.pred[3]
inners <-cbind(angle[jj], TA.pred.fit[jj], TA.pred.lwr[jj], TA.
   ↪ pred.upr[jj],
                angle.pred.fit[jj], angle.pred.lwr[jj],angle.pred.
                   ↪ upr[jj])
outers<-rbind(outers, inners)
}

outers<- data.frame(outers)
write.csv(outers,file = "Combined_Outers.csv",row.names=FALSE)

outer.cols <-c("Angle","Pred.fit","Pred.lower","Pred.upper","CI.
   ↪ fit","CI.lower","CI.upper")
colnames(outers)<-outer.cols

old.output <- output
output <- outers

ymin<-min(output$Angle)
ymax<-max(output$Angle)

mypath <- file.path("C:/Users/Jefferys/Desktop/Thesis_Jefferys/
   ↪ Hemospat/LRN/",paste("Combined_Prediction", ".png", sep = ""
   ↪ ))
```

```
png(file = mypath, width = 1000, height = 600)
#mytitle = paste("Prediction Values for Combined Hemospat Data")
plot(output$Angle, output$CI.fit , type="l", ylim=c(ymin,ymax),
   ↪ xlab="Measured Angle", ylab="True Angle", main="Prediction
   ↪ Values Resulting from Measured Values for Combined Lead
   ↪ Round Nose Hemospat Data with Confidence Intervals")
lines( output$Angle,output$CI.upper , lty=2, col="blue")
lines(output$Angle,output$CI.lower , lty=2, col="blue")
#for (i in 1:length(output$Angle)){
#  x.temp <- c(output$Angle[i],output$Angle[i])
#  y.temp <- c(output$CI.lower[i],output$CI.upper[i])
#  lines(x.temp,y.temp)
#}
lines(output$Angle,output$Pred.upper , lty=2, col="red")
lines(output$Angle,output$Pred.lower , lty=2, col="red")
#for (i in 1:length(output$Angle)){
#  x.temp <- c(output$Angle[i],output$Angle[i])
#  y.temp <- c(output$Pred.lower[i],output$Pred.upper[i])
#  lines(x.temp,y.temp)
#}
abline(v=45, col="grey")
abline(v=50, col="grey")
abline(v=60, col="grey")
abline(v=75, col="grey")
abline(v=90, col="grey")
dev.off()
#output <- old.output

#start of methods loop
method_type <- as.character(unique(linmod$Method))

##########################################Methods
#adjust method being used here
i <- "Outside"
#for(i in method_type){
  linmodsub <- subset(linmod, linmod$Method == as.character(i))
```

```
hemo1 <- lm(True_Angle ~ Calculated_Degrees, data = linmodsub)
summary(hemo1)

normrsq<- c()
gradients1 <- c()
intercepts1 <- c()
adjrsq <- c()
pvalueint <- c()
pvaluevar <- c()
sterrorint <- c()
sterrorvar <- c()

gradients1[i] <- as.numeric(hemo1$coefficients[2])
intercepts1[i] <- as.numeric(hemo1$coefficients[1])
normrsq[i] <- summary(hemo1)$r.squared
adjrsq[i] <- summary(hemo1)$adj.r.squared
pvalueint[i] <- summary(hemo1)$coefficients[1,4]
pvaluevar[i] <- summary(hemo1)$coefficients[2,4]
sterrorint[i] <- summary(hemo1)$coefficients[1,2]
sterrorvar[i] <- summary(hemo1)$coefficients[2,2]
tvalueint[i] <- summary(hemo1)$coefficients[1,3]
tvaluevar[i] <- summary(hemo1)$coefficients[2,3]

output.df1 <-cbind(intercepts1[i],sterrorint[i],tvalueint[i],
   ↪ pvalueint[i],normrsq[i])
output.df2 <- cbind(gradients1[i],sterrorvar[i],tvaluevar[i],
   ↪ pvaluevar[i],adjrsq[i])

finaloutput2 <- rbind(output.df1,output.df2)
write.csv(finaloutput2,file = paste(as.character(i),"_Data_Model
   ↪ .csv"),row.names=FALSE)

#residuals plots
res = residuals(hemo1)
pred = fitted(hemo1)
```

```
mypath <- file.path("C:/Users/Jefferys/Desktop/Thesis_Jefferys/
    ↪ Hemospat/LRN",paste("Residuals_for", as.character(i), ".
    ↪ png", sep = ""))
png(file = mypath, width = 1000, height = 600)
mytitle = paste("Residuals_versus_Fitted_Values_for_Method", as.
    ↪ character(i), "Using_Lead_Round_Nose_Bullets")
plot(pred,res,xlab = "Fitted_Value", ylab= "Residuals", main =
    ↪ mytitle)
abline(h=0,lty=2)
dev.off()

res = sort(residuals(hemo1))
n = length(res)
z = qnorm(ppoints(n))
mypath <- file.path("C:/Users/Jefferys/Desktop/Thesis_Jefferys/
    ↪ Hemospat/LRN",paste("Normal_QQ_Plot", as.character(i), ".
    ↪ png", sep = ""))
png(file = mypath, width = 1000, height = 600)
mytitle = paste("Normal_Q-Q_Plot_for_Method", as.character(i),"
    ↪ Using_Lead_Round_Nose_Bullets")
plot(z,res,xlab="Theoretical_Quantiles",ylab="Sample_Quantiles",
    ↪  main = mytitle)
abline(lm(res~z))
dev.off()

res = residuals(hemo1)
mx = mean(res)
##Note the residual standard error
#not the simple SD of the residuals
#is the estimate of the SD of the residuals
#residual SE is the best estimate for sigma (estimating SD of
    ↪ residuals)
sx = summary(hemo1)$sigma
mypath <- file.path("C:/Users/Jefferys/Desktop/Thesis_Jefferys/
    ↪ Hemospat/LRN",paste("Histogram_for", as.character(i), ".
    ↪ png", sep = ""))
```

```
png(file = mypath, width = 1000, height = 600)
mytitle = paste("Histogram for Method", as.character(i), "Using
    ↪ Lead Round Nose Bullets")
hist(res, prob=TRUE, xlab="Residuals", main =mytitle, ylim=c
    ↪ (0,0.04))
x = seq(min(res)-0.5*sx, max(res)+0.5*sx, length=200)
y = dnorm(x, mx, sx)
lines(x,y,lty=2)
box()
dev.off()

mypath <- file.path("C:/Users/Jefferys/Desktop/Thesis_Jefferys/
    ↪ Hemospat/LRN",paste("Linear Model of", as.character(i), ".
    ↪ png", sep = ""))
png(file = mypath, width = 1000, height = 600)
mytitle = paste("Linear Model of Method", as.character(i), "
    ↪ Using Lead Round Nose Bullets with Prediction and
    ↪ Confidence Intervals")
plot(True_Angle ~ Calculated_Degrees, data = linmodsub,xlim=c
    ↪ (30,90), main=mytitle, xlab="Measured Angle",ylab="True
    ↪ Angle")
new.Calculated_Degrees = seq(min(linmodsub$Calculated_Degrees),
    ↪ max(linmodsub$Calculated_Degrees),length = 90)
True_Angle.pred.ci = predict(hemo1,data.frame(Calculated_Degrees
    ↪  =new.Calculated_Degrees),interval = "confidence")
True_Angle.pred.pred = predict(hemo1,data.frame(Calculated_
    ↪ Degrees = new.Calculated_Degrees),interval = "prediction")
lines(new.Calculated_Degrees, True_Angle.pred.ci[, 1])
lines(new.Calculated_Degrees,True_Angle.pred.ci[, 2] , lty = 2,
    ↪ col = "blue")
lines( new.Calculated_Degrees, True_Angle.pred.ci[, 3] , lty =
    ↪ 2, col = "blue")
lines( new.Calculated_Degrees,True_Angle.pred.pred[, 2], lty =
    ↪ 2, col = "red")
lines( new.Calculated_Degrees, True_Angle.pred.pred[, 3] , lty =
    ↪  2, col = "red")
```

```
testval <- c(45,75,90)
l.colors <- c("green","orange","darkgrey")
for (i in 1:length(testval)){
  abline(v=testval[i],col=l.colors[i])
  new.Calculated_Degrees <- c(testval[i])

  xmax1 <- predict(hemo1,data.frame(Calculated_Degrees =new.
    ↪ Calculated_Degrees),interval="prediction")
  xg1 <- c(0,testval[i])
  yg1 <- c(xmax1[,3],xmax1[,3])
  lines(xg1,yg1,lty=2,col=l.colors[i])
  xg2 <- c(0,testval[i])
  yg2 <- c(xmax1[,2],xmax1[,2])
  lines(xg2,yg2,lty=2,col=l.colors[i])
  xg3 <- c(0,testval[i])
  yg3 <- c(xmax1[,1],xmax1[,1])
  lines(xg3,yg3,lty=1,col=l.colors[i])
  xmax2 <- predict(hemo1,data.frame(Calculated_Degrees =new.
    ↪ Calculated_Degrees),interval="confidence")
  xg4 <- c(0,testval[i])
  yg4 <- c(xmax2[,2],xmax2[,2])
  lines(xg4,yg4,lty=3,col=l.colors[i])
  xg5 <- c(0,testval[i])
  yg5 <- c(xmax2[,3],xmax2[,3])
  lines(xg5,yg5,lty=3,col=l.colors[i])
}
dev.off()

#adjust what i is based on method being used
i <- "Outside"

outers<-c()
inners<-c()
angle <- c()
TA.pred.fit <- c()
```

```
TA.pred.lwr <- c()
TA.pred.upr <- c()
angle.pred.fit <- c()
angle.pred.lwr <- c()
angle.pred.upr <- c()

for (jj in 45:90) {

  angle[jj] <- jj
  CD <- c(jj)
  TA.pred = predict(hemo1, data.frame(Calculated_Degrees=CD),
    ↪ interval = "confidence")
  angle.pred = predict(hemo1, data.frame(Calculated_Degrees=CD),
    ↪  interval = "prediction")
  TA.pred.fit[jj] <- angle.pred[1]
  TA.pred.lwr[jj] <- angle.pred[2]
  TA.pred.upr[jj] <- angle.pred[3]
  angle.pred.fit[jj] <- TA.pred[1]
  angle.pred.lwr[jj] <- TA.pred[2]
  angle.pred.upr[jj] <- TA.pred[3]
  inners <-cbind(angle[jj], TA.pred.fit[jj], TA.pred.lwr[jj], TA
    ↪ .pred.upr[jj],
                 angle.pred.fit[jj], angle.pred.lwr[jj],angle.
                   ↪ pred.upr[jj])
  outers<-rbind(outers, inners)
}

outers<- data.frame(outers)
write.csv(outers,file = paste(as.character(i),"_Outers.csv"),row
  ↪ .names=FALSE)

outer.cols <-c("Angle","Pred.fit","Pred.lower","Pred.upper","CI.
  ↪ fit","CI.lower","CI.upper")
colnames(outers)<-outer.cols

old.output <- output
```

```
output <- outers

ymin<-min(output$Angle)
ymax<-max(output$Angle)

mypath <- file.path("C:/Users/Jefferys/Desktop/Thesis_Jefferys/
    ↪ Hemospat/LRN",paste("Final_Model_of", as.character(i), ".
    ↪ png", sep = ""))
png(file = mypath, width = 1000, height = 600)
mytitle = paste("Prediction_Values_Resulting_from_Measured_
    ↪ Values_for_Method", as.character(i),"Using_Lead_Round_Nose
    ↪ _Bullets_with_Confidence_Intervals")
plot(output$Angle, output$CI.fit , type="l",xlim=c(45,90), ylim=c
    ↪ (ymin,ymax), xlab="Measured_Angle", ylab="True_Angle",
    ↪ main=mytitle)
lines( output$Angle,output$CI.upper , lty=2, col="blue")
lines(output$Angle,output$CI.lower , lty=2, col="blue")
#for (i in 1:length(output$Angle)){
#  x.temp <- c(output$Angle[i],output$Angle[i])
#  y.temp <- c(output$CI.lower[i],output$CI.upper[i])
#  lines(x.temp,y.temp)
#}
lines(output$Angle,output$Pred.upper , lty=2, col="red")
lines(output$Angle,output$Pred.lower , lty=2, col="red")
#for (i in 1:length(output$Angle)){
#  x.temp <- c(output$Angle[i],output$Angle[i])
#  y.temp <- c(output$Pred.lower[i],output$Pred.upper[i])
#  lines(x.temp,y.temp)
#}
abline(v=45, col="grey")
abline(v=50, col="grey")
abline(v=60, col="grey")
abline(v=75, col="grey")
abline(v=90, col="grey")
dev.off()
# #output <- old.output
```

```
  #
  # write.csv(output_final, file = paste(substr(linmodsub$Method[i
    ↪ ],1,2),"_Data_Methods.csv"),row.names=FALSE)
#}
###end script for LRN Hemospat
```

8.2 Script for side view bullet deformation

File preparation

```
###begin set up file code for bullet deformation
getwd()
setwd("C:/Users/Jefferys/Desktop/Thesis_Jefferys/Bullet_Angle_
  ↪ Photos/LRN/90_Degrees/Results")

path = "C:/Users/Jefferys/Desktop/Thesis_Jefferys/Bullet_Angle_
  ↪ Photos/LRN/90_Degrees/Results"
file.names <- dir(path, pattern =".csv")

for(i in 1:length(file.names)){
  Angle <- read.table(file.names[i],header=TRUE, sep=",",
    ↪ stringsAsFactors=FALSE)

  trueangle1 <- 90 #adjust

  yprime <- 2500-Angle$Y

  dataname <- substr(file.names[i],9,10)
  method <- substr(file.names[i],12,13)
  points <- substr(file.names[i],15,16)

  newAngle <- cbind(dataname,Angle,yprime)

  yint1 <- min(newAngle$X)
  yint2 <- max(newAngle$X)
  yprimemax <- max(newAngle$yprime)
```

```
linear <- lm(formula = newAngle$yprime ~ newAngle$X, data =
    ↪ newAngle)
linear$coefficients
gradient <- as.numeric(linear$coefficients[2])
intercept <- as.numeric(linear$coefficients[1])
rsquared <- summary(linear)$r.squared

mypath <- file.path("C:/Users/Jefferys/Desktop/Thesis_Jefferys/
    ↪ Bullet_Angle_Photos/LRN/90_Degrees/Results/Graphs",paste("
    ↪ Graph_of_", substr(file.names[i],1,16), ".png", sep = ""))
png(file = mypath, width = 1000, height = 600)
mytitle = paste("Linear_Model_of", substr(file.names[i],1,16))
plot(newAngle$X,newAngle$yprime, main = mytitle, ylab ="Y-
    ↪ Coordinates", xlab = "X-Coordinates")
abline(coef = c(intercept,gradient))
dev.off()

theoreticalrad <- atan(gradient)
rad2deg <- function(rad) {(rad * 180) / (pi)}
theoreticaldeg3 <- rad2deg(theoreticalrad)
theodeg <- 90-theoreticaldeg3#adjust based on slope

error <- abs(((trueangle1-theodeg)/trueangle1)*100)

output <- cbind(dataname, method, points, gradient, intercept,
    ↪ rsquared, trueangle1, theoreticaldeg3,theodeg, error)
colnames(output) <- c("Data_Name","Method","Points","Gradient","
    ↪ Y-Intercept","R-Squared_Value","True_Angle","Theoretical_
    ↪ Degrees","Calculated_Degrees","Percent_Error")

setwd("C:/Users/Jefferys/Desktop/Thesis_Jefferys/Bullet_Angle_
    ↪ Photos/LRN/90_Degrees/Results/Data_Files")
write.csv(output,file = paste(substr(file.names[i],1,16),"_Data.
    ↪ csv"),row.names=FALSE)
setwd("C:/Users/Jefferys/Desktop/Thesis_Jefferys/Bullet_Angle_
    ↪ Photos/LRN/90_Degrees/Results/")
```

```
}
setwd("C:/Users/Jefferys/Desktop/Thesis_Jefferys/Bullet_Angle_
    ↪ Photos/LRN/90_Degrees/Results/Data_Files")
fileNames <- Sys.glob("*.csv")
tables <- lapply(fileNames, read.csv, header = TRUE)
combined.df <- do.call(rbind, tables)
write.csv(combined.df, "C:/Users/Jefferys/Desktop/Thesis_Jefferys/
    ↪ Bullet_Angle_Photos/LRN/90_Degrees/Results/Combined_Data_90_
    ↪ 2.csv")#adjust
###end script for file set up bullet deformation
```

FMJ bullets

```
######################beginning of bullet angle main combination
    ↪ script
setwd("C:/Users/Jefferys/Desktop/Thesis_Jefferys/Bullet_Angle_
    ↪ Photos/FMJ/New")

dat1 <- read.csv("Combined_Data_90.csv")
dat2 <- read.csv("Combined_Data_75.csv")
dat3 <- read.csv("Combined_Data_60.csv")
dat4 <- read.csv("Combined_Data_50.csv")
dat5 <- read.csv("Combined_Data_45.csv")

complete.dat <- rbind(dat1,dat2,dat3,dat4,dat5)
complete.dat <- complete.dat[ order(complete.dat[,8]), ]
write.csv(complete.dat, file="Combined_Data_All.csv")

#####begin linear model
linmod <- read.table("Combined_Data_All.csv",header=TRUE, sep=",",
    ↪  stringsAsFactors=FALSE)

bullet <- lm(True_Angle ~ Calculated_Degrees, data = linmod)
#bullet <- lm(linmod$Calculated_Degrees ~ linmod$True_Angle, data
    ↪ = linmod)
summary(bullet)
```

```
# range <- range(linmod$Calculated_Degrees)
# xrange <-seq(28.8,90.8,0.1)

normrsq<- c()
gradients1 <- c()
intercepts1 <- c()
adjrsq <- c()
pvalueint <- c()
pvaluevar <- c()
sterrorint <- c()
sterrorvar <- c()

gradients1 <- as.numeric(bullet$coefficients[2])
intercepts1 <- as.numeric(bullet$coefficients[1])
normrsq <- summary(bullet)$r.squared
adjrsq <- summary(bullet)$adj.r.squared
pvalueint <- summary(bullet)$coefficients[1,4]
pvaluevar <- summary(bullet)$coefficients[2,4]
sterrorint <- summary(bullet)$coefficients[1,2]
sterrorvar <- summary(bullet)$coefficients[2,2]
tvalueint <- summary(bullet)$coefficients[1,3]
tvaluevar <- summary(bullet)$coefficients[2,3]

output.df1 <-cbind(intercepts1,sterrorint,tvalueint,pvalueint,
  ↪ normrsq)
output.df2 <- cbind(gradients1,sterrorvar,tvaluevar,pvaluevar,
  ↪ adjrsq)

final.output <- rbind(output.df1,output.df2)
write.csv(final.output,file ="Combined_Data_BulletAngle_All_2.csv"
  ↪ ,row.names=FALSE)

#stats
res = residuals(bullet)
pred = fitted(bullet)
```

```
png(file = "Residual_Combined_BulletAngle.png", width = 1000,
    ↪ height = 600)
plot(pred,res,xlab = "Fitted_Value", ylab= "Residuals",main ="
    ↪ Residuals_versus_Fitted_Values_for_Combined_Full_Metal_
    ↪ Jacket_Bullet_Angle_Data")
abline(h=0,lty=2)
#qqnorm(res)
dev.off()

res = sort(residuals(bullet))
n = length(res)
z = qnorm(ppoints(n))
png(file = "QQplot_Combined_BulletAngle.png", width = 1000, height
    ↪  = 600)
plot(z,res,xlab="Theoretical_Quantiles",ylab="Sample_Quantiles",
    ↪ main="Normal_Q-Q_Plot_for_Combined_Full_Metal_Jacket_Bullet_
    ↪ Angle_Data")
abline(lm(res~z))
dev.off()

res = residuals(bullet)
mx = mean(res)
##Note the residual standard error
#not the simple SD of the residuals
#is the estimate of the SD of the residuals
#residual SE is the best estimate for sigma (estimating SD of
    ↪ residuals)
sx = summary(bullet)$sigma
png(file = "Histogram_Combined_BulletAngle.png", width = 1000,
    ↪ height = 600)
hist(res, prob=TRUE, xlab="Residuals",main="Histogram_of_Combined_
    ↪ Full_Metal_Jacket_Bullet_Angle_Data", ylim=c(0,0.060))
x = seq(min(res)-0.5*sx, max(res)+0.5*sx, length=200)
y = dnorm(x, mx, sx)
lines(x,y,lty=2)
box()
```

```
dev.off()

##############################
png(file = "Linear_Model_of_Combined_LRN.png" , width = 1000,
    ↪ height = 600)
plot(True_Angle ~ Calculated_Degrees, data = linmod, main="Linear_
    ↪ Model_of_Combined_Full_Metal_Jacket_Bullet_Angle_Data_with_
    ↪ Confidence_and_Prediction_Intervals", ylab="True_Angle",xlab
    ↪ ="Measured_Angle")
new.Calculated_Degrees = seq(min(linmod$Calculated_Degrees),max(
    ↪ linmod$Calculated_Degrees),length = 450)
True_Angle.pred.ci = predict(bullet,data.frame(Calculated_Degrees
    ↪ =new.Calculated_Degrees),interval = "confidence")
True_Angle.pred.pred = predict(bullet,data.frame(Calculated_
    ↪ Degrees = new.Calculated_Degrees),interval = "prediction")
lines(new.Calculated_Degrees, True_Angle.pred.ci[, 1])
lines(new.Calculated_Degrees,True_Angle.pred.ci[, 2] , lty = 2,
    ↪ col = "blue")
lines( new.Calculated_Degrees, True_Angle.pred.ci[, 3] , lty = 2,
    ↪ col = "blue")
lines( new.Calculated_Degrees,True_Angle.pred.pred[, 2], lty = 2,
    ↪ col = "red")
lines( new.Calculated_Degrees, True_Angle.pred.pred[, 3] , lty =
    ↪ 2, col = "red")

testval <- c(55,75,90)
l.colors <- c("green","orange","darkgrey")
for (i in 1:length(testval)){
  abline(v=testval[i],col=l.colors[i])
  new.Calculated_Degrees <- c(testval[i])

  xmax1 <- predict(bullet,data.frame(Calculated_Degrees =new.
      ↪ Calculated_Degrees),interval="prediction")
  xg1 <- c(0,testval[i])
  yg1 <- c(xmax1[,3],xmax1[,3])
  lines(xg1,yg1,lty=2,col=l.colors[i])
```

```
  xg2 <- c(0,testval[i])
  yg2 <- c(xmax1[,2],xmax1[,2])
  lines(xg2,yg2,lty=2,col=l.colors[i])
  xg3 <- c(0,testval[i])
  yg3 <- c(xmax1[,1],xmax1[,1])
  lines(xg3,yg3,lty=1,col=l.colors[i])
  xmax2 <- predict(bullet,data.frame(Calculated_Degrees =new.
    ↪ Calculated_Degrees),interval="confidence")
  xg4 <- c(0,testval[i])
  yg4 <- c(xmax2[,2],xmax2[,2])
  lines(xg4,yg4,lty=3,col=l.colors[i])
  xg5 <- c(0,testval[i])
  yg5 <- c(xmax2[,3],xmax2[,3])
  lines(xg5,yg5,lty=3,col=l.colors[i])
}
dev.off()

###prediction intervals
#prediction code for model
outers<-c()
inners<-c()
angle <- c()
TA.pred.fit <- c()
TA.pred.lwr <- c()
TA.pred.upr <- c()
angle.pred.fit <- c()
angle.pred.lwr <- c()
angle.pred.upr <- c()

for (jj in 45:90) {

  angle[jj] <- jj
  CD <- c(jj)
  TA.pred = predict(bullet, data.frame(Calculated_Degrees=CD),
    ↪ interval = "confidence")
```

```
  angle.pred = predict(bullet, data.frame(Calculated_Degrees=CD),
     ↪ interval = "prediction")
  TA.pred.fit[jj] <- angle.pred[1]
  TA.pred.lwr[jj] <- angle.pred[2]
  TA.pred.upr[jj] <- angle.pred[3]
  angle.pred.fit[jj] <- TA.pred[1]
  angle.pred.lwr[jj] <- TA.pred[2]
  angle.pred.upr[jj] <- TA.pred[3]
  inners <-cbind(angle[jj], TA.pred.fit[jj], TA.pred.lwr[jj], TA.
     ↪ pred.upr[jj],
                 angle.pred.fit[jj], angle.pred.lwr[jj],angle.pred
                    ↪ .upr[jj])
  outers<-rbind(outers, inners)
}

outers<- data.frame(outers)
write.csv(outers,file = "Combined_BulletAngle_Outers.csv",row.
   ↪ names=FALSE)

outer.cols <-c("Angle","Pred.fit","Pred.lower","Pred.upper","CI.
   ↪ fit","CI.lower","CI.upper")
colnames(outers)<-outer.cols

old.output <- output
output <- outers

ymin<-min(output$Angle)
ymax<-max(output$Angle)

mypath <- file.path("C:/Users/Jefferys/Desktop/Thesis_Jefferys/
   ↪ Bullet_Angle_Photos/FMJ/New/",paste("Combined_BulletAngle_
   ↪ Prediction", ".png", sep = ""))
png(file = mypath, width = 1000, height = 600)
#mytitle = paste("Prediction Values for Combined bulletspat Data")
plot(output$Angle,output$CI.fit , type="l", ylim=c(30,105), xlim=c
   ↪ (ymin,ymax), ylab="True_Angle", xlab="Measured_Angle", main=
```

```
   ↪ "Prediction Values Resulting from Measured Values for
   ↪ Combined Full Metal Jacket Bullet Angle Data with Confidence
   ↪ Intervals")
lines( output$Angle,output$CI.upper , lty=2, col="blue")
lines(output$Angle,output$CI.lower , lty=2, col="blue")
#for (i in 1:length(output$Angle)){
#  x.temp <- c(output$Angle[i],output$Angle[i])
#  y.temp <- c(output$CI.lower[i],output$CI.upper[i])
#  lines(x.temp,y.temp)
#}
lines(output$Angle,output$Pred.upper , lty=2, col="red")
lines(output$Angle,output$Pred.lower , lty=2, col="red")
#for (i in 1:length(output$Angle)){
#  x.temp <- c(output$Angle[i],output$Angle[i])
#  y.temp <- c(output$Pred.lower[i],output$Pred.upper[i])
#  lines(x.temp,y.temp)
#}
abline(v=45, col="grey")
abline(v=50, col="grey")
abline(v=60, col="grey")
abline(v=75, col="grey")
abline(v=90, col="grey")
dev.off()

############################################################

#start of methods loop
method_type <- as.character(unique(linmod$Method))

#Methods
i <- "VV"
#for(i in method_type){
  linmodsub <- subset(linmod, linmod$Method == as.character(i))

  bullet1 <- lm(True_Angle ~ Calculated_Degrees, data = linmodsub)
  summary(bullet1)
```

```
normrsq<- c()
gradients1 <- c()
intercepts1 <- c()
adjrsq <- c()
pvalueint <- c()
pvaluevar <- c()
sterrorint <- c()
sterrorvar <- c()
tvalueint <- c()
tvaluevar <- c()

gradients1[i] <- as.numeric(bullet1$coefficients[2])
intercepts1[i] <- as.numeric(bullet1$coefficients[1])
normrsq[i] <- summary(bullet1)$r.squared
adjrsq[i] <- summary(bullet1)$adj.r.squared
pvalueint[i] <- summary(bullet1)$coefficients[1,4]
pvaluevar[i] <- summary(bullet1)$coefficients[2,4]
sterrorint[i] <- summary(bullet1)$coefficients[1,2]
sterrorvar[i] <- summary(bullet1)$coefficients[2,2]
tvalueint[i] <- summary(bullet1)$coefficients[1,3]
tvaluevar[i] <- summary(bullet1)$coefficients[2,3]

output.df1 <-cbind(intercepts1[i],sterrorint[i],tvalueint[i],
   ↪ pvalueint[i],normrsq[i])
output.df2 <- cbind(gradients1[i],sterrorvar[i],tvaluevar[i],
   ↪ pvaluevar[i],adjrsq[i])

finaloutput2 <- rbind(output.df1,output.df2)
write.csv(finaloutput2,file = paste(as.character(i),"_Data_Model
   ↪ .csv"),row.names=FALSE)

# plot(linmodsub$Calculated_Degrees,linmodsub$True_Angle, main =
   ↪  mytitle, ylab ="Calculated Angle", xlab = "True Angle")
# abline(coef = c(intercepts[i],gradients[i]))
# abline(coef = c(0,1))
```

```
# dev.off()

################residuals plots
res = residuals(bullet1)
pred = fitted(bullet1)
mypath <- file.path("C:/Users/Jefferys/Desktop/Thesis_Jefferys/
    ↪ Bullet_Angle_Photos/FMJ/New/",paste("Residuals_for", as.
    ↪ character(i), ".png", sep = ""))
png(file = mypath, width = 1000, height = 600)
mytitle = paste("Residuals_versus_Fitted_Values_for_Method", as.
    ↪ character(i),"Using_Full_Metal_Jacket_Bullets")
plot(pred,res,xlab = "Fitted_Value", ylab= "Residuals",main=
    ↪ mytitle)
abline(h=0,lty=2)
dev.off()

# ################################QQplot
res = sort(residuals(bullet1))
n = length(res)
z = qnorm(ppoints(n))
mypath <- file.path("C:/Users/Jefferys/Desktop/Thesis_Jefferys/
    ↪ Bullet_Angle_Photos/FMJ/New/",paste("Normal_QQ_Plot", as.
    ↪ character(i), ".png", sep = ""))
png(file = mypath, width = 1000, height = 600)
mytitle = paste("Normal_Q-Q_Plot_for_Method", as.character(i),"
    ↪ Using_Full_Metal_Jacket_Bullets")
plot(z,res,xlab="Theoretical_Quantiles",ylab="Sample_Quantiles",
    ↪  main=mytitle)
abline(lm(res~z))
dev.off()

# ############################Histogram
res = residuals(bullet1)
mx = mean(res)
##Note the residual standard error
#not the simple SD of the residuals
```

```
#is the estimate of the SD of the residuals
#residual SE is the best estimate for sigma (estimating SD of
    ↪ residuals)
sx = summary(bullet1)$sigma
mypath <- file.path("C:/Users/Jefferys/Desktop/Thesis_Jefferys/
    ↪ Bullet_Angle_Photos/FMJ/New/",paste("Histogram_for", as.
    ↪ character(i), ".png", sep = ""))
png(file = mypath, width = 1000, height = 600)
mytitle = paste("Histogram_for_Method", as.character(i), "Using_
    ↪ Full_Metal_Jacket_Bullets")
hist(res, prob=TRUE, xlab="Residuals",main=mytitle,ylim=c
    ↪ (0,0.080))
x = seq(min(res)-0.5*sx, max(res)+0.5*sx, length=200)
y = dnorm(x, mx, sx)
lines(x,y,lty=2)
box()
dev.off()

######################Confidence Plot
mypath <- file.path("C:/Users/Jefferys/Desktop/Thesis_Jefferys/
    ↪ Bullet_Angle_Photos/FMJ/New/",paste("Linear_Model_of", as.
    ↪ character(i), ".png", sep = ""))
png(file = mypath, width = 1000, height = 600)
mytitle = paste("Linear_Model_of_Method", as.character(i), "
    ↪ Using_Full_Metal_Jacket_Bullets_with_Prediction_and_
    ↪ Confidence_Intervals")
plot(True_Angle ~ Calculated_Degrees, data = linmodsub, main=
    ↪ mytitle, ylab="True_Angle",xlab="Measured_Angle")
new.Calculated_Degrees = seq(min(linmodsub$Calculated_Degrees),
    ↪ max(linmodsub$Calculated_Degrees),length = 90)
True_Angle.pred.ci = predict(bullet1,data.frame(Calculated_
    ↪ Degrees =new.Calculated_Degrees),interval = "confidence")
True_Angle.pred.pred = predict(bullet1,data.frame(Calculated_
    ↪ Degrees = new.Calculated_Degrees),interval = "prediction")
lines(new.Calculated_Degrees, True_Angle.pred.ci[, 1])
```

```
lines(new.Calculated_Degrees,True_Angle.pred.ci[, 2] , lty = 2,
    ↪ col = "blue")
lines( new.Calculated_Degrees, True_Angle.pred.ci[, 3] , lty =
    ↪ 2, col = "blue")
lines( new.Calculated_Degrees,True_Angle.pred.pred[, 2], lty =
    ↪ 2, col = "red")
lines( new.Calculated_Degrees, True_Angle.pred.pred[, 3] , lty =
    ↪  2, col = "red")

testval <- c(60,75,90)
l.colors <- c("green","orange","darkgrey")
for (i in 1:length(testval)){
  abline(v=testval[i],col=l.colors[i])
  new.Calculated_Degrees <- c(testval[i])

  xmax1 <- predict(bullet1,data.frame(Calculated_Degrees =new.
      ↪ Calculated_Degrees),interval="prediction")
  xg1 <- c(0,testval[i])
  yg1 <- c(xmax1[,3],xmax1[,3])
  lines(xg1,yg1,lty=2,col=l.colors[i])
  xg2 <- c(0,testval[i])
  yg2 <- c(xmax1[,2],xmax1[,2])
  lines(xg2,yg2,lty=2,col=l.colors[i])
  xg3 <- c(0,testval[i])
  yg3 <- c(xmax1[,1],xmax1[,1])
  lines(xg3,yg3,lty=1,col=l.colors[i])
  xmax2 <- predict(bullet1,data.frame(Calculated_Degrees =new.
      ↪ Calculated_Degrees),interval="confidence")
  xg4 <- c(0,testval[i])
  yg4 <- c(xmax2[,2],xmax2[,2])
  lines(xg4,yg4,lty=3,col=l.colors[i])
  xg5 <- c(0,testval[i])
  yg5 <- c(xmax2[,3],xmax2[,3])
  lines(xg5,yg5,lty=3,col=l.colors[i])
}
dev.off()
```

```
##################################


#i needs changed to method being used
i <- "VV"

#####################prediction
outers<-c()
inners<-c()
angle <- c()
TA.pred.fit <- c()
TA.pred.lwr <- c()
TA.pred.upr <- c()
angle.pred.fit <- c()
angle.pred.lwr <- c()
angle.pred.upr <- c()

for (jj in 45:90) {

  angle[jj] <- jj
  CD <- c(jj)
  TA.pred = predict(bullet1, data.frame(Calculated_Degrees=CD),
    ↪ interval = "confidence")
  angle.pred = predict(bullet1, data.frame(Calculated_Degrees=CD
    ↪ ), interval = "prediction")
  TA.pred.fit[jj] <- angle.pred[1]
  TA.pred.lwr[jj] <- angle.pred[2]
  TA.pred.upr[jj] <- angle.pred[3]
  angle.pred.fit[jj] <- TA.pred[1]
  angle.pred.lwr[jj] <- TA.pred[2]
  angle.pred.upr[jj] <- TA.pred[3]
  inners <-cbind(angle[jj], TA.pred.fit[jj], TA.pred.lwr[jj], TA
    ↪ .pred.upr[jj],
                 angle.pred.fit[jj], angle.pred.lwr[jj],angle.
                   ↪ pred.upr[jj])
  outers<-rbind(outers, inners)
```

```
}

outers<- data.frame(outers)
write.csv(outers,file = paste(as.character(i),"_Outers.csv"),row
    ↪ .names=FALSE)

outer.cols <-c("Angle","Pred.fit","Pred.lower","Pred.upper","CI.
    ↪ fit","CI.lower","CI.upper")
colnames(outers)<-outer.cols

old.output <- output
output <- outers

ymin<-min(output$Angle)
ymax<-max(output$Angle)

mypath <- file.path("C:/Users/Jefferys/Desktop/Thesis_Jefferys/
    ↪ Bullet_Angle_Photos/FMJ/New/",paste("Final_Model_of", as.
    ↪ character(i), ".png", sep = ""))
png(file = mypath, width = 1000, height = 600)
mytitle = paste("Prediction_Values_Resulting_from_Measured_
    ↪ Values_for_Method", as.character(i), "Using_Full_Metal_
    ↪ Jacket_Bullets_with_Confidence_Intervals")
plot(output$Angle,output$CI.fit , type="l", ylim=c(30,105), xlim=
    ↪ c(ymin,ymax), ylab="True_Angle", xlab="Measured_Angle",
    ↪ main=mytitle)
lines( output$Angle,output$CI.upper , lty=2, col="blue")
lines(output$Angle,output$CI.lower , lty=2, col="blue")
#for (i in 1:length(output$Angle)){
#  x.temp <- c(output$Angle[i],output$Angle[i])
#  y.temp <- c(output$CI.lower[i],output$CI.upper[i])
#  lines(x.temp,y.temp)
#}
lines(output$Angle,output$Pred.upper , lty=2, col="red")
lines(output$Angle,output$Pred.lower , lty=2, col="red")
#for (i in 1:length(output$Angle)){
```

```
  #   x.temp <- c(output$Angle[i], output$Angle[i])
  #   y.temp <- c(output$Pred.lower[i], output$Pred.upper[i])
  #   lines(x.temp, y.temp)
  #}
  abline(v=45, col="grey")
  abline(v=50, col="grey")
  abline(v=60, col="grey")
  abline(v=75, col="grey")
  abline(v=90, col="grey")
  dev.off()
#}
###############Beginning of Points Models
   ↪ ##################################
#Points
point_type2 <- as.character(unique(linmod$Points))

i <- "15"
#for(i in point_type2){
  linmodsub <- subset(linmod, linmod$Points == as.character(i))

  bullet2 <- lm(True_Angle ~ Calculated_Degrees, data = linmodsub)

  normrsq<- c()
  gradients1 <- c()
  intercepts1 <- c()
  adjrsq <- c()
  pvalueint <- c()
  pvaluevar <- c()
  sterrorint <- c()
  sterrorvar <- c()

  gradients1[i] <- as.numeric(bullet2$coefficients[2])
  intercepts1[i] <- as.numeric(bullet2$coefficients[1])
  normrsq[i] <- summary(bullet2)$r.squared
  adjrsq[i] <- summary(bullet2)$adj.r.squared
  pvalueint[i] <- summary(bullet2)$coefficients[1,4]
```

```
pvaluevar[i] <- summary(bullet2)$coefficients[2,4]
sterrorint[i] <- summary(bullet2)$coefficients[1,2]
sterrorvar[i] <- summary(bullet2)$coefficients[2,2]
tvalueint[i] <- summary(bullet2)$coefficients[1,3]
tvaluevar[i] <- summary(bullet2)$coefficients[2,3]

output.df1 <-cbind(intercepts1[i],sterrorint[i],tvalueint[i],
    ↪ pvalueint[i],normrsq[i])
output.df2 <- cbind(gradients1[i],sterrorvar[i],tvaluevar[i],
    ↪ pvaluevar[i],adjrsq[i])

finaloutput2 <- rbind(output.df1,output.df2)
write.csv(finaloutput2,file = paste(as.character(i),"_Data_Model
    ↪ .csv"),row.names=FALSE)

mytitle = paste("Linear Model of Combined Data Points",as.
    ↪ character(i))
plot(linmodsub$Calculated_Degrees,linmodsub$True_Angle, main =
    ↪ mytitle, ylab ="Calculated Angle", xlab = "True Angle")
abline(coef = c(intercepts2[i],gradients2[i]))

#residuals plots
res = residuals(bullet2)
pred = fitted(bullet2)
mypath <- file.path("C:/Users/Jefferys/Desktop/Thesis_Jefferys/
    ↪ Bullet Angle Photos/FMJ/New/",paste("Residuals for", as.
    ↪ character(i), ".png", sep = ""))
png(file = mypath, width = 1000, height = 600)
mytitle = paste("Residuals versus Fitted Values for", as.
    ↪ character(i),"Point Method Using Full Metal Jacket Bullets
    ↪ ")
plot(pred,res,xlab = "Fitted Value", ylab= "Residuals",main=
    ↪ mytitle)
abline(h=0,lty=2)
dev.off()
```

```
##qqplot
res = sort(residuals(bullet2))
n = length(res)
z = qnorm(ppoints(n))
mypath <- file.path("C:/Users/Jefferys/Desktop/Thesis_Jefferys/
    ↪ Bullet_Angle_Photos/FMJ/New/",paste("Normal_QQ_Plot", as.
    ↪ character(i), ".png", sep = ""))
png(file = mypath, width = 1000, height = 600)
mytitle = paste("Normal_Q-Q_Plot_for", as.character(i), "Point_
    ↪ Method_Using_Full_Metal_Jacket_Bullets")
plot(z,res,xlab="Theoretical_Quantiles",ylab="Sample_Quantiles",
    ↪  main=mytitle)
abline(lm(res~z))
dev.off()

#histogram
res = residuals(bullet2)
mx = mean(res)
##Note the residual standard error
#not the simple SD of the residuals
#is the estimate of the SD of the residuals
#residual SE is the best estimate for sigma (estimating SD of
    ↪ residuals)
sx = summary(bullet2)$sigma
mypath <- file.path("C:/Users/Jefferys/Desktop/Thesis_Jefferys/
    ↪ Bullet_Angle_Photos/FMJ/New/",paste("Histogram_for", as.
    ↪ character(i), ".png", sep = ""))
png(file = mypath, width = 1000, height = 600)
mytitle = paste("Histogram_for", as.character(i), "Point_Method_
    ↪ Using_Full_Metal_Jacket_Bullets")
hist(res, prob=TRUE, xlab="Residuals",main=mytitle, ylim=c
    ↪ (0,0.070))
x = seq(min(res)-0.5*sx, max(res)+0.5*sx, length=200)
y = dnorm(x, mx, sx)
lines(x,y,lty=2)
box()
```

```
dev.off()

mypath <- file.path("C:/Users/Jefferys/Desktop/Thesis_Jefferys/
    ↪ Bullet_Angle_Photos/FMJ/New/",paste("Linear_Model_of", as.
    ↪ character(i), ".png", sep = ""))
png(file = mypath, width = 1000, height = 600)
mytitle = paste("Linear_Model_of", as.character(i), "Point_
    ↪ Method_Using_Full_Metal_Jacket_Bullets_with_Prediction_and
    ↪ _Confidence_Intervals")
plot(True_Angle ~ Calculated_Degrees, data = linmodsub, main=
    ↪ mytitle, xlab="Measured_Angle",ylab="True_Angle")
new.Calculated_Degrees = seq(min(linmodsub$Calculated_Degrees),
    ↪ max(linmodsub$Calculated_Degrees),length = 90)
True_Angle.pred.ci = predict(bullet2,data.frame(Calculated_
    ↪ Degrees =new.Calculated_Degrees),interval = "confidence")
True_Angle.pred.pred = predict(bullet2,data.frame(Calculated_
    ↪ Degrees = new.Calculated_Degrees),interval = "prediction")
lines(new.Calculated_Degrees, True_Angle.pred.ci[, 1])
lines(new.Calculated_Degrees,True_Angle.pred.ci[, 2] , lty = 2,
    ↪ col = "blue")
lines( new.Calculated_Degrees, True_Angle.pred.ci[, 3] , lty =
    ↪ 2, col = "blue")
lines( new.Calculated_Degrees,True_Angle.pred.pred[, 2], lty =
    ↪ 2, col = "red")
lines( new.Calculated_Degrees, True_Angle.pred.pred[, 3] , lty =
    ↪  2, col = "red")

testval <- c(55,75,90)
l.colors <- c("green","orange","darkgrey")
for (i in 1:length(testval)){
  abline(v=testval[i],col=l.colors[i])
  new.Calculated_Degrees <- c(testval[i])

  xmax1 <- predict(bullet2,data.frame(Calculated_Degrees =new.
      ↪ Calculated_Degrees),interval="prediction")
  xg1 <- c(0,testval[i])
```

```
  yg1 <- c(xmax1[,3],xmax1[,3])
  lines(xg1,yg1,lty=2,col=l.colors[i])
  xg2 <- c(0,testval[i])
  yg2 <- c(xmax1[,2],xmax1[,2])
  lines(xg2,yg2,lty=2,col=l.colors[i])
  xg3 <- c(0,testval[i])
  yg3 <- c(xmax1[,1],xmax1[,1])
  lines(xg3,yg3,lty=1,col=l.colors[i])
  xmax2 <- predict(bullet2,data.frame(Calculated_Degrees =new.
    ↪ Calculated_Degrees),interval="confidence")
  xg4 <- c(0,testval[i])
  yg4 <- c(xmax2[,2],xmax2[,2])
  lines(xg4,yg4,lty=3,col=l.colors[i])
  xg5 <- c(0,testval[i])
  yg5 <- c(xmax2[,3],xmax2[,3])
  lines(xg5,yg5,lty=3,col=l.colors[i])
}
dev.off()

#i needs changed to points being used
i <- "15"

outers<-c()
inners<-c()
angle <- c()
TA.pred.fit <- c()
TA.pred.lwr <- c()
TA.pred.upr <- c()
angle.pred.fit <- c()
angle.pred.lwr <- c()
angle.pred.upr <- c()

for (jj in 45:90) {

  angle[jj] <- jj
  CD <- c(jj)
```

```
  TA.pred = predict(bullet2, data.frame(Calculated_Degrees=CD),
    ↪ interval = "confidence")
  angle.pred = predict(bullet2, data.frame(Calculated_Degrees=CD
    ↪ ), interval = "prediction")
  TA.pred.fit[jj] <- angle.pred[1]
  TA.pred.lwr[jj] <- angle.pred[2]
  TA.pred.upr[jj] <- angle.pred[3]
  angle.pred.fit[jj] <- TA.pred[1]
  angle.pred.lwr[jj] <- TA.pred[2]
  angle.pred.upr[jj] <- TA.pred[3]
  inners <-cbind(angle[jj], TA.pred.fit[jj], TA.pred.lwr[jj], TA
    ↪ .pred.upr[jj],
                 angle.pred.fit[jj], angle.pred.lwr[jj],angle.
                   ↪ pred.upr[jj])
  outers<-rbind(outers, inners)
}

outers<- data.frame(outers)
write.csv(outers,file = paste(as.character(i),"_Outers.csv"),row
  ↪ .names=FALSE)

outer.cols <-c("Angle","Pred.fit","Pred.lower","Pred.upper","CI.
  ↪ fit","CI.lower","CI.upper")
colnames(outers)<-outer.cols

old.output <- output
output <- outers

ymin<-min(output$Angle)
ymax<-max(output$Angle)

mypath <- file.path("C:/Users/Jefferys/Desktop/Thesis_Jefferys/
  ↪ Bullet_Angle_Photos/FMJ/New/",paste("Final_Model_of", as.
  ↪ character(i), ".png", sep = ""))
png(file = mypath, width = 1000, height = 600)
```

```
  mytitle = paste("Prediction Values Resulting from Measured
    ↪ Values for",as.character(i),"Point Method Using Full Metal
    ↪ Jacket Bullets with Confidence Intervals")
  plot(output$Angle,output$CI.fit, type="l", ylim=c(30,105), xlim=
    ↪ c(ymin,ymax), ylab="True Angle", xlab="Measured Angle",
    ↪ main=mytitle)
  lines( output$Angle,output$CI.upper , lty=2, col="blue")
  lines(output$Angle,output$CI.lower , lty=2, col="blue")
  #for (i in 1:length(output$Angle)){
  #  x.temp <- c(output$Angle[i],output$Angle[i])
  #  y.temp <- c(output$CI.lower[i],output$CI.upper[i])
  #  lines(x.temp,y.temp)
  #}
  lines(output$Angle,output$Pred.upper , lty=2, col="red")
  lines(output$Angle,output$Pred.lower , lty=2, col="red")
  #for (i in 1:length(output$Angle)){
  #  x.temp <- c(output$Angle[i],output$Angle[i])
  #  y.temp <- c(output$Pred.lower[i],output$Pred.upper[i])
  #  lines(x.temp,y.temp)
  #}
  abline(v=45, col="grey")
  abline(v=50, col="grey")
  abline(v=60, col="grey")
  abline(v=75, col="grey")
  abline(v=90, col="grey")
  dev.off()
#}
##########################end of bullet angle script
```

LRN bullets

```
#######################beginning of bullet angle main combination
  ↪ script
setwd("C:/Users/Jefferys/Desktop/Thesis_Jefferys/Bullet Angle
  ↪ Photos/LRN/Combined")

dat1 <- read.csv("Combined_Data_90.csv")
```

```
dat2 <- read.csv("Combined_Data_75.csv")
dat3 <- read.csv("Combined_Data_60.csv")
dat4 <- read.csv("Combined_Data_50.csv")
dat5 <- read.csv("Combined_Data_45.csv")

complete.dat <- rbind(dat1,dat2,dat3,dat4,dat5)
complete.dat <- complete.dat[ order(complete.dat[,8]), ]
write.csv(complete.dat, file="Combined_Data_All.csv")

#####begin linear model
linmod <- read.table("Combined_Data_All.csv",header=TRUE, sep=",",
   ↪  stringsAsFactors=FALSE)

bullet <- lm(True_Angle ~ Calculated_Degrees, data = linmod)
#bullet <- lm(linmod$Calculated_Degrees ~ linmod$True_Angle, data
   ↪ = linmod)
summary(bullet)

# range <- range(linmod$Calculated_Degrees)
# xrange <-seq(28.8,90.8,0.1)

normrsq<- c()
gradients1 <- c()
intercepts1 <- c()
adjrsq <- c()
pvalueint <- c()
pvaluevar <- c()
sterrorint <- c()
sterrorvar <- c()

gradients1 <- as.numeric(bullet$coefficients[2])
intercepts1 <- as.numeric(bullet$coefficients[1])
normrsq <- summary(bullet)$r.squared
adjrsq <- summary(bullet)$adj.r.squared
pvalueint <- summary(bullet)$coefficients[1,4]
pvaluevar <- summary(bullet)$coefficients[2,4]
```

```
sterrorint <- summary(bullet)$coefficients[1,2]
sterrorvar <- summary(bullet)$coefficients[2,2]
tvalueint <- summary(bullet)$coefficients[1,3]
tvaluevar <- summary(bullet)$coefficients[2,3]

output.df1 <-cbind(intercepts1,sterrorint,tvalueint,pvalueint,
    ↪ normrsq)
output.df2 <- cbind(gradients1,sterrorvar,tvaluevar,pvaluevar,
    ↪ adjrsq)

final.output <- rbind(output.df1,output.df2)
write.csv(final.output,file ="Combined_Data_BulletAngle_All.csv",
    ↪ row.names=FALSE)

#stats
res = residuals(bullet)
pred = fitted(bullet)
png(file = "Residual_Combined_BulletAngle.png", width = 1000,
    ↪ height = 600)
plot(pred,res,xlab = "Fitted Value", ylab= "Residuals",main ="
    ↪ Residuals versus Fitted Values for Combined Lead Round Nose
    ↪ Bullet Angle Data")
abline(h=0,lty=2)
#qqnorm(res)
dev.off()

res = sort(residuals(bullet))
n = length(res)
z = qnorm(ppoints(n))
png(file = "QQplot_Combined_BulletAngle.png", width = 1000, height
    ↪  = 600)
plot(z,res,xlab="Theoretical Quantiles",ylab="Sample Quantiles",
    ↪ main="Normal Q-Q Plot for Combined Lead Round Nose Bullet
    ↪ Angle Data")
abline(lm(res~z))
dev.off()
```

```
res = residuals(bullet)
mx = mean(res)
##Note the residual standard error
#not the simple SD of the residuals
#is the estimate of the SD of the residuals
#residual SE is the best estimate for sigma (estimating SD of
   ↪ residuals)
sx = summary(bullet)$sigma
png(file = "Histogram_Combined_BulletAngle.png", width = 1000,
   ↪ height = 600)
hist(res, prob=TRUE, xlab="Residuals",main="Histogram_of_Combined_
   ↪ Lead_Round_Nose_Bullet_Angle_Data", ylim=c(0,0.040))
x = seq(min(res)-0.5*sx, max(res)+0.5*sx, length=200)
y = dnorm(x, mx, sx)
lines(x,y,lty=2)
box()
dev.off()

png(file = "Linear_Model_of_Combined_LRN.png" , width = 1000,
   ↪ height = 600)
plot(True_Angle ~ Calculated_Degrees, data = linmod, main="Linear_
   ↪ Model_of_Combined_Lead_Round_Nose_Bullet_Angle_Data_with_
   ↪ Confidence_and_Prediction_Intervals", xlab="Measured_Angle",
   ↪ ylab="True_Angle")
new.Calculated_Degrees = seq(min(linmod$Calculated_Degrees),max(
   ↪ linmod$Calculated_Degrees),length = 450)
True_Angle.pred.ci = predict(bullet,data.frame(Calculated_Degrees
   ↪ =new.Calculated_Degrees),interval = "confidence")
True_Angle.pred.pred = predict(bullet,data.frame(Calculated_
   ↪ Degrees = new.Calculated_Degrees),interval = "prediction")
lines(new.Calculated_Degrees, True_Angle.pred.ci[, 1])
lines(new.Calculated_Degrees,True_Angle.pred.ci[, 2] , lty = 2,
   ↪ col = "blue")
lines( new.Calculated_Degrees, True_Angle.pred.ci[, 3] , lty = 2,
   ↪ col = "blue")
```

```
lines( new.Calculated_Degrees,True_Angle.pred.pred[, 2], lty = 2,
    ↪ col = "red")
lines( new.Calculated_Degrees, True_Angle.pred.pred[, 3] , lty =
    ↪ 2, col = "red")

testval <- c(45,75,90)
l.colors <- c("green","orange","darkgrey")
for (i in 1:length(testval)){
  abline(v=testval[i],col=l.colors[i])
  new.Calculated_Degrees <- c(testval[i])

  xmax1 <- predict(bullet,data.frame(Calculated_Degrees =new.
      ↪ Calculated_Degrees),interval="prediction")
  xg1 <- c(0,testval[i])
  yg1 <- c(xmax1[,3],xmax1[,3])
  lines(xg1,yg1,lty=2,col=l.colors[i])
  xg2 <- c(0,testval[i])
  yg2 <- c(xmax1[,2],xmax1[,2])
  lines(xg2,yg2,lty=2,col=l.colors[i])
  xg3 <- c(0,testval[i])
  yg3 <- c(xmax1[,1],xmax1[,1])
  lines(xg3,yg3,lty=1,col=l.colors[i])
  xmax2 <- predict(bullet,data.frame(Calculated_Degrees =new.
      ↪ Calculated_Degrees),interval="confidence")
  xg4 <- c(0,testval[i])
  yg4 <- c(xmax2[,2],xmax2[,2])
  lines(xg4,yg4,lty=3,col=l.colors[i])
  xg5 <- c(0,testval[i])
  yg5 <- c(xmax2[,3],xmax2[,3])
  lines(xg5,yg5,lty=3,col=l.colors[i])
}
dev.off()


###prediction intervals
#prediction code for model
```

```
outers<-c()
inners<-c()
angle <- c()
TA.pred.fit <- c()
TA.pred.lwr <- c()
TA.pred.upr <- c()
angle.pred.fit <- c()
angle.pred.lwr <- c()
angle.pred.upr <- c()

for (jj in 45:90) {

  angle[jj] <- jj
  CD <- c(jj)
  TA.pred = predict(bullet, data.frame(Calculated_Degrees=CD),
     ↪ interval = "confidence")
  angle.pred = predict(bullet, data.frame(Calculated_Degrees=CD),
     ↪ interval = "prediction")
  TA.pred.fit[jj] <- angle.pred[1]
  TA.pred.lwr[jj] <- angle.pred[2]
  TA.pred.upr[jj] <- angle.pred[3]
  angle.pred.fit[jj] <- TA.pred[1]
  angle.pred.lwr[jj] <- TA.pred[2]
  angle.pred.upr[jj] <- TA.pred[3]
  inners <-cbind(angle[jj], TA.pred.fit[jj], TA.pred.lwr[jj], TA.
     ↪ pred.upr[jj],
                 angle.pred.fit[jj], angle.pred.lwr[jj],angle.pred
                    ↪ .upr[jj])
  outers<-rbind(outers, inners)
}

outers<- data.frame(outers)
write.csv(outers,file = "Combined_BulletAngle_Outers.csv",row.
   ↪ names=FALSE)
```

```
outer.cols <-c("Angle","Pred.fit","Pred.lower","Pred.upper","CI.
    ↪ fit","CI.lower","CI.upper")
colnames(outers)<-outer.cols

old.output <- output
output <- outers

ymin<-min(output$Angle)
ymax<-max(output$Angle)

mypath <- file.path("C:/Users/Jefferys/Desktop/Thesis_Jefferys/
    ↪ Bullet_Angle_Photos/LRN/Combined/",paste("Combined_
    ↪ BulletAngle_Prediction", ".png", sep = ""))
png(file = mypath, width = 1000, height = 600)
#mytitle = paste("Prediction Values for Combined bulletspat Data")
plot(output$Angle , output$CI.fit , type="l", ylim=c(30,105), xlim=
    ↪ c(ymin,ymax), ylab="True_Angle", xlab="Measured_Angle", main
    ↪ ="Prediction_Values_Resulting_from_Measured_Values_for_
    ↪ Combined_Lead_Round_Nose_Bullet_Angle_Data_with_Confidence_
    ↪ Intervals")
lines( output$Angle,output$CI.upper , lty=2, col="blue")
lines(output$Angle,output$CI.lower , lty=2, col="blue")
#for (i in 1:length(output$Angle)){
#  x.temp <- c(output$Angle[i],output$Angle[i])
#  y.temp <- c(output$CI.lower[i],output$CI.upper[i])
#  lines(x.temp,y.temp)
#}
lines(output$Angle,output$Pred.upper , lty=2, col="red")
lines(output$Angle,output$Pred.lower , lty=2, col="red")
#for (i in 1:length(output$Angle)){
#  x.temp <- c(output$Angle[i],output$Angle[i])
#  y.temp <- c(output$Pred.lower[i],output$Pred.upper[i])
#  lines(x.temp,y.temp)
#}
abline(v=45, col="grey")
abline(v=50, col="grey")
```

```
abline(v=60, col="grey")
abline(v=75, col="grey")
abline(v=90, col="grey")
dev.off()

##########################################################

#start of methods loop
method_type <- as.character(unique(linmod$Method))

#Methods
i <- "AA" #can use this to do one at a time
#for(i in method_type){
  linmodsub <- subset(linmod, linmod$Method == as.character(i))

  bullet1 <- lm(True_Angle ~ Calculated_Degrees, data = linmodsub)
  summary(bullet1)

  normrsq<- c()
  gradients1 <- c()
  intercepts1 <- c()
  adjrsq <- c()
  pvalueint <- c()
  pvaluevar <- c()
  sterrorint <- c()
  sterrorvar <- c()
  tvalueint <- c()
  tvaluevar <- c()

  gradients1[i] <- as.numeric(bullet1$coefficients[2])
  intercepts1[i] <- as.numeric(bullet1$coefficients[1])
  normrsq[i] <- summary(bullet1)$r.squared
  adjrsq[i] <- summary(bullet1)$adj.r.squared
  pvalueint[i] <- summary(bullet1)$coefficients[1,4]
  pvaluevar[i] <- summary(bullet1)$coefficients[2,4]
  sterrorint[i] <- summary(bullet1)$coefficients[1,2]
```

```
sterrorvar[i] <- summary(bullet1)$coefficients[2,2]
tvalueint[i] <- summary(bullet1)$coefficients[1,3]
tvaluevar[i] <- summary(bullet1)$coefficients[2,3]

output.df1 <-cbind(intercepts1[i],sterrorint[i],tvalueint[i],
    ↪ pvalueint[i],normrsq[i])
output.df2 <- cbind(gradients1[i],sterrorvar[i],tvaluevar[i],
    ↪ pvaluevar[i],adjrsq[i])

finaloutput2 <- rbind(output.df1,output.df2)
write.csv(finaloutput2,file = paste(as.character(i),"_Data_Model
    ↪ .csv"),row.names=FALSE)

# plot(linmodsub$Calculated_Degrees,linmodsub$True_Angle, main =
    ↪  mytitle, ylab ="Calculated Angle", xlab = "True Angle")
# abline(coef = c(intercepts[i],gradients[i]))
# abline(coef = c(0,1))
# dev.off()

################residuals plots
res = residuals(bullet1)
pred = fitted(bullet1)
mypath <- file.path("C:/Users/Jefferys/Desktop/Thesis_Jefferys/
    ↪ Bullet_Angle_Photos/LRN/Combined/",paste("Residuals_for",
    ↪ as.character(i), ".png", sep = ""))
png(file = mypath, width = 1000, height = 600)
mytitle = paste("Residuals_versus_Fitted_Values_for_Method", as.
    ↪ character(i),"Using_Lead_Round_Nose_Bullets")
plot(pred,res,xlab = "Fitted_Value", ylab= "Residuals",main=
    ↪ mytitle)
abline(h=0,lty=2)
dev.off()

# ##################################QQplot
res = sort(residuals(bullet1))
n = length(res)
```

```
z = qnorm(ppoints(n))
mypath <- file.path("C:/Users/Jefferys/Desktop/Thesis_Jefferys/
    ↪ Bullet_Angle_Photos/LRN/Combined/",paste("Normal_QQ_Plot",
    ↪  as.character(i), ".png", sep = ""))
png(file = mypath, width = 1000, height = 600)
mytitle = paste("Normal_Q-Q_Plot_for_Method", as.character(i),"
    ↪ Using_Lead_Round_Nose_Bullets")
plot(z,res,xlab="Theoretical_Quantiles",ylab="Sample_Quantiles",
    ↪  main=mytitle)
abline(lm(res~z))
dev.off()

##########################Histogram
res = residuals(bullet1)
mx = mean(res)
##Note the residual standard error
#not the simple SD of the residuals
#is the estimate of the SD of the residuals
#residual SE is the best estimate for sigma (estimating SD of
    ↪ residuals)
sx = summary(bullet1)$sigma
mypath <- file.path("C:/Users/Jefferys/Desktop/Thesis_Jefferys/
    ↪ Bullet_Angle_Photos/LRN/Combined/",paste("Histogram_for",
    ↪ as.character(i), ".png", sep = ""))
png(file = mypath, width = 1000, height = 600)
mytitle = paste("Histogram_for_Method", as.character(i), "Using_
    ↪ Lead_Round_Nose_Bullets")
hist(res, prob=TRUE, xlab="Residuals",main=mytitle,ylim=c
    ↪ (0,0.04))
x = seq(min(res)-0.5*sx, max(res)+0.5*sx, length=200)
y = dnorm(x, mx, sx)
lines(x,y,lty=2)
box()
dev.off()

######################Confidence Plot
```

```
mypath <- file.path("C:/Users/Jefferys/Desktop/Thesis_Jefferys/
    ↪ Bullet_Angle_Photos/LRN/Combined/",paste("Linear_Model_of"
    ↪ , as.character(i), ".png", sep = ""))
png(file = mypath, width = 1000, height = 600)
mytitle = paste("Linear_Model_of_Method", as.character(i), "
    ↪ Using_Lead_Round_Nose_Bullets_with_Prediction_and_
    ↪ Confidence_Intervals")
plot(True_Angle ~ Calculated_Degrees, data = linmodsub, ylim=c
    ↪ (30,90),xlim=c(35,90), main=mytitle, xlab="Measured_Angle"
    ↪ ,ylab="True_Angle")
new.Calculated_Degrees = seq(min(linmodsub$Calculated_Degrees),
    ↪ max(linmodsub$Calculated_Degrees),length = 90)
True_Angle.pred.ci = predict(bullet1,data.frame(Calculated_
    ↪ Degrees =new.Calculated_Degrees),interval = "confidence")
True_Angle.pred.pred = predict(bullet1,data.frame(Calculated_
    ↪ Degrees = new.Calculated_Degrees),interval = "prediction")
lines(new.Calculated_Degrees, True_Angle.pred.ci[, 1])
lines(new.Calculated_Degrees,True_Angle.pred.ci[, 2] , lty = 2,
    ↪ col = "blue")
lines( new.Calculated_Degrees, True_Angle.pred.ci[, 3] , lty =
    ↪ 2, col = "blue")
lines( new.Calculated_Degrees,True_Angle.pred.pred[, 2], lty =
    ↪ 2, col = "red")
lines( new.Calculated_Degrees, True_Angle.pred.pred[, 3] , lty =
    ↪  2, col = "red")

testval <- c(45,75,90)
l.colors <- c("green","orange","darkgrey")
for (i in 1:length(testval)){
  abline(v=testval[i],col=l.colors[i])
  new.Calculated_Degrees <- c(testval[i])

  xmax1 <- predict(bullet1,data.frame(Calculated_Degrees =new.
      ↪ Calculated_Degrees),interval="prediction")
  xg1 <- c(0,testval[i])
  yg1 <- c(xmax1[,3],xmax1[,3])
```

```
  lines(xg1,yg1,lty=2,col=l.colors[i])
  xg2 <- c(0,testval[i])
  yg2 <- c(xmax1[,2],xmax1[,2])
  lines(xg2,yg2,lty=2,col=l.colors[i])
  xg3 <- c(0,testval[i])
  yg3 <- c(xmax1[,1],xmax1[,1])
  lines(xg3,yg3,lty=1,col=l.colors[i])
  xmax2 <- predict(bullet1,data.frame(Calculated_Degrees =new.
    ↪ Calculated_Degrees),interval="confidence")
  xg4 <- c(0,testval[i])
  yg4 <- c(xmax2[,2],xmax2[,2])
  lines(xg4,yg4,lty=3,col=l.colors[i])
  xg5 <- c(0,testval[i])
  yg5 <- c(xmax2[,3],xmax2[,3])
  lines(xg5,yg5,lty=3,col=l.colors[i])
}
dev.off()


#i gets changed in the above code
#it needs to be set again to the method being used
i <- "AA"

####################prediction
outers<-c()
inners<-c()
angle <- c()
TA.pred.fit <- c()
TA.pred.lwr <- c()
TA.pred.upr <- c()
angle.pred.fit <- c()
angle.pred.lwr <- c()
angle.pred.upr <- c()

for (jj in 45:90) {
```

```
  angle[jj] <- jj
  CD <- c(jj)
  TA.pred = predict(bullet1, data.frame(Calculated_Degrees=CD),
    ↪ interval = "confidence")
  angle.pred = predict(bullet1, data.frame(Calculated_Degrees=CD
    ↪ ), interval = "prediction")
  TA.pred.fit[jj] <- angle.pred[1]
  TA.pred.lwr[jj] <- angle.pred[2]
  TA.pred.upr[jj] <- angle.pred[3]
  angle.pred.fit[jj] <- TA.pred[1]
  angle.pred.lwr[jj] <- TA.pred[2]
  angle.pred.upr[jj] <- TA.pred[3]
  inners <-cbind(angle[jj], TA.pred.fit[jj], TA.pred.lwr[jj], TA
    ↪ .pred.upr[jj],
                 angle.pred.fit[jj], angle.pred.lwr[jj],angle.
                   ↪ pred.upr[jj])
  outers<-rbind(outers, inners)
}

outers<- data.frame(outers)
write.csv(outers,file = paste(as.character(i),"_Outers.csv"),row
  ↪ .names=FALSE)

outer.cols <-c("Angle","Pred.fit","Pred.lower","Pred.upper","CI.
  ↪ fit","CI.lower","CI.upper")
colnames(outers)<-outer.cols

old.output <- output
output <- outers

ymin<-min(output$Angle)
ymax<-max(output$Angle)

mypath <- file.path("C:/Users/Jefferys/Desktop/Thesis_Jefferys/
  ↪ Bullet_Angle_Photos/LRN/Combined/",paste("Final_Model_of",
  ↪  as.character(i), ".png", sep = ""))
```

```
  png(file = mypath, width = 1000, height = 600)
  mytitle = paste("Prediction Values Resulting from Measured
    ↪ Values for Method", as.character(i), "Using Lead Round
    ↪ Nose Bullets with Confidence Intervals")
  plot(output$Angle,output$CI.fit , type="l", ylim=c(ymin,ymax),
    ↪ ylab="True Angle", xlab="Measured Angle", main=mytitle)
  lines( output$Angle,output$CI.upper , lty=2, col="blue")
  lines(output$Angle,output$CI.lower , lty=2, col="blue")
  #for (i in 1:length(output$Angle)){
  #  x.temp <- c(output$Angle[i],output$Angle[i])
  #  y.temp <- c(output$CI.lower[i],output$CI.upper[i])
  #  lines(x.temp,y.temp)
  #}
  lines(output$Angle,output$Pred.upper , lty=2, col="red")
  lines(output$Angle,output$Pred.lower , lty=2, col="red")
  #for (i in 1:length(output$Angle)){
  #  x.temp <- c(output$Angle[i],output$Angle[i])
  #  y.temp <- c(output$Pred.lower[i],output$Pred.upper[i])
  #  lines(x.temp,y.temp)
  #}
  abline(v=45, col="grey")
  abline(v=50, col="grey")
  abline(v=60, col="grey")
  abline(v=75, col="grey")
  abline(v=90, col="grey")
  dev.off()
#}

###############Beginning of Points Models
   ↪ ##################################
#Points
point_type2 <- as.character(unique(linmod$Points))

i <- "15"
#for(i in point_type2){
  linmodsub <- subset(linmod, linmod$Points == as.character(i))
```

```
bullet2 <- lm(True_Angle ~ Calculated_Degrees, data = linmodsub)

normrsq<- c()
gradients1 <- c()
intercepts1 <- c()
adjrsq <- c()
pvalueint <- c()
pvaluevar <- c()
sterrorint <- c()
sterrorvar <- c()

gradients1[i] <- as.numeric(bullet2$coefficients[2])
intercepts1[i] <- as.numeric(bullet2$coefficients[1])
normrsq[i] <- summary(bullet2)$r.squared
adjrsq[i] <- summary(bullet2)$adj.r.squared
pvalueint[i] <- summary(bullet2)$coefficients[1,4]
pvaluevar[i] <- summary(bullet2)$coefficients[2,4]
sterrorint[i] <- summary(bullet2)$coefficients[1,2]
sterrorvar[i] <- summary(bullet2)$coefficients[2,2]
tvalueint[i] <- summary(bullet2)$coefficients[1,3]
tvaluevar[i] <- summary(bullet2)$coefficients[2,3]

output.df1 <-cbind(intercepts1[i],sterrorint[i],tvalueint[i],
   ↪ pvalueint[i],normrsq[i])
output.df2 <- cbind(gradients1[i],sterrorvar[i],tvaluevar[i],
   ↪ pvaluevar[i],adjrsq[i])

finaloutput2 <- rbind(output.df1,output.df2)
write.csv(finaloutput2,file = paste(as.character(i),"_Data_Model
   ↪ .csv"),row.names=FALSE)

# mytitle = paste("Linear Model of Combined Data Points",as.
   ↪ character(i))
# plot(linmodsub$Calculated_Degrees,linmodsub$True_Angle, main =
   ↪  mytitle, ylab ="Calculated Angle", xlab = "True Angle")
```

```
# abline(coef = c(intercepts2[i],gradients2[i]))
#residuals plots

res = residuals(bullet2)
pred = fitted(bullet2)
mypath <- file.path("C:/Users/Jefferys/Desktop/Thesis_Jefferys/
    ↪ Bullet_Angle_Photos/LRN/Combined",paste("Residuals_for",
    ↪ as.character(i), ".png", sep = ""))
png(file = mypath, width = 1000, height = 600)
mytitle = paste("Residuals_versus_Fitted_Values_for", as.
    ↪ character(i),"Point_Method_Using_Lead_Round_Nose_Bullets")
plot(pred,res,xlab = "Fitted_Value", ylab= "Residuals",main=
    ↪ mytitle)
abline(h=0,lty=2)
dev.off()

# res = residuals(bullet2)
# qqnorm(res)
# qqline(res)

##qqplot
res = sort(residuals(bullet2))
n = length(res)
z = qnorm(ppoints(n))
mypath <- file.path("C:/Users/Jefferys/Desktop/Thesis_Jefferys/
    ↪ Bullet_Angle_Photos/LRN/Combined",paste("Normal_QQ_Plot",
    ↪ as.character(i), ".png", sep = ""))
png(file = mypath, width = 1000, height = 600)
mytitle = paste("Normal_Q-Q_Plot_for", as.character(i), "Point_
    ↪ Method_Using_Lead_Round_Nose_Bullets")
plot(z,res,xlab="Theoretical_Quantiles",ylab="Sample_Quantiles",
    ↪  main=mytitle)
abline(lm(res~z))
dev.off()

#histogram
```

```
res = residuals(bullet2)
mx = mean(res)
##Note the residual standard error
#not the simple SD of the residuals
#is the estimate of the SD of the residuals
#residual SE is the best estimate for sigma (estimating SD of
    ↪ residuals)
sx = summary(bullet2)$sigma
mypath <- file.path("C:/Users/Jefferys/Desktop/Thesis_Jefferys/
    ↪ Bullet_Angle_Photos/LRN/Combined",paste("Histogram_for",
    ↪ as.character(i), ".png", sep = ""))
png(file = mypath, width = 1000, height = 600)
mytitle = paste("Histogram_for", as.character(i), "Point_Method_
    ↪ Using_Lead_Round_Nose_Bullets")
hist(res, prob=TRUE, xlab="Residuals",main=mytitle, ylim=c
    ↪ (0,0.04))
x = seq(min(res)-0.5*sx, max(res)+0.5*sx, length=200)
y = dnorm(x, mx, sx)
lines(x,y,lty=2)
box()
dev.off()



mypath <- file.path("C:/Users/Jefferys/Desktop/Thesis_Jefferys/
    ↪ Bullet_Angle_Photos/LRN/Combined",paste("Linear_Model_of",
    ↪  as.character(i), ".png", sep = ""))
png(file = mypath, width = 1000, height = 600)
mytitle = paste("Linear_Model_of", as.character(i), "Point_
    ↪ Method_Using_Lead_Round_Nose_Bullets_with_Prediction_and_
    ↪ Confidence_Intervals")
plot(True_Angle ~ Calculated_Degrees, data = linmodsub, main=
    ↪ mytitle, xlab="Measured_Angle",ylab="True_Angle")
new.Calculated_Degrees = seq(min(linmodsub$Calculated_Degrees),
    ↪ max(linmodsub$Calculated_Degrees),length = 90)
```

```
True_Angle.pred.ci = predict(bullet2,data.frame(Calculated_
    ↪ Degrees =new.Calculated_Degrees),interval = "confidence")
True_Angle.pred.pred = predict(bullet2,data.frame(Calculated_
    ↪ Degrees = new.Calculated_Degrees),interval = "prediction")
lines(new.Calculated_Degrees, True_Angle.pred.ci[, 1])
lines(new.Calculated_Degrees,True_Angle.pred.ci[, 2] , lty = 2,
    ↪ col = "blue")
lines( new.Calculated_Degrees, True_Angle.pred.ci[, 3] , lty =
    ↪ 2, col = "blue")
lines( new.Calculated_Degrees,True_Angle.pred.pred[, 2], lty =
    ↪ 2, col = "red")
lines( new.Calculated_Degrees, True_Angle.pred.pred[, 3] , lty =
    ↪  2, col = "red")

testval <- c(45,75,90)
l.colors <- c("green","orange","darkgrey")
for (i in 1:length(testval)){
  abline(v=testval[i],col=l.colors[i])
  new.Calculated_Degrees <- c(testval[i])

  xmax1 <- predict(bullet2,data.frame(Calculated_Degrees =new.
      ↪ Calculated_Degrees),interval="prediction")
  xg1 <- c(0,testval[i])
  yg1 <- c(xmax1[,3],xmax1[,3])
  lines(xg1,yg1,lty=2,col=l.colors[i])
  xg2 <- c(0,testval[i])
  yg2 <- c(xmax1[,2],xmax1[,2])
  lines(xg2,yg2,lty=2,col=l.colors[i])
  xg3 <- c(0,testval[i])
  yg3 <- c(xmax1[,1],xmax1[,1])
  lines(xg3,yg3,lty=1,col=l.colors[i])
  xmax2 <- predict(bullet2,data.frame(Calculated_Degrees =new.
      ↪ Calculated_Degrees),interval="confidence")
  xg4 <- c(0,testval[i])
  yg4 <- c(xmax2[,2],xmax2[,2])
  lines(xg4,yg4,lty=3,col=l.colors[i])
```

```
  xg5 <- c(0,testval[i])
  yg5 <- c(xmax2[,3],xmax2[,3])
  lines(xg5,yg5,lty=3,col=l.colors[i])
}
dev.off()

#change i to the points being used
i <- "15"

#########outers
outers<-c()
inners<-c()
angle <- c()
TA.pred.fit <- c()
TA.pred.lwr <- c()
TA.pred.upr <- c()
angle.pred.fit <- c()
angle.pred.lwr <- c()
angle.pred.upr <- c()

for (jj in 45:90) {

  angle[jj] <- jj
  CD <- c(jj)
  TA.pred = predict(bullet2, data.frame(Calculated_Degrees=CD),
    ↪ interval = "confidence")
  angle.pred = predict(bullet2, data.frame(Calculated_Degrees=CD
    ↪ ), interval = "prediction")
  TA.pred.fit[jj] <- angle.pred[1]
  TA.pred.lwr[jj] <- angle.pred[2]
  TA.pred.upr[jj] <- angle.pred[3]
  angle.pred.fit[jj] <- TA.pred[1]
  angle.pred.lwr[jj] <- TA.pred[2]
  angle.pred.upr[jj] <- TA.pred[3]
  inners <-cbind(angle[jj], TA.pred.fit[jj], TA.pred.lwr[jj], TA
    ↪ .pred.upr[jj],
```

```
                    angle.pred.fit[jj], angle.pred.lwr[jj],angle.
                        ↪ pred.upr[jj])
  outers<-rbind(outers, inners)
}

outers<- data.frame(outers)
write.csv(outers,file = paste(as.character(i),"_Outers.csv"),row
    ↪ .names=FALSE)

outer.cols <-c("Angle","Pred.fit","Pred.lower","Pred.upper","CI.
    ↪ fit","CI.lower","CI.upper")
colnames(outers)<-outer.cols

old.output <- output
output <- outers

ymin<-min(output$Angle)
ymax<-max(output$Angle)

mypath <- file.path("C:/Users/Jefferys/Desktop/Thesis_Jefferys/
    ↪ Bullet_Angle_Photos/LRN/Combined",paste("Final_Model_of",
    ↪ as.character(i), ".png", sep = ""))
png(file = mypath, width = 1000, height = 600)
mytitle = paste("Prediction_Values_Resulting_from_Measured_
    ↪ Values_for", as.character(i), "Point_Method_Using_Lead_
    ↪ Round_Nose_Bullets_with_Confidence_Intervals")
plot(output$Angle,output$CI.fit, type="l", ylim=c(ymin,ymax),
    ↪ ylab="True_Angle", xlab="Measured_Angle", main=mytitle)
lines( output$Angle,output$CI.upper , lty=2, col="blue")
lines(output$Angle,output$CI.lower , lty=2, col="blue")
#for (i in 1:length(output$Angle)){
#  x.temp <- c(output$Angle[i],output$Angle[i])
#  y.temp <- c(output$CI.lower[i],output$CI.upper[i])
#  lines(x.temp,y.temp)
#}
lines(output$Angle,output$Pred.upper , lty=2, col="red")
```

```
  lines(output$Angle,output$Pred.lower , lty=2, col="red")
  #for (i in 1:length(output$Angle)){
  #  x.temp <- c(output$Angle[i],output$Angle[i])
  #  y.temp <- c(output$Pred.lower[i],output$Pred.upper[i])
  #  lines(x.temp,y.temp)
  #}
  abline(v=45, col="grey")
  abline(v=50, col="grey")
  abline(v=60, col="grey")
  abline(v=75, col="grey")
  abline(v=90, col="grey")
  dev.off()
#}
##########################end of bullet angle script
```

8.3 Script for multiple linear regression

```
###begin script for MLR
library(lattice)
library(graphics)
library(scatterplot3d)
library(fields)

setwd("C:/Users/Jefferys/Desktop/Thesis_Jefferys/Final_Data/FMJ")

linmod <- read.table("Complete_Data.csv",header=TRUE, sep=",",
    ↪ stringsAsFactors=FALSE)

mult <- lm(True_Angle ~ X_Patch*Minor, data = linmod)
summary(mult)

####Contour plot
pa.seq <- seq(-400, 2000, 10)
mi.seq <- seq(2400, 3600, 10)

len.pa.seq <- length(pa.seq)
```

```
len.mi.seq <- length(mi.seq)

outputPred <- matrix(,nrow=len.pa.seq, ncol=len.mi.seq)

xx <- 1
yy <- 1

for (pa in pa.seq){
  for (mi  in mi.seq){
    out <- predict(mult,data.frame(X_Patch=pa, Minor=mi),interval=
      ↪ "prediction")
    #cat(out[1])
    outputPred[xx,yy] <- out[3]#####add in 1, 2, 3 for fit,lower,
      ↪ upper intervals
    yy <- yy+1
  }
  yy <- 1
  xx<-xx+1
}

####change names in code for lower, upper, and fitted
png(file = "ContourFMJUpper.png", width = 600, height = 600)
image.plot(outputPred, axes=F, ylab="Minor",xlab="X_Patch")
contour(outputPred, add = TRUE)
title(main="Upper Predictions Using X_Patch and Minor for Full
  ↪ Metal Jacket Bullets")
xat<-seq(0,1,length.out = 7)
yat <-seq(0,1,length.out = 5)
x.labels<- c(-400,0,400,800,1200,1600,2000)
y.labels <- c(2400,2700,3000, 3300, 3600)
axis(side=1, at=xat, labels = x.labels)
axis(side=2, at=yat, labels = y.labels)
dev.off()

#single prediction to check plots
```

```
out <- predict(mult,data.frame(True_Angle = 70),interval="
    ↪ prediction")
out2 <- predict(mult,data.frame(X_Patch=0, Minor=3300),interval="
    ↪ prediction")
out3 <- predict(mult,data.frame(X_Patch=400, Minor=3100),interval=
    ↪ "prediction")
out4 <- predict(mult,data.frame(X_Patch=1300, Minor=2400),interval
    ↪ ="prediction")
out5 <- predict(mult,data.frame(X_Patch=1900, Minor=3300),interval
    ↪ ="prediction")
#end of contour

normrsq<- c()
gradients1 <- c()
intercepts1 <- c()
adjrsq <- c()
pvalueint <- c()
pvaluevar <- c()
sterrorint <- c()
sterrorvar <- c()
intercepts2 <-c()
intercepts3 <- c()
pvaluevar2 <-c()
pvaluevar3 <-c()
tvaluevar2 <- c()
tvaluevar3 <- c()
sterrorvar2 <- c()
sterrorvar3 <- c()

gradients1 <- as.numeric(mult$coefficients[2])
intercepts1 <- as.numeric(mult$coefficients[1])
intercepts2 <-as.numeric(mult$coefficients[3])
intercepts3 <- as.numeric(mult$coefficients[4])

normrsq <- summary(mult)$r.squared
adjrsq <- summary(mult)$adj.r.squared
```

```
pvalueint <- summary(mult)$coefficients[1,4]
pvaluevar <- summary(mult)$coefficients[2,4]
pvaluevar2 <-summary(mult)$coefficients[3,4]
pvaluevar3 <-summary(mult)$coefficients[4,4]

sterrorint <- summary(mult)$coefficients[1,2]
sterrorvar <- summary(mult)$coefficients[2,2]
sterrorvar2 <- summary(mult)$coefficients[3,2]
sterrorvar3 <- summary(mult)$coefficients[4,2]

tvalueint <- summary(mult)$coefficients[1,3]
tvaluevar <- summary(mult)$coefficients[2,3]
tvaluevar2 <- summary(mult)$coefficients[3,3]
tvaluevar3 <- summary(mult)$coefficients[4,3]

output.df1 <-cbind(intercepts1,sterrorint,tvalueint,pvalueint,
   ↪ normrsq)
output.df2 <- cbind(gradients1,sterrorvar,tvaluevar,pvaluevar,
   ↪ adjrsq)
output.df3 <- cbind(intercepts2,sterrorvar2,tvaluevar2,pvaluevar2,
   ↪ normrsq)
output.df4 <- cbind(intercepts3,sterrorvar3,tvaluevar3,pvaluevar3,
   ↪ adjrsq)

final.output <- rbind(output.df1,output.df2,output.df3,output.df4)
write.csv(final.output,file="Combined_Data_MLRFMJbullets_All.csv"
   ↪ ,row.names=FALSE)

#plot of residuals
res = residuals(mult)
pred = fitted(mult)
png(file = "Residual_Combined_MLRFMJ.png", width = 1000, height =
   ↪ 600)
```

```
plot(pred,res,xlab = "Fitted Value", ylab= "Residuals",main ="
    ↪ Residuals versus Fitted Values using X Patch x Minor for
    ↪ Full Metal Jacket Bullet Data")
abline(h=0,lty=2)
dev.off()

#qqplot
res = sort(residuals(mult))
n = length(res)
z = qnorm(ppoints(n))
png(file = "QQplot Combined MLRFMJ.png", width = 1000, height =
    ↪ 600)
plot(z,res,xlab="Theoretical Quantiles",ylab="Sample Quantiles",
    ↪ main="Normal Q-Q Plot using X Patch x Minor for Full Metal
    ↪ Jacket Bullet Data")
abline(lm(res~z))
dev.off()

#histogram
res = residuals(mult)
mx = mean(res)
sx = summary(mult)$sigma
png(file = "Histogram Combined MLRFMJ.png", width = 1000, height =
    ↪  600)
hist(res, prob=TRUE, xlab="Residuals",main="Histogram of X Patch x
    ↪ Minor for Full Metal Jacket Bullet Data")
x = seq(min(res)-0.5*sx, max(res)+0.5*sx, length=200)
y = dnorm(x, mx, sx)
lines(x,y,lty=2)
box()
dev.off()

#3D plot
png(file = "Scatterplot3d.png", width = 1000, height = 600)
par(mai=c(1.2,1.2,2,1.8))#bottom, left, top, right
linmod$pcolor[linmod$True Angle==90] <- "red"
```

```
linmod$pcolor[linmod$True_Angle==75] <- "blue"
linmod$pcolor[linmod$True_Angle==60] <- "darkgreen"
linmod$pcolor[linmod$True_Angle==50] <- "purple"
linmod$pcolor[linmod$True_Angle==45] <- "black"
with(linmod, {
  scatterplot3d(linmod$Minor, linmod$X_Patch, linmod$True_Angle,
                pch=16,
                highlight.3d=FALSE,
                type="h",
                main="3D Scatter Plot of Minor, X_Patch, and True
                    ↪ Angle with Vertical Lines",color=pcolor,xlab
                    ↪ ="Minor",zlab="True Angle",ylab="X_Patch")
  legend("topleft", inset=c(.0025,-0.0050),       # location and
     ↪ inset
         bty="n", cex=1,,                  # suppress legend box,
            ↪ shrink text 50%
         title="Angles",
         c("45", "50", "60","75","90"), fill=c("black","red","blue
            ↪ ","darkgreen","purple"))
})
dev.off()

#xy plot
png(file = "XYplotFMJ.png", width = 1000, height = 600)
par(mai=c(1.2,1.2,1.2,1.8))#bottom, left, top, right
xyplot(linmod$Minor~linmod$X_Patch,grid=TRUE, group = linmod$True_
   ↪ Angle,main="XY Plot of X_Patch and Minor for Full Metal
   ↪ Jacket Bullet Data", pch=15, xlab="X_Patch",ylab="Minor",
       auto.key=list(space="right", columns=1,title="Angles",
                     points=TRUE,
                     type = c("p", "smooth"),pch=16, lwd = 4))
dev.off()

####Regular linear model Plots
png(file = "Xpatchplot.png", width = 1000, height = 600)
```

```
plot(X_Patch ~ True_Angle, data = linmod,xlab="True Angle",main="
    ↪ Scatterplot of X_Patch versus True_Angle for Full Metal
    ↪ Jacket Bullet Data")
dev.off()
png(file = "MinorPlot.png", width = 1000, height = 600)
plot(Minor ~ True_Angle , data = linmod,xlab="True Angle",main="
    ↪ Scatterplot of Minor versus True_Angle for Full Metal Jacket
    ↪ Bullet Data")
dev.off()
###end of MLR script

#begin extension script for testing and training
#library(s20x)
library(lattice)
library(graphics)

set.seed(123)

setwd("C:/Users/Jefferys/Desktop/Thesis_Jefferys/Final_Data/FMJ")

linmod <- read.table("Complete_Data.csv",header=TRUE, sep=",",
    ↪ stringsAsFactors=FALSE)

outer<-c()

for (j in 1:5000){
  ## 90% of the sample size
  smp_size <- floor(0.8 * nrow(linmod))

  ## set the seed to make your partition reproductible

  train_ind <- sample(seq_len(nrow(linmod)), size = smp_size)

  train <- linmod[train_ind, ]
  test <- linmod[-train_ind, ]
```

```
  mult <- lm(True_Angle ~ Minor*X_Patch, data = train)

  inner<-c()
  angle.p <- c()
  angle.t <- c()
  angle.p.l <- c()
  angle.p.u <- c()

  for (i in 1:length(test$Minor)){
    out <- predict(mult,data.frame(X_Patch=as.numeric(test$X_Patch
      ↪ [i]), Minor=as.numeric(test$Minor[i])),interval="
      ↪ prediction")
    #cat(out[1])
    angle.p[i] <- out[1]
    angle.p.l[i] <- out[2]
    angle.p.u[i] <- out[3]
    angle.t[i] <- as.numeric(test$True_Angle[i])
  }

  inner <- cbind(angle.p,angle.t,angle.p.l,angle.p.u)

  outer <-rbind(outer,inner)

}

outer.df <-data.frame(outer)

#generate the plot
png(file = "xyplottesttrain.png", width = 800, height = 600)
xyplot(outer.df$angle.p~outer.df$angle.t, jitter.x = T, pch=".",
   ↪ main="Measured Values Resulting from Test and Training Sets
   ↪ using Minor and X_Patch\n (1000 Iterations , 20% Testing , 80%
   ↪ Training)",xlab="True Angle",ylab="Measured Angle")
dev.off()
#end testing and training script
```

8.4 Script for principal component analysis

FMJ bullets

```
###begin FMJ PCA script

library(devtools)
install_github("ggbiplot", "vqv")

library(ggbiplot)
library(caret)
library(scatterplot3d)
library(hexbin)

setwd("C:/Users/Jefferys/Desktop/Thesis_Jefferys/All_PCA/FMJ")

filer <- read.csv("C:/Users/Jefferys/Desktop/Thesis_Jefferys/All_
    ↪ PCA/FMJ/FMJ_Data_FS.csv")

all.dat <- cbind(filer,PC)
write.csv(all.dat, file="C:/Users/Jefferys/Desktop/Thesis_Jefferys/
    ↪ All_PCA/FMJ/All_Data.csv", row.names = FALSE)

##########################

filer$True_Angle <- as.factor(filer$True_Angle)
log.var <- filer[, 4:9]
ir.angle <- filer[, 2]
trans <- preProcess(log.var, method=c("BoxCox", "center", "scale")
    ↪ )
PC <- predict(trans, log.var)
ir.pca_2 <- prcomp(PC, center = FALSE)

#prints the standard deviations and rotations
print(ir.pca_2$sdev)
stdpc <- ir.pca_2$sdev
rotpc <- ir.pca_2$rotation
```

```
data.all <- rbind(stdpc,rotpc)
write.csv(data.all, file="C:/Users/Jefferys/Desktop/Thesis_
    ↪ Jefferys/All_PCA/FMJ/Data_All_RotationsSD.csv")

###Proportion of Variance
s <- summary(ir.pca_2, scale = TRUE)

proppc <- s$importance[2, ]
cumlativepc <- s$importance[3, ]

data.all2 <- rbind(proppc,cumlativepc)
write.csv(data.all2, file="C:/Users/Jefferys/Desktop/Thesis_
    ↪ Jefferys/All_PCA/FMJ/Data_All_Proportion.csv")

###Scree plot for PCs
png(file = "ScreePlotFMJ.png", width = 1000, height = 600)
plot(PC, type = "l",ylim=c(0,4),main="Scree_Plot_for_Full_Metal_
    ↪ Jacket_Bullet_Data")
dev.off()

#Plot of 1 and 2
g <- ggbiplot(ir.pca_2,choices = c(1,2), obs.scale = 1, var.scale
    ↪ = 1,
              groups = ir.angle, ellipse = TRUE,
              circle = FALSE, ellipse.prob = 0.95)
g <- g + scale_color_discrete(name = '')
g <- g + theme(legend.direction = 'horizontal',
               legend.position = 'top')
g <- g + ggtitle("Biplot_of_Full_Metal_Jacket_Bullet_Data_(PC1_and
    ↪ _PC2)")
png(file = "BiplotFMJ1_2.png", width = 1000, height = 667)
print(g)
dev.off()

#Plot of 1 and 3
```

```
g <- ggbiplot(ir.pca_2,choices = c(3,4), obs.scale = 1, var.scale
    ↪ = 1,
                groups = ir.angle, ellipse = TRUE,
                circle = FALSE, ellipse.prob = 0.95)
g <- g + scale_color_discrete(name = '')
g <- g + theme(legend.direction = 'horizontal',
                legend.position = 'top')
g <- g + ggtitle("Biplot of Full Metal Jacket Data (PC3 and PC4)")
png(file = "BiplotFMJ3_4.png", width = 1000, height = 632)
print(g)
dev.off()

##########################################
ninety.mean <- apply(filer[filer$True_Angle=="90",4:9], 2, mean)
ninety.cov <- cov(filer[filer$True_Angle=="90",4:9])

seventyfive.mean <- apply(filer[filer$True_Angle=="75",4:9], 2,
    ↪ mean)
seventyfive.cov <- cov(filer[filer$True_Angle=="75",4:9])

sixty.mean <- apply(filer[filer$True_Angle=="60",4:9], 2, mean)
sixty.cov <- cov(filer[filer$True_Angle=="60",4:9])

fifty.mean <- apply(filer[filer$True_Angle=="50",4:9], 2, mean)
fifty.cov <- cov(filer[filer$True_Angle=="50",4:9])

fourtyfive.mean <- apply(filer[filer$True_Angle=="45",4:9], 2,
    ↪ mean)
fourtyfive.cov <- cov(filer[filer$True_Angle=="45",4:9])

#Make new random data based on the calculated biometry info. each
    ↪ species
#The MASS package allows for the calculation of correlated/
    ↪ covarying random
#numbers using this information.
require(MASS)
```

```
set.seed(1)

new.90 <- c()
new.75 <- c()
new.60 <- c()
new.50 <- c()
new.45 <- c()

n <- 20000
new.90 <- mvrnorm(n, ninety.mean, ninety.cov)
new.75 <- mvrnorm(n, seventyfive.mean, seventyfive.cov)
new.60 <- mvrnorm(n, sixty.mean, sixty.cov)
new.50 <- mvrnorm(n, fifty.mean, fifty.cov)
new.45 <- mvrnorm(n, fourtyfive.mean, fourtyfive.cov)

combine.data <- rbind(new.90,new.75,new.60,new.50,new.45)

# combine <- preProcess(combine.data, method=c("BoxCox", "center",
  ↪ "scale"))
# PC1 <- predict(combine, combine.data)
# ir.pca_2 <- prcomp(PC1, center = FALSE)
# pred.combine <-predict(ir.pca_2,combine.data)

###############
filer$True_Angle <- as.factor(filer$True_Angle)
log.var2 <- combine.data[, 1:6]
trans <- preProcess(log.var2, method=c("BoxCox", "center", "scale"
  ↪ ))
PC1 <- predict(trans, log.var2)
ir.pca_23 <- prcomp(PC1, center = FALSE)

pred.combine <-predict(ir.pca_23)
pred.90 <- pred.combine[1:20000,1:6]
pred.75 <- pred.combine[20001:40000,1:6]
pred.60 <- pred.combine[40001:60000,1:6]
pred.50 <- pred.combine[60001:80000,1:6]
```

```
pred.45 <- pred.combine[80001:100000,1:6]
##########Coefficients Plot
require(ggplot2)

#PC1 AND PC2
theta <- seq(0,2*pi,length.out = 100)
circle <- data.frame(x = cos(theta), y = sin(theta))
p <- ggplot(circle,aes(x,y)) + geom_path()

loadings <- data.frame(ir.pca_2$rotation,
                       .names = row.names(ir.pca_2$rotation))
p <- p + ggtitle("Coefficients of Variables for Full Metal Jacket
    ↪ Bullet Data (PC1 and PC2)")
p <- p + geom_text(data=loadings,
              mapping=aes(x = PC1, y = PC2, label = .names, colour
                  ↪  = .names)) +
  coord_fixed(ratio=1) +
  labs(x = "PC1", y = "PC2")
png(file = "CoefficientFMJ1_2.png", width = 700, height = 600)
par(mai=c(1.2,0.5,1.2,0.5))#bottom, left, top, right
print(p)
dev.off()
#PC1 AND PC3
theta <- seq(0,2*pi,length.out = 100)
circle <- data.frame(x = cos(theta), y = sin(theta))
p <- ggplot(circle,aes(x,y)) + geom_path()

loadings <- data.frame(ir.pca_2$rotation,
                       .names = row.names(ir.pca_2$rotation))
p <- p + ggtitle("Coefficients of Variables for Full Metal Jacket
    ↪ Bullet Data (PC1 and PC3)")
p <- p + geom_text(data=loadings,
                   mapping=aes(x = PC1, y = PC3, label = .names,
                       ↪ colour = .names)) +
  coord_fixed(ratio=1) +
  labs(x = "PC1", y = "PC3")
```

```
png(file = "CoefficientFMJ1_3.png", width = 700, height = 600)
par(mai=c(1.2,0.5,1.2,0.5))#bottom, left, top, right
print(p)
dev.off()

####Projected Plots
filer$True_Angle <-as.numeric(filer$True_Angle)

SPP <- filer$True_Angle
COLOR <- c("blue","darkorange4","darkgreen","red","purple")

##PC1 AND PC2
pc <- c(1,2)
#png(file = "PredictedonOriginal.png", width = 1000, height = 600)
par(mai=c(1.2,1.2,1.2,1.8))#bottom, left, top, right
plot(pred.45[,1],pred.45[,2] ,col="cornflowerblue", pch=1,xlim=c
    ↪ (-4,4),ylim=c(-2,2), ylab="PC2 (15.3%)",xlab="PC1 (63.2%)")
points(pred.90[,1],pred.90[,2], col="plum", pch=1)
points(pred.75[,1],pred.75[,2], col="brown", pch=1)
points(pred.60[,1],pred.60[,2], col="green", pch=1)
points(pred.50[,1],pred.50[,2], col="darkorange", pch=1)
points(ir.pca_2$x[,1], ir.pca_2$x[,2],col=COLOR[SPP], pch=16)
title(main="Projected Predicted PCs (Test Set = 20000) and
    ↪ Original Data (Training Set = 10) using PC1 and PC2")
legend("topright", inset=c(-0.15,0),col=c("purple","plum","red","
    ↪ brown","darkgreen","green","darkorange4","darkorange","blue"
    ↪ ,"cornflowerblue"),xpd = TRUE, legend=c("Original 90","
    ↪ Predicted 90","Original 75","Predicted 75","Original 60","
    ↪ Predicted 60","Original 50","Predicted 50","Original 45","
    ↪ Predicted 45"), pch=c(16,1,16,1,16,1,16,1,16,1), title="
    ↪ Angles")
#dev.off()

#Recording the prediction values
PC_val <-ir.pca_2$x[,1]
PC_val2 <-ir.pca_2$x[,2]
```

```
PC1_90 <- pred.90[,1]
PC2_90 <- pred.90[,2]

PC1_75 <- pred.75[,1]
PC2_75 <- pred.75[,2]

PC1_60 <- pred.60[,1]
PC2_60 <- pred.60[,2]

PC1_50 <- pred.50[,1]
PC2_50 <- pred.50[,2]

PC1_45 <- pred.45[,1]
PC2_45 <- pred.45[,2]

outer <-cbind(PC_val,PC_val2,PC1_90,PC2_90,PC1_75,PC2_75,PC1_60,
    ↪ PC2_60,PC1_50,PC2_50,PC1_45,PC2_45)
write.csv(outer, file="C:/Users/Jefferys/Desktop/Thesis_Jefferys/
    ↪ All_PCA/FMJ/Outer_Data_1_2.csv")

# #Code Hexbin=========================
# plot(hexbin(pred.90[,1], pred.90[,2], xbins = 50, shape = 1,
#         xbnds = range(pred.90[,1]), ybnds = range(pred.90[,2]),
#         xlab = NULL, ylab = NULL, IDs = FALSE))
#
# points(pred.90[,1],pred.90[,2], col="plum", pch=1)

#PC1 AND PC3
pc <- c(1,2)
png(file = "PredictedonOriginal_1_3.png", width = 1000, height =
    ↪ 600)
par(mai=c(1.2,1.2,1.2,1.8))#bottom, left, top, right
plot(pred.45[,1],pred.45[,3] ,col="cornflowerblue", pch=1,xlim=c
    ↪ (-4,4),ylim=c(-2,2), ylab="PC2_(15.3%)",xlab="PC1_(63.2%)")
points(pred.90[,1],pred.90[,3], col="plum", pch=1)
```

```
points(pred.75[,1],pred.75[,3], col="brown", pch=1)
points(pred.60[,1],pred.60[,3], col="green", pch=1)
points(pred.50[,1],pred.50[,3], col="darkorange", pch=1)
points(ir.pca_2$x[,1], ir.pca_2$x[,3],col=COLOR[SPP], pch=16)
title(main="Projected Predicted PCs (Test Set = 20000) and
    ↪ Original Data (Training Set = 10) using PC1 and PC3")
legend("topright", inset=c(-0.15,0),col=c("purple","plum","red","
    ↪ brown","darkgreen","green","darkorange4","darkorange","blue"
    ↪ ,"cornflowerblue"),xpd = TRUE, legend=c("Original 90","
    ↪ Predicted 90","Original 75","Predicted 75","Original 60","
    ↪ Predicted 60","Original 50","Predicted 50","Original 45","
    ↪ Predicted 45"), pch=c(16,1,16,1,16,1,16,1,16), title="
    ↪ Angles")
dev.off()

#####################3D Plots
pc1.rot <- ir.pca_2$rotation[,1]
pc2.rot <- ir.pca_2$rotation[,2]
pc3.rot <- ir.pca_2$rotation[,3]

row.PC <- nrow(PC)
col.PC <- ncol(PC)
out.PC1 <- c()
out.PC2 <- c()
out.PC3 <- c()
inner.PC1 <- 0
inner.PC2 <- 0
inner.PC3 <- 0

i <- 1
j <- 1

for(i in 1:row.PC){
  for(j in 1:6){
    inner.PC1 <- inner.PC1+PC[i,j]*pc1.rot[j]
    inner.PC2 <- inner.PC2+PC[i,j]*pc2.rot[j]
```

```
    inner.PC3 <- inner.PC3+PC[i,j]*pc2.rot[j]
  }
  out.PC1[i] <- inner.PC1
  out.PC2[i] <- inner.PC2
  out.PC3[i] <- inner.PC3
  inner.PC1 <- 0
  inner.PC2 <- 0
  inner.PC3 <- 0
}
#3D plot
png(file = "Scatterplot3dFMJpca.png", width = 1000, height = 600)
par(mai=c(1.2,1.2,2,1.8))#bottom, left, top, right
filer$pcolor[filer$True_Angle==90] <- "plum"
filer$pcolor[filer$True_Angle==75] <- "brown"
filer$pcolor[filer$True_Angle==60] <- "green"
filer$pcolor[filer$True_Angle==50] <- "darkorange"
filer$pcolor[filer$True_Angle==45] <- "cornflowerblue"
with(filer, {
  scatterplot3d(out.PC1, out.PC2, out.PC3,
                pch=16,
                highlight.3d=FALSE,
                type="h",
                main="3D Scatter Plot for Full Metal Jacket
                    ↪ Bullets (PC1, PC2, PC3) with Vertical Lines"
                    ↪ ,color=pcolor,xlab="PC1 (63.2% variance
                    ↪ explained)",zlab="PC3 (12.0% variance
                    ↪ explained)",ylab="PC2 (15.3% variance
                    ↪ explained)")
  legend("topleft", inset=c(.0025,-0.0050),      # location and
    ↪ inset
         bty="n", cex=1,,              # suppress legend box,
           ↪ shrink text 50%
         title="Angles",
         c("45", "50", "60","75","90"), fill=c("cornflowerblue","
           ↪ darkorange","green","brown","plum"))
})
```

```
dev.off()
#end of script FMJ PCA
```

LRN bullets

```
#begin PCA LRN script
library(devtools)
library(ggbiplot)
library(caret)
library(scatterplot3d)

setwd("C:/Users/Jefferys/Desktop/Thesis_Jefferys/All_PCA/LRN")

filer <- read.csv("C:/Users/Jefferys/Desktop/Thesis_Jefferys/All_
    ↪ PCA/LRN/Complete_Data_LRN.csv")

filer$True_Angle <- as.factor(filer$True_Angle)
log.var <- filer[, 4:9]
ir.angle <- filer[, 2]
trans <- preProcess(log.var, method=c("BoxCox", "center", "scale")
    ↪ )
PC <- predict(trans, log.var)
ir.pca_2 <- prcomp(PC, center = FALSE)

summary(ir.pca_2)
print(ir.pca_2)

#Whole file
all.dat <- cbind(filer ,PC)
write.csv(all.dat, file="C:/Users/Jefferys/Desktop/Thesis_Jefferys/
    ↪ All_PCA/LRN/All_Data_LRN.csv", row.names = FALSE)

#prints the standard deviations and rotations
print(ir.pca_2$sdev)
stdpc <- ir.pca_2$sdev
rotpc <- ir.pca_2$rotation
```

```
data.all <- rbind(stdpc,rotpc)
write.csv(data.all, file="C:/Users/Jefferys/Desktop/Thesis_
    ↪ Jefferys/All_PCA/LRN/Data_All_RotationsSD.csv")

###Proportion of Variance
s <- summary(ir.pca_2, scale = TRUE)

proppc <- s$importance[2, ]
cumlativepc <- s$importance[3, ]

data.all2 <- rbind(proppc,cumlativepc)
write.csv(data.all2, file="C:/Users/Jefferys/Desktop/Thesis_
    ↪ Jefferys/All_PCA/LRN/Data_All_Proportion.csv")

###Scree plot for PCs
png(file = "ScreePlotLRN.png", width = 1000, height = 600)
plot(ir.pca_2, type = "l",ylim=c(0,2.5),main="Scree_Plot_for_Lead_
    ↪ Round_Nose_Bullet_Data", xlab="Eigenvalue")
dev.off()

#Plot of 1 and 2
g <- ggbiplot(ir.pca_2,choices = c(1,2), obs.scale = 1, var.scale
    ↪ = 1,
              groups = ir.angle, ellipse = TRUE,
              circle = FALSE, ellipse.prob = 0.95)
g <- g + scale_color_discrete(name = '')
g <- g + theme(legend.direction = 'horizontal',
               legend.position = 'top')
g <- g + ggtitle("Biplot_of_Lead_Round_Nose_Bullet_Data_(PC1_and_
    ↪ PC2)")
png(file = "BiplotLRN1_2.png", width = 1000, height = 1000)
print(g)
dev.off()

#Plot of 1 and 3
```

```
g <- ggbiplot(ir.pca_2,choices = c(3,4), obs.scale = 1, var.scale
  ↪ = 1,
              groups = ir.angle, ellipse = TRUE,
              circle = FALSE)
g <- g + scale_color_discrete(name = '')
g <- g + theme(legend.direction = 'horizontal',
               legend.position = 'top')
g <- g + ggtitle("Biplot of Lead Round Nose Bullet Data (PC3 and
  ↪ PC4)")
png(file = "BiplotLRN3_4.png", width = 1000, height = 705)
print(g)
dev.off()

#Plot of 1 and 3
g <- ggbiplot(ir.pca_2,choices = c(1,4), obs.scale = 1, var.scale
  ↪ = 1,
              groups = ir.angle, ellipse = TRUE,
              circle = FALSE)
g <- g + scale_color_discrete(name = '')
g <- g + theme(legend.direction = 'horizontal',
               legend.position = 'top')
g <- g + ggtitle("Biplot of Lead Round Nose Bullet Data (PC1 and
  ↪ PC4)")
png(file = "BiplotLRN1_4.png", width = 1000, height = 471)
print(g)
dev.off()

#Plot of 3 and 4
g <- ggbiplot(ir.pca_2,choices = c(3,4), obs.scale = 1, var.scale
  ↪ = 1,
              groups = ir.angle, ellipse = TRUE,
              circle = FALSE)
g <- g + scale_color_discrete(name = '')
g <- g + theme(legend.direction = 'horizontal',
               legend.position = 'top')
```

```
g <- g + ggtitle("Biplot of Lead Round Nose Bullet Data (PC3 and
    ↪ PC4)")
png(file = "BiplotLRN3_4.png", width = 1000, height = 705)
print(g)
dev.off()

########################################
###Create new data sets for each of the three species.
#Biometric values are based on the distributions of the original
    ↪ data means
#and the covariances between these parameters.
ninety.mean <- apply(filer[filer$True_Angle=="90",4:9], 2, mean)
ninety.cov <- cov(filer[filer$True_Angle=="90",4:9])

seventyfive.mean <- apply(filer[filer$True_Angle=="75",4:9], 2,
    ↪ mean)
seventyfive.cov <- cov(filer[filer$True_Angle=="75",4:9])

sixty.mean <- apply(filer[filer$True_Angle=="60",4:9], 2, mean)
sixty.cov <- cov(filer[filer$True_Angle=="60",4:9])

fifty.mean <- apply(filer[filer$True_Angle=="50",4:9], 2, mean)
fifty.cov <- cov(filer[filer$True_Angle=="50",4:9])

fourtyfive.mean <- apply(filer[filer$True_Angle=="45",4:9], 2,
    ↪ mean)
fourtyfive.cov <- cov(filer[filer$True_Angle=="45",4:9])

#Make new random data based on the calculated biometry info. each
    ↪ species
#The MASS package allows for the calculation of correlated/
    ↪ covarying random
#numbers using this information.
require(MASS)
set.seed(1)
```

```
new.90 <- c()
new.75 <- c()
new.60 <- c()
new.50 <- c()
new.45 <- c()

n <- 20000
new.90 <- mvrnorm(n, ninety.mean, ninety.cov)
new.75 <- mvrnorm(n, seventyfive.mean, seventyfive.cov)
new.60 <- mvrnorm(n, sixty.mean, sixty.cov)
new.50 <- mvrnorm(n, fifty.mean, fifty.cov)
new.45 <- mvrnorm(n, fourtyfive.mean, fourtyfive.cov)

combine.data <- rbind(new.90,new.75,new.60,new.50,new.45)

# combine <- preProcess(combine.data, method=c("BoxCox", "center",
  ↪ "scale"))
# PC1 <- predict(combine, combine.data)
# ir.pca_2 <- prcomp(PC1, center = FALSE)
# pred.combine <-predict(ir.pca_2,combine.data)

###############
filer$True_Angle <- as.factor(filer$True_Angle)
log.var2 <- combine.data[, 1:6]
trans <- preProcess(log.var2, method=c("BoxCox", "center", "scale"
  ↪ ))
PC1 <- predict(trans, log.var2)
ir.pca_23 <- prcomp(PC1, center = FALSE)

nup <- n*5

pred.combine <-predict(ir.pca_23)
pred.90 <- pred.combine[1:20000,1:6]
pred.75 <- pred.combine[20001:40000,1:6]
pred.60 <- pred.combine[40001:60000,1:6]
pred.50 <- pred.combine[60001:80000,1:6]
```

```
pred.45 <- pred.combine[80001:100000,1:6]

#Recording the prediction values
PC_val <-ir.pca_2$x[,1]
PC_val2 <-ir.pca_2$x[,2]

PC1_90 <- pred.90[,1]
PC2_90 <- pred.90[,2]

PC1_75 <- pred.75[,1]
PC2_75 <- pred.75[,2]

PC1_60 <- pred.60[,1]
PC2_60 <- pred.60[,2]

PC1_50 <- pred.50[,1]
PC2_50 <- pred.50[,2]

PC1_45 <- pred.45[,1]
PC2_45 <- pred.45[,2]

outer <-cbind(PC_val,PC_val2,PC1_90,PC2_90,PC1_75,PC2_75,PC1_60,
   ↪ PC2_60,PC1_50,PC2_50,PC1_45,PC2_45)
write.csv(outer,file="C:/Users/Jefferys/Desktop/Thesis_Jefferys/
   ↪ All_PCA/LRN/Outer_Data_1_2.csv")

##########Coefficients Plot
require(ggplot2)

#PC1 AND PC2
theta <- seq(0,2*pi,length.out = 100)
circle <- data.frame(x = cos(theta), y = sin(theta))
p <- ggplot(circle,aes(x,y)) + geom_path()

loadings <- data.frame(ir.pca_2$rotation,
                       .names = row.names(ir.pca_2$rotation))
```

```
p <- p + ggtitle("Coefficients of Variables for Lead Round Nose
    ↪ Bullet Data (PC1 and PC2)")
p <- p + geom_text(data=loadings,
                   mapping=aes(x = PC1, y = PC2, label = .names,
                       ↪ colour = .names)) +
  coord_fixed(ratio=1) +
  labs(x = "PC1", y = "PC2")
png(file = "CoefficientLRN1_2.png", width = 700, height = 600)
par(mai=c(1.2,0.5,1.2,0.5))#bottom, left, top, right
print(p)
dev.off()
#PC1 AND PC3
theta <- seq(0,2*pi,length.out = 100)
circle <- data.frame(x = cos(theta), y = sin(theta))
p <- ggplot(circle,aes(x,y)) + geom_path()

loadings <- data.frame(ir.pca_2$rotation,
                       .names = row.names(ir.pca_2$rotation))
p <- p + ggtitle("Coefficients of Variables for Lead Round Nose
    ↪ Bullet Data (PC1 and PC3)")
p <- p + geom_text(data=loadings,
                   mapping=aes(x = PC1, y = PC3, label = .names,
                       ↪ colour = .names)) +
  coord_fixed(ratio=1) +
  labs(x = "PC1", y = "PC3")
png(file = "CoefficientLRN1_3.png", width = 700, height = 600)
par(mai=c(1.2,0.5,1.2,0.5))#bottom, left, top, right
print(p)
dev.off()
#PC1 AND PC4
theta <- seq(0,2*pi,length.out = 100)
circle <- data.frame(x = cos(theta), y = sin(theta))
p <- ggplot(circle,aes(x,y)) + geom_path()

loadings <- data.frame(ir.pca_2$rotation,
                       .names = row.names(ir.pca_2$rotation))
```

```
p <- p + ggtitle("Coefficients of Variables for Lead Round Nose
    ↪ Bullet Data (PC1 and PC4)")
p <- p + geom_text(data=loadings,
                   mapping=aes(x = PC1, y = PC4, label = .names,
                     ↪ colour = .names)) +
  coord_fixed(ratio=1) +
  labs(x = "PC1", y = "PC4")
png(file = "CoefficientLRN1_4.png", width = 700, height = 600)
par(mai=c(1.2,0.5,1.2,0.5))#bottom, left, top, right
print(p)
dev.off()

####Projected Plots
filer$True_Angle <-as.numeric(filer$True_Angle)

SPP <- filer$True_Angle
COLOR <- c("blue","darkorange4","darkgreen","red","purple")

#PC1 AND PC2
pc <- c(1,2)
png(file = "PredictedonOriginal_LRN.png", width = 1000, height =
    ↪ 600)
par(mai=c(1.2,1.2,1.2,1.8))#bottom, left, top, right
plot(pred.45[,1],pred.45[,2] ,col="cornflowerblue", pch=1,xlim=c
    ↪ (-4,4),ylim=c(-2,2), ylab="PC2 (25.5%)",xlab="PC1 (35.3%)")
points(pred.90[,1],pred.90[,2], col="plum", pch=1)
points(pred.75[,1],pred.75[,2], col="brown", pch=1)
points(pred.60[,1],pred.60[,2], col="green", pch=1)
points(pred.50[,1],pred.50[,2], col="darkorange", pch=1)
points(ir.pca_2$x[,1], ir.pca_2$x[,2],col=COLOR[SPP], pch=16)
title(main="Projected Predicted PCs (Test Set = 20000) and
    ↪ Original Data (Training Set = 10) using PC1 and PC2")
legend("topright", inset=c(-0.15,0),col=c("purple","plum","red","
    ↪ brown","darkgreen","green","darkorange4","darkorange","blue"
    ↪ ,"cornflowerblue"),xpd = TRUE, legend=c("Original 90","
    ↪ Predicted 90","Original 75","Predicted 75","Original 60","
```

```
    ↪ Predicted 60","Original 50","Predicted 50","Original 45","
    ↪ Predicted 45"), pch=c(16,1,16,1,16,1,16,1,16,1), title="
    ↪ Angles")
dev.off()

#PC1 AND PC3
pc <- c(1,2)
png(file = "PredictedonOriginal_1_3.png", width = 1000, height =
    ↪ 600)
par(mai=c(1.2,1.2,1.2,1.8))#bottom, left, top, right
plot(pred.45[,1],pred.45[,3] ,col="cornflowerblue", pch=1,xlim=c
    ↪ (-4,4),ylim=c(-2,2), ylab="PC3 (20.7%)",xlab="PC1 (35.3%)")
points(pred.90[,1],pred.90[,3], col="plum", pch=1)
points(pred.75[,1],pred.75[,3], col="brown", pch=1)
points(pred.60[,1],pred.60[,3], col="green", pch=1)
points(pred.50[,1],pred.50[,3], col="darkorange", pch=1)
points(ir.pca_2$x[,1], ir.pca_2$x[,3],col=COLOR[SPP], pch=16)
title(main="Projected Predicted PCs (Test Set = 20000) and
    ↪ Original Data (Training Set = 10) using PC1 and PC3")
legend("topright", inset=c(-0.15,0),col=c("purple","plum","red","
    ↪ brown","darkgreen","green","darkorange4","darkorange","blue"
    ↪ ,"cornflowerblue"),xpd = TRUE, legend=c("Original 90","
    ↪ Predicted 90","Original 75","Predicted 75","Original 60","
    ↪ Predicted 60","Original 50","Predicted 50","Original 45","
    ↪ Predicted 45"), pch=c(16,1,16,1,16,1,16,1,16,1), title="
    ↪ Angles")
dev.off()

#PC1 AND PC4
pc <- c(1,2)
png(file = "PredictedonOriginal_1_4.png", width = 1000, height =
    ↪ 600)
par(mai=c(1.2,1.2,1.2,1.8))#bottom, left, top, right
plot(pred.45[,1],pred.45[,4] ,col="cornflowerblue", pch=1,xlim=c
    ↪ (-4,4),ylim=c(-2,2), ylab="PC4 (11.3%)",xlab="PC1 (35.3%)")
points(pred.90[,1],pred.90[,4], col="plum", pch=1)
```

```
points(pred.75[,1],pred.75[,4], col="brown", pch=1)
points(pred.60[,1],pred.60[,4], col="green", pch=1)
points(pred.50[,1],pred.50[,4], col="darkorange", pch=1)
points(ir.pca_2$x[,1], ir.pca_2$x[,4],col=COLOR[SPP], pch=16)
title(main="Projected Predicted PCs (Test Set = 20000) and
    ↪ Original Data (Training Set = 10) using PC1 and PC4")
legend("topright", inset=c(-0.15,0),col=c("purple","plum","red","
    ↪ brown","darkgreen","green","darkorange4","darkorange","blue"
    ↪ ,"cornflowerblue"),xpd = TRUE, legend=c("Original 90","
    ↪ Predicted 90","Original 75","Predicted 75","Original 60","
    ↪ Predicted 60","Original 50","Predicted 50","Original 45","
    ↪ Predicted 45"), pch=c(16,1,16,1,16,1,16,1,16), title="
    ↪ Angles")
dev.off()

#####################3D Plots
pc1.rot <- ir.pca_2$rotation[,1]
pc2.rot <- ir.pca_2$rotation[,2]
pc3.rot <- ir.pca_2$rotation[,3]

row.PC <- nrow(PC)
col.PC <- ncol(PC)
out.PC1 <- c()
out.PC2 <- c()
out.PC3 <- c()
inner.PC1 <- 0
inner.PC2 <- 0
inner.PC3 <- 0

i <- 1
j <- 1

for(i in 1:row.PC){
  for(j in 1:6){
    inner.PC1 <- inner.PC1+PC[i,j]*pc1.rot[j]
    inner.PC2 <- inner.PC2+PC[i,j]*pc2.rot[j]
```

```
    inner.PC3 <- inner.PC3+PC[i,j]*pc2.rot[j]
  }
  out.PC1[i] <- inner.PC1
  out.PC2[i] <- inner.PC2
  out.PC3[i] <- inner.PC3
  inner.PC1 <- 0
  inner.PC2 <- 0
  inner.PC3 <- 0
}
png(file = "Scatterplot3dLRNpca.png", width = 1000, height = 600)
par(mai=c(1.2,1.2,2,1.8))#bottom, left, top, right
filer$pcolor[filer$True_Angle==90] <- "plum"
filer$pcolor[filer$True_Angle==75] <- "brown"
filer$pcolor[filer$True_Angle==60] <- "green"
filer$pcolor[filer$True_Angle==50] <- "darkorange"
filer$pcolor[filer$True_Angle==45] <- "cornflowerblue"
with(filer, {
  scatterplot3d(out.PC1, out.PC2, out.PC3,
                pch=16,
                highlight.3d=FALSE,
                type="h",
                main="3D Scatter Plot for Lead Round Nose Bullets
                    ↪ (PC1, PC2, PC3) with Vertical Lines",color=
                    ↪ pcolor,xlab="PC1 (35.3% variance explained)"
                    ↪ ,zlab="PC3 (20.7% variance explained)",ylab=
                    ↪ "PC2 (25.5% variance explained)")
  legend("topleft", inset=c(.0025,-0.0050),      # location and
    ↪ inset
         bty="n", cex=1,,              # suppress legend box,
           ↪ shrink text 50%
         title="Angles",
         c("45", "50", "60","75","90"), fill=c("cornflowerblue","
           ↪ darkorange","green","brown","plum"))
})
dev.off()
#end PCA LRN script
```

9. References

[1] MidwayUSA. Remington bullets 9mm (355 diameter) 115 grain full metal jacket. Retrieved from http://www.midwayusa.com/product/1601144112/, 2015.

[2] E. Vermeij, M. Rijnders, P. Pieper, and R. Hermsen. Interaction of bullets with intermediate targets: Material transfer and damage. *Forensic Sci. Int.*, (223):125–135, 2012.

[3] Rensselaer Polytechnic Institute. Snell's law. Retrieved from http://www.rpi.edu/dept/phys/.

[4] Locke Scientific. *Reference Glasses and Silicone Oils for Refractive Index Determination.*

[5] R. Wilcox. Refractive index determination using the central focal masking technique with dispersion colors. *Am. Mineral.*, (68):1126–1236, 1983.

[6] W. McCrone, L. McCrone, and J. Delly. *Polarized light microscopy.* Ann Arbor Science Publishers Inc., 1978.

[7] Pathtech. ffTA GRIM3. Retrieved from https://www.pathtech.com.au/product/ffta-grim3/.

[8] Research Group Electrochemical and Surface Engineering. Auger electron spectroscopy - aes. Retrieved from http://www.surfgroup.be/aes.

[9] J. Goldstein, D. Newbury, D. Joy, P. Echlin, E. Lifshin, L Sawyer, and J. Michael. *Scanning Electron Microscopy and X-ray Microanalysis.* Springer Science and Businesss Media, LLC, 2003.

[10] The Subsurface Life in Mineral Environment Team. Manganese. Retrieved from http://www.caveslime.org/fmd/manganese.

[11] Australian Microscopy and Microanalysis Research Center. X-ray mapping. Retrieved from http://www.ammrf.org.au/myscope/analysis/eds/mapping, 2014.

[12] J. Curran. *Introduction to data analysis with R for forensic scientists.* CRC Press, 2010.

[13] T. Holderness. Plotting confidence intervals of linear regression in python. Retrieved from https://tomholderness.wordpress.com/2013/01/10/, 2013.

[14] R. Wehrens. *Chemometrics with R!* Springer, 2011.

[15] National Institute of Standards and Technology (NIST). Box-Cox normality plot. Retrieved from http://www.itl.nist.gov/div898/handbook/eda/section3/boxcoxno.htm.

[16] J. Andrasko and A. Maehly. The discrimination between samples of window glass by combining physical and chemical techniques. *J. Forensic Sci.*, (23):250–262, 1978.

[17] C. Munger, K. Gates, and C. Hamburg. Determining the refractive index variation within panes of vehicle windshield glass. *J. Forensic Sci.*, (59), 2014.

[18] P. Kirk. *Crime investigation physical evidence and the police laboratory.* Interscience Publishers, Inc., 1953.

[19] J. Almirall, J. Buckleton, J. Curran, and T. Hicks. *Examination of glass.* CRC Press, 2000.

[20] B. Caddy. *Forensic examination of glass and paint: analysis and interpretation.* CRC Press, 2002.

[21] P. DeForest, R. Gaensslen, and H. Lee. *Forensic science: An introduction to criminalistics.* McGraw-Hill Humanities/Social Sciences/Languages, 1983.

[22] M. Haag and L. Haag. *Shooting incident reconstruction.* Academic Press, 2011.

[23] R. Saferstein. *Criminalistics: An introduction to forensic science.* Prentice Hall, Inc., 2004.

[24] R. Gardon. *Elasticity and strength in glasses: Glass: Science and technology*, volume 5. Academic Press, 2012.

[25] D. Deskins. Firearms and toolmarks section. Kentucky State Police Eastern Laboratory, 2015.

[26] Lead round nose (lrn) bullets explained. Retrieved from http://ammo.net/bullet-type/lead-round-nose-lrn, 2015.

[27] N. Leghorn. What are the different types of bullets, and what do they do? Retrieved from http://www.thetruthaboutguns.com/2013/07/foghorn/, 2013.

[28] J. Wallace. *Chemical analysis of firearms, ammunition, and gunshot residue*. CRC Press, 2008.

[29] Ballistics, ogives, and bullet shapes (part 1). Retrieved from http://mathscinotes.com/2011/01/ballistics-ogives-and-bullet-shapes-part-1/, 2011.

[30] W. Goldsmith and S. Finnegan. Penetration and perforation processes in metal targets at and above ballistic velocities. *Int. J. Mech. Sci.*, (13):843–866, 1971.

[31] J. Horswell. *The practice of crime scene investigation*. CRC Press, 2004.

[32] N. Petraco and P. DeForest. Trajectory reconstructions i: Trace evidence in flight. *J. Forensic Sci.*, (35):1284–1296, 1990.

[33] D. Stoney and J. Thornton. The forensic significance of the correlation of density and refractive index in glass evidence. *Forensic Sci. Int.*, (29):147–157, 1985.

[34] H. Ritland. Relation between refractive index and density of a glass at constant temperature. *J. Am. Ceram. Soc.*, (38):86–88, 1955.

[35] J. Girard. *Criminalistics: Forensic science, crime, and terrorism*. Jones & Bartlett Publishers, 2013.

[36] S. Bell and K. Morris. *An introduction to microscopy*. CRC, 2009.

[37] Scientific Working Group for Material Analysis (SWGMAT). Collection, handling, and identification of glass. 2005.

[38] Scientific Working Group for Materials Analysis (SWGMAT). Glass refractice index determination. 2005.

[39] B. Wheeler and L. Wilson. *Practical forensic microscopy: A Laboratory manual*. John Wiley & Sons, 2011.

[40] D. Bell and A. Garratt-Reed. *Energy dispersive X-ray analysis in the electron microscope*. Garland Science, 2003.

[41] W. Rasband. ImageJ. Retrieved from http://imagej.nih.gov/ij/, 1997-2014.

[42] National Institutes of Health. ImageJ User Guide. Retrieved from https://imagej.nih.gov/ij/docs/guide/146-30.html, 2012.

[43] R Development Core Team. *R: A Language and Environment for Statistical Computing*. 2014.

[44] RStudio Inc. About RStudio. Retrieved from http://www.rstudio.com/about.

[45] C. Zaiontz. Real statistics using Excel. Retrieved from http://www.real-statistics.com/regression/confidence-and-prediction-intervals/.

[46] GraphPad Software Inc. The distinction between confidence intervals, prediction intervals and tolerance intervals. Retrieved from http://www.graphpad.com/support/faqid/1506/, 2009.

[47] P. Gemperline. Principle component analysis, 2006.

[48] G. Zadora and Z. Brozek-Mucha. SEM-EDX-a useful tool for forensic examinations. *Mater. Chem. Phys.*, (81), 2003.

[49] R. Falcone, G. Sommariva, and M. Verita. WDXRF, EPMA and SEM/EDX quantitative chemical analyses of small glass samples. *Microchim. Acta*, (155):137–140, 2006.

[50] B. Karger, A. Hoekstra, and P. Schmidt. Trajectory reconstruction from trace evidence on spent bullets. *Int. J. Legal Med.*, (115):16–22, 2001.

[51] K. Wong and J. Jacobson. Angle of impact determination from bullet holes. *Journal of Forensic Identification*, 63, 2013.

[52] S. Baviskar. A quick & automated method for measuring cell area using ImageJ. *The American Biology Teacher*, (73):554–556, 2011.

[53] J. Brecko, A. Mathys, W. Dekoninck, M. Leponce, D. VandenSpiegel, and P. Semal. Focus stacking: Comparing commercial top-end set-ups with a semi-automatic low budget approach. A possible solution for mass digitization of type specimens. *ZooKeys*, 464:1–23, 2014.

[54] A. Maloney, C. Nicloux, K. Maloney, and F. Heron. One-sided impact spatter and area-of-origin calculations. *Jounal of Forensic Identification*, 61, 2011.

[55] K. Maloney, J. Killeen, and A. Maloney. The use of hemospat to include bloodstains located on nonorthogonal surfaces in area-of-origin calculations. *Journal of Forensic Identifcation*, 59, 2009.

[56] W. Rowe and S. Hanson. Range-of-fire estimates from regression analysis applied to the spreads of shotgun pellet patterns: Results of a blind study. *Forensic Sci. Int.*, (28):239–250, 1985.

[57] K. Heaney and W. Rowe. The application of linear regression to range-of-fire estimates based on the spread of shotgun pellet patterns. *J. Forensic Sci.*, 28(2):433–436, 1983.

[58] J. Wray, J. McNeil, and W. Rowe. Comparison of methods for estimating range of fire based on the spread of buckshot patterns. *J. Forensic Sci.*, 28(4):846–857, 1983.

[59] K. Virkler and I. Lednev. Blood species identification for forensic purposes using Raman Spectroscopy combined with advanced statistical analysis. *Anal. Chem.*, 81(18):7773–7777, 2009.

[60] C. Muehlethaler, G. Massonnet, and P. Esseiva. The application of chemometrics on Infrared and Raman Spectra as a tool for the forensic analysis of paints. *Forensic Sci. Int.*, 2011.

[61] J. Osborne. Improving your data transformations: Applying the Box-Cox transformation. *Practical Assessment, Research & Evaluation*, 15(12), 2010.

[62] FORident Software. HemoSpat bloodstain pattern analysis software. Retrieved from https://hemospat.com/.

[63] FORident Software. HemoSpat features. Retrieved from https://hemospat.com/features/.

[64] Inc. Cognisys. StackShot - automated macro rail for focus stacking. Retrieved from https://www.cognisys-inc.com/products/stackshot/stackshot.php.

[65] Nikon Corporation. Camera control pro 2. Retrieved from http://imaging.nikon.com/lineup/software/.

[66] Zerene Systems LLC. Zerene Stacker – the basics. Retrieved from http://zerenesystems.com/cms/stacker, 2015.

[67] LLC Zerene Systems. FAQ: Frequently asked questions. Retrieved from http://zerenesystems.com/cms/stacker/docs/faqlist, 2016.

[68] B. Reta. Firearms and toolmarks section. West Virginia State Police Crime Laboratory.